Cátia Vanessa Rodrigues Tavares

Sensores de fibra ótica para arquiteturas *e-Health*

Fiber optic sensors for e-Health architectures

Universidade de Aveiro
2022

Cátia Vanessa Rodrigues Tavares

Sensores de fibra ótica para arquiteturas *e-Health*

Fiber optic sensors for e-Health architectures

Tese apresentada à Universidade de Aveiro para cumprimento dos requisitos necessários à obtenção do grau de Doutor em Engenharia Física, realizada sob a orientação científica do Doutor Paulo Fernando da Costa Antunes, Professor Auxiliar do Departamento de Física da Universidade de Aveiro, e do Doutor Hugo Humberto Plácido da Silva, Professor Auxiliar Convidado do Departamento de Bioengenharia do Instituto Superior Técnico.

O júri / The jury

Presidente / President   Prof. Doutor Óscar Emanuel Chave Mealha
professor catedrático da Universidade de Aveiro

Vogais / Examiners committee   Prof. Doutor José Luís Campos de Oliveira Santos
professor catedrático da Universidade do Porto

Prof. Doutor Henrique Leonel Gomes
professor associado com agregação da Universidade de Coimbra

Profa. Doutora Filomena Maria da Rocha Menezes de Oliveira Santos
professora associada com agregação da Universidade do Minho

Profa. Doutora Margarida Maria Resende Vieira Facão
professora auxiliar da Universidade de Aveiro

Prof. Doutor Paulo Fernando da Costa Antunes
professor auxiliar da Universidade de Aveiro

À minha filha, Maria do Mar

Agradecimentos /Acknowledgement

Começo por agradecer aos meus orientadores. Ao Professor Paulo Antunes pela oportunidade de poder realizar este trabalho, pela orientação, pelo apoio e compreensão e pelo bom ambiente que sempre tentou transmitir aos seus alunos. Foi um gosto enorme e um orgulho trabalhar consigo!

Ao Professor Hugo Plácido da Silva, que embora mais distante esteve sempre disponível para me orientar e ajudar neste percurso.

Ao Instituto de Nanoestruturas, Nanomodelação e Nanofabricação, Departamento de Física e Instituto de Telecomunicações pelas condições de acolhimento proporcionadas no desenvolvimento do trabalho apresentado nesta Tese.

Um especial agradecimento à Doutora Fátima Domingues e à Doutora Nélia Alberto que me ensinaram a dar os primeiros passos no real mundo da investigação e que me orientaram muitas vezes ao longo deste percurso. À Doutora Cátia Leitão, pela ajuda no meu crescimento profissional, pelas nossas conversas e ensinamentos.

Aos meus colegas e amigos do Departamento de Física, Tiago, Susana, Micael, Marta e Luís pelo apoio, pelas conversas diárias e pela constante boa disposição.

A todos os meus amigos, obrigada pela vossa amizade.

À minha família.

Um agradecimento especial e de coração aos meus pais e irmão, pelo apoio, paciência, ajuda e amor incondicional. Um agradecimento também os meus sogros e cunhada por todo o apoio e ajuda com a minha filha. Sem vocês, teria sido mais difícil.

Ao amor da minha vida, a minha filha Maria do Mar pelo amor incondicional.

Por último, mas de todo o menos importante, ao Gonçalo, meu amigo, marido e companheiro, muito obrigada pelo incentivo para abraçar esta aventura, pela tua ajuda, mas sobretudo pelo apoio, paciência e amor.

O meu sincero obrigada a todos.

Palavras-chave   Sensores de fibra ótica, redes de Bragg em fibra ótica, sensores de pressão, sensores de cisalhamento, sensores de frequência cardiaca e respiratória

Resumo   Neste trabalho foram desenvolvidos e otimizados sensores em fibra ótica para aplicações biomédicas em soluções vestíveis e não intrusivas/ou invisíveis.
Tendo em conta que se pretende que os dispositivos desenvolvidos não interfiram com os movimentos e o dia-a-dia do utilizador, os sensores de fibra ótica apresentam inúmeras vantagens quando comparados com os sensores eletrónicos convencionais, de entre várias, destacam-se: tamanho e peso reduzido, biocompatibilidade, segurança, imunidade a interferências eletromagnéticas e elevada sensibilidade.

Numa primeira etapa, foram desenvolvidos dispositivos vestíveis com sensores de fibra ótica baseados em redes de Bragg (FBG) para incorporar em palmilhas de modo a monitorizar diferentes parâmetros da marcha com base na análise da pressão exercida em várias zonas da palmilha. Ainda no âmbito deste tema, adicionalmente, foram desenvolvidos sensores utilizando a mesma tecnologia de sensoriamento, mas capazes de monitorizar simultaneamente pressão e forças de cisalhamento. Este trabalho foi pioneiro e permitiu monitorizar um dos principais responsáveis pela ulceração dos pés em pessoas com diabetes: o cisalhamento.

Numa fase posterior, o estudo centrou-se na temática relacionada com o aparecimento de úlceras em pessoas com mobilidade reduzida e utilizadores de cadeiras de rodas. De modo a contribuir para a mitigação deste flagelo, procurou-se desenvolver um sistema composto por uma rede de sensores de fibra ótica capaz de monitorizar a pressão em vários pontos de uma cadeira de rodas e não só aferir a pressão em cada ponto, mas monitorizar a postura do cadeirante e aconselhá-lo a mudar de postura com regularidade, de modo a diminuir a probabilidade de ocorrência desta patologia. Ainda dentro desta aplicação, foi publicado um outro trabalho onde o sensor não só monitoriza a pressão como também a temperatura em cada um dos pontos de análise, conseguindo aferir assim indiretamente o cisalhamento.

Numa outra fase, foi realizado o estudo e desenvolvimento de sensores de fibra ótica de plástico para monitorizar a postura corporal de um utilizador de uma cadeira de escritório. Simultaneamente, foi desenvolvido um software capaz de monitorizar e mostrar ao utilizador todos os dados adquiridos em tempo real e advertir o utilizador de posturas incorretas, bem como aconselhar para pausas no trabalho.

Numa quarta fase, o estudo centrou-se no desenvolvimento de sensores altamente sensíveis embebidos em materiais impressos 3D. O sensor é composto por uma fibra ótica com uma FBG e o corpo do sensor por um material polimérico flexível, denominado "*Flexible*". O sensor foi impresso numa impressora 3D e durante a sua impressão foi incorporada a fibra ótica. O sensor demonstrou ser altamente sensível e foi capaz de monitorizar frequência respiratória e cardíaca, tanto em soluções vestíveis (peito e pulso) como em soluções "invisíveis" (cadeira de escritório).

Abstract   In this work, optical fiber sensors were developed and optimized for biomedical applications in wearable and non-intrusive and/or invisible solutions.

As it was intended that the developed devices would not interfere with the user's movements and their daily life, the fibre optic sensors presented several advantages when compared to conventional electronic sensors, among others, the following stand out: size and reduced weight, biocompatibility, safety, immunity to electromagnetic interference and high sensitivity.

In a first step, wearable devices with fibre optic sensors based in Fiber Bragg gratings (FBG) were developed to be incorporated into insoles to monitor different walking parameters based on the analysis of the pressure exerted on several areas of the insole. Still within this theme, other sensors were developed using the same sensing technology, but capable of monitoring pressure and shear forces simultaneously. This work was pioneering and allowed monitoring one of the main causes of foot ulceration in people with diabetes: shear.

At a later stage, the study focused on the issue related with the appearance of ulcers in people with reduced mobility and wheelchair users. In order to contribute to the mitigation of this scourge, a system was developed composed of a network of fibre optic sensors capable of monitoring the pressure at various points of the wheelchair. It not only measures the pressure at each point, but also monitors the posture of the wheelchair user and advises him/her to change posture regularly to reduce the probability of this pathology occurring. Still within this application, another work was developed where the sensor not only monitored the pressure but also the temperature in each of the analysis points, thus indirectly measuring shear.

In another phase, plastic fibre optic sensors were studied and developed to monitor the body posture of an office chair user. Simultaneously, software was developed capable of monitoring and showing the user all the acquired data in real time and warning for incorrect postures, as well as advising for work breaks.

In a fourth phase, the study focused on the development of highly sensitive sensors embedded in materials printed by a 3D printer. The sensor was composed of an optical fibre with a FBG and the sensor body of a flexible polymeric material called "*Flexible*". This material was printed on a 3D printer and during its printing the optical fibre was incorporated. The sensor proved to be highly sensitive and was able to monitor respiratory and cardiac rate, both in wearable solutions (chest and wrist) and in "invisible" solutions (office chair).

INDEX

MANUSCRIPT 1

> REPLACE THIS LINE WITH YOUR PAPER IDENTIFICATION NUMBER (DOUBLE-CLICK HERE TO EDIT) <   1

Insole optical fiber sensor architecture for remote gait analysis - an eHealth Solution

M. Fátima Domingues, Nélia Alberto, Cátia Leitão, Cátia Tavares, Eduardo Rocon de Lima, Ayman Radwan, Victor Sucasas, Jonathan Rodriguez, Paulo André, Paulo Antunes

5

Insole optical fiber sensor architecture for remote gait analysis - an eHealth Solution

M. Fátima Domingues, Nélia Alberto, Cátia Leitão, Cátia Tavares, Eduardo Rocon de Lima, Ayman Radwan, Victor Sucasas, Jonathan Rodriguez, Paulo André, Paulo Antunes

Abstract— The advances and fast spread of mobile devices and technologies, we witness today, have extended its advantages over medical and health practice supported by mobile devices, giving rise to the growing research of Internet of Things (IoT), especially the e-Health field. The features provided by mobile technologies revealed to be of major importance when we consider the continuous aging of population and the consequent increase of its debilities. In addition to the increase of lifetime span of population, also the increase of health risks and their locomotive impairments increases, requiring a close monitoring and continuous evaluation. Such monitoring should be as non-invasive as possible, in order not to compromise the mobility and the day-to-day activities of citizens. Therefore, we present the development of a non-invasive optical fiber sensor architecture adaptable to a shoe sole for plantar pressure remote monitoring, which is suitable to be integrated in an IoT e-Health solution to monitor the wellbeing of individuals. The paper explores the production of the optical fiber sensor multiplexed network (using Fiber Bragg Gratings) to monitor the foot plantar pressure distribution during gait (walking movement). From the acquired gait data, it is possible to infer health conditions of the patient's foot and spine posture. To guarantee the patients mobility, the proposed system consists of an optical fiber sensor network integrated with a wireless transceiver to enable efficient ubiquitous monitoring of patients. The paper shows the calibration and measurement results, which reflect the accuracy of the proposed system, under normal walking in controlled area.

Index Terms— Internet of Things; e-Health; Gait analysis; Plantar pressure; Fiber Bragg gratings; Optical fiber sensing.

I. INTRODUCTION

The vast progress and spread of mobile and networking technologies has boosted the use of mobile devices' features in healthcare services applications, widening the interest of research communities, from the delivery of standard services like entertainment and communications, to the innovation of smart architectures and methods that can improve the autonomy and safety of people. The rise of e-Health, under the global scope of Internet of Things (IoT), aims to improve both the quality of the healthcare services provided to the patients, as well as the life quality of people (specifically patients), by providing them with the autonomy and mobility during their daily activities.

Additionally, the demographic and lifestyle changes of population also instigate an increase in health risks, demanding more close (continuous) health monitoring. e-Health, which is a rapid emerging area of IoT, can be the solution to decrease the risk of such health debilities and allow patients to continue with and normal lifestyle.

The use of electronic and mobile technologies in healthcare context, increases the quality of health services provided to patients and helps medical staff in the premature display of patients' anomalous health conditions.

The developments and new ambitions for the e-Health topic appear as the natural consequence of the technological evolution witnessed in the past decade. The monitoring process of individual health condition, rehabilitation status, or assistance requires the use of advanced and accurate systems, whose functions are centered in the interaction with humans not only on a physical level but also on a cognitive one. When considering wearable body physiological sensor networks, with wireless connection to a monitoring and decision center, those networks should be comfortably wearable by patients, in order to collect parameters for healthcare monitoring purposes, without compromising their lifestyle. Regarding the human-mobile devices interaction, the main challenges reside

M. Fátima Domingues is with the Instituto de Telecomunicações, Campus Universitário de Santiago, 3810-193 Aveiro, Portugal; Department of Physics & I3N, University of Aveiro, Campus Universitário de Santiago, 3810-193 Aveiro, Portugal and Centro de Automática y Robótica, CSIC-UPM ctra. Campo Real, 28500 Arganda del Rey, Madrid, Spain (e-mail: fatima.domingues@ua.pt)

Nélia Alberto is with Instituto de Telecomunicações, Campus Universitário de Santiago, 3810-193 Aveiro, Portugal and Centre for Mechanical Technology and Automation, Department of Mechanical Engineering, University of Aveiro, 3810-193 Aveiro, Portugal (e-mail: nelia@ua.pt).

Cátia Leitão is with Department of Physics & I3N, University of Aveiro, Campus Universitário de Santiago, 3810-193 Aveiro, Portugal (e-mail: catia.leitao@ua.pt).

Eduardo Rocon de Lima is with Centro de Automática y Robótica, CSIC-UPM, ctra. Campo Real, 28500 Arganda del Rey, Madrid, Spain (e-mail: erocon@iai.csic.es).

Catia Tavares, Ayman Radwan and Victor Sucasas are with Instituto de Telecomunicações, Campus Universitário de Santiago, 3810-193 Aveiro, Portugal (e-mail: catia.tavares@ua.pt; aradwan, vsucasas@av.it.pt).

Jonathan Rodriguez is with the Instituto de Telecomunicações, Campus Universitário de Santiago, 3810-193 Aveiro, Portugal; and the University of South Wales, Pontypridd, United Kingdom, CF37 1DL (e-mail: jonathan.rodriguez@southwales.ac.uk).

Paulo André is with Department of Electrical and Computer Engineering, Instituto de Telecomunicações, IST, Technical University of Lisbon, 1049-001 Lisbon, Portugal (e-mail: paulo.andre@lx.it.pt).

Paulo Antunes is with Department of Physics & I3N, University of Aveiro, Campus Universitário de Santiago, 3810-193 Aveiro, and with Instituto de Telecomunicações, Campus Universitário de Santiago, 3810-193 Aveiro, Portugal Portugal (e-mail: pantunes@ua.pt).

in safety, privacy, size/weight and power consumption of devices [1]. Such challenges should be taken more seriously, when users are elderly or impaired with incapacitating diseases.

To improve the life quality of physically impaired citizens and increase the mobility of elder citizens, we developed a non-invasive e-Health architecture which includes optical fiber sensors (OFSs) integrated into a shoe-sole for continuous remote monitoring of foot plantar pressure during gait (walking).

The plantar pressure distribution on the foot plantar surface is a reliable and important indicator with regards to foot health condition and gait pattern, from which, information like the wellbeing of the spinal cord or regarding the foot ulcerations evolution (in case of patients with diabetes) can be inferred. In the particular case of diabetes, the patients tend to develop foot ulcerations, which can be detected by high/abnormal forefoot plantar pressure [2]. So, accurate and controlled evaluation of the plantar pressure is vital to reduce and eventually avoid the risk of such pathologies.

The sensing mechanism used in the proposed architecture is based on Fiber Bragg Gratings (FBG) technology. This sensing elements are inscribed in the optical fiber core and the use of these OFSs is one of the innovations of the presented work, that comprises all the advantages inherent to OFSs, including robustness yet flexibility, the immunity to electromagnetic interference, the intrinsic electric safety (no electricity is needed at the measuring point), the ability to multiplex several sensors into the same optical fiber cable (optimal for sensing networks), among others. The sensing network is connected to an interrogation system, responsible for the acquisition of the sensed modulated signal. Both structures, the sensing network and interrogator, are connected through a secured body network, to a mobile gateway responsible to collect and analyze all sensed data and capable of ubiquitously connecting to the cloud.

The presented architecture is planned to be user-friendly and with the least impact possible on the shoe and foot anatomy (non-invasive), which is achievable due to the reduced size of the optical fiber; hence mobile, allowing the patient to be monitored during her/his normal daily activities. Such innovative aspect of the presented architecture will mitigate the drawbacks of currently used electronic devices, which restricts the experiments within the laboratory and consequently the natural execution of movements such as walking or running [3]. The optical sensor network is projected in order to satisfy the demands for small size and reduced power consumption, as well as high resolution in the acquisition of the data from the gait movement. The proposed shoe insole, incorporated with a network of optical fiber sensors, is an ambulatory accurate solution to continuously monitor body physical parameters.

In this paper, we emphasize on the calibration and successful implementation of the FBG sensing network in the insole. The presented measures show the accuracy of the implemented FBG network in monitoring the plantar pressure distribution during gait, since it is able to produce a typical gait pattern curve.

The remainder of the paper is organized as follows. In Section II the system architecture is presented and described.

Section III presents the FBG concept, its production and implementation. Section IV introduces the energy-efficient body network and mobile gateway, in addition to security issues. Section V presents the results obtained with the instrumented shoe insole. Section VI concludes.

II. REMOTE SENSING SYSTEM ARCHITECTURE

This section explores the architecture proposed for the remote monitoring of the foot plantar pressure and health condition. The designed system, shown in Fig. 1, comprises three key elements: the optical fiber sensing network (FBG sensors), the interrogator system and the wireless mobile connection.

The first part, responsible for the data sensing and therefore, the key innovative component of the system, is the FBG sensing network. This network consists of an optical fiber (incorporated in a shoe sole) containing six multiplexed FBGs, placed in the key points for the analysis of the foot health condition.

For the analysis of the data acquired, it is essential to have an interrogator system, able to acquire the signal modulated in the sensing points, and which is a function of the plantar pressure induced by the patients. In this configuration, the used interrogator is an off-the-shelf solution, the Ibsen® I-MON 512 USB, [4].

To complete the remote plantar pressure monitoring architecture, a mobile wireless gateway, responsible for the data process and wireless transmission to the decision centers, will also be incorporated.

Therefore, with the architecture presented, we developed a framework for monitoring the health conditions of citizens and provide automated visual feedback using state of the art technologies (i.e. advanced optical fiber sensors technology, secured energy-efficient wireless broadband access systems, smart actuators).
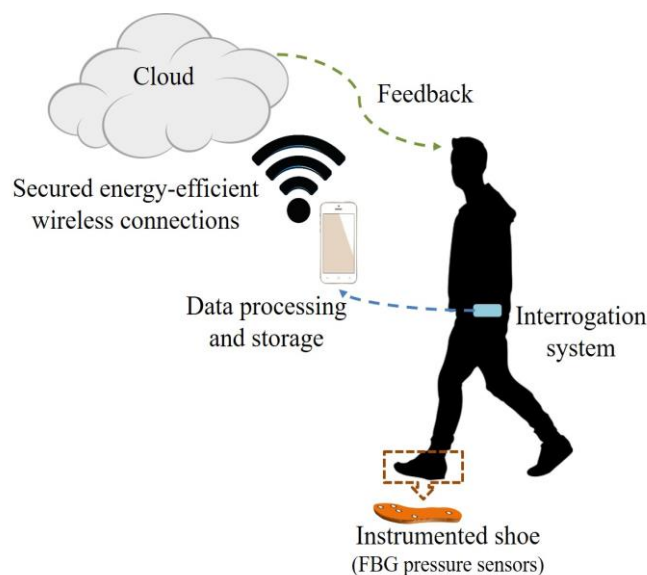

Fig. 1. Architecture of the proposed health monitoring system.

Bearing in mind the challenges and requirements related to such sensitive topic, the main goal was to develop a non-invasive monitoring system through the development of a showcase focusing on an "in-shoe" integrated network of optical fiber sensors, to support health promotion, patient-centric care, and well-being at home or during daily activities.

It is worth mentioning that this paper concentrates on the calibration and measurement of the developed FBG sensing network, showing the achieved accuracy of the proposed sensing architecture and its success in monitoring foot pressure during gait. The integration of the whole system is planned for future work.

III. PLANTAR PRESSURE FBG INSOLE PRODUCTION

A. Fiber Bragg Gratings sensing mechanism

The continuous progress in optical fiber technology offers major key of advantages not only for application in telecommunications field, but also for its use in biomedical sciences and as sensing mechanisms [5-9].

Regarding its features for sensing applications, optical fiber offers considerable advantages over similar electronic solutions, which makes OFS technology a cost-effective choice for sensing devices. Their flexibility, robustness, compact size, multiplexing ability (one optical fiber can comprise several sensing elements), their immunity to electromagnetic interference, and intrinsic electric safety (no need for electricity at the measuring point) are among their featured advantages [6, 7].

Within the various existing optical fiber sensing solutions, FBG sensors are now a well-established technology that offers all the optimum optical fiber features, allied with high efficiency, sensitivity and resolution [6-9].

This sensing elements (FBGs) can be described as the longitudinal periodic modification of the optical fiber core refractive index. Such perturbation can be induced by UV laser, and it consists of a wavelength reflective grating in the fiber core that follows the Bragg condition [7].

For sensing purposes, at the point where the FBG is inscribed, a component of the optical signal injected in the fiber is reflected, that component is named the Bragg wavelength. Application wise, when an optical source emits a spectral broadband optical signal into the fiber, at the FBG location, the component correspondent to the Bragg wavelength will be reflected. Regarding the transmitted signal, that same spectrum component will be missing [7], as schematized in Fig. 2. By monitoring the wavelength reflected by the grating – the Bragg wavelength – it is possible to monitor the parameters that induce the wavelength shift of the FBG sensor, namely temperature and/or strain [7].

The Bragg wavelength, λ_{Bragg}, is the function of the fiber core effective refractive index, n_{eff}, and the grating period, Λ, and can be expressed as [7]:

$$\lambda_{Bragg} = 2n_{eff}\Lambda \qquad (1)$$

As a result, the Bragg wavelength shift can be induced by changes in both the grating period and/or the effective refractive index [10].
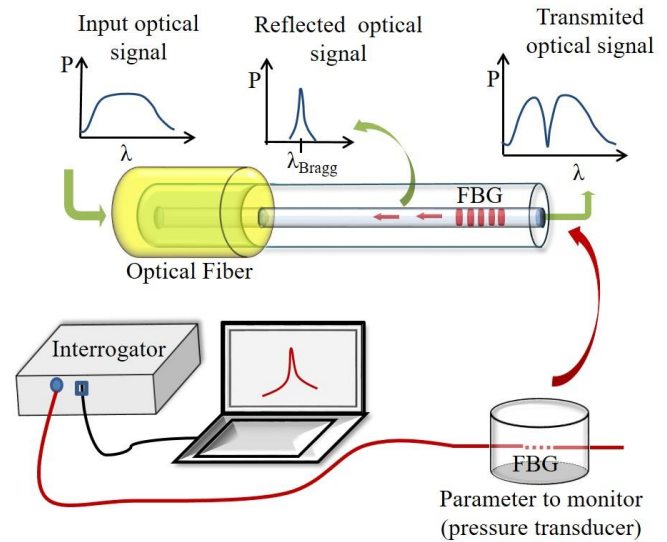

Fig. 2. Schematic diagram of the FBGs sensing mechanism.

Such dependence of the Bragg wavelength shift, $\Delta\lambda_{Bragg}$, makes this structures sensitive to strain and temperature variations. The relation between the $\Delta\lambda_{Bragg}$, and strain ($\Delta\varepsilon$) and/or temperature (ΔT) is translated by Equation (2), where the first term refers to the strain effect on λ_{Bragg} and the second term stands for the temperature effect [7]:

$$\Delta\lambda_{Bragg} = \lambda_{Bragg}(1-\alpha\rho)\Delta\varepsilon + \lambda_{Bragg}(\alpha+\xi)\Delta T \qquad (2)$$

α, ρ, and ξ are, respectively, the thermal expansion, the photoelastic and the thermo-optic coefficients of the fiber [7].

Regarding the strain influence in the $\Delta\lambda_{Bragg}$, it is due to the photo-elastic effects induced in the fiber by any physical elongation or deformation, which leads the fiber grating period to change. Temperature wise, the thermal dependence of the fiber on the refractive index is the responsible for the Bragg wavelength shift. A thermal expansion of the optical fiber will change the refractive index of the fiber at the FBG location, and consequently, will induce the Bragg wavelength to shift [7].

Such reliance of the Bragg wavelength on the temperature and strain variations gives this sensing element the accuracy necessary to render them optimum sensing solutions for the monitoring of such parameters at specific locations.

B. Insole design for plantar pressure and gait monitor with a FBG network

In the proposed architecture, an FBG sensing network was incorporated into a shoe insole in order to monitor the plantar pressure distribution in patients' feet during gait. The material used for the insole bulk structure was cork, which was chosen due its optimal characteristics for such application, as it is a material with thermal isolation, a near zero Poisson ratio and the malleability necessary to integrate the sensors and to adapt to the shoe and walk pattern [11].

As a first step towards the sensing sole production, 6 FBGs were inscribed and multiplexed into a GF1 photosensitive optical fiber (Thorlabs®) cable, using the phase mask technique and a KrF excimer UV laser, with a pulse energy of 5 mJ and a pulse repetition of 500 Hz.

The cork sole was then designed and machined in order to incorporate the network of 6 FBG sensors, which were allocated in the key points for the plantar pressure analysis (heel, midfoot, metatarsal and toe areas) [3], [12], [13], as shown in Fig. 3.

Considering the load pressure involved in the gait movement, it is necessary to provide extra resistance and protection to the optical fiber sensing elements. Addressing that purpose, the sensors were embedded in an epoxy resin cylindrical structures (1.0 cm diameter and 0.5 cm height), which was then incorporated within the cork sole.
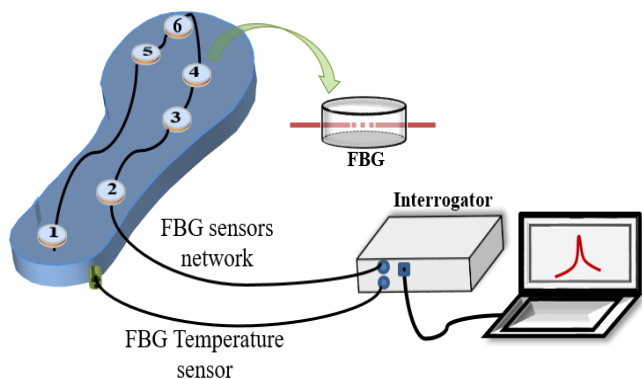

Fig. 3. Schematic diagram of the shoe insole containing the FBGs network.

Moreover, an FBG temperature sensor [7] was incorporated in the insole (close to the FBG placed in point 1), to guarantee that the thermal isolation provided by the cork is effective and the FBG plantar pressure sensors are not affected by the body temperature, or any external temperature changes.

Although in this particular application the temperature sensor was used as a control mechanism over the feedback of the pressure sensors, its application as a body temperature sensor can also be beneficial and considered in a wider system development.

IV. UBIQUITOUS SECURED ENERGY-EFFICIENT CONNECTIVITY

The proposed system includes a wireless transceiver, capable of ubiquitously connecting to a cloud-based monitoring application. The system can use a stand-alone wireless device dedicated to the monitoring architecture or an app, which is planned to be developed in future work to be installed on patients' smart phones. As mentioned above, the paper concentrates on the implementation and calibration of the FBG sensing network and only briefly discusses main ideas and issues of the design of ubiquitous secured energy efficient wireless connectivity.

Energy Efficiency: This system is developed to continuously monitor the well-being of a patient or an elder citizen; therefore, it requires to function for long periods,

without the need for re-charging, in order not to compromise user mobility. Energy efficiency is then a top priority of the wireless connectivity of such system. To provide ubiquity under the constraint of limited battery capacity, different wireless technologies simultaneously exist, and the mobile gateway is designed to be intelligent enough to choose the interface that produces the best energy efficiency (i.e. amount of data transmitted per joule of energy spent). The system also considers cooperative communications, clustering, or data aggregation, if energy savings can be achieved, as shown in our previous work [14], [15].

The gateway also uses a new form of smart caching of sensed data and transmission based on the wireless medium conditions. The system is designed to be smart to transmit data when good channel conditions exist, while sensed data is cached and transmitted at later times otherwise. We have shown the concept of smart uplink caching in previous work [16]. The system is also intelligent to be alerted when there is an emergency; hence data has to be forwarded immediately to inform a specialist.

Security: e-Health is an emerging technology, which is yet to be widely adopted by public. People, especially older generations, may be reluctant to embrace such technology for fear of their privacy being violated; hence security and privacy are essential, if e-Health is to achieve its full potential of improving the life quality of citizens. Hence, privacy-preserving mechanisms are of paramount importance to foster a rapid penetration of e-Health applications in the market. The state-of-the-art in privacy-preserving systems includes several solutions such as anonymous credentials [17], Public Key Infrastructure [18], group signatures [19], and pseudo-identities [20]. Pseudonym-based schemes are the most efficient approach in terms of computational complexity and latency. However, existing pseudonym-based solutions have common disadvantages: i) a permanent contact with a trusted authority that pseudonyms are required; ii) the update and distribution of the anonymity revocation lists for misuse detection is not scalable. Our solution goes beyond the state-of-the-art by providing an autonomous privacy preserving system, which is low-complex for low-capable devices, which can also provide efficient anonymity revocation. For that, we propose to use a system with self-generated pseudonyms and anonymity-revocation based on delegation, following our approach in [21]. The design and implantation of such security scheme will be presented in our future work.

V. CALIBRATION AND IMPLEMENTATION MEASUREMENTS

Before implementing the insole for plantar pressure monitoring, its 6 FBG sensing elements were calibrated to different pressure load values ranging from 10 N up to 200 N (Shimadzu® AGS-5kND mechanical test machine). The load sets were applied independently in each sensing point (from FBG 1 to FBG 6), using a probe with a diameter of 1.0 cm.

During each load set, the reflected Bragg wavelength shift of the respective FBGs was acquired by an interrogation system. The interrogation system comprises the optical source with high spectral width (Amonics, ALS-CL-17-B-FA), the optical circulator and an optical spectrometer (Ibsen, I-MON E).

The calibration values for the sensing element in position 2 and 3 (FBG 2 and FBG 3) are presented in Fig. 4, in which the linear dependence of the Bragg wavelength shift with the applied pressure is evident.
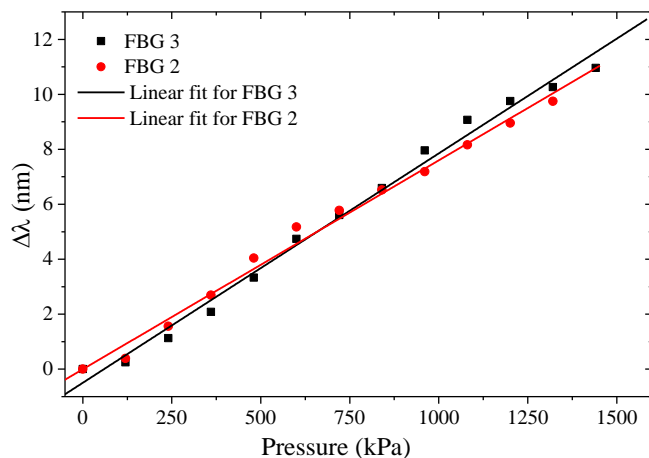

Fig. 4. Calibration of the FBG sensors to pressure (Points are the experimental values and line refers to the linear fit, $R^2 \sim 0.99$).

For these elements, FBG2 and FBG 3, the sensitivity coefficient achieved was 7.6±0.23 pm/kPa and 8.3±0.24 pm/kPa, respectively. Similar values were obtained for the other sensing elements.

Subsequent to the calibration, the insole was tested in the monitoring of the plantar pressure during gait. For that purpose, the insole was placed inside a shoe, and the wavelength shift induced in the 6 critical points during the gait movement was monitored.

Gait is the horizontal displacement of the body center of mass, and it requires, in a normal gait cycle, that the body posture is sustained alternatively by the foot, just by placing one foot forward, followed by the other [22].

In that way, gait is a cycle movement which can be categorized by two main phases: *stance phase* and the *swing phase*. The first corresponds to the period of time in which the foot is in contact with the ground and it starts when the heel first strikes the floor, lasting until the moment the toe becomes the last contact point (toe off). The *swing phase*, on the other hand, represents the lack of contact with the floor, and it starts when the toe ceases to be in contact with the ground, persisting till the moment the heel strikes the floor again, then starting a new gait cycle. For an individual with no abnormalities, the stance phase (at a normal pace) corresponds to about ~62% of the entire gait cycle [13, 23].

By monitoring the plantar pressure in the gait cycles of an individual/patient, we are making a systematic examination of their locomotion parameters (body posture shifts, spinal cord condition, foot structure and possible ulcerations), which can be used for diagnosis, posture correction and/or early treatment and assessment of patients [23].

The foot plantar pressure fluctuation during gait is also induced in the instrumented cork sole. Such pressure oscillations will lead to the shift in the reflected Bragg wavelength, which was acquired with the interrogator for the 6 FBGs sensors.

After converting the wavelength shift acquired, considering the sensitivity coefficient previously obtained (Fig. 4), the plantar pressure distribution induced in the cork sole over the gait movement was inferred, as it is shown in Fig. 5, for the 6 FBGs, during 3 gait cycles.

From the results obtained with the proposed insole sensor network, it becomes clear the repeatability of the data, given the similar response of the sensors over the three gait cycles depicted in Fig. 5. From the data acquired with the sole, we can also detect the sequence in which the sensors are activated (maximum amplitude registered), which was also in accordance to what is expected in a gait movement [3, 13]. FBG 1 is activated first, at the beginning of the stance phase of the gait cycle, when the heel starts its contact with the floor. With the evolution of the cycle, FBG 2 and FBG 3 (located at the middle-foot and beginning of the metatarsal) are activated at the start of foot-flat stage during the single support. Following the gait movement, FBG 4 and FBG 5, located at the metatarsal positions, have a stronger response at the fore-foot contact during the terminal double support, and finally, FBG 6, located at the toe area, is activated at the toe-off moment, marking the end of the stance phase and the beginning of the swing phase of the gait cycle.

The plantar pressure typical curve for the gait movement can be obtained by the addition of each of the 6 sensors feedback. The resulting final gait curve (considering our implementation) was computed and is also displayed in Fig. 5. Such figure shows that, with the implemented FBG network, it is possible to acquire an accurate gait pattern curve, as previously reported in literature [3, 13].

Based on the gait curve shape and pressure values, it is possible to detect potential foot ulcerations due to diseases, such as diabetes and even to infer postural condition of the spine. When comparing to previous reports using electronic devices [24], we can affirm that the feedback of the plantar pressure monitoring solution presented is within the expected behavior, which confirms that the method implemented is a reliable solution for such application.

Its synergic conjugation with a stand-alone wireless device is seen as a ubiquitous mobile solution that allows the continuous monitoring of physical postural parameters of impaired citizens. From such monitoring, the healthcare providers can access the patient's condition and detect any anomaly in their therapy or health status and if needed, provide the necessary feedback/corrections.

Regarding the temperature control sensor, presented also in Fig. 5 (top), we can observe that it remains constant, validating the thermal isolation of the cork used for the instrumented sole production.
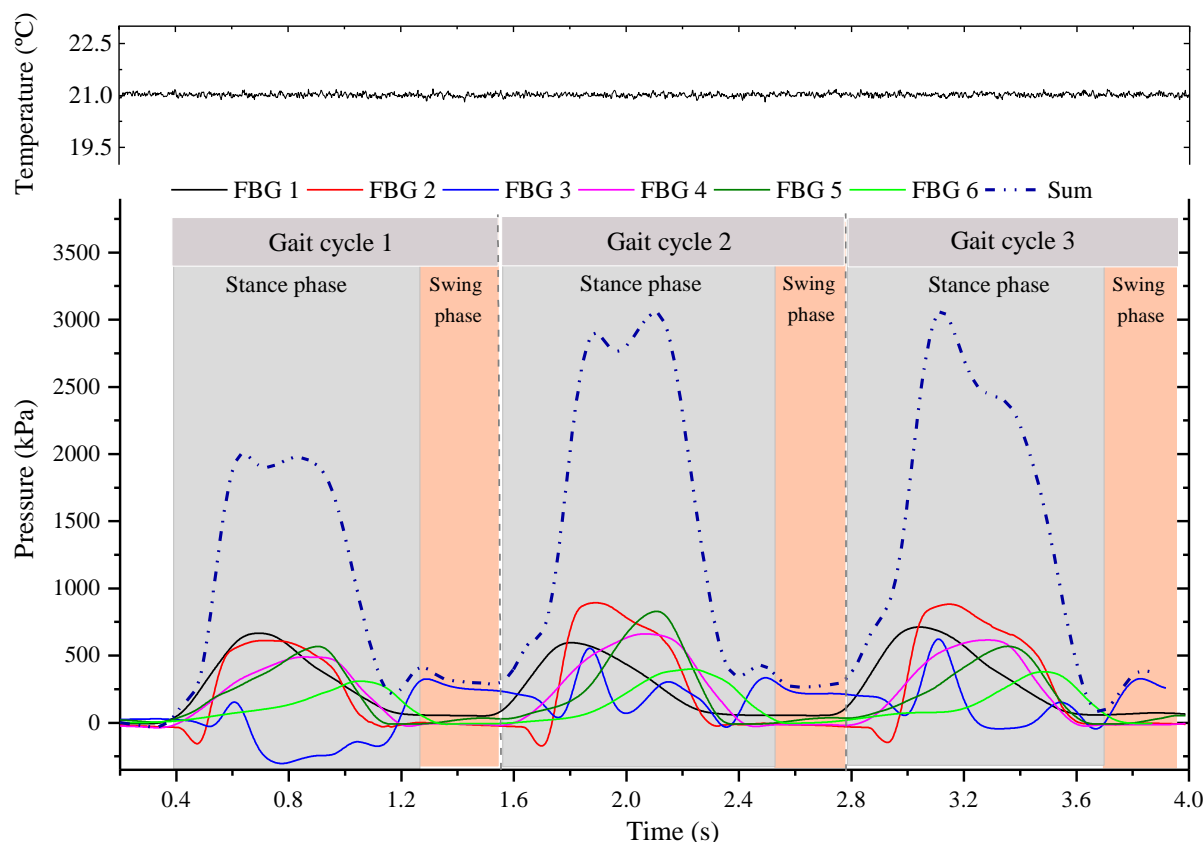
Fig. 5. Plantar pressure acquired data for the 6 sensors in the cork insole. Dashed curve corresponds to the final gait pattern curve.

VI. CONCLUSION

The fast progress of mobile technologies brought a new insight into healthcare systems and practices, igniting the research and development of the e-Health topic, a rapid emerging field of IoT.

The continuous aging of population and the development of chronic diseases often associated to it (such as diabetes or locomotive impairments) demands for a thorough monitoring of the patients, with a methodology that is as cost effective as possible. In contributing towards such noble objective, we presented a new optical fiber based sensing architecture for remote monitoring of foot plantar pressure distribution. The information retrieved form the plantar pressure distribution can provide valuable insights about foot health condition, which is able to provide information with regards to other diseases, such as the condition of the spine and/or the foot ulcerations due to diabetes.

The proposed architecture is composed of three main components, namely a sensing network consisting of 6 FBG sensors placed in key points around a cork shoe sole, an interrogator, for the acquisition of the modulated optical signal generated by the FBG sensors, and a mobile gateway which is responsible for ubiquitous connectivity to the cloud.

The calibration and measurements obtained with the proposed monitoring system were presented. From the results attained, we demonstrate the accuracy and reliability of the sensing network to monitor the foot plantar pressure distribution during gait.

The architecture presented is a small non-invasive system, designed to monitor the foot plantar pressure during gait, without compromising patient's mobility nor interfere in their daily activities. Moreover, the projected mobile gateway (secured and energy-efficient) will be responsible for the constant monitoring of patients/citizens. In that way, if an emergency or high risk situation occurs, prompt alerts can be send to the monitoring center (medical center/hospital/care taker), in order to provide fast response/assistance.

This article has been accepted for publication in a future issue of this journal, but has not been fully edited. Content may change prior to final publication. Citation information: DOI 10.1109/JIOT.2017.2723263, IEEE Internet of Things Journal

> REPLACE THIS LINE WITH YOUR PAPER IDENTIFICATION NUMBER (DOUBLE-CLICK HERE TO EDIT) <   7

REFERENCES

[1] A. Al-Fuqaha, M. Guizani, M. Mohammadi, M. Aledhari and M. Ayyas, "Internet of things: A survey on enabling technologies, protocols, and applications," IEEE Communications Surveys & Tutorials, vol. 17, no. 4, pp. 2347-2376, 2015.

[2] E. Morag and P. R. Cavanagh, "Morag E, Cavanagh PR. Structural and functional predictors of regional peak pressures under the foot during walking," Journal of biomechanics, vol. 32, no. 4, pp. 359-370, 1999.

[3] A. H. Abdul Razak, A. Zayegh, R. K. Begg and Y. Wahab, "Foot plantar pressure measurement system: a review," Sensors, vol. 12, no. 7, pp. 9884-9912, 2012.

[4] Ibsen, [Online]. Available: ibsen. com/products/interrogation-monitors/i-mon-usb/i-mon-256-512-usb/.

[5] P. Antunes, M. F. Domingues, N. Alberto and P. André, "Optical fiber microcavity strain sensors produced by the catastrophic fuse effect," IEEE Photonics Technology Letters, vol. 26, no. 1, pp. 78-81, 2014.

[6] P. Antunes, C. Leitão, H. Rodrigues, R. Travanca, J. Lemos-Pinto, A. Costa, H. Varum and P. André, "Optical fiber Bragg grating based accelerometers and applications," in Accelerometers: Principles, Structure and Applications, Nova Publishers, 2013.

[7] N. Alberto, L. Bilro, P. Antunes, C. Leitão, H. Lima and P. André, "Optical fiber technology for eHealthcare," in Handbook of Research on ICTs and Management Systems for Improving Efficiency in Healthcare and Social Care, IGI Global, pp. 180-200, 2013.

[8] C. Leitão, L. Bilro, N. Alberto, P. Antunes, H. Lima, P. André, R. Nogueira and J. L. Pinto, "Feasibility studies of Bragg probe for non-invasive carotid pulse waveform assessment," Journal of Biomedical Optics, vol. 18, no. 1, pp. 017006-1 - 017006-6, 2013.

[9] V. Mishra, N. Singh, U. Tiwari and P. Kapur, "Fiber grating sensors in medicine: Current and emerging applications," Sensors and Actuators A: Physical, vol. 167, no. 2, pp. 279-290, 2011.

[10] K. Hill and G. Meltz, "Fiber Bragg grating technology fundamentals and overview," Journal of Lightwave Technology, vol. 15, no. 8, pp. 1263-1276, 1997.

[11] Silva, S. P., M. A. Sabino, E. M. Fernandes, V. M. Correlo, L. F. Boesel, and R. L. Reis. "Cork: properties, capabilities and applications." International Materials Reviews 50, no. 6, pp. 345-365. 2005.

[12] W. Tao, T. Liu, R. Zheng and H. Feng, "Gait analysis using wearable sensors," Sensors, vol. 12, no. 2, pp. 2255-2283, 2012.

[13] Domingues, Maria Fátima, Cátia Tavares, Cátia Leitão, Anselmo Frizera-Neto, Nélia Alberto, Carlos Marques, Ayman Radwan et al. "Insole optical fiber Bragg grating sensors network for dynamic vertical force

monitoring." Journal of Biomedical Optics 22, no. 9, pp. 091507-091507, 2017.

[14] A. Radwan and J. Rodriguez, "Energy saving in multi-standard mobile terminals through short-range cooperation," EURASIP Journal on Wireless Communications and Networking, vol. 1, pp. 1-15, 2012.

[15] F. B. Saghezchi, A. Radwan, J. Rodriguez, and T. Dagiuklas, "Coalition Formation Game toward Green Mobile Terminals in Heterogeneous Wireless Networks," in IEEE Wireless Communications, vol. 20, no. 5, pp. 85-91, Nov. 2013.

[16] A. Radwan, M. F. Domingues, and J. Rodriguez, "Mobile Caching-enabled Small-cells for Delay-tolerant e-Health Apps," in proc. IEEE Conference on Communications (ICC'17), May 2017.

[17] M. Raya and J.-P. Hubaux, "The security of vehicular ad hoc networks," in Proceedings of the 3rd ACM Workshop on Security of Ad Hoc and Sensor Networks, SASN '05, pages 11–21, New York, NY, USA, 2005.

[18] X. Liu, Z. Fang and L. Shi, "Securing vehicular ad hoc networks," in 2nd International Conference on Pervasive Computing and Applications, ICPCA 2007, pages 424–429, July 2007.

[19] X. Lin, X. Sun, P. H. Ho and X. Shen, "GSIS: A secure and privacy-preserving protocol for vehicular communications," IEEE Transactions on vehicular technology, vol. 56, no. 6, pp. 3442-3456, 2007.

[20] R. Lu, X. Lin, Z. Shi and X. Shen, "A Lightweight Conditional Privacy-Preservation Protocol for Vehicular Traffic-Monitoring Systems," IEEE Intelligent Systems, vol. 28, no. 3, pp. 62-65, 2013.

[21] V. Sucasas, G. Mantas, F. B. Saghezchi, A. Radwan and J. Rodriguez, "An autonomous privacy-preserving authentication scheme for intelligent transportation systems," Computer Security, vol. 60, pp. 193-205, 2016.

[22] Kim, C. Maria, and Janice J. Eng. "Symmetry in vertical ground reaction force is accompanied by symmetry in temporal but not distance variables of gait in persons with stroke." Gait & posture 18, no. 1, pp. 23-28, 2003.

[23] de Castro, Marcelo P., Sofia C. Abreu, Helena Sousa, Leandro Machado, Rubim Santos, and Joao Paulo Vilas-Boas. "In-shoe plantar pressures and ground reaction forces during overweight adults' overground walking." Research quarterly for Exercise and Sport 85, no. 2, pp. 188-197, 2014.

[24] Lopez-Meyer, Paulo, George D. Fulk, and Edward S. Sazonov. "Automatic detection of temporal gait parameters in poststroke individuals." IEEE Transactions on Information Technology in Biomedicine 15, no. 4, pp. 594-601, 2011.

This article has been accepted for publication in a future issue of this journal, but has not been fully edited. Content may change prior to final publication. Citation information: DOI 10.1109/JIOT.2017.2723263, IEEE Internet of Things Journal

> REPLACE THIS LINE WITH YOUR PAPER IDENTIFICATION NUMBER (DOUBLE-CLICK HERE TO EDIT) <   8

ABOUT THE AUTHORS

Maria Fátima Domingues received her PhD in Physics Engineering, from the University of Aveiro, Portugal in 2014 and she is currently a research Fellow at Instituto de Telecomunicações-Aveiro, I3N-Physiscs Department, University of Aveiro, Portugal & Consejo Superior de Investigaciones Científicas (CSIC)-Madrid, Spain holding Post-doc grant from the Fundação para a Ciencia e a Tecnologia (FCT-Portugal). Her current research interests include new solutions of optical fiber sensors and its application in robotic exoskeletons and e-Health.

Nélia Alberto graduated with the degree in Physics and Chemistry from University of Aveiro, Portugal, in 2005. The Ph.D. degree in Physics was received in 2011, from the same university. She is currently working as a Post-Doctoral researcher at the Instituto de Telecomunicações and Centre for Mechanical Technology and Automation (Aveiro). Her main research interests include the study, development and application of optical fiber based devices for sensing applications.

Cátia Sofia Jorge Leitão was born in Porto, in 1987. She received is M.S. degree in Biomedical Engineering, specialization in Biomedical Instrumentation and Biomaterials, from University of Coimbra in 2010. From 2010 to 2012 she was research fellow, and from 2013 to 2016, PhD student in Physical Engineering in University of Aveiro. Currently, she is a postdoctoral researcher at I3N & Physics Department of University of Aveiro, Portugal. Her main research interests are optical fiber sensors applied to non-invasive cardiovascular monitoring, mainly in arterial pulse waveform acquisition and its implications on cardiovascular risk assessment.

Cátia Tavares was born in Aveiro, Portugal, in July 1992. She received the Master degree in Physics Engineering from the University of Aveiro, Portugal in 2016. She is currently working as a researcher fellow at the Instituto de Telecomunicações-Aveiro and I3N-Physiscs Department, University of Aveiro, Portugal. Her current research interests include de development of optical fiber sensors for eHealth solutions and its application in physical rehabilitation.

Eduardo Rocon received a Ph.D. degree in 2006 from the Universidad Politécnica de Madrid. His researched activity was awarded with the Georges Giralt PhD Award as the best PhD robotics thesis in Europe and the EMBEC scientific award. He is current a tenure researcher at the Bioengineering Group at the Consejo Superior de Investigaciones Científicas (CSIC). His research interests include rehabilitation, neurophysiology, biomechanics, adaptive signal processing, and human machine interaction.

Ayman Radwan received his Ph.D. from Queen's University (Canada), in 2009. He is a senior Research Engineer (Investigador Auxiliar) with the Instituto de Telecomunicações. Radwan is mainly specialized in coordination and management of EU funded projects. He participated in the coordination of multiple EU projects. He is currently the Project coordinator of CELTIC+ project "MUSCLES", as well as participating in the coordination of the ITN-SECRET. He also acted as the Technical Manager of FP7-C2POWER project and as the coordinator of CELTIC+ "Green-T" project. His research interests include IoT, 5G, and green communications.

Victor Sucasas obtained his Ph.D. on Electronic Engineering at University of Surrey (UK) in 2016. He has extensive research experience as a researcher at Instituto de Telecomunicações - Aveiro, Portugal and as a PhD student at University of Surrey, Guildford, UK, where he worked on European projects FP7-GREENET, ECSEL-SWARMs and CATRENE-H2O. Over the past 6 years, he has been an active researcher in several fields such as wireless ad hoc networks, internet of things, network security and privacy preserving systems.

Jonathan Rodriguez received his Master's degree in Electronic and Electrical Engineering and Ph.D from the University of Surrey (UK), in 1998 and 2004 respectively. Since 2005, he is a researcher at the Instituto de Telecomunicações, Portugal. In 2017, he was appointed Professor of Mobile Communications at the University of South Wales (UK). He is author of more than 360 scientific works, and his professional affiliations include: Senior Member of the IEEE, Chartered Engineer (CEng), and Fellow of the IET (2015). His research interests include: 5G Mobile Architectures, IoT, Radio Resource Management and RF design.

Paulo S. B. André received the Ph.D. degree in Physics, and the Agregação title (habilitation) degree from the Universidade de Aveiro, Portugal, in 2002 and 2011, respectively. He joined the Instituto Superior Técnico, University of Lisbon, in 2013, as an Associate Professor, lecturing on telecommunications. His is a IEEE senior member and his research interests include the study /simulation of photonic and optoelectronic components, optical sensors, integrated optics, photonic graphene applications, multiwavelength optical communications systems, and passive optical networks.

Paulo F. C. Antunes received the Ph.D. in Physics Engineering in 2011 from the Aveiro University, Portugal. He is currently an Assistant Researcher at the I3N-Aveiro (Institute of Nanostructures, Nanomodelling and Nanofabrication), he is also with the University of Aveiro Physics Department and the Instituto de Telecomunicações. His current research interests include the study and simulation of fiber Bragg gratings, data acquisition, optical sensing solutions for static and dynamic applications, including medical and structural monitoring.

MANUSCRIPT 2

Insole optical fiber Bragg grating sensors network for dynamic vertical force monitoring

Maria Fátima Domingues
Cátia Tavares
Cátia Leitão
Anselmo Frizera-Neto
Nélia Alberto
Carlos Marques
Ayman Radwan
Jonathan Rodriguez
Octavian Postolache
Eduardo Rocon
Paulo André
Paulo Antunes

Insole optical fiber Bragg grating sensors network for dynamic vertical force monitoring

Maria Fátima Domingues
Cátia Tavares
Cátia Leitão
Anselmo Frizera-Neto
Nélia Alberto
Carlos Marques
Ayman Radwan
Jonathan Rodriguez
Octavian Postolache
Eduardo Rocon
Paulo André
Paulo Antunes

SPIE.

Insole optical fiber Bragg grating sensors network for dynamic vertical force monitoring

Maria Fátima Domingues,[a,b,c,*] **Cátia Tavares,**[a] **Cátia Leitão,**[a,c] **Anselmo Frizera-Neto,**[d] **Nélia Alberto,**[a,e]
Carlos Marques,[a,c] **Ayman Radwan,**[a] **Jonathan Rodriguez,**[a] **Octavian Postolache,**[f] **Eduardo Rocon,**[b]
Paulo André,[g] **and Paulo Antunes**[a,c]
[a]Instituto de Telecomunicações, Campus Universitário de Santiago, Aveiro, Portugal
[b]Centro de Automática y Robótica, CSIC-UPM, Arganda del Rey, Madrid, Spain
[c]University of Aveiro, Department of Physics and I3N, Campus Universitário de Santiago, Aveiro, Portugal
[d]Federal University of Espírito Santo, Department of Electrical Engineering, Goiabeiras, Vitória, Brazil
[e]University of Aveiro, Centre for Mechanical Technology and Automation, Department of Mechanical Engineering, Aveiro, Portugal
[f]Lisbon University Institute, ISCTE-IUL, Instituto de Telecomunicações, Lisbon, Portugal
[g]University of Lisbon, Instituto Superior Técnico, Instituto de Telecomunicações and Department of Electrical and Computer Engineering, Lisbon, Portugal

Abstract. In an era of unprecedented progress in technology and increase in population age, continuous and close monitoring of elder citizens and patients is becoming more of a necessity than a luxury. Contributing toward this field and enhancing the life quality of elder citizens and patients with disabilities, this work presents the design and implementation of a noninvasive platform and insole fiber Bragg grating sensors network to monitor the vertical ground reaction forces distribution induced in the foot plantar surface during gait and body center of mass displacements. The acquired measurements are a reliable indication of the accuracy and consistency of the proposed solution in monitoring and mapping the vertical forces active on the foot plantar sole, with a sensitivity up to 11.06 pm/N. The acquired measurements can be used to infer the foot structure and health condition, in addition to anomalies related to spine function and other pathologies (e.g., related to diabetes); also its application in rehabilitation robotics field can dramatically reduce the computational burden of exoskeletons' control strategy. The proposed technology has the advantages of optical fiber sensing (robustness, noninvasiveness, accuracy, and electromagnetic insensitivity) to surpass all drawbacks verified in traditionally used sensing systems (fragility, instability, and inconsistent feedback). © *2017 Society of Photo-Optical Instrumentation Engineers (SPIE)* [DOI: 10.1117/1.JBO.22.9.091507]

Keywords: gait vertical ground reaction force; gait plantar pressure; physical rehabilitation; optical fiber sensors; insole fiber Bragg gratings network.

Paper 160820SSPR received Nov. 30, 2016; accepted for publication Feb. 8, 2017; published online Feb. 28, 2017.

1 Introduction

The continuous aging of the population and lifetime expectation increase entail health risks that require a close monitoring of elder citizens and patients. With the witnessed demographic shift in the world's population allied to a growing sedentary lifestyle, the demand for remote, continuous, and dynamic healthcare monitoring systems to enhance the quality of life is increasing.[1] Such solutions should enable debilitated people to sustain a fulfilling lifestyle by monitoring and controlling their physical incapacities.[2]

Aiming to contribute toward enhancing the life quality of physically debilitated and elder citizens, this work proposes an optical fiber sensors' network solution adaptable into an insole for vertical ground reaction forces (VGRF) and plantar pressure monitoring. The assessment of these parameters is of great importance for the gait analysis health evaluation. Additionally, by mapping the ground reaction forces during gait, it is possible to understand the effect induced in the body.[3–5]

Gait represents the movement of the body center of mass (BCM) through a horizontal trajectory and it implies, in a normal gait cycle, that the feet alternate in their ability to sustain the body posture, by placing one foot forward followed by the next.[6] Therefore, gait is a cycle activity that can be divided into two main phases: stance, when the foot is in contact with the ground and swing, when such contact ceases. The stance phase starts when the heel strikes (HS) the ground, lasting until the moment the toe becomes the last contact point [toe off (TO)]. The swing phase starts when the toe ceases its contact with the ground and lasts till the instant the HS the floor again, the point at which a new gait cycle starts. For normal individuals, walking at a normal pace, the stance phase corresponds to about ∼62% of the entire gait cycle.[4]

Gait analysis can be referred to as the systematic examination of the locomotion, and it can be used in the evaluation of pretreatment, for surgical decisions and postoperative assessment of patients.[4] The distribution of the VGRF and plantar pressure on the surface of the foot during its contact with the ground provides valuable information regarding abnormal posture shifts, the spinal cord well-being, as well as the foot structure and condition.[7] Also, there are pathologies that can be related to an abnormal VGRF and plantar pressure, such as the high risk for ulceration in diabetic patients with high forefoot plantar pressure

*Address all correspondence to: Maria Fátima Domingues, E-mail: fatima.domingues@ua.pt

during gait.[8] Therefore, the accurate monitoring of the VGRF and plantar pressure distribution is vital to avoid and reduce the risk of such pathologies.

Additionally, for the rehabilitation robotics field, the development of a flexible insole pressure sensor, to measure and analyze force distribution on a patient's foot, would represent a real breakthrough. The possibility of having this information directly from a sensor could dramatically reduce the computational burden of exoskeletons' control strategy because currently it is estimated based on very complex biomechanical models.[9]

The dynamic and continuous monitor of gait parameters requires that the sensing mechanisms implemented are mobile, with limited or nonexistent wiring, preferably adaptable to a shoe, low cost, and with low power consumption.[10] Although a considerable number of solutions for plantar pressure have been already reported, they are mainly based on electronic or imaging devices, presenting some drawbacks such as fragility, instability, and inconsistent feedback.[10,11]

As an alternative to these electronic devices, optical-fiber-based sensors offer a smaller (diameter of several hundred micrometers), robust, minimally invasive, biocompatible, highly accurate, electromagnetic insensitive, electrical isolation (no electrical power at the measuring point), and a multiplexable solution, allowing several sensors into the same fiber cable.[12,13] The optical fiber technology is widely spread and used to monitor parameters, such as pressure, temperature, humidity, strain, refractive index, angular displacements, and acceleration, among others.[12–19] Also, optical fiber sensing technology has already been used to monitor static VGRF and plantar pressure values.[20–22] Nevertheless, to date, no reports on dynamic continuous measurements during gait have been presented.[21,22] On that note, the achievement of our work regarding the dynamic and continuous optical data acquisition during gait is of great significance for the field.

The proposed optical system architecture to monitor VGRF consists of a network of fiber Bragg grating (FBG) sensors incorporated into an insole, matching the sensing requirements mentioned before (mobile, with limited wiring, adaptable to a shoe, low cost, and low power consumption), allied to the high accuracy and all the advantages of optical fiber sensing.

The FBGs can be described as periodic perturbations of the refractive index of the fiber core along the longitudinal axis of the optical fiber. The grating structure can be induced by an ultraviolet (UV) laser, which is used to create a selective wavelength reflective structure that follows the Bragg condition.[14,15] The sensing principle relies on the monitoring of the wavelength reflected by the inscribed grating (λ_B-Bragg wavelength) and its variation as a function of the parameter under study (e.g., strain and/or temperature). The Bragg wavelength shift, $\Delta\lambda_B$, can be related to strain ($\Delta\varepsilon$) and/or temperature (ΔT) variations by the following:

$$\Delta\lambda_B = S_\varepsilon \times \Delta\varepsilon + S_T \times \Delta T, \tag{1}$$

where S_ε and S_T are the sensor sensitivities to strain and temperature variations, respectively. The first term is associated to the strain influence on λ_B, whereas the second term represents the temperature effect in the same parameter.[16]

After this initial introduction, in the following section (Sec. 2), the description of the insole design, production, assembling, and calibration are presented. Section 3 deals with the results and analysis of the data acquired during the testing of the developed solutions for VGRF monitoring. Finally, the main conclusions retrieved from this work are pointed out in the Sec. 4.

2 Insole Development and Production

In this section, the development and calibration of a new platform based on the optical fiber sensing technology to monitor the VGRF and plantar pressure during gait are presented. This solution can be used as a fixed platform or as an insole adaptable to a shoe.

2.1 Insole Incorporation of the Fiber Bragg Grating Network

The optical platform is composed of a cork sole, with 1.0-cm thickness, in which FBG sensors were incorporated in critical points of analysis [heel, midfoot, metatarsal, and toe areas, Fig. 1(a)] to monitor the VGRF,[10,23] as shown in Figs. 1(b) and 1(c).

The cork was the material chosen to embed the sensors due to its excellent properties for this application, namely thermal isolation, malleability, and a near-zero Poisson ratio.[24] The first is extremely relevant, once the body temperature may influence the FBGs sensing feedback. By using a thermal isolation material, no compensation is needed in the acquired Bragg
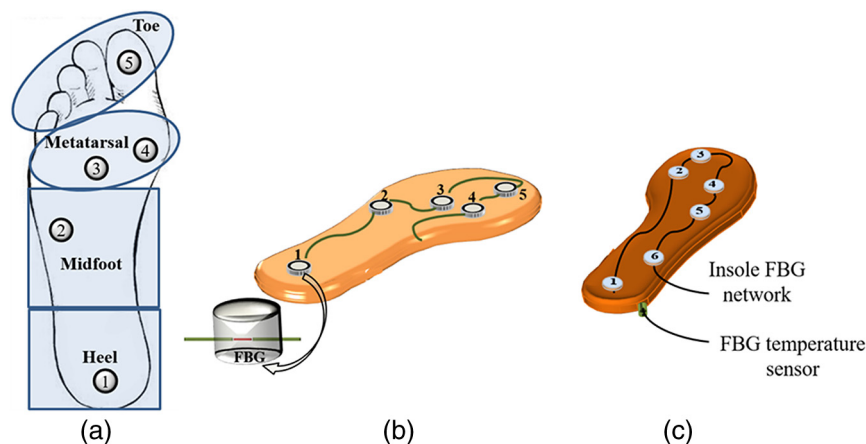

Fig. 1 Schematic representation of (a) the foot plantar main areas, (b) the sensors network implemented for a fixed platform, and (c) the sensors network implemented for the insole adapted in a shoe.
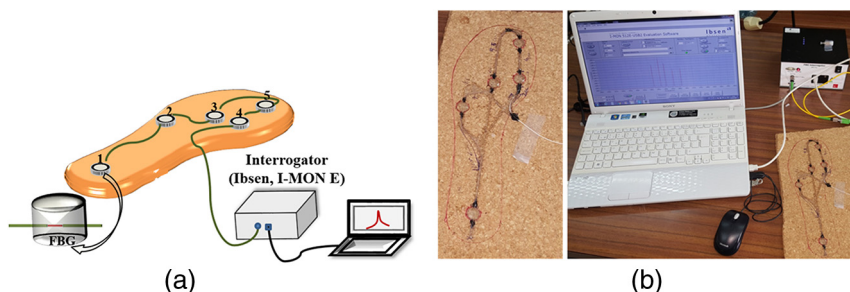
Fig. 2 Fixed platform monitoring system: (a) schematic representation and (b) photograph.

wavelength. Also, the malleable properties of the cork make it easy to incorporate the sensing elements in the required points of analysis, which additionally facilitates the sole implementation in any type of shoe configuration. Moreover, and although malleable to handle, it also provides the necessary resistance to prevent the optical fiber network to be damaged or broken during the gait movement. Finally, its near-zero Poisson ratio is an advantage to its use, once the pressure applied in one area of the plantar surface will not influence the other areas, allowing in that way to isolate the pressure points, preventing sensor's cross talk.[24]

The FBG sensing elements were inscribed and multiplexed into a GF1-photosensitive optical fiber (Thorlabs®) cable, using an UV KrF Bragg Star™ Industrial-LN pulsed KrF excimer laser operating at 248 nm, applying pulses with energy of 5 mJ and repetition rate of 500 Hz. Phase masks customized for 248-nm UV laser were chosen for the 1550-nm spectral region grating inscription (Ibsen Photonics). In order to protect and provide extra resistance to the optical fiber sensing elements, the FBGs were encapsulated in epoxy resin (Liquid Lens™) cylinder structures (1.0-cm diameter and 0.5-cm height). Each sensing element consists of such cylindrical epoxy structure with the FBG at the middle position. The entire FBG sensing network (epoxy structure included) was incorporated within the cork structures, in order to obtain a compact (no air gap within it) insole.

Two solutions were developed, one to be used as a fixed platform [Fig. 1(b)] containing five FBG-based sensors and another to act as an instrumented insole to be adapted into a shoe [Fig. 1(c)] with six FBG sensors. The second solution was intended to be able to monitor all the critical points[10,23] for VGRF analysis, but due to equipment restrictions, only six points were considered.

For the insole, an FBG temperature sensor was also inserted into the cork near the first sensing point. This procedure was implemented to guarantee that the sensing points are not influenced by any temperature change, and if they are, it can be properly compensated.

2.2 Monitoring System Assemble and Calibration

For the monitoring and calibration of both systems, the FBG sensing network was connected to a portable interrogation system constituted of a battery, a miniaturized broadband optical ASE module (B&A Technology Co., As4500), an optical circulator (Thorlabs, 6015-3), and an optical spectrometer (Ibsen, I-MON 512E-USB). The latter operates at a maximum rate of 960 Hz, with a wavelength resolution of 5 pm, responsible for the acquisition of the Bragg wavelength shift, which is

proportional to the vertical force applied on the sensing element points, as shown in Fig. 2.

Prior to its implementation for VGRF determination, the developed platform and insole were calibrated. This procedure was made with one load sequence on each isolated sensor. The contact area was of 1.0 cm (diameter of the loading prove used during the calibration process). For that purpose, different load values, ranging from 0 to 170 N, in 10-N steps increment, were induced in the FBG sensing elements, using a Shimadzu® AGS-5 kND mechanical test machine. The reflected Bragg wavelength shift of each FBG in the network was registered for each load value. The calibration values for the five sensing points in the fixed platform are presented in Fig. 3.

A linear dependence of the Bragg wavelength shift with the applied loads was obtained, with sensitivity coefficients ranging from 3.38 pm/N (FBG 4) to 11.06 pm/N (FBG 2). The differences in the strain sensitivities may be related to the methodology used to incorporate the FBGs in the insole. As the cork used is a porous material, different amounts of the epoxy resin may have infiltrated into its surroundings. Also, although major effort was made to keep all the FBGs at the same depth of the cylinder epoxy resin, some deviations might have occurred, due to the resin's initial liquid properties. Nonetheless, such facts do not influence the obtained final results, once all the sensing elements were independently calibrated. In future works, special attention will be given to this aspect.

The sensitivity coefficients, for each FBG sensor, in the platform and insole implementations, were later applied to retrieve
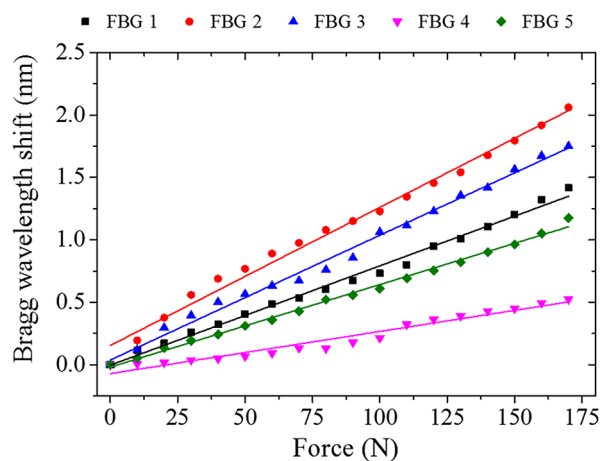

Fig. 3 Bragg wavelength shift as function of the applied vertical force. Points are correspondent to the experimental data and the lines to the linear fits ($0.953 < R^2 < 0.995$).

the vertical force value from the acquired Bragg wavelength shift data.

3 Vertical Ground Reaction Forces Platform Testing and Insole Integration

After the calibration, three sets of studies were implemented in order to verify the reliability of both the fixed platform and the insole developed.

3.1 Platform Testing

The VGRF induced in the sensing elements during a normal gait movement was analyzed with the platform fixed at the ground, as shown in Fig. 4. The response of each sensing element to the VGRF during a gait cycle was repeated and acquired five times. The feedback of the platform to the displacement of the BCM was also evaluated.

In Fig. 5, the acquired data are presented, from which it is possible to verify that the sensing network response is similar for the five passages, confirming the repeatability of the sensor's response.
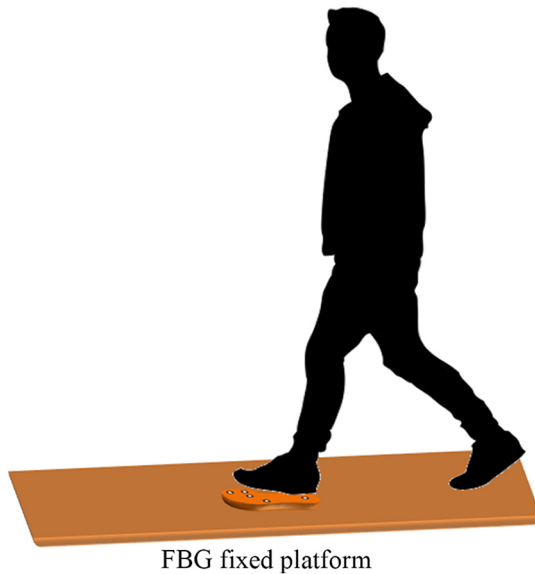
FBG fixed platform

Fig. 4 Schematic diagram of the protocol implemented for gait analysis using the fixed platform.
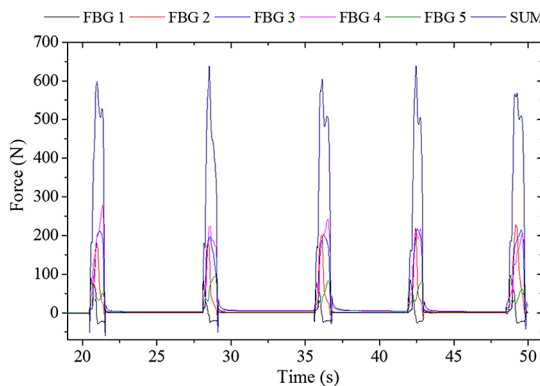
Fig. 5 VGRF obtained during the five steps and the resulting curve of all the sensors response sum for each step.

A detailed view of the stance period of the gait cycle is shown in Fig. 6. It is possible to retrieve the sequence in which the sensors are activated and the VGRF associated at each point under analysis. The observed maximum amplitude obtained for each sensor was temporally registered according to what is expected in a gait movement,[4] verifying a typical VGRF curve during the stance period of the gait cycle.[4]

The stance period is initiated when the heel touches the ground, HS; after the contact of the heel with the ground, the foot is moved toward a stable support position for the body in which the hip joint becomes aligned with the ankle joint; this phase is called midstance phase (MS). The purpose of the following movements is to propel the BCM forward, which is initiated by the rise of the heel (HR) and its loss of contact with the ground. In this movement, the last point of contact of the foot with the ground should be the toe at the moment known as the TO, which also corresponds to the end of the stance phase in a gait cycle.[4]

According to the layout of the sensing network, it can be observed that the beginning of the HS moment is marked by the FBG1 with greater response, which is expected, as this sensor is placed at the heel. This response is maintained until the MS stage (in which all the sensors are activated) finishes. It can also be verified that at the HR's initial moment, the VGRF values registered for the sensor FBG 1 considerably drop, and the most accentuated forces are registered for the sensors placed in the metatarsals areas (FBG 2, 3, and 4). Also, at this moment, the VGRF registered at the toe location by the sensor FBG 5 becomes more accentuated and hits its maximum as the toe becomes the last point of support in the stance phase at the TO stage.

From the positive feedback of the fixed platform during the performed tests, it becomes evident that the method implemented is an adequate solution for VGRF monitoring during gait. Moreover, from the analysis of the forces registered during the stance phase, it is also possible to infer and monitor the plantar pressures of individuals.[4,10,23]

The BCM displacements, in the body sagittal and frontal planes of motion, were also analyzed using the same platform. For that purpose, an 85-kg male, was asked to place his foot on the sensing platform and to execute a series of BCM movements (with a 5-s duration each), starting by standing still with the BCM centered (C), followed by an anterior (A) position and
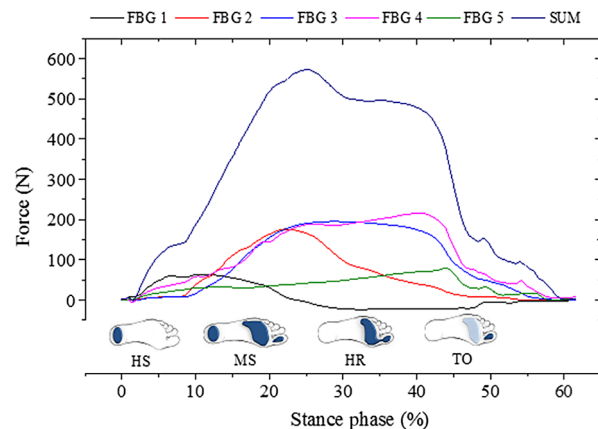

Fig. 6 Average VGRF obtained during the stance period (62%), from the individual steps analyzed (the regions of the foot touching the platform in each gait step are in dark blue).
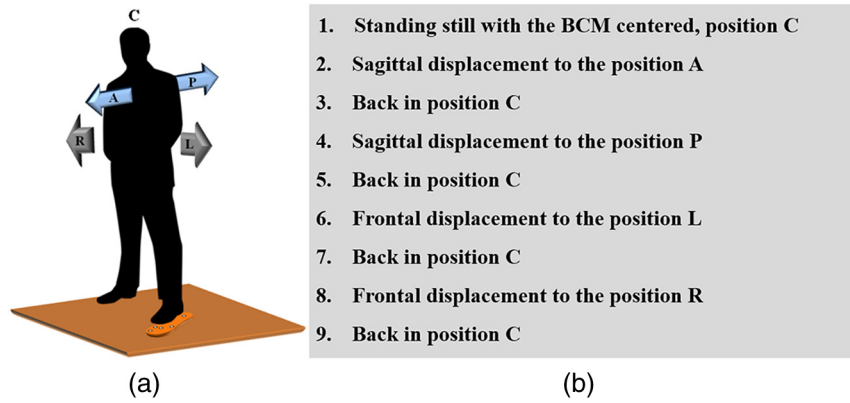
1. **Standing still with the BCM centered, position C**
2. **Sagittal displacement to the position A**
3. **Back in position C**
4. **Sagittal displacement to the position P**
5. **Back in position C**
6. **Frontal displacement to the position L**
7. **Back in position C**
8. **Frontal displacement to the position R**
9. **Back in position C**

(a)   (b)

Fig. 7 (a) Schematic diagram of the protocol implemented for the analysis of the BCM displacement (sagittal and frontal displacements in blue and gray, respectively) and (b) descriptive protocol (the subject remained in each position for 5 s).

then back to the original position (C) from which goes to posterior (P) position and then resting again at the center (C). After the sagittal displacement, a frontal displacement was executed, in which the subject moved the BCM first to the left (L), back in the center (C) and then to the right (R), and finally back in the center (C). In Fig. 7, the implemented protocol is schematized.

During the protocol implementation, the Bragg wavelength shift induced in the sensing network was acquired and the corresponding VGRFs were retrieved. Figure 8 presents the response of each sensor, during the different moments of the tests performed.

In the anterior movement, an increase of the vertical forces registered by the sensors positioned in the metatarsal and toe areas is evident, while the sensor placed in the heel section indicates a decrease of the VGRF. On the other hand, during the posterior displacement of the BCM, the VGRF at the heel area is more accentuated, while the force values at the toe and metatarsal areas decrease.

Regarding the centered position of BCM (C), the areas that are mostly actuated in the platform are the metatarsal and midfoot areas, indicating that those zones are the more pressed ones in the ground in the sustainment of the subject's body weight, while standing.

The behavior monitored by the FBGs network is within the expected; hence, in the anterior movement of the BCM, the body weight will be mainly distributed by the metatarsal and toe areas, while in the posterior movement, it will be mostly supported by the heel area.

Regarding the frontal plane displacements, the sensors located at the extremities of the platform (FBG 2 and 4) should be the ones presenting a higher variation of the VGRF. In fact, it is noticeable that during such movements, the sensor placed in position 2 registers the increase of vertical force, when the BCM is displaced to the left, while the sensor placed in position 4 shows a similar behavior when the BCM is moved to the right. Regarding the sensors positioned at the central of the metatarsal
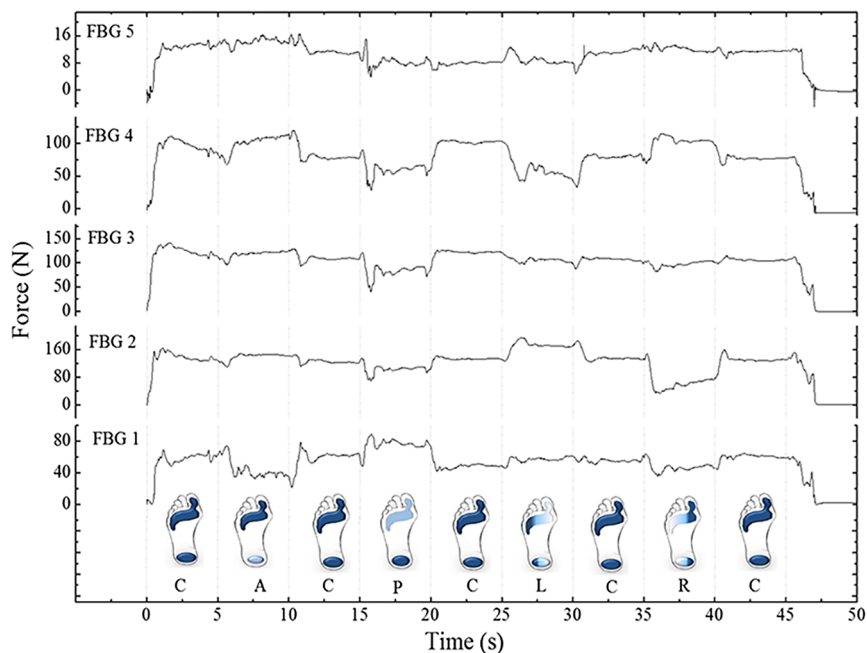

Fig. 8 Representation of the vertical forces detected during the BCM displacements [the VGRF intensity on each foot location is colored, in the scheme, from light (less intensity) to dark (more intense) blue].

area, the value registered through the frontal protocol implementation is mostly constant, which indicates that in such BCM displacement, the vertical force is mostly shifted between the left and the right metatarsal areas.

3.2 Instrumented Shoe

In order to perform a dynamic and autonomous VGRF monitoring during gait, an insole with six FBG sensors network was designed and adapted to a shoe, as shown in Fig. 9.

In addition to the sensing network for VGRF monitoring, an FBG temperature sensor[16] was also adapted to the insole in order to monitor the temperature variations and guarantee that the Bragg wavelength shift registered during the gait cycles is only the result of the VGRF actuating on the sensing elements. In fact, due to the cork thermal isolation characteristics,[24] it is expected that the body temperature will not influence the Bragg wavelength shift of the sensing network, once its sensing elements are placed within the cork sole and not in direct contact

with the body. The wavelength shift values obtained for the temperature sensor confirms what was previously stated, as its value remained constant during the gait cycles experiments, as presented in Fig. 10.

Regarding the gait cycles analysis, the subject, in this case, a 45-kg female, was instructed to walk in a normal pace, during which the Bragg wavelength was acquired by the interrogation system. In Fig. 10, the vertical forces, registered in the insole sensing network for three gait cycles, are presented, in addition to the temperature recorded during the test.

Similar to the behavior registered in the fixed platform (Sec. 3.1), the elements initially actuated are the ones placed within the heel area (FBG 1 and 6), followed by the metatarsal area (FBG 5, 4, and 2) and ending with the element within the toe area (FBG 3) at the conclusion of the stance phase.

Also, from the gait cycles monitoring, the different phases in the gait cycle, namely the stance phase that characterizes ~68% of the gait cycle for the subject tested, and the swing phase, during which the foot is not in contact with the ground, are clearly
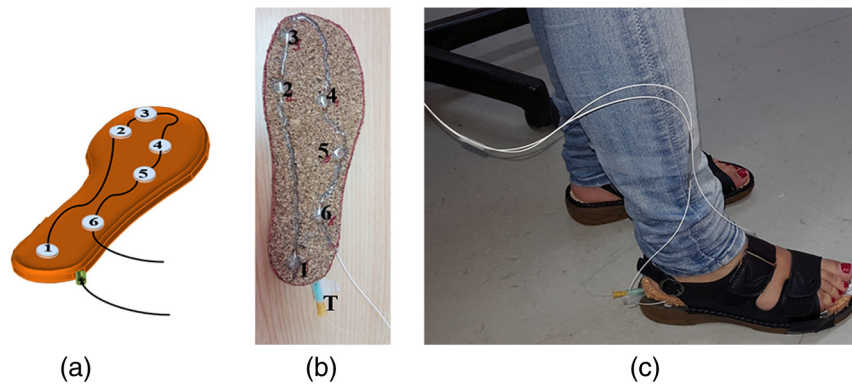

(a)　　　　　　　　(b)　　　　　　　　(c)

Fig. 9 (a) Schematic representation of the designed insole, (b) photograph of the insole with the sensing network and temperature sensor, and (c) photograph of the instrumented shoe.
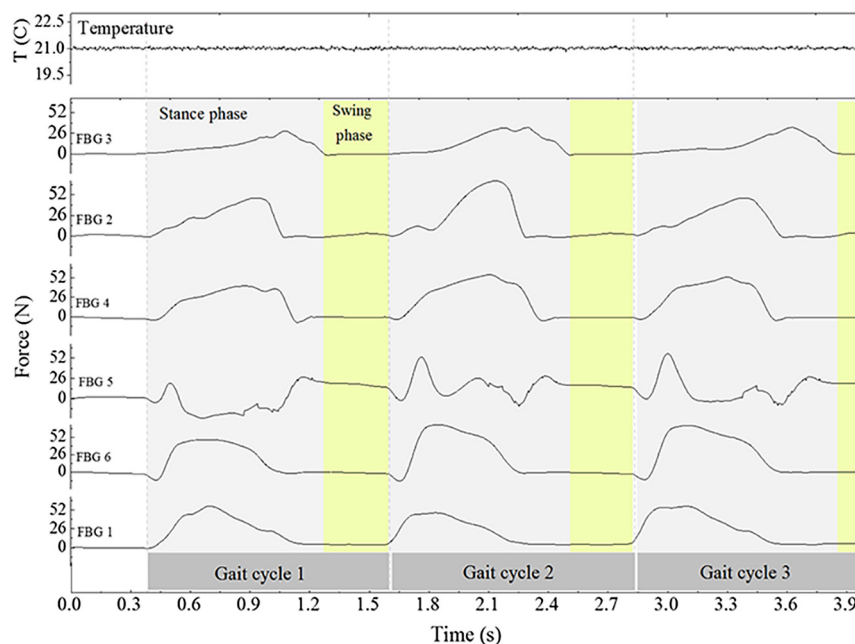

Fig. 10 Temperature and the vertical forces registered in the insole sensing network for three gait cycles.

distinguished. During the latter phase, the VGRF is not present, and therefore, the Bragg wavelength shift of all the sensing elements is mostly constant during that phase.

4 Conclusion

In this work, an optical fiber sensing architecture to monitor the VGRF induced in the foot plantar surface during gait and BCM displacements is presented. The paper shows the design and implementation of a platform with a five FBGs network, placed in key points to monitor the VGRF on the foot surface during gait cycles and the BCM displacements. Also, an insole instrumented with a six FBGs network was designed and implemented within a shoe for dynamic monitoring of gait.

The calibration and laboratory measurements for both solutions are presented. The results obtained demonstrate the accuracy and reliability of the proposed systems to monitor the VGRF during the tests implemented. Moreover, due to the reduced size and resilience of the sensing network, the proposed solutions are a noninvasive tool to monitor the vertical forces induced on the foot plantar surface without impairing the mobility of the user.

The analysis of the vertical forces distribution can provide important data toward the foot plantar pressure mapping, which enables inferring vital information with regards to the foot structure and health condition, in addition to the detection of any anomaly related to the spinal function. Moreover, such plantar pressure mapping can be also applied in the detection of high-risk alerts related to pathologies, such as the foot ulceration in patients with diabetes. Additionally, the development of a flexible insole pressure sensor for the rehabilitation robotics field would represent a real advance in the monitor and analysis of a patient's foot force distribution allowing to considerably reduce the computational burden of exoskeletons' control strategy, currently based on very complex biomechanical models. The proposed noninvasive solution represents a step forward in the field of e-Health toward providing continuous and close monitoring of impaired patients and/or elder citizens, while maintaining their mobility and without compromising their life quality or their daily activities.

Disclosures

The authors have no relevant financial interests in the paper, and no other potential conflicts of interest to disclose.

Acknowledgments

References

1. World Health Organization, "World report on ageing and health," 2015, http://www.who.int/ageing/publications/world-report-2015/en/ (February 2017).
2. I. Korhonen, J. Parkka, and M. Van Gils, "Health monitoring in the home of the future," *IEEE Eng. Med. Biol. Mag.* **22**(3), 66–73 (2003).
3. M. P. de Castro et al., "In-shoe plantar pressures and ground reaction forces during overweight adults' overground walking," *Res. Q. Exercise Sport* **85**(2), 188–197 (2014).
4. T. Marasović, M. Cecic, and V. Zanchi, "Analysis and interpretation of ground reaction forces in normal gait," *WSEAS Trans. Syst.* **8**(9), 1105–1114 (2009).
5. C. Kim and J. Eng, "Symmetry in vertical ground reaction force is accompanied by symmetry in temporal but not distance variables of gait in persons with stroke," *Gait Posture* **18**(1), 23–28 (2003).
6. J. Perry, *Gait Analysis: Normal and Pathological Function*, p. 524, Slack, Inc., Thorofare, New Jersey (1992).
7. R. J. Abboud, "(i) Relevant foot biomechanics," *Curr. Orthop.* **16**(3), 165–179 (2002).
8. E. Morag and P. R. Cavanagh, "Structural and functional predictors of regional peak pressures under the foot during walking," *J. Biomech.* **32**(4), 359–370 (1999).
9. C. Bayón et al., "Locomotor training through a novel robotic platform for gait rehabilitation in pediatric population: short report," *J. NeuroEng. Rehabil.* **13**(1), 98 (2016).
10. A. Razak et al., "Foot plantar pressure measurement system: a review," *Sensors* **12**(7), 9884–9912 (2012).
11. T. Sim et al., "Predicting complete ground reaction forces and moments during gait with insole plantar pressure information using a wavelet neural network," *J. Biomech. Eng.* **137**(9), 091001 (2015).
12. P. Roriz et al., "From conventional sensors to fibre optic sensors for strain and force measurements in biomechanics applications: a review," *J. Biomech.* **47**(6), 1251–1261 (2014).
13. D. J. Webb et al., "First in-vivo trials of a fiber Bragg grating based temperature profiling system," *J. Biomed. Opt.* **5**(1), 45–50 (2000).
14. P. Antunes et al., "Biaxial optical accelerometer and high-angle inclinometer with temperature and cross-axis insensitivity," *IEEE Sens. J.* **12**(7), 2399–2406 (2012).
15. C. Leitão et al., "Feasibility studies of Bragg probe for noninvasive carotid pulse waveform assessment," *J. Biomed. Opt.* **18**(1), 017006 (2013).
16. N. Alberto et al., "Optical fiber technology for eHealthcare," in *Handbook of Research on ICTs and Management Systems for Improving Efficiency in Healthcare and Social Care*, pp. 180–200, IGI Global, Hershey (2013).
17. N. Alberto et al., "Three-parameter optical fiber sensor based on a tilted fiber Bragg grating," *Appl. Opt.* **49**(31), 6085–6091 (2010).
18. G. Wehrle et al., "A fibre optic Bragg grating strain sensor for monitoring ventilator movements," *Meas. Sci. Technol.* **12**(7), 805–809 (2001).
19. H. J. Kalinowski et al., "Application of fibre Bragg grating sensors in biomechanics," in *Chapter in Trends in Photonics 2010*, J. Canning, Ed., pp. 315–343, Research Signpost , Kerala, India (2010).
20. J. Z. Hao et al., "Design of a foot-pressure monitoring transducer for diabetic patients based on FBG sensors," in *16th Annual Meeting of the IEEE Lasers and Electro-Optics Society (LEOS '03)*, Vol. 1 (2003).
21. T. C. Liang, J. J. Lin, and L. Y. Guo, "Plantar pressure detection with fiber Bragg gratings sensing system," *Sensors* **16**(10), 1766 (2016).
22. R. Suresh et al., "Development of a high resolution plantar pressure monitoring pad based on fiber Bragg grating (FBG) sensors," *Technol. Health Care* **23**(6), 785–794 (2015).
23. S. C. Wearing et al., "A comparison of gait initiation and termination methods for obtaining plantar foot pressures," *Gait Posture* **10**(3), 255–263 (1999).
24. S. P. Silva et al., "Cork: properties, capabilities and applications," *Int. Mater. Rev.* **50**(6), 345–365 (2005).

Maria Fátima Domingues received her PhD in physics engineering from the University of Aveiro, Portugal, in 2014 and she is currently

a research fellow at the Instituto de Telecomunicações-Aveiro, I3N-Physiscs Department, University of Aveiro, Portugal and Consejo Superior de Investigaciones Científicas (CSIC)-Madrid, Spain holding postdoc grant from the Fundação para a Ciencia e a Tecnologia (FCT-Portugal). Her current research interests include new solutions of optical fiber sensors and its application in robotic exoskeletons and e-Health.

Cátia Tavares received her master degree in physics engineering from the University of Aveiro, Portugal in 2016. She is currently working as a researcher fellow at the Instituto de Telecomunicações-Aveiro and I3N-Physiscs Department, University of Aveiro, Portugal. Her current research interests include de development of optical fiber sensors for eHealth solutions and its application in physical rehabilitation.

Cátia Leitão received her MS degree in biomedical engineering, specialization in biomedical instrumentation and biomaterials, from University of Coimbra in 2010. From 2010 to 2012 she was research fellow, and from 2013 to 2016, PhD student in physical engineering in University of Aveiro. Currently, she is a postdoctoral researcher at I3N & Physics Department of University of Aveiro, Portugal. Her main research interests are optical fiber sensors applied to noninvasive cardiovascular monitoring, mainly in arterial pulse waveform acquisition and its implications on cardiovascular risk assessment.

Anselmo Frizera-Neto received his BS degree in electrical engineering from the Federal University of Espirito Santo UFES, Brazil, in 2006 and his PhD in electronics from the Universidad de Alcalá, Spain, in 2010. From 2006 to 2010, he was a researcher with the Bioengineering Group, Spanish National Research Council. He is currently a lecturer and researcher at the Electrical Engineering Department, UFES. His research interests include rehabilitation robotics, human–machine interaction, optical fiber sensors and movement analysis.

Nélia Alberto graduated with the degree in physics and chemistry from University of Aveiro, Portugal, in 2005. She received her PhD in physics from the same university in 2011. She is currently working as a postdoctoral researcher at the Instituto de Telecomunicações and Centre for Mechanical Technology and Automation in Aveiro. Her main research interests include the study, development and application of optical fiber based devices for sensing applications.

Carlos Marques received the PhD in physics engineering from the University of Aveiro, Portugal, in 2013. He was a Marie Curie fellow in the AIPT, Aston University, Birmingham, U.K from 2014 to 2016. Currently, he is a research fellow in the Instituto de Telecomunicações and Physics Department & I3N, University of Aveiro, Portugal. He authored or coauthored more than 85 journal and conference technical papers with emphasis on optical communications and sensing using optical fiber technology.

Ayman Radwan received his PhD from Queen's University, Canada, in 2009. He is a senior research engineer (Investigador Auxiliar) with the Instituto de Telecomunicações. He is mainly specialized in co-ordination and management of EU funded projects. He participated in the coordination of multiple EU projects. He is currently the project coordinator of CELTIC+ project "MUSCLES", as well as participating in the coordination of the ITN-SECRET. His research interests include IoT, 5G, and green communications.

Jonathan Rodriguez received his masters degree in electronic and electrical engineering and PhD from the University of Surrey UK, in 1998 and 2004 respectively. Since 2005, he is a researcher at the Instituto de Telecomunicacoes, Portugal. He is author of more than 300 scientific works, and his professional affiliations include: senior member of the IEEE and chartered engineer (CEng) since 2013, and fellow of the IET (2015).

Octavian Postolache is assistant professor at ISCTE-Lisbon University Institute and senior researcher at Instituto de Telecomunicacoes. He received his PhD in 1999 in electrical engineering from "Gh. Asachi" Technical University of Iasi and the habilitation from Instituto Superior Tecnico, Lisbon, in 2016. He is an IEEE IMS distinguished lecturer, IEEE IMS Portugal chair and IMS TC-13 chair. His fields of interests are smart sensors for biomedical and environmental applications, pervasive computing for healthcare, WSN and IoT, and advanced signal processing for biomedical applications.

Eduardo Rocon received his PhD from the Universidad Politécnica de Madrid in 2006. His research activity was awarded with the Georges Giralt PhD award as the best PhD robotics thesis in Europe and the EMBEC scientific award. He is current a tenure researcher at the Bioengineering Group at the Consejo Superior de Investigaciones Científicas (CSIC). His research interests include rehabilitation, neurophysiology, biomechanics, adaptive signal processing, and human machine interaction.

Paulo André received his PhD in physics, and the Agregação title (habilitation) degree from the Universidade de Aveiro, Portugal, in 2002 and 2011, respectively. He joined the Instituto Superior Técnico, University of Lisbon, in 2013, as an associate professor, lecturing on telecommunications. He is an IEEE senior member and his research interests include the study /simulation of photonic and optoelectronic components, optical sensors, integrated optics, photonic graphene applications, multiwavelength optical communications systems, and passive optical networks.

Paulo Antunes received his PhD in physics engineering from the Aveiro University, Portugal, in 2011. He is currently an assistant researcher at the I3N-Aveiro (Institute of Nanostructures, Nanomodelling and Nanofabrication), he is also with the University of Aveiro Physics Department and the Instituto de Telecomunicações. His current research interests include the study and simulation of fiber Bragg gratings, data acquisition, optical sensing solutions for static and dynamic applications, including medical and structural monitoring.

MANUSCRIPT 3

sensors

MDPI

Article

Gait Shear and Plantar Pressure Monitoring: A Non-Invasive OFS Based Solution for e-Health Architectures

Cátia Tavares [1,2,*], M. Fátima Domingues [1,3], Anselmo Frizera-Neto [4], Tiago Leite [2], Cátia Leitão [1,2], Nélia Alberto [1], Carlos Marques [1], Ayman Radwan [1], Eduardo Rocon [3], Paulo André [5] and Paulo Antunes [1,2]

[1] Instituto de Telecomunicações, Campus Universitário de Santiago, Aveiro 3810-193, Portugal; fatima.domingues@ua.pt (M.F.D.); catia.leitao@ua.pt (C.L.); nelia@ua.pt (N.A.); carlos.marques@ua.pt (C.M.); aradwan@av.it.pt (A.R.); pantunes@ua.pt (P.A.)

[2] Department of Physics & I3N, University of Aveiro, Campus Universitário de Santiago, Aveiro 3810-193, Portugal; tmpl@ua.pt

[3] CSIC-UPM, Ctra. Campo Real, Arganda del Rey 28500, Madrid, Spain; e.rocon@csic.es

[4] Telecommunications Laboratory, Electrical Engineering Department, Federal University of Espírito Santo, Espírito Santo 29075-910, Brazil; frizera@ieee.org

[5] Department of Electrical and Computer Engineering and Instituto de Telecomunicações, Instituto Superior Técnico, University of Lisbon, Lisbon 1049-001, Portugal; paulo.andre@lx.it.pt

* Correspondence: catia.tavares@ua.pt; Tel.: +351-234-377-900

check for updates

Gait Shear and Plantar Pressure Monitoring: A Non-Invasive OFS Based Solution for e-Health Architectures

Cátia Tavares [1,2,*] , M. Fátima Domingues [1,3], Anselmo Frizera-Neto [4] , Tiago Leite [2], Cátia Leitão [1,2] , Nélia Alberto [1] , Carlos Marques [1] , Ayman Radwan [1] , Eduardo Rocon [3] , Paulo André [5] and Paulo Antunes [1,2]

[1] Instituto de Telecomunicações, Campus Universitário de Santiago, Aveiro 3810-193, Portugal; fatima.domingues@ua.pt (M.F.D.); catia.leitao@ua.pt (C.L.); nelia@ua.pt (N.A.); carlos.marques@ua.pt (C.M.); aradwan@av.it.pt (A.R.); pantunes@ua.pt (P.A.)

[2] Department of Physics & I3N, University of Aveiro, Campus Universitário de Santiago, Aveiro 3810-193, Portugal; tmpl@ua.pt

[3] CSIC-UPM, Ctra. Campo Real, Arganda del Rey 28500, Madrid, Spain; e.rocon@csic.es

[4] Telecommunications Laboratory, Electrical Engineering Department, Federal University of Espírito Santo, Espírito Santo 29075-910, Brazil; frizera@ieee.org

[5] Department of Electrical and Computer Engineering and Instituto de Telecomunicações, Instituto Superior Técnico, University of Lisbon, Lisbon 1049-001, Portugal; paulo.andre@lx.it.pt

* Correspondence: catia.tavares@ua.pt; Tel.: +351-234-377-900

Abstract: In an era of unprecedented progress in sensing technology and communication, health services are now able to closely monitor patients and elderly citizens without jeopardizing their daily routines through health applications on their mobile devices in what is known as e-Health. Within this field, we propose an optical fiber sensor (OFS) based system for the simultaneous monitoring of shear and plantar pressure during gait movement. These parameters are considered to be two key factors in gait analysis that can help in the early diagnosis of multiple anomalies, such as diabetic foot ulcerations or in physical rehabilitation scenarios. The proposed solution is a biaxial OFS based on two in-line fiber Bragg gratings (FBGs), which were inscribed in the same optical fiber and placed individually in two adjacent cavities, forming a small sensing cell. Such design presents a more compact and resilient solution with higher accuracy when compared to the existing electronic systems. The implementation of the proposed elements into an insole is also described, showcasing the compactness of the sensing cells, which can easily be integrated into a non-invasive mobile e-Health solution for continuous remote gait monitoring of patients and elder citizens. The reported results show that the proposed system outperforms existing solutions, in the sense that it is able to dynamically discriminate shear and plantar pressure during gait.

Keywords: gait analysis; e-Health application; physical rehabilitation; shear and plantar pressure sensor; biaxial optical fiber sensor; multiplexed fiber Bragg gratings

1. Introduction

Between 2015 and 2050, the world's population aged over 60 years is expected to double from about 12% up to 22% (up to about 2 billion), with the group aged 80 years and over growing most rapidly (predictably will quadruple from approximately 100 million to 434 million people) [1]. Many elderly and patient groups experience varying degrees of mobility impairments, which require closer monitoring. Assistive devices play a pivotal role in their lives and have a great impact on their ability

to live independently and perform basic daily tasks. The assistive products market is set to expand significantly in response to the ageing population and disability trends, with a global market for home medical equipment expected to grow from \$27.8 billion in 2015 to nearly \$44.3 billion by 2020 [2]. This growing demand for e-Health solutions will improve healthcare services and quality of life by providing autonomy and mobility during daily activities.

Non-invasive continuous monitoring of an individual's health conditions, rehabilitation status, or assistance appears as a natural evolution of current healthcare services by providing patients with continuous remote support when required while guaranteeing autonomy and free mobility. Following this direction and towards improving the quality of life of physically impaired citizens by increasing their mobility, our team has been working on different practical solutions for the continuous remote monitoring of patients [3–5].

The monitoring and analysis of the shear and plantar pressure involved in gait is crucial for the evaluation of patients under physical rehabilitation processes, as well as for the control of rehabilitation exoskeletons in order to correct abnormal plantar pressures due to the uneven load distribution resulting from poor foot sensitivity [6,7]. Moreover, shear in particular, plays a major role in the diagnosis of foot ulceration in diabetic patients. The existence of shear forces presupposes friction between the skin-foot and the shoe. An abnormal increase of shear forces in a given plantar area can cause callosities or the so-called pressure ulcers. This health condition can occur when the tissue is compressed under pressure during gait/walk. Diabetic patients tend to lose sensitivity in the extremities of the body and the feet are one of the most affected areas. By losing sensitivity in the foot plantar areas, the patient involuntarily begins to modify the gait pattern and to adopt less correct postures that lead to the appearance of wounds, which due to their insensitivity in most cases are discovered late. An early discovery of irregularities in the gait pattern of individuals at risk is the first step in reducing the occurrence of ulceration and its treatment. Although shear stress has been identified as a pathogenic factor in the development of plantar ulcers, due to a lack of validated shear stress sensing devices, only studies related to plantar pressures are widely reported [6]. During the last few decades some methods have been proposed for the measurement of plantar shear stress [6], nonetheless, there is a lack of systems able to accurately monitor shear and plantar pressure simultaneously during gait. The work reported in this paper intends to fill such a gap while providing an ambulatory solution based on state-of-the-art optical fiber sensing technology able to be integrated as an enabler in e-Health architectures.

As a first step, we have developed a non-invasive solution for the continuous remote monitoring of foot plantar pressure during gait (walking). Our previous efforts have concentrated on pressure distribution through a strategically placed network of optical fiber sensors (OFSs) [3–5]. In the present work, we take a step forward by presenting the design and implementation of a fiber Bragg grating (FBG)-based platform for the simultaneous measurement of shear force (F_S) and vertical force (F_V), which can be useful in various applications in addition to e-Health. The proposed architecture comprises a compact and accurate biaxial OFS-based on two in-line FBGs (FBG1 and FBG2) placed individually in two adjacent cavities. For the demodulation of the optical signal registered by the designed optical sensing cell, a system of two equations was used, correlating the sensitivities of both FBGs with the F_V and F_S forces [8]. Moreover, we also present the design and integration of the sensing architecture in an insole for continuous monitoring of F_S and F_V (from which is calculated the plantar pressure), during the gait movement of patients.

The rest of this paper is organized as follows. Section 2 provides a survey of the state-of-the-art technology in monitoring shear and vertical forces, highlighting the advantages of the proposed solution. Section 3 introduces the design and calibration of the sensors and the implemented experimental protocols. Section 4 showcases the implantation of five sensing cells in an insole for gait analysis purposes. Section 5 discusses a potential e-Health architecture based on optical fiber sensors for gait analysis. The conclusion is drawn in Section 6.

2. Related Work

Vertical force sensors are nowadays required for a wide number of applications in diverse areas such as industrial production and structural health monitoring, artificial intelligence, robotic exoskeletons, and other health applications [3–5,9–16]. There are several types of F_V sensors, which are characterized essentially by the transduction mechanisms and technology used for converting forces into electrical signals, such as piezo resistivity and capacitance [11,14–16]. In addition to these electronic mechanisms, other transduction methods, such as OFSs are frequently used for the measurement of these type of forces [3–5,17].

Apart from the F_V sensors, devices with additional sensing properties, such as temperature and shear, are highly desired in equipment for medical applications. Specifically, sensors capable of simultaneously measuring F_V and F_S are highly required for the haptic perception of robotic hands, prosthetic skin, and to monitor the stress under the foot to prevent its ulceration [3–6,18–23].

Several studies have been published, using different technologies for the simultaneous sensing of F_V and F_S, namely strain gauge technology [21,24], piezoelectric materials [22,25], capacitive sensors [26], micro strip antennas, and coils [27] to name a few. All these types of sensors have the great disadvantage of using electricity at the point of contact with the user of the equipment, non-immunity to electromagnetic radiation, and thus require the use of several electric cables, usually one for each sensor cell, when multiple points are monitored simultaneously. As an example of the drawbacks presented by electronic devices, the sensor developed by Chen et al. can only be used as a static equipment because, despite having a small detection area of 1.9 cm × 1.9 cm, the overall structure of the sensor is very large [24]. In the work presented by Heywood et al., problems with the electrical insulation of the four layers that constitute the sensor to avoid the short circuits were reported [26]. Also, the work developed by Moahmmad et al. has limitations on the maximum pressure that it can withstand, which is about 0.25 psi [27]. In this context, OFSs appear as an alternative technology to sense these variables, with several advantages over their electronic counterparts. Such advantages include their immunity to electromagnetic interference, remote operation and sensing capability, small dimensions, lightweight, and geometrical versatility, making the technology increasingly used as sensing devices in several areas, with special significance in the biomedical engineering and biomechanics areas [3–5,9,28,29].

Although few, there are already some works reporting the development of optical fiber based F_V and F_S sensors. In 2000, Koulaxouzidis et al. demonstrated that three optical fibers with one FBG each (one on the horizontal and the other two on the diagonals), embedded in a block of solid elastomer, could be used for the measurement of in-shoe shear stress [30]. The Bragg wavelength shift was found to be almost linear under shear stress, in the range between −120 kPa and 120 kPa, yielding to a sensitivity of 4.35 pm/kPa. In 2013, Zhang et al. used a similar method to produce a sensor for the measurement of the same parameters. However, in this case only two optical fibers with FBGs were used (one on the horizontal and the other on the diagonal directions), embedded in a soft polydimethylsiloxane matrix [8]. The sensitivities achieved were 0.82 pm/Pa for vertical pressure and 1.33 pm/Pa for shear. Moreover, in 2005, Wang et al. used a different sensing mechanism, consisting of an array of optical fibers, lying in perpendicular rows and columns separated by elastomeric pads [31]. In their design, the measurements of plantar and shear pressures are based on intensity attenuation in the fibers due to physical deformation. The pressure measurement relies on the force induced light loss from the two affected crossing fibers, while the shear measurement depends on relative position changes in these pressure points between the two fiber mesh layers. This method was later used by other researchers [32–34], where they tried to improve the quality of the obtained data, but still with the disadvantage of a high number of fibers for each measuring point, hence its high complexity and large sensor size.

Although some previous efforts reported the use of OFSs, all those works have used complex designs with more than one optical fiber, which increases their fragility and lowers their application feasibility.

With the aim of reducing the complexity of the sensing device without compromising its performance, we present the design and implementation of an FBG-based sensor for simultaneous measurement of F_V and F_S. Our proposed solution stands out from previously reported ones because of the minimalism of the sensor structure and its accurate feedback. In an insole with several points of analysis it is important to use the least invasive technology possible, to reduce the amount of fiber inside the insole (with a limited size and thickness), and decrease the number of fracture and possible rupture points along the fiber. As this detection method has the ability to multiplex several sensors in the same fiber, it was possible to design an insole with several points of analysis using only one optical fiber.

3. Sensing Cell Design and Implementation

3.1. Sensing Cell Design

In the designed architecture, we used a sensing system comprising two multiplexed FBGs with a 2 mm-length, FBG1 and FBG2, spaced by 9 mm, inscribed in a photosensitive optical fiber (GF1, Thorlabs® Newton, NJ, USA), using the phase mask method with a UV KrF pulsed excimer laser (Bragg StarTM Industrial-LN, Coherent, Dieburg, Germany) operating at 248 nm. A 5 mJ pulse energy was applied with a repetition rate of 500 Hz. The central Bragg wavelength of the FBGs is 1560.9 nm and 1557.6 nm, for FBG1 and FBG2, respectively.

The optical fiber containing the multiplexed FBGs was incorporated in a small cell (9.0 mm × 16.0 mm × 5.5 mm) composed by two cavities, as shown in Figure 1. The cavity in which the FBG1 was placed (cavity 1) was mechanically isolated with a cork wall with a thickness of 2 mm, while the cavity containing the FBG2 (cavity 2) was designed and 3D printed with a hard polymer (polylactic acid, PLA) with a 1.2 mm thick wall. To protect the optical fiber and provide the necessary robustness to the sensing cell, both cavities were then filled with a thermosetting epoxy resin [17], which becomes a semi-rigid structure bounded to the optical fiber, after the curing process. Despite the epoxy resin stiffness, the applied F_V and F_S still induce deformation in the cell area and consequently in the optical fiber sensors without compromising their feedback. It should be noted that no bonding points were added in the cross section between the optical fiber and the cavities' boundaries. In that way, a vertical force applied in the cell top area will compress the epoxy resin vertically, inducing the stretching of the fiber embedded in its interior. On the other hand, a horizontal force, applied along the longitudinal axis of the fiber (left to right on the image), will compress the resin and the fiber containing the sensors against the PLA hard wall.
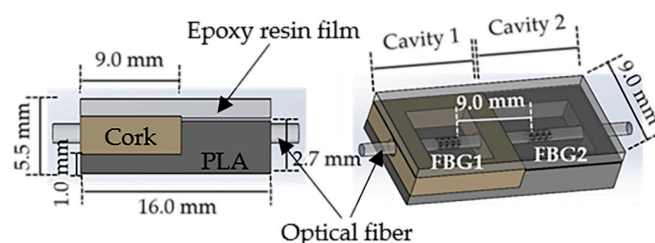

Figure 1. Schematic illustration of the designed sensing cell for simultaneous vertical forces (F_V) and shear forces (F_S) measurement.

Due to its near zero Poisson coefficient [35], the cork walls in cavity 1 provide the necessary mechanical isolation from lateral forces (applied out of the sensing cell area), while, simultaneously, offering the necessary elasticity for the FBG1 to be actuated under vertical forces and longitudinal shear stresses.

Additionally, in order to induce different sensitivities in the FBGs, the walls of cavity 1 were designed to be slightly higher than the walls of cavity 2 (gap of 0.8 mm), and in that way, the response

obtained from FBG1 can be enhanced when compared with the FBG2, since the latter is more concealed due to the hard polymer wall. To make the contact area uniform, a 2 mm thick layer of epoxy resin was placed on the top of the sensing cell, as shown in Figure 1.

3.2. Calibration and Performance Testing Methodology

The optical sensing cell feedback is processed in terms of the Bragg wavelength shift ($\Delta\lambda$). The dependence of this parameter with the strain variations ($\Delta\varepsilon$) can be translated by Equation (1) [4]:

$$\Delta\lambda = K_\varepsilon . \Delta\varepsilon \tag{1}$$

where K_ε is the sensor sensitivity to strain variations.

For the demodulation of the reflected optical signal, it was necessary to calibrate each FBG, independently, to F_V and F_S. To do so, a 3-axial electronic force sensor, composed of one biaxial (MBA400, Futek, Irvine, CA, USA) and one uniaxial (TPP-3/75, Transdutec, Barcelona, Spain) unit was used. The designed optical fiber based sensing cell (designated hereinafter as FBGs cell) was firmly attached to the three-axial sensing unit in order to guarantee that any perturbation induced in the FBGs cell would be also registered by the electronic sensing mechanism. Figure 2 is a schematic representation of the experimental setup implemented.
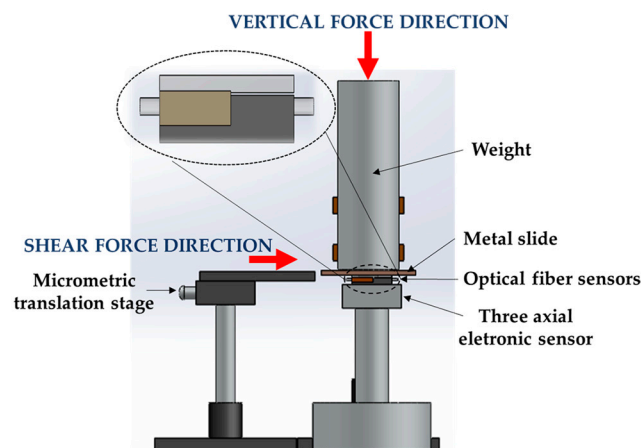

Figure 2. Representation of the experimental setup for the calibration and testing of the fiber Bragg grating (FBGs) cell.

The data retrieved from the electronic sensor was acquired through an analog-to-digital converter (USB-6008, National Instruments, Austin, TX, USA), while the optical signal given by the FBGs cell was acquired by an interrogation system (I-MON 512 USB, Ibsen, Farum, Denmark).

For the calibration of the FBGs cell to F_S, a metal slide placed between the sensing units and a metal cylinder bar (3 kg) was horizontally dragged with the help of a translation stage [8], as shown in Figure 2. The translation stage pushed the metal slide parallel to the sensors' top area, inducing an F_S in both sensing units (electronic and optical). During this test, the F_V was maintained constant ($\Delta F_V \approx 0$ N). For the calibration to F_V, a variable force was applied on the cylindrical bar, while the F_S was kept constant ($\Delta F_S \approx 0$ N). During these procedures (F_S and F_V calibration), the values registered by both sensing systems were simultaneously acquired for further comparison/calibration.

After the calibration, in order to evaluate the FBGs performance under the simultaneous application of F_V and F_S, the procedures described previously were performed simultaneously: the metal slide was propelled horizontally while an F_V was applied in the cylindrical bar, as seen in Figure 2. During the implementation of this protocol, both sensors (electronic and optical) were

simultaneously acquiring the data modulated in the sensing units. The obtained results are presented and discussed in the next subsections.

Also, the system hysteresis was tested, by inducing increasing and decreasing vertical forces in the sensing cell.

3.3. Calibration Results

Figure 3 shows the data simultaneously acquired by the electronic and optical systems, for the F_V (a) and F_S (b) characterization procedures. The F_V characterization, Figure 3a, clearly shows the increase of the registered pressure with the load applied over time. In the case of the optical sensor, this increase is translated by a continuous wavelength shift towards higher wavelengths in both FBGs. Such a shift is caused by the longitudinal distension (stretching) of the resin under vertical compression, which will induce the elongation of the embedded optical fiber and consequently the positive Bragg wavelength shift. In the representation of the shear calibration data (see Figure 3b), the periodic variations induced by the translation stage movements are visible in both sensors.
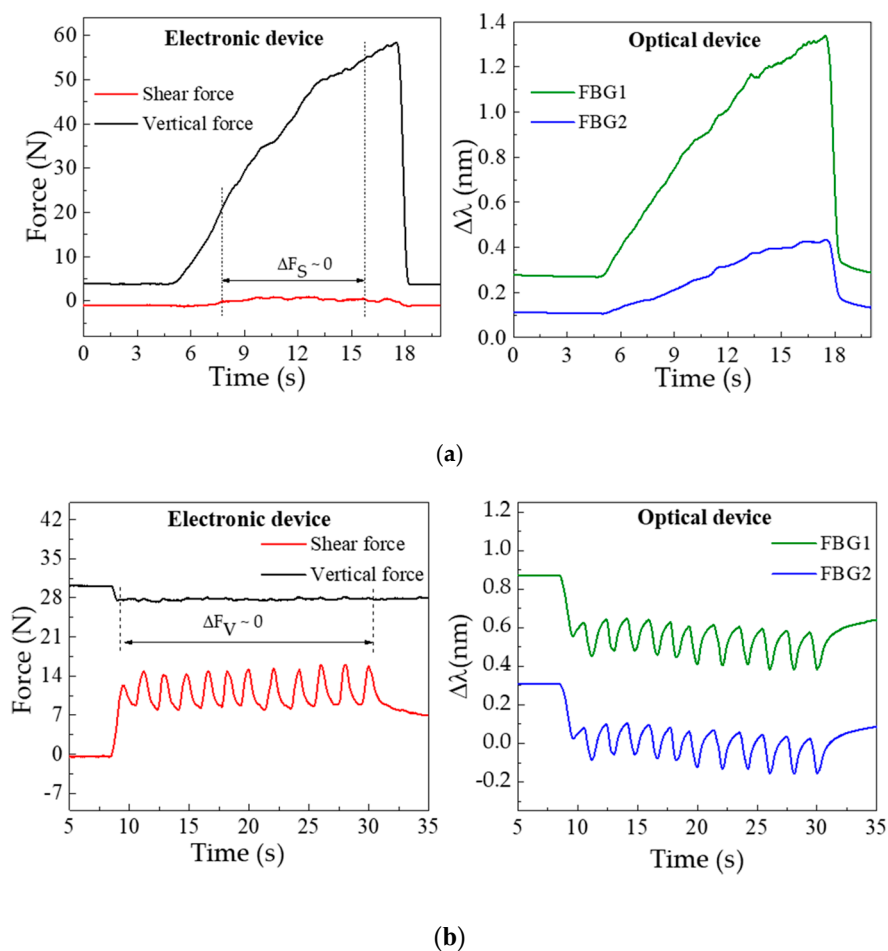

(a)

(b)

Figure 3. Data acquired by the three-axial electronic (left) and optical fiber (right) based systems, for the (**a**) vertical and (**b**) shear forces characterization.

In the electronic device, the increasing force corresponds to the movement of the translation stage given by one complete turn of the micrometric screw (360°). Once that turn is complete there is a relaxing moment till the new turn is started, which corresponds to the decrease (return to initial state) of the applied force. In the represented characterization process, there is a total of 12 turns. In the

optical sensor response, this data is inverted, hence the shear applied in the cell will longitudinally compress the resin and the embedded optical fiber, resulting in a negative Bragg wavelength shift.

From the characterization procedures, the sensitivities of FBG1 and FBG2 were calculated for both the F_V and F_S applied. Towards that, for each value registered by the three-axial electronic sensor, the correspondent Bragg wavelength shift (given by the optical sensor) was correlated, as presented in Figure 4.
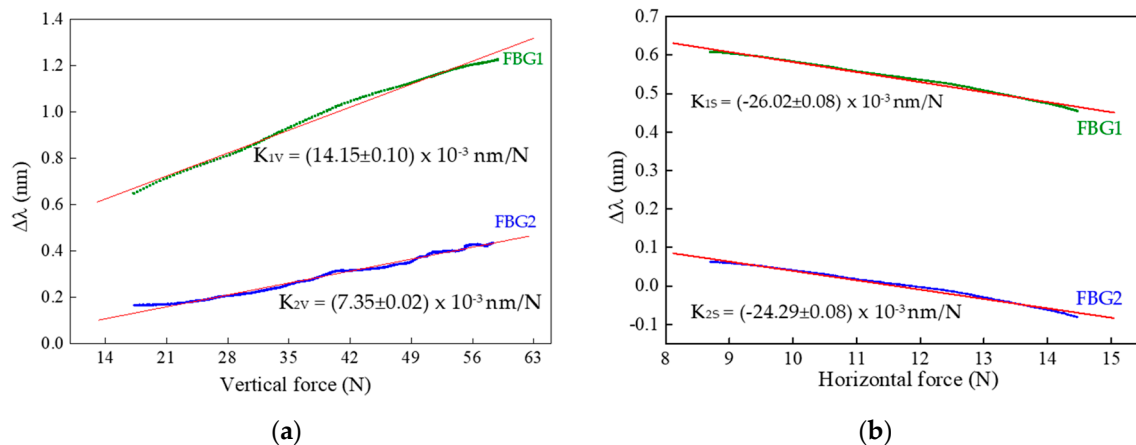

Figure 4. Calibration data obtained for FBG1 and FBG2 during the variation of the applied forces: (**a**) vertical (with $\Delta F_S \approx 0$ N) and (**b**) shear (with $\Delta F_V \approx 0$ N). Symbols are the acquired data and the red line corresponds to the linear fit ($R^2 > 0.99$).

From the calibration representation, a linear dependence of the Bragg wavelength shift with the applied force is verified. The sensitivities obtained for FBG1 and FBG2 as a function of the vertical (K_{1V} and K_{2V}) and shear forces (K_{1S} and K_{2S}) were:

$K_{1V} = (14.15 \pm 0.10) \times 10^{-3}$ nm/N, $K_{1S} = -26.02 \pm 0.08) \times 10^{-3}$ nm/N,
$K_{2V} = (7.35 \pm 0.02) \times 10^{-3}$ nm/N, $K_{2S} = (-24.29 \pm 0.08) \times 10^{-3}$ nm/N.

The substantial discrepancy in the vertical force sensitivity values obtained for the two FBGs is due to the height difference between the walls of cavity 1 and 2, since there is a gap of 0.8 mm between the wall of cavity 2 and the top of the cell. However, once the fiber is not fixed in any point of the cell, its longitudinal movements are similarly transmitted to FBG1 and FBG2, and therefore their sensitivities to shear forces are not as different as that of the vertical forces.

The results obtained for the hysteresis tests are presented in Figure 5. The maximum values found were 0.07 nm for FBG1 and 0.05 nm for FBG2.
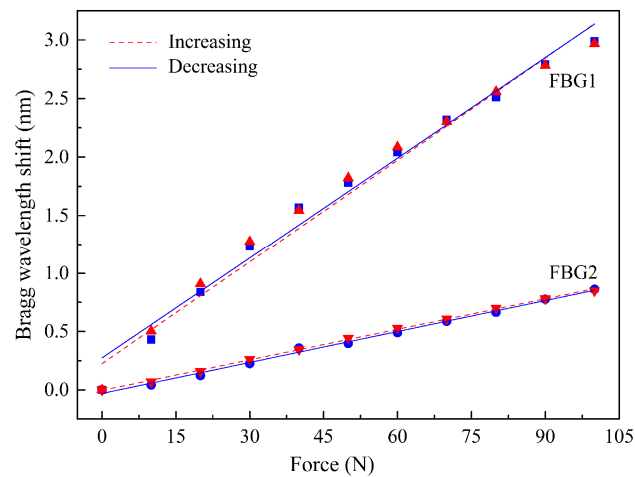
Figure 5. Bragg wavelength shifts as function of increasing and decreasing loadings.

3.4. Implementation: Simultaneous F_V and F_S Loadings

After the calibration, and using the same experimental setup as depicted in Figure 2, the sensor was tested for simultaneous F_S and F_V loadings. The Bragg wavelength shifts, modulated in the optical fiber sensors under simultaneous shear and vertical loadings, can be related to the applied forces by a two-equation system [8]:

$$\begin{bmatrix} F_V \\ F_S \end{bmatrix} = \begin{bmatrix} K_{1V} & K_{1S} \\ K_{2V} & K_{2S} \end{bmatrix}^{-1} \begin{bmatrix} \Delta\lambda_{FBG1} \\ \Delta\lambda_{FBG2} \end{bmatrix} \quad \begin{bmatrix} F_V \\ F_S \end{bmatrix} = \begin{bmatrix} 14.15 \times 10^{-3} & -26.02 \times 10^{-3} \\ 7.35 \times 10^{-3} & -24.29 \times 10^{-3} \end{bmatrix}^{-1} \begin{bmatrix} \Delta\lambda_{FBG1} \\ \Delta\lambda_{FBG2} \end{bmatrix} \quad (2)$$

where $\Delta\lambda_{FBG1}$ and $\Delta\lambda_{FBG2}$ are the Bragg wavelength shift of FBG1 and FBG2, respectively.

In Figure 6, the values acquired for the electronic and optical sensing units during this test are presented, as well as the data acquired after the application of Equation (2). The plot in Figure 6a corresponds to the values registered by the 3-axial electronic force sensor, while the data depicted in Figure 6b are the corresponding Bragg wavelength shift values acquired through the optical sensing cell.
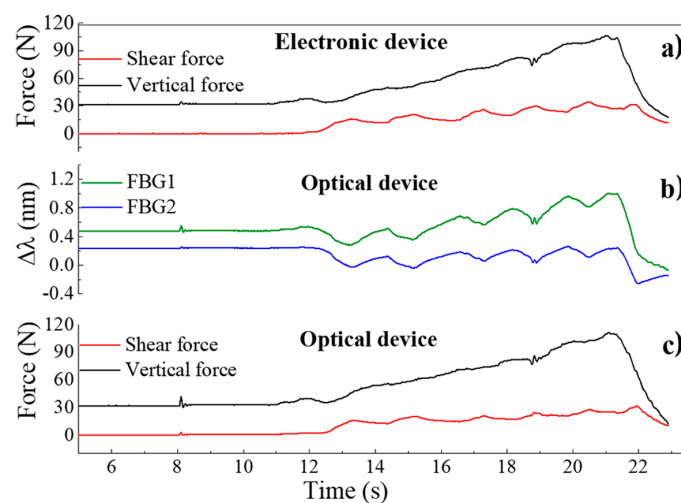

Figure 6. Response to the applied forces as a function of time for the: (**a**) electronic sensor; (**b**) FBGs cell, with the response as Bragg wavelength shift; (**c**) FBGs cell, the forces are calculated by applying Equation (2) to the registered wavelength shifts.

After applying Equation (2) to the $\Delta\lambda$ values obtained from the optical sensing unit, it is possible to obtain the correspondent force values, as presented in Figure 6c, which match the values acquired by the electronic sensors. Moreover, when comparing both sensors' responses, the differences between the curves obtained by the optical and the electronic sensor have a normalized root mean square error value of $RMSE_V = 0.025$ for F_V and $RMSE_S = 0.053$ for F_S, as presented in Figure 7, indicating the reliable performance of the optical sensor and its suitability to monitor F_V and F_S, simultaneously.
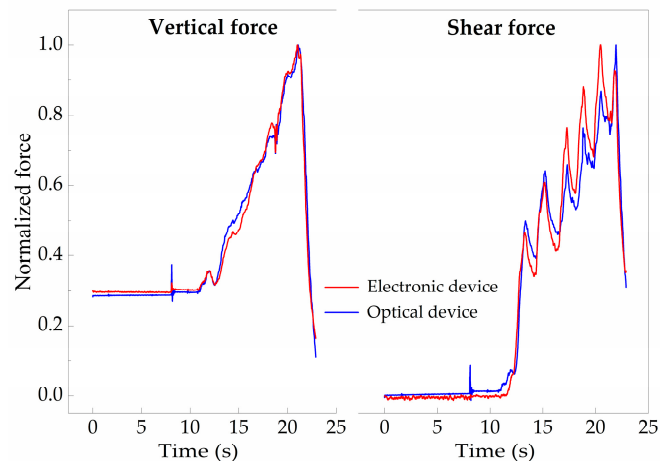

Figure 7. Comparison between the normalized values acquired with the three-axial sensor and the FBGs cell ($RMSE_V = 0.025$ and $RMSE_S = 0.053$).

The compactness, accuracy and reliability of the presented solution is demonstrated in shoe insoles for non-invasive gait pattern analysis (Section 4), however, its application in rehabilitation exoskeleton robots has great potential and will also be considered in our future work.

4. Gait Simultaneous Shear and Plantar Pressure Monitoring

In this section, we present the integration of the sensing architecture described before in an insole for the continuous and simultaneous monitoring of shear and plantar pressure during gait. This proposed solution is compact in size, non-invasive and could be used continuously during a daily routine, without jeopardizing the mobility of patients nor their autonomy while providing an early assessment of the gait pattern abnormalities of individuals at risk.

4.1. Insole Design and Implementation

Considering the foot plantar anatomy, the most at risk areas to develop neuropathic ulcers are the regions covering the bony prominences, where the load is heavily applied. Such areas are located under the metatarsal heads. Nonetheless, the shear stress measured in the great toe and heel are also reported as key points of analysis [6].

During gait, the value of vertical reaction forces and anterior-posterior (AP) forces (shear) are related to the body weight. As for vertical forces, a typical maximum (over the plantar area) is obtained with a force corresponding to 120% of the body weight at the early stance and toe-off moments [36,37]. For the anterior posterior forces, they are considerably smaller and can reach up to 25% of the body weight [36,37]. Locally wise, the area in which the vertical force will have a higher amplitude is the heel area, with a force that can reach up to 80% of the body weight [37].

Bearing in mind such key areas and gait pattern features, we have designed and produced an insole incorporating a total of five sensing cells, similar to the one described in Section 3. A single optical fiber, containing a total of 10 FBGs, was incorporated in the insole, as depicted in Figure 8.
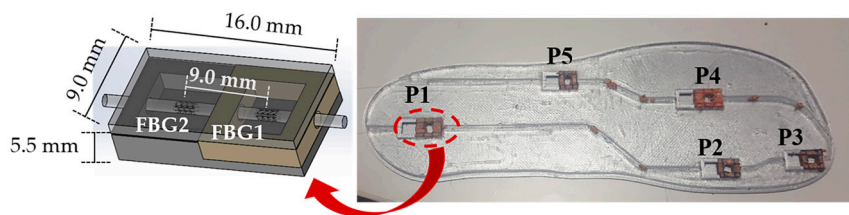
Figure 8. Photograph of the insole used for shear and plantar pressure monitor, incorporating five FBGs cells (as also schemed).

The FBGs cells were placed in the key points of analysis for the foot plantar pressure and shear stress monitor, namely, heel (P1), midfoot (P5), metatarsal (P2 and P4) and toe (P3). The Bragg wavelength and grating periodicity for each FBG are presented in Table 1.

Table 1. Bragg wavelength and grating periodicity for each FBG.

		Bragg Wavelength (nm)	**Grating Period (nm)**
P1	FBG1	1535.1	522.1
	FBG2	1547.1	526.2
P2	FBG1	1540.4	524.0
	FBG2	1543.8	525.1
P3	FBG1	1549.2	527.0
	FBG2	1555.7	529.1
P4	FBG1	1537.1	522.8
	FBG2	1552.8	528.2
P5	FBG1	1557.9	529.9
	FBG2	1561.4	531.1

4.2. Shear and Plantar Pressure Results

With the developed system, by monitoring the wavelength shift experienced by the FBGs in each cell, it is possible to simultaneously monitor the patient's gait pattern, as well as the plantar pressure (corresponding to the vertical force mention in previous sections, for unit of area) and shear stress distribution. Nonetheless, prior to its dynamic application, it is necessary to calibrate each sensing cell to pressure and shear. In that way, the procedure described in Section 3.2 was performed individually for each sensing cell, from which the sensitivities values K_{1V}, K_{2V} (to vertical forces) and K_{1S}, K_{2S} (to shear) were obtained for each FBGs cell.

Figure 9 displays the optical spectra obtained for the developed insole during the vertical force calibration of the FBGs cell "P5". Since the whole system is placed in one optical fiber with 10 multiplexed FBGs, the Bragg wavelength corresponding to each FBG is also visible. However, during the calibration process, only the FBGs corresponding to the sensing cell inserted in P5 responds to the local applied loads. Such a characteristic confirms the good isolation of the designed sensing cell to forces applied in its surroundings, and its suitability for a precise local analysis. Additionally, the presented design (size, number and location of the sensing cells) can be customized according to a doctor prescription and each patient/situation's specific needs.

After calibration, the insole was placed in a shoe for a dynamic monitoring test. During the test, the interrogation system was continuously acquiring the Bragg wavelength shift registered in each point, while the subject (female with 45 kg) was walking.
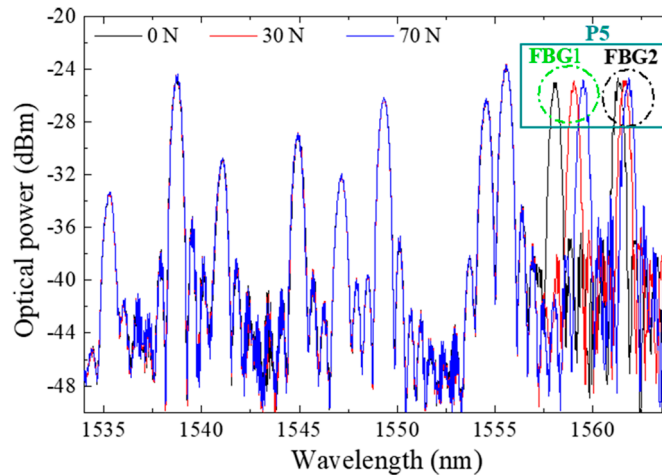
Figure 9. Optical spectra obtained during the pressure calibration of FBGs cell "P5".

Figure 10 represents the registered Bragg wavelength shift for each FBG, in the 5 points, during a 3 s gait. Due to a malfunction in the interrogation system, the Bragg wavelength acquired for FBG1 in P1 had extensive value gaps along time (Bragg wavelength returned as zero) and therefore its values were ignored.

For the global set of the remaining sensing cells, it is clear that each point is activated according to the pressure pattern expected during gait. The stance phase (foot in contact with the floor) and swing phase (foot without contact with the floor) are also clear in this representation [3].
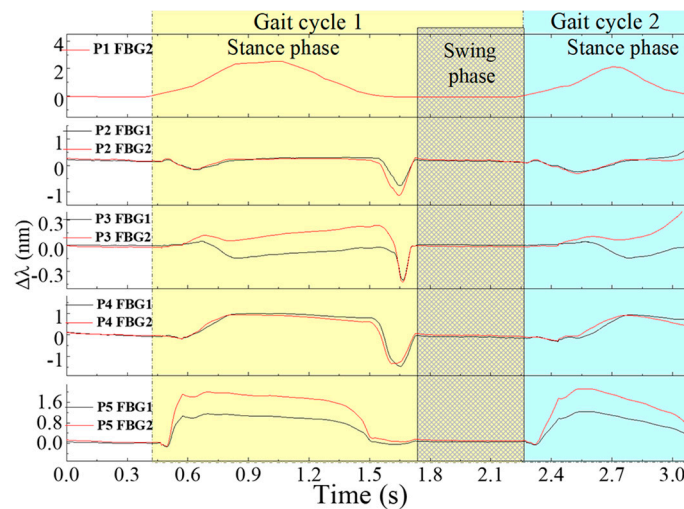
Figure 10. Bragg wavelength shifts in time, registered for each FBG in the 5 points of analysis.

Moreover, the instant in which the shear is a dominant force in the gait cycle is clearly visible (end of the stance phase), as well as the areas in which it is more predominant, namely, the metatarsal (P2 and P4) and the toe (P3) areas.

In order to retrieve the values of plantar vertical and shear forces from the raw data plotted in Figure 10, we apply Equation (2) to each point. The resultant curve, obtained for point 2, located at one of the metatarsal heads (critical point for shear analysis), is depicted in Figure 11.

Figure 11. Plantar pressure and shear stress retrieved from the sensing cells in the insole during gait.
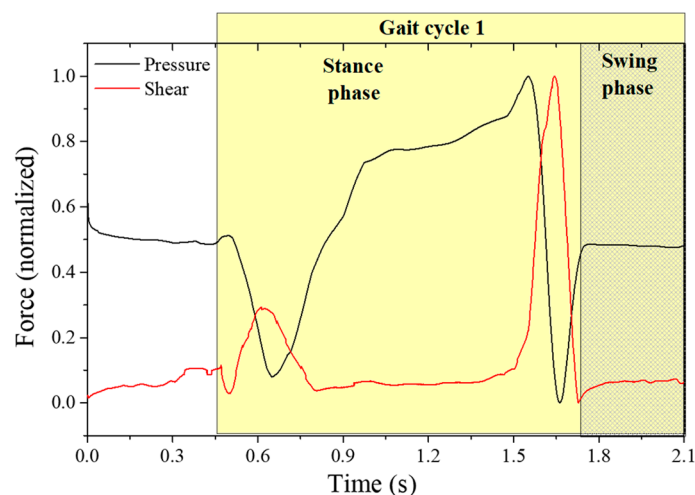
As it can be seen, it is possible to differentiate the plantar vertical force and the AP shear stress curve, as reported previously [3,6]. From the obtained curves, it is also observed that the maximum shear stress occurs first in the beginning of the foot-flat phase and again, with higher intensity, at the rising of the heel and the toe-off phase, which corresponds to the backward acceleration force under the metatarsal areas [6].

It is worth noting here that the shear stress evaluated with the referred system is the AP longitudinal shear, and to evaluate the medial-lateral stress, a different sensing cell configuration should be designed. However, and as stated before (and shown in Figure 9), lateral forces do not affect the proposed sensing cells performances for AP shear stress and plantar pressure. Also, it should be noticed that the estimated dynamic range can reach up to at least ~350 N (considering the sensor at heel area, where a typical vertical force of 80% of the body weight is applied).

So, the designed system presented in this paper is a reliable solution for the simultaneous monitoring of plantar pressure and shear stress during gait. Although the developed insole is composed of resin, which is a semi-rigid material, due to its flexibility and the small thickness used for this application, it is possible to be integrated inside the orthopedic insoles, for more comfortable wear. Its application as e-Health tool can provide a clear advantage to patients prone to develop neuropathic ulcers, by early alerting them to correct their posture and walking pattern [4,38]. Also, the incorporation of such devices in rehabilitation exoskeletons will allow the mitigation of the existing gap regarding the monitoring of shear forces.

5. Suitable Non-Invasive e-Health Solution

It has been emphasized throughout this paper the importance of the compact size of the sensing architecture, in addition to its resilience. These two properties render the architecture suitable for integration within a non-invasive e-Health system for the continuous monitoring of patients and elderly citizens. The proposed insole design, described in Section 4, would comprise one part of the whole mobile e-Health solution, used to continuously monitor patients for irregularities in their gait movement. The envisioned overall non-invasive monitoring solution is shown in Figure 12. The system comprises three components: the sensing element, the interrogator system, and the mobile app on a smartphone. The first part, which is the optical fiber sensing architecture, has been extensively explained throughout the paper. It is basically represented by the insole integrated with the optical FBGs cells, as explained in previous section.

The second part is the interrogator system, required to acquire the signal modulated in the sensing points. This can be translated into shear and vertical pressure, based on the proposed system of two equations, as explained in Section 3.
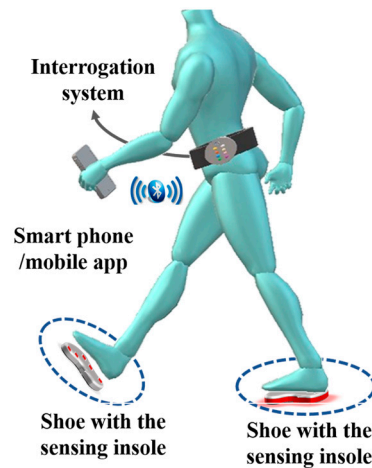

Figure 12. Non-invasive e-Health optical fiber sensing architecture for shear and plantar pressure gait analysis.

The last component is a mobile app installed on a smartphone. The mobile app has multiple roles. First, it is used as a data processing tool to analyze the acquired measurements from the sensing system. Second, the app uses the smartphone as a gateway for transmitting the measured data to the cloud, as shown in our previous work [3]. Additionally, the app can be used to display the results, when required by the patient. The user (patient or his/her doctor) is able to use the app to view the statistics from the measured data over a period of time. Although the system is continuously measuring the pressures, the main requirement is not the instantaneous display of measured values, but the average overall performance of monitored patients/elders during their actual daily routines. Hence the results are continuously transmitted to the cloud for a more elaborate analysis by medical personnel (i.e., the doctor, nurse or physical therapist), eliminating the requirement for high computational and energy capabilities at the mobile device [38]. It is worth mentioning here that the overall e-Health solution is still under development and results obtained from the system will be presented in future work.

6. Conclusions

In this work, a novel compact and efficient optical fiber based solution for the simultaneous sensing of vertical and shear forces is presented. The proposed architecture is accurate and resilient compared to existing solutions. The results obtained from the developed sensing cell show similar behavior to the three-axial electronic force sensor used for comparison, with a $RMSE_V = 0.025$ and $RMSE_S = 0.053$ between them. These values show that the developed device achieved the necessary accuracy while offering all the optical fiber sensor technology advantages, like immunity to electromagnetic interference and humid environments. Moreover, the proposed one-dimensional configuration is a reliable solution, which facilitates the production and incorporation of the sensing cell elements in other devices. Additionally, the presented sensing element, being able to infer and discriminate shear from vertical forces, has a great potential for incorporation into insoles for the measurement of plantar pressure (vertical force) and shear force. This measurement has high potential in different contexts/scenarios, including the prevention and study of pressure ulcers or in monitoring the performance of athletes during training; in electronic skin (e-skin) technologies; intelligent and rehabilitation robotic exoskeletons; human-machine interaction devices or even biomimetic prosthesis.

As for future work, it is our intention to optimize the cell to be able to retrieve both shear forces, anteroposterior and medial lateral, and validate its functionality within several individuals of both genders and of different age groups. Furthermore, its integration in an overall non-invasive e-Health architecture is being assembled, which will allow us to evaluate the forces during gait remotely and in a real time, enabling the monitoring of patients and elder citizens during their active lifestyle routines, without jeopardizing their mobility or freedom.

Conflicts of Interest: The authors declare no conflict of interest. The founding sponsors had no role in the design of the study; in the collection, analyses, or interpretation of data; in the writing of the manuscript, and in the decision to publish the results.

References

1. World Health Organization. Aging and Health. Available online: http://www.who.int/mediacentre/factsheets/fs404/en/ (accessed on 13 February 2018).
2. McWilliams, A. Global Markets and Technologies for Home Medical Equipment. Available online: https://www.bccresearch.com/market-research/healthcare/home-medical-equipment-technologies-market-report-hlc054d.html (accessed on 20 April 2018).
3. Domingues, F.; Tavares, C.; Leitão, C.; Frizera-Neto, A.; Alberto, N.; Marques, C.; Radwan, A.; Rodriguez, J.; Postolache, O.; Racon, E.; et al. Insole optical fiber Bragg grating sensors network for dynamic vertical force monitoring. *J. Biomed. Opt.* **2017**, *22*. [CrossRef] [PubMed]
4. Domingues, F.; Alberto, N.; Leitão, C.; Tavares, C.; Lima, E.; Radwan, A.; Sucasas, V.; Rodriguez, J.; André, P.; Antunes, P. Insole optical fiber sensor architecture for remote gait analysis-an eHealth Solution. *IEEE Internet Thing J.* **2017**. [CrossRef]
5. Domingues, M.F; Tavares, C.; Alberto, N.; Leitão, C.; Antunes, P.; André, P.; Rocon, E.; Sucasas, V.; Radwan, A.; Rodriguez, J. Non-invasive insole optical fiber sensor architecture for monitoring foot anomalies. In Proceedings of the IEEE Global Communications Conference, Singapore, 4–8 December 2017.
6. Rajala, S.; Lekkala, J. Plantar shear stress measurements—A Review. *Clin. Biomech.* **2014**, *29*, 475–483. [CrossRef] [PubMed]
7. Bayón, C.; Lerma, S.; Ramírez, O.; Serrano, J.I.; Del Castillo, M.D.; Raya, R.; Belda-Lois, J.M.; Martínez, I.; Rocon, E. Locomotor training through a novel robotic platform for gait rehabilitation in pediatric population. *J. Neuroeng. Rehabil.* **2016**, *13*, 98. [CrossRef] [PubMed]
8. Mohammad, I.; Huang, H. Pressure and shear sensing based on microstrip antennas. *Proc. SPIE* **2012**, *8345*. [CrossRef]
9. Leitão, C.; Antunes, P.; Pinto, J.; Bastos, J.; André, P. Carotid distension waves acquired with a fiber sensor as an alternative to tonometry for central arterial systolic pressure assessment in young subjects. *Measurement* **2017**, *95*, 45–49. [CrossRef]
10. Hammock, M.; Chortos, A.; Tee, B.; Tok, J.; Bao, Z. 25th Anniversary Article: The Evolution of Electronic Skin (E-Skin): A Brief History, Design Considerations, and Recent Progress. *Adv. Mater.* **2013**, *25*, 5997. [CrossRef] [PubMed]

11. Luo, N.; Dai, W.; Li, C.; Zhou, Z.; Lu, L.; Poon, C.; Chen, S.-C.; Zhang, Y.; Zhao, N. Flexible piezoresistive sensor patch enabling ultralow power cuffless blood pressure measurement. *Adv. Funct. Mater.* **2016**, *26*, 1178–1187. [CrossRef]

12. Jung, S.; Kim, J.; Kim, J.; Choi, S.; Lee, J.; Park, I.; Hyeon, T.; Kim, D. Reverse-micelle-induced porous pressure-sensitive rubber for wearable human-machine interfaces. *Adv. Mater.* **2014**, *26*, 4825–4830. [CrossRef] [PubMed]

13. Mesquita, E.; Arede, A.; Silva, R.; Rocha, P.; Gomes, A.; Pinto, N.; Varum, H.; Antunes, P. Structural health monitoring of the retrofitting process, characterization and reliability analysis of a masonry heritage construction. *J. Civ. Struct. Health Monit.* **2017**, *7*, 405–428. [CrossRef]

14. Minami, K.; Kokubo, Y.; Maeda, I.; Hibino, S. Analysis of actual pressure point using the power flexible capacitive sensor during chest compression. *J. Anesth.* **2017**, *31*, 152–155. [CrossRef] [PubMed]

15. Voinea, J.; Butnariu, S.; Mogan, G. Measurement and geometric modelling of human spine posture for medical rehabilitation purposes using a wearable monitoring system based on inertial sensors. *Sensors* **2016**, *17*, 3. [CrossRef] [PubMed]

16. Choi, S.; Cho, H.; Lissenden, C. Selection of shear horizontal wave transducers for robotic nondestructive inspection in harsh environments. *Sensors* **2016**, *17*, 5. [CrossRef] [PubMed]

17. Ferreira, L.; Antunes, P.; Domingues, F.; Silva, P.; André, P. Monitoring of sea bed level changes in nearshore regions using fiber optic sensors. *Measurement* **2012**, *45*, 1527–1533. [CrossRef]

18. Zang, Y.; Zhang, F.; Di, C.; Zhu, D. Advances of flexible pressure sensors toward artificial intelligence and health care applications. *Mater. Horiz.* **2015**, *2*, 140–156. [CrossRef]

19. Tiwana, M.; Shashank, A.; Redmond, S.; Lovell, N. Characterization of a capacitive tactile shear sensor for application in robotic and upper limb prostheses. *Sens. Actuators A Phys.* **2011**, *165*, 164–172. [CrossRef]

20. Puangmali, P.; Althoefer, K.; Seneviratne, L.; Murphy, D.; Dasgupta, P. State-of-the-art in force and tactile sensing for minimally invasive surgery. *IEEE Sens. J.* **2008**, *8*, 371–381. [CrossRef]

21. Chen, W.; Lee, P.; Park, S.; Lee, S.; Shim, V.; Lee, T. A novel gait platform to measure isolated plantar metatarsal forces during walking. *J. Biomech.* **2010**, *43*, 2017–2021. [CrossRef] [PubMed]

22. Kärki, S.; Lekkala, J.; Kuokkanen, H.; Halttunen, J. Development of a piezoelectric polymer film sensor for plantar normal and shear stress measurements. *Sens. Actuators A Phys.* **2009**, *154*, 57–64. [CrossRef]

23. Hamatani, M.; Mori, T.; Oe, M.; Noguchi, H.; Takehara, K.; Amemiya, A.; Ohashi, Y.; Ueki, K.; Kadowaki, T.; Sanada, H. Factors associated with callus in patients with diabetes, focused on plantar shear stress during gait. *J. Diabetes Sci. Technol.* **2016**, *10*, 1–7. [CrossRef] [PubMed]

24. Yavuz, M.; Erdemir, A.; Botek, G.; Hirschman, G.; Bardsley, L.; Davis, B. Peak plantar pressure and shear locations—Relevance to diabetic patients. *Diabetes Care* **2007**, *30*, 2643–2645. [CrossRef] [PubMed]

25. Razian, M.; Pepper, M. Design, development, and characteristics of an in-shoe triaxial pressure measurement transducer utilizing a single element of piezoelectric copolymer film. *IEEE Trans. Neural Syst. Rehabil. Eng.* **2003**, *11*, 288–293. [CrossRef] [PubMed]

26. Heywood, E.J.; Jeutter, D.C.; Harris, G.F. Tri-axial plantar pressure sensor: Design, calibration and characterization. In Proceedings of the 26th Annual International Conference of the IEEE Engineering in Medicine and Biology Society, San Francisco, CA, USA, 1–5 September 2004.

27. Alberto, N.; Bilro, L.; Antunes, P.; Leitão, C.; Lima, H.; André, P.; Nogueira, R.; Pinto, J.L. Optical fiber technology for e-Healthcare. In *Handbook of Research on ICTs and Management Systems for Improving Efficiency in Healthcare and Social Care*; IGI Global: Hershey PA, USA, 2013; pp. 180–200.

28. Domingues, F.; Radwan, A. Optical fiber sensors in IoT. In *Optical Fiber Sensors for IoT and Smart Devices*; Springer: Cham, Switzerland, 2017; pp. 73–86.

29. Koulaxouzidis, A.; Holmes, M.; Roberts, C.; Handerek, V. A shear and vertical stress sensor for physiological measurements using fibre Bragg gratings. In Proceedings of the 22nd Annual International Conference of the IEEE Engineering in Medicine and Biology Society, Chicago, IL, USA, 23–28 July 2000.

30. Zhang, Z.; Tao, X. Soft fiber optic sensors for precision measurement of shear stress and pressure. *IEEE Sens. J.* **2013**, *13*, 1478–1482. [CrossRef]

31. Wang, W.; Ledoux, W.; Sangeorzan, B.; Reinhall, P. A shear and plantar pressure sensor based on fibre-optic bend loss. *J. Rehabil. Res. Dev.* **2005**, *42*, 315–326. [CrossRef] [PubMed]

32. Liu, C.; Chou, G.; Liang, X.; Reinhall, P.; Wang, W. Design of a multi-layered optical bend loss sensor for pressure and shear sensing. *Proc. SPIE* **2007**, *6532*. [CrossRef]

33. Soetanto, W.; Nguyen, N.; Wang, W. Fiber optic plantar pressure/shear sensor. *Proc. SPIE* **2011**, *7984*. [CrossRef]

34. Chang, C.; Liu, C.; Soetanto, W.; Wang, W. A platform-based foot pressure/shear sensor. *Proc. SPIE* **2012**, *8348*. [CrossRef]

35. Silva, S.; Sabino, M.; Fernandes, E.; Correlo, V.; Boesel, L.; Reis, R. Cork: Properties, capabilities and applications. *Int. Mater. Rev.* **2005**, *50*, 345–365. [CrossRef]

36. Perry, J.; Davids, J.R. Gait analysis: normal and pathological function. *J. Pediatr. Orthop.* **1992**, *12*, 815. [CrossRef]

37. Wearing, S.C.; Urry, S.R.; Smeathers, J.E. Ground reaction forces at discrete sites of the foot derived from pressure plate measurements. *Foot Ankle Int.* **2001**, *22*, 653–661. [CrossRef] [PubMed]

38. Radwan, A.; Domingues, M.F.; Rodriguez, J. Mobile caching-enabled small-cells for delay-tolerant e-Health apps. In Proceedings of the 2017 IEEE International Conference on Communications Workshops, Paris, France, 21–25 May 2017; pp. 103–108.

MANUSCRIPT 4

Optically Instrumented Insole for Gait Plantar and Shear Force Monitoring

CÁTIA TAVARES[1,2,3], FLÁVIA LEITE[1,2,3], MARIA DE FÁTIMA DOMINGUES[3], (Member, IEEE), TIAGO PAIXÃO[1,2], NÉLIA ALBERTO[3], ANTÓNIO RAMOS[4], HUGO SILVA[5,6], (Senior Member, IEEE), AND PAULO FERNANDO DA COSTA ANTUNES[1,2,3]

[1]Department of Physics, University of Aveiro, Campus Universitário de Santiago, 3810-193 Aveiro, Portugal
[2] Institute for Nanostructures, Nanomodelling and Nanofabrication (I3N), University of Aveiro, Campus Universitário de Santiago, 3810-193 Aveiro, Portugal
[3]Instituto de Telecomunicações, University of Aveiro, Campus Universitário de Santiago, 3810-193 Aveiro, Portugal
[4]Centre for Mechanical Technology and Automation, Department of Mechanical Engineering, University of Aveiro, Campus Universitário de Santiago, 3810-193 Aveiro, Portugal
[5]Instituto Superior Técnico, Universidade de Lisboa (IST-UL), 1049-001 Lisbon, Portugal
[6]PLUX –Wireless Biosignals, S.A, 1050-059 Lisbon, Portugal

Optically Instrumented Insole for Gait Plantar and Shear Force Monitoring

CÁTIA TAVARES[1,2,3], **FLÁVIA LEITE**[1,2,3], **MARIA DE FÁTIMA DOMINGUES**[3], **(Member, IEEE),**
TIAGO PAIXÃO[1,2], **NÉLIA ALBERTO**[3], **ANTÓNIO RAMOS**[4],
HUGO SILVA[5,6], **(Senior Member, IEEE), AND PAULO FERNANDO DA COSTA ANTUNES**[1,2,3]

[1]Department of Physics, University of Aveiro, Campus Universitário de Santiago, 3810-193 Aveiro, Portugal
[2]Institute for Nanostructures, Nanomodelling and Nanofabrication (I3N), University of Aveiro, Campus Universitário de Santiago, 3810-193 Aveiro, Portugal
[3]Instituto de Telecomunicações, University of Aveiro, Campus Universitário de Santiago, 3810-193 Aveiro, Portugal
[4]Centre for Mechanical Technology and Automation, Department of Mechanical Engineering, University of Aveiro, Campus Universitário de Santiago, 3810-193 Aveiro, Portugal
[5]Instituto Superior Técnico, Universidade de Lisboa (IST-UL), 1049-001 Lisbon, Portugal
[6]PLUX –Wireless Biosignals, S.A, 1050-059 Lisbon, Portugal

Corresponding authors: Cátia Tavares (catia.tavares@ua.pt) and M. Fátima Domingues (fatima.domingues@ua.pt)

ABSTRACT In this work, a fiber Bragg gratings (FBGs) based sensing insole, capable of simultaneously measure plantar force (PF) and shear force (SF) is proposed. The insole has four measuring points, strategically located for a full gait analysis. Each sensing point contains a sensor-cell which consists of a polylactic acid (PLA) structure, covered by an epoxy resin layer, and crossed by one optical fiber with two FBGs, FBG1 and FBG2, respectively. Due to the specific design of the system, the FBG1 is sensitive to both forces (with higher sensitivity to the PF), while the FBG2 is designed to detect only the SF. The instrumented insole was tested during static and gait exercises, and the results, obtained for the PF and SF monitoring, were according to those theoretically expected.

INDEX TERMS Foot plantar sensor, gait cycle anomalies, multiplexed fiber Bragg gratings, pressure ulcers, shear force sensor.

I. INTRODUCTION

With the progressive increase in life expectancy, a continuous monitoring of the aging citizens' health is a necessary requirement to ensure a healthy life [1]. Everyone wants to improve life quality, making the development of devices to monitor the physical capabilities essential to ensure that they are not weakened, or, when this happens, that any prescribed rehabilitation treatment is being done in a correct way and is being effective [2]. The advances in research areas like e-Health are driven by the purpose of providing solutions (including the sensing systems) that increase the quality of life of patients, as well as the necessary help to medical staff in the early diagnosis of anomalies. These sensing systems and e-Health enablers must be capable to help elder generations and patients with chronic illness to live an active life, without compromising their daily routines. To improve

the quality of life of citizens with reduced mobility, our research team has been working in different practical optical fiber-based solutions for the continuous remote monitoring of patients' health [3]–[5].

The motivation for this work is to develop a fiber optic sensor system to detect abnormalities in the gait cycle that may be related to serious pathologies in the spine, as well as the detection of warning signals related to the appearance of pressure ulcers in the feet. These sensors can also be used in rehabilitation aids, like in the so-called exoskeletons.

This paper reports the optimization of a fiber Bragg gratings (FBGs) based device able to measure plantar force (PF) and shear force (SF). The proposed solution, designed as sensor-cell, is a polylactic acid (PLA) structure, covered by an epoxy resin layer and crossed by an optical fiber with two inscribed FBGs (FBG1 and FBG2). For the insole instrumentation, this sensor-cell was replicated, and positioned at four key points for the foot plantar forces analysis.

The associate editor coordinating the review of this manuscript and approving it for publication was Sukhdev Roy.

Pressure ulcers are localized lesions in the skin, or underlying tissues, that appear due to the decrease of the blood circulation inflicted by an increased pressure in specific areas of the body [6]. According to the study reported in [7], the average hospital treatment costs associated with stage IV pressure ulcers and related complications were $129,248 for hospital-acquired ulcers during 1 admission, and $124,327 for community-acquired ulcers over an average of 4 admissions [7]. Beyond their treatment financial cost, the untreated (or lately detected) pressure ulcers can also lead to limb amputations or even death of the patients.

As this serious pathology is commonly related to the foot, the existence of devices (typically insoles) able to predict its development in an early stage is of the utmost importance [8]. In that way, the device developed by our team aims to help in such early detection, since it is able to monitor the two fundamental parameters for the appearance and worsening of pressure ulcers: the foot plantar and shear forces [9]–[11]. The foot plantar force (PF) consists on the vertical reaction of the ground to the patient weight, and the shear force (SF) is related with the horizontal forces between the foot and the ground, and often referred in many published works as the responsible for this pathology [8].

Several authors highlight feet areas such as heel, midfoot, first metatarsal and hallux as the key points for the plantar and shear monitoring [12]–[14]. The typical distribution of PF and SF is depicted in Fig. 1, where the blue regions correspond to the areas with lower applied force, and the red ones are the areas where higher values of force are expected. In this figure, the four key points (black dots) where the sensor-cells were positioned are also identified. These points correspond to the expected higher values of PF and SF, and, therefore, the areas with more predisposition to the appearance of pressure ulcers.

FIGURE 1. Typical plantar and shear forces distribution in the foot, with the areas with higher (red) and lower (blue) forces. Identification of the sensor-cells position (black dots).

In the sensor market, there are many electronic devices available for the analysis of plantar pressure, such as pressure distribution platforms, imaging technologies with image processing software, and in-shoe systems. These solutions are generally equipped with piezoelectric and/or piezoresistive sensors and capacitive sensors [15], [16]. All these are electronic solutions, possessing relevant disadvantages

that can potentially be mitigated by optical fiber technology. Furthermore, the solutions to simultaneously monitor shear and plantar forces are scarce and financially costly.

Optical fiber sensors (OFS) have been widely used into different areas, and in the last years its application in the biomedical fields has been greatly explored [17]. OFS are used for temperature control during several surgical procedures [18]; very low pressure levels for intracapillary measurements [19], medium pressure levels in finger interactive forces monitoring [20], and for higher pressure levels such as the pressure exerted by the body human [2], [3]. They have also been used for heart [21] and respiratory rate measuring [22], among others. When compared to their electronic counterparts, the advantages of these type of sensors include immunity to electromagnetic interferences, the ability to multiplex several sensors in a single optical fiber, and the possibility to be used in the presence of humidity without any special encapsulation, since no electric current is needed at the measurement point, making them intrinsically safer [17]. Also, due to its high accuracy and resolution, it is possible to achieve a level of detail in the deformation process, that the electronic sensors lack.

The monitoring of the vertical and tangential forces in biomedical applications, like analysis of plantar forces, or prosthetic applications, using OFS with FBG has also been considerably investigated.

In 2000, Koulaxouzidis *et al.* presented the first tangential and vertical forces sensor for physiological measurements. Nevertheless, the sensor was quite complex since it was composed by three FBGs embedded in a rubber block in three different orientations. When subjected to forces, the material is deformed, and consequently a variation on the reflected Bragg wavelength is observed [23]. Later, in 2013, Zhu's team presented a similar sensor, however they used two polymer FBGs (PFBGs) embedded in polydimethylsiloxanes (PDMS) block [24]. In 2016, Chethana *et al.* presented a 3D force measurement platform, based on several FBG sensors [25]. Later, it was reported the use of a cork insole with an FBG network [26] and PFBG network [27] sensors located at key points for the analysis of vertical force during gait. In 2018, our research group proposed a biaxial optical fiber sensor with two FBGs, using only one optical fiber, for simultaneous shear stress and vertical pressure monitoring [28]. Months later, the same research group reported the application of these sensors in an insole to monitor these same parameters in five different zones in the sole of the foot, to prevent/diagnose diabetic feet and disturbances in the synchronization of the lower limbs [29]. Each of these sensor-cells was composed by cork, PLA, epoxy resin and two in-line FBGs recorded on a single optical fiber [28], [29]. In the following year, the same authors proposed a bio-inspired cell-sensor capable of measuring the same physical parameters, but with a simpler production process, due to the use of a 3D printer to make the sensor-cell body, and without cork [30]. In 2020, Mai *et al.* proposed a similar solution, with the same working principle to fulfill the same purpose, but with two

sensor-cells and two distinct optical fibers: one to measure normal force, and the other to measure shear force [31].

Concerning to the prosthetic application, in 2017, an FBG-instrumented prosthetic silicone liner that provides cushioning for the residual limb and can successfully measure interface pressures inside prosthetic sockets of lower-limb amputees was proposed [32]. The liner is made of two silicone layers between which twelve FBG sensors were embedded at locations of clinical interest to measure pressure. A year later, it was reported the use of FBGs embedded into a carbon fiber reinforced polymer transtibial prosthesis to evaluate the user's gait, and its own performance [33]. The FBGs were positioned vertically and horizontally within the structure, and they have been used for load and strain force evaluation during real-time experiments with a candidate at different speeds on a treadmill. In 2019, a novel method to simultaneously measure the normal and shear strains using two FBGs sensors embedded into a foam liner that sits at the prosthetic interface was proposed [34]. The results show a very good agreement of measured normal and shear strains for loads below 20 N.

With this paper, we propose a new instrumented insole capable of simultaneously measuring plantar and shear forces at the same point of analysis. There is only one published work that fulfills the same purpose [29], however it presents some complexity of production due to the manual cutting of all the pieces involved in the sensor-cell production (pieces of only a few millimeters in dimension). So, we are now presenting a new sensor-cell design that reduces the production complexity, since only two materials are used and fewer manual production steps are involved, due to the use of 3D printing to produce the body of the sensor-cell and the base of the insole. With this proposed configuration, a higher ratio between each direction sensitivity was obtained, which is less prone to cross sensitivity effects.

This paper is organized in 5 sections: Section I is the introduction; Section II presents the FBG sensing principle; Section III focuses on the sensor-cell design, simulations and experimental characterization; Section IV shows the implementation of the sensor-cells on the insole and their performance during static and dynamic tests; Section V presents the overall device architecture; and Section VI outlines the main conclusions.

II. FBG SENSING PRINCIPLE

FBGs are produced by laterally exposing the optical fiber to a periodic pattern of, typically, an UV light. After exposure, they present a periodic perturbation in the refractive index of the fiber core, which is sensitive to external perturbations, such as temperature and strain variations. When an optical fiber containing an FBG is illuminated by a broadband light source, only a small set of wavelengths that meet the Bragg condition are reflected, being all the others transmitted. The Bragg condition is given by the following equation:

$$\lambda_B = 2n_{eff}\Lambda \tag{1}$$

where λ_B is the reflected Bragg wavelength, n_{eff} is the effective refractive index of the optical fiber core, and Λ is the grating period.

Any temperature (ΔT) and/or strain (Δl) variations will be translated in a Bragg wavelength shift ($\Delta\lambda_B$) in accordance with the following equation:

$$\Delta\lambda_B = \Delta\lambda_{B,l} + \Delta\lambda_{B,T}$$
$$\Delta\lambda_B = 2\left(\Lambda\frac{\partial n_{eff}}{\partial l} + n_{eff}\frac{\partial\Lambda}{\partial l}\right)\Delta l$$
$$+ 2\left(\Lambda\frac{\partial n_{eff}}{\partial T} + n_{eff}\frac{\partial\Lambda}{\partial T}\right)\Delta T$$
$$\Delta\lambda_B = S_l\Delta l + S_T\Delta T \tag{2}$$

where the first term is the strain induced Bragg wavelength shift, and the last the thermal effect on the same parameter. S_l and S_T represent the strain and temperature sensitivity coefficients of the FBG, respectively.

In this work, each sensor-cell was produced with two in-line FBGs separated by 9.5 mm. The FBGs were inscribed into a photosensitive optical fiber (GF1 Thorlabs), using a pulsed Q-switched Nd: YAG laser system (LOTIS TII LS-2137U Laser), lasing at the fourth harmonic (266 nm). The FBGs were recorded through the phase mask technique, employing a laser pump energy of 25 J, a repetition rate of 10 Hz, and an exposure time of $\sim$1 min.

III. SENSOR-CELL DEVELOPMENT
A. DESIGN AND PRODUCTION
In our previously work [29], a complex sensor-cell production was used, involving three different materials and several manual production steps. The complex assembly methodologies make it difficult to replicate the sensor-cells, and therefore it adds a higher probability of errors in its construction and implementation feedback.

The present work intends to be a step forward from the previous sensing system, with a sensor-cell design providing an alternative solution that overcomes these two disadvantages. For that, the sensor-cell was designed to be printed in PLA on a 3D printer (Ultimaker 3D Extended), to facilitate the production process, to guarantee better reproducibility conditions, and to ensure the discrimination of the plantar and shear forces, with one of the two FBGs being only sensitive to the shear force.

Each sensor-cell is composed by an optical fiber (represented in green color in Fig. 2) containing two in-line FBGs, which were incorporated into a PLA piece (in blue color in the Fig. 2) and epoxy resin to protect the cell and to fill a cavity, which is within the zone 1 (in red color in Fig. 2).

The cell's base is composed by two zones: zone 1, which contains the cavity designed to accommodate the FBG mostly sensitive to vertical force (FBG1), while zone 2 contains the FBG that should be sensitive only to shear force (FBG2) (Fig. 2a). This sensor-cell has a dimension of 19.00 mm $\times$ 8.00 mm $\times$ 5.00 mm and a hole along its entire length at a height of 2.70 mm from the base, with a diameter of 0.80 mm
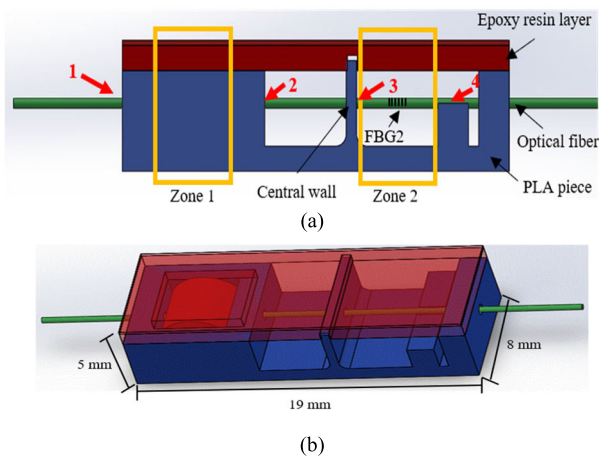
FIGURE 2. Sensor-cell design with the evidence of the materials and zones (a), and dimensions (b).

for the fiber allocation (Fig. 2b). The central wall, limiting zone 2, has a height of 4.20 mm (to be anchored in the epoxy top layer), a thickness of 0.90 mm and a curvature with the connection to its base with a radius of 0.75 mm. Such dimensions allow its longitudinal movement but constrains its vertical and transversal ones. These dimensions were set based on the theoretical analysis described in the following section.

The optical fiber containing the two FBGs was first placed in the PLA piece, with the FBG1 positioned in the middle of the cavity (zone 1), and the FBG2 (sensitive to shear) located between the central wall and the small wall. Then, the optical fiber was glued to the PLA at four points (1, 2, 3 and 4 identified in red in Fig. 2a: first between the first and the second points; second, between the third and the fourth points. In the second bonding, between points 3 and 4, the optical fiber was tensioned (with a tension corresponding to a Bragg wavelength shift of around 1 nm). Between the second and third points, the fiber is not tensioned, so that the forces undergo by FBG1 do not influence the forces applied in FBG2, and vice-versa. The aim of the lower wall between the points 3 and 4 is to support the optical fiber between those fixed points. After the fiber bonding process, the cavity of the zone 1 was filled with epoxy resin (Advanced from Liquid Lens^{TM}), represented in red in Fig. 2. Lastly, a resin layer with a thickness of approximately 1 mm was placed over all the PLA piece. The main function of this layer is to provide to the sensor-cell a protection in terms of physical integrity, and to allow the FBG2 to be sensitive to the shear forces felt on its surface. This second purpose is only possible because this layer has a groove to fit the central wall of the base. In other words, the surface of the sensor-cell when exposed to tangential forces (shear) will move the central wall, which is thin enough to undergo slight lateral displacements, but thick enough not to break.

As the FBG1 was embedded in the resin, it will be sensitive to all events to which the resin is subjected, namely both plantar and shear forces.

The shear felt on the insoles always behaves in the same way: runs from the toes towards the heel. Therefore, the sensor-cell will be placed on the insole so that the shear occurs in the direction from FBG1 to FBG2. Due to the cell design, it is expected that the FBG1 will be stretched in the presence of PF, whereas for FBG2 this happens for the case of SF, since it was glued to a wall that is only expected to undergo shear.

Previous works report that the maximum pressure exerted on the sole of the foot during walking is about 0.27 MPa [11], but once an FBG embedded in epoxy resin has a much higher compression limit, about 1.57 MPa [35], our sensor-cell is a good solution for the pressure range to which an insole is exposed during walking.

B. FINITE ELEMENT SIMULATION

The sensor-cell behavior was simulated using finite element modeling with "SolidWorks Simulation" software, considering the expected maxima values of plantar and shear forces reported in the literature, of 42 N and 8 N, respectively [11]. This simulation allowed to visualizing and understand the behavior of the sensor-cell, and to optimize the characteristics of the central wall. From the results presented in Fig. 3 we can conclude that, for a plantar force of 42 N, the cavity 1, and consequently, the FBG1 suffer the most deformation, while the FBG2 in zone 2 does not show significant changes (the presence of a greenish color allows to predict that there is only a very small movement of the central wall).
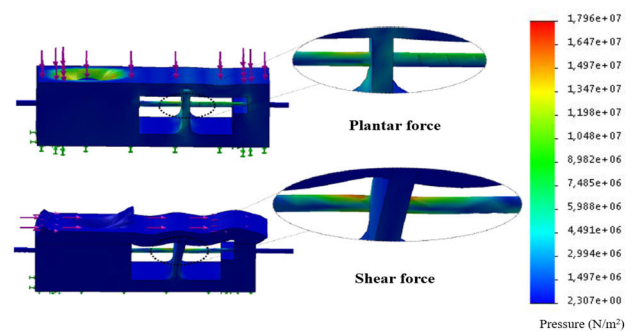
FIGURE 3. Simulation results of the behavior of the sensor-cell when a plantar and shear forces are applied.

For the case of a shear force of 8 N, it is shown that the resin at the top of the cavity 1 moves significantly, so it is expected that the FBG1 is sensitive to this force. In relation to FBG2, it is also observed that the optical fiber near the central wall undergoes some tension (presence of red color). So, as expected, both FBGs will be sensitive to shear force (Fig. 3). Several sensor-cells, with different central wall dimensions, were also simulated to attain the most suitable wall characteristics that should induce a greater sensitivity to shear forces, without compromising the wall structure. The results revealed that the wall should have the following dimensions: 4.20 mm of height, 0.90 mm of thickness and a curvature radius with the base of 0.75 mm.

FIGURE 4. Schematic representation of the experimental setup used to calibrate the FBGs.

C. EXPERIMENTAL CHARACTERIZATION

Prior to the sensor-cell application, it is crucial to calibrate each FBG independently for each of the forces, aiming to convert its wavelength shift into the respective force value applied to the sensor-cell. So, for the calibration, an electronic multiaxial force sensor (LFX-A-1KN Kyowa) was used. The sensor-cell was fixed to the electronic sensor, with the aid of double-sided tape, allowing the forces to be felt simultaneously in both devices (over both electronic sensor and sensor-cell). The data from the electronic sensor was acquired through an analog-to-digital converter (ADC) (USB6008,

National Instruments), while the optical signal provided by the sensor-cell was acquired by an optical interrogator (I-Mon512, Ibsen), with an acquisition rate of 912 Hz. A schematic representation of the implemented experimental setup is depicted in Fig. 4.

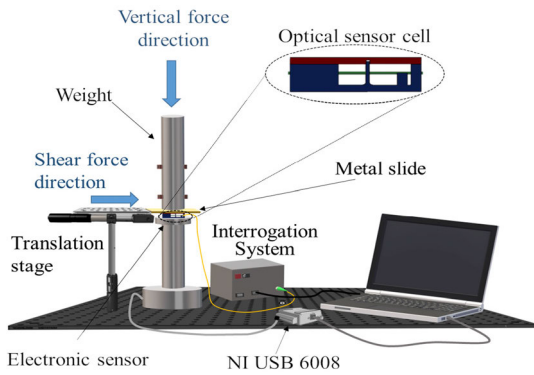To calibrate the sensor-cell to shear force, a metal plate was placed between the sensor-cell and a weight, which was properly tightened, preventing the movement over the plate. The plate was then pushed horizontally using a micrometric screw (translation stage) (Fig. 4). Thus, the plate slid parallel to the surface of the sensors (optical and electronic), causing SF (shear force) in both sensors, while the PF (plantar force) remained constant ($\Delta PF \approx 0$ N). For the vertical force calibration, several weights were used, in order to vary the force that was applied vertically in the sensor-cell, while the shear force was set constant ($\Delta SF \approx 0$ N).

During the PF and SF calibrations, the data from both sensors were simultaneously acquired for later comparison.

Figure 5 presents the data acquired by the reference electronic and optical devices, during the PF and SF calibrations. In Figs. 5a and 5b there is an increase (in module) of the force exerted on the sensor due to the placement of the weights over time and, as predicted, the SF remained constant ($\Delta SF \approx 0$ N). In the case of the optical sensor, this increase is observed by the Bragg wavelength shift on the two FBGs, being this behavior more accentuated for the FBG1, as expected (Fig. 5b).
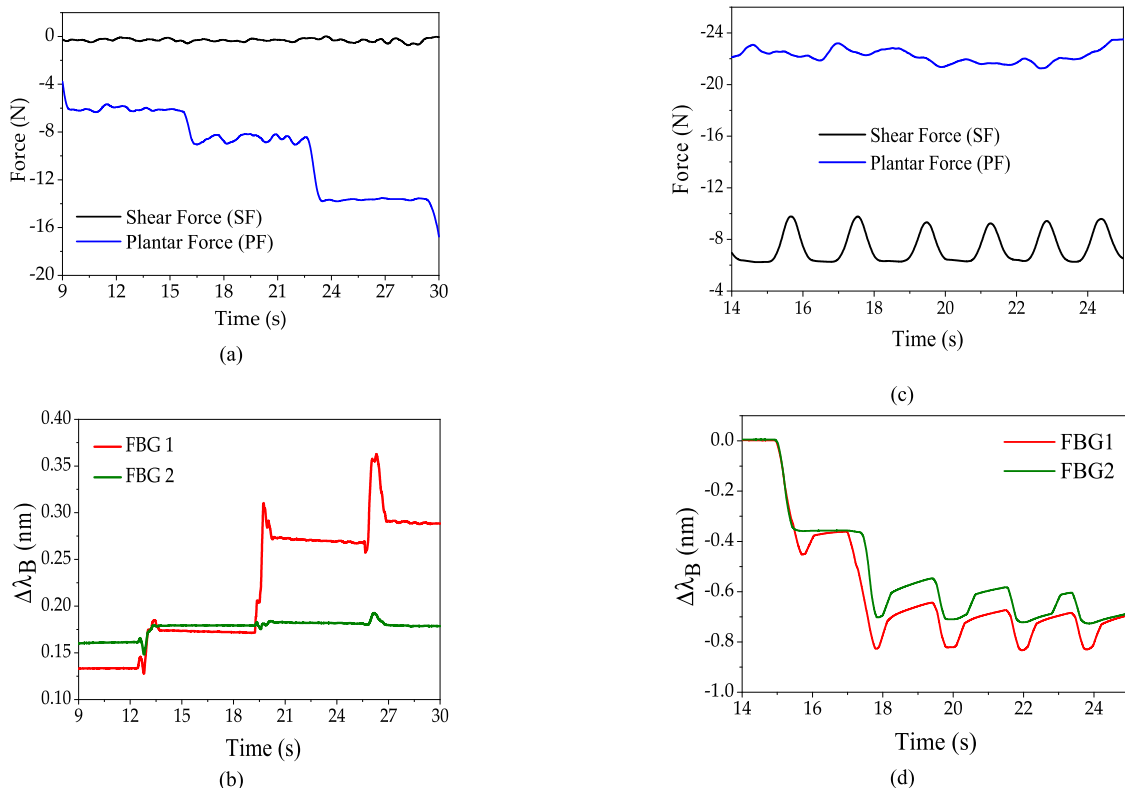

(a)

(b)

(c)

(d)

FIGURE 5. Data acquired by the electronic ((a) and (c)) and optical ((b) and (d)) devices, for the PF ((a) and (b)) and SF ((c) and (d)) forces.
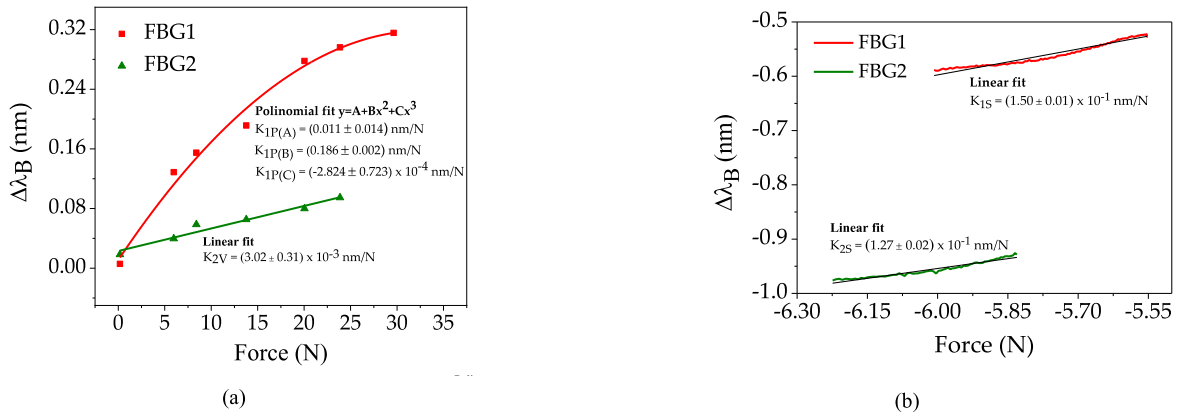
FIGURE 6. Bragg wavelengths shift as function of the PF (a) and SF (b), and their respective linear and/or polynomial fitting curves.

In the data acquired during the shear calibration (Figs. 5c and 5d), the periodic variations induced by the micrometer screw are observed in the response of both sensors. On the electronic device, one turn on the screw (equivalent to pushing the metal plate for a short period of time) corresponds to the zone of increased force, followed by a moment of relaxation (decrease force), until the screw is turned again. As the plantar force on the cell was kept constant throughout this procedure, the data acquired by the electronic sensor shows very small oscillations.

Aiming at the determination of the FBG1 and FBG2 sensitivities to plantar and shear forces, the data acquired with the electronic and optical sensors were correlated, being the results present in the Fig. 6.

The graphs show that there is a linear dependence of the FBG1 and FBG2 responses with the applied shear forces. When applying a vertical force, it was verified that the FBG2 present a linear response, whereas FBG1 has a polynomial behavior (Fig. 6a), mainly due to the elastic response of the resin. The sensitivities obtained for each of the FBGs to the plantar force (K_{1P} and K_{2P}) and to the shear force (K_{1S} and K_{2S}) are summarized in Table 1. Additionally, for the polynomial fit to the FBG1 data we have the coefficients A, B and C instead of just a single sensitivity value (called $K_{1P(A)}$, $K_{1P(B)}$ and $K_{1P(C)}$, respectively).

TABLE 1. Sensitivity coefficients (values in nm/N).

	PF	SF
FBG1	$K_{1P(A)}$= 0.011±0.014 $K_{1P(B)}$= 0.186±0.002 $K_{1P(C)}$= -2.824±0.723 x 10^{-4}	K_{1S}= (1.500±0.010) x 10^{-1}
FBG2	K_{2P}= (3.020±0.310) x 10^{-3}	K_{2S}= (1.270±0.020) x 10^{-1}

The wavelength shift of the FBGs can be related with the plantar (ΔF_P) and shear forces (ΔF_S) through the following system of equations:

$$\Delta\lambda_{B1} = \left(K_{1P(A)} + K_{1P(B)}.\Delta F_P + K_{1P(C)}.\Delta F_P^2\right) + K_{1S}.\Delta F_S$$
$$\Delta\lambda_{B2} = K_{2P}.\Delta F_P + K_{2S}.\Delta F_S \qquad (3)$$

After applying Equation (3) to the raw data of $\Delta\lambda_B$ values obtained from the optical device, it was possible to calculate the values of the corresponding force. Figure 7 compares the response of the optical and the electronic sensors (in terms of normalized forces), when the PF and SF were simultaneously applied. In Fig. 7a is presented the plantar force, while Fig. 7b depicts the shear force. The difference between the curves has a normalized mean square error of $RMSE_P = 0.119$ for the plantar force, and $RMSE_S = 0.153$ for the shear force.

The sensor-cell's response time and measurement repeatability were tested (Fig. 8) by placing and removing an identical load 10 times over a sensor-cell. From this test, it can be concluded that the average response time is 0.38 s for load applications and 0.44 s for load relief, and the sensor-cell present a negligible hysteresis, since it recovers its optical signal characteristics after several loading cycles.

IV. IMPLEMENTATION OF THE SENSOR-CELLS IN AN INSOLE

The insole was designed for the incorporation of four sensor-cells, being its structure printed in PLA on the 3D printer (BCN3D - R19). The four sensor-cells were strategically positioned at key points for the analysis of the gait cycle, namely heel (P1), 1st metatarsal (P2), hallux (P3) and 4th and 5th metatarsus area (P4), Fig. 9. Due to the multiplexing capabilities of FBGs, the number of sensor-cells can be increased, and their position can be adjusted according to the user's requirements. Here, we only present a proof-of-concept of the developed design, with four sensor-cells, placed at the locations more prone to develop ulcers due to the shear movement.

The insole contains eight FBGs inscribed into GF1 Nufern's photosensitive optical fiber multiplexed into two optical fiber cables, with Bragg wavelengths ranging from 1530 to
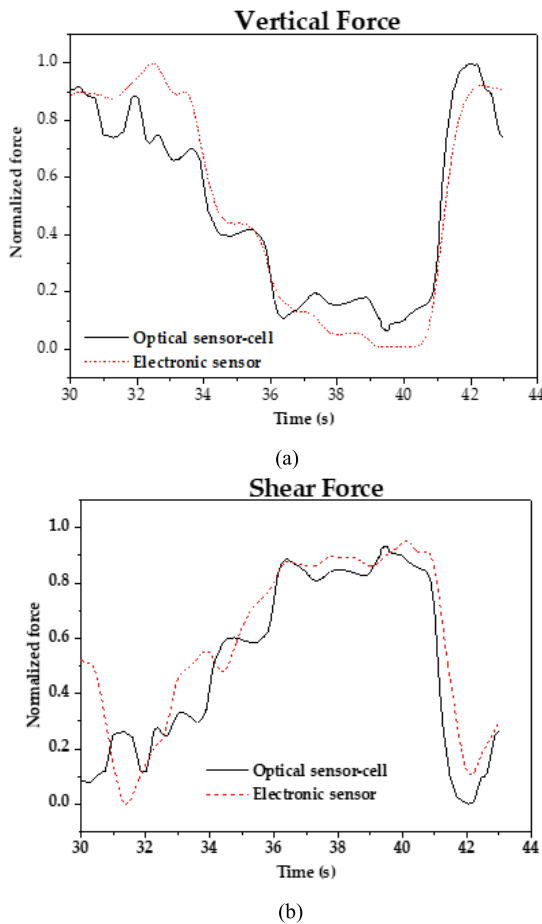
Vertical Force (a)

Shear Force (b)

FIGURE 7. Comparison of the normalized plantar (a) and shear (b) forces, acquired with the electronic device and the developed optical sensor.
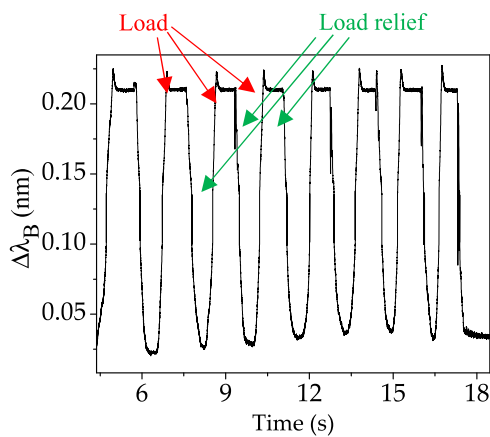
FIGURE 8. Determination of the response time and measurement repeatability of a sensor-cell.

FIGURE 9. (a) Design of the insole PLA structure; (b) Instrumented insole with four sensor-cells and one temperature sensor.

coupler into 1 channel of the optical interrogator, aiming to avoid a tight curvature on the big toe, and consequently a signal attenuation.

Besides the PLA-base, the insole is composed by an epoxy resin layer (with a thickness of $\approx$1 mm) that provides strength, comfort, and protection to the optical fibers.

Figure 9b shows a picture of the insole after its instrumentation with the four sensor-cells. For simplicity, we adopted a nomenclature using a number and a letter. The 1, 2, 3 and 4 refer to the sensor-cell position, and the letters S and P concern to the shear and plantar forces. As example, 1S will represent the shear force for the sensor-cell in the position 1.

In order to evaluate the sensors temperature stabilization time, an FBG temperature sensor (FBG_T) was also adapted to the insole in order to monitor the temperature variations. This evaluation, prior to the insole implementation, shows that the Bragg wavelength shift registered during the gait cycles is the result of only the applied forces actuating on the sensor-cells, as no significant temperature variations occur after the stabilization period (Temp, Fig. 9b).

To determine the temperature stabilization time, FBG_T was monitored during 30 minutes with insole worn (Fig. 10). From the graph, it can be deduced that the value of the wavelength shift stabilizes after around 3 minutes.
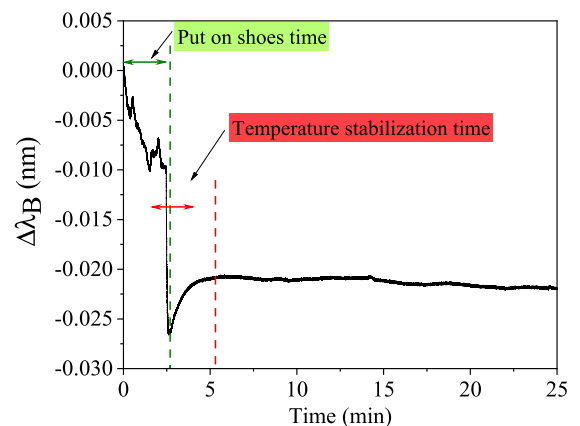
FIGURE 10. Determination of the temperature stabilization time.

1562 nm. One of the optical fiber cables is placed on the right side of the insole and has only the sensor-cell 4 (P4); the other fiber is on the left side and has the sensor-cells 1, 2 and 3 (P1, P2 and P3). Although it was possible to use only one optical fiber cable, we decided to use two optical fibers, and to multiplex the signal using an external 2 × 1 optical
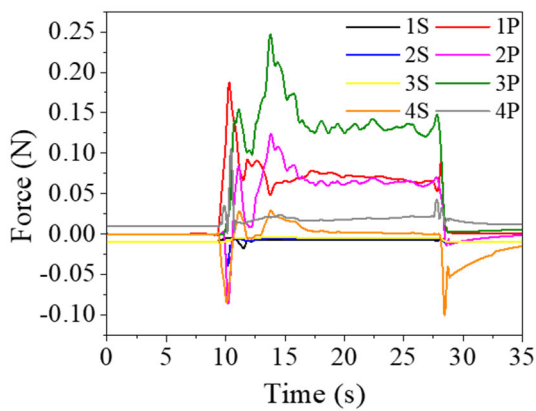
FIGURE 11. Instrumented insole's data acquired during the stability test of the center of mass.

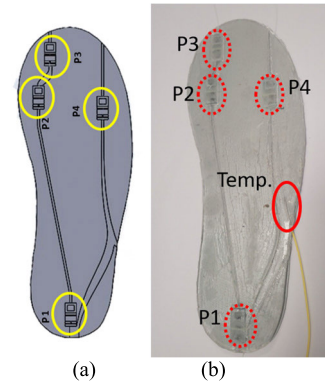
FIGURE 12. Behavior of the insole's four sensor-cells over four steps, with a zoom-in of the 1st step section, and with photograph of the instrumented insole to aid in the location of each sensor-cell in the insole.

The performance of the insole was first evaluated during a static test, in which one subject (female, 46 kg) remained static with the right foot supported on the entire surface of the insole, for about 20 s (Fig. 11). This test aims to evaluate the performance of the insole during the center of mass stability study, and to evaluate its response to plantar and shear force values.

The data presented in Fig. 11 can be analyzed by sections, according to the time/ evolution of the test and the respective stability of the center of mass: from 0 to 10 s is the time corresponding to the start of the test without any force applied to the insole; from 10 to 17 s is the allocation of the foot on the shoe with the insole and adjustment of the center of mass; from 17 to 28 s is the period that should be considered for analyzing the stability of the center of mass; and finally, the period after 28 s, corresponds to the insole exit.

By observing the data in Fig.11, it can be concluded that the sensors identified with the letter P (plantar) behave as expected: with positive Bragg wavelength shift, meaning that they have suffered positive vertical forces. We can also conclude that 3P was the zone that suffered the greatest force, which corresponds to the big toe area. The lowest value was registered for the 4P, which corresponds to the 4th and 5th metatarsal area. Regarding the sensors identified with the letter S (shear), their signal kept constant, with only visible changes in the process of placing and removing the foot in the insole, when a higher value of shear is also expected.

The tests were also carried out to evaluate the performance of the insole during the gait. For this, some slow steps were performed by the subject using the insole. It is important to note here that, this evaluation was only performed, after the insole were worn for 10 minutes, to ensure that the insole reaches the body temperature, thus minimizing the temperature influence. In Figure 12 it is represented four gait cycles acquired for the right foot during the insole performance evaluation. For graphical simplification, the timescale was reset to zero, close to the tests beginning.

As it can be seen in Fig. 12, in some locations (like P3), it is possible to clearly differentiate the plantar and the shear force
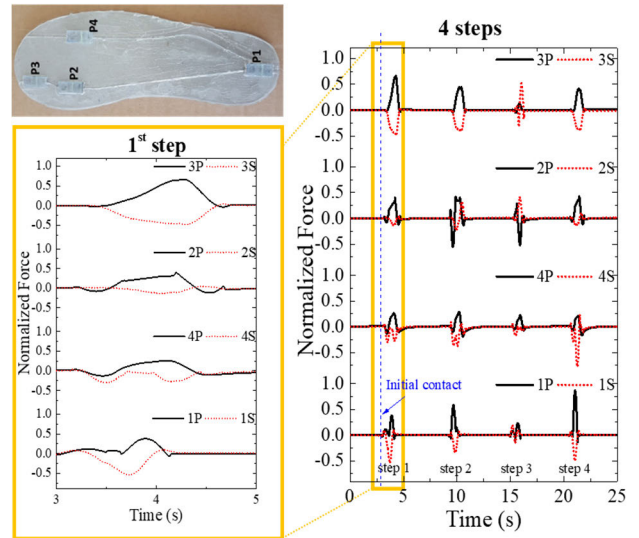
exerted in the anteroposterior direction [14]. This location at the toe area is known to induce a more prominent effect of shear, right before the toe off moment of the gait cycle. Also, as expected by the design of the sensor-cell, the sensitivity of the FBG1 is greater when plantar forces are applied, whereas the sensitivity of the FBG2 is higher for shear forces.

It is also possible to verify that the shear forces recorded are more pronounced at the beginning, and at the end of each step, which is in accordance with expected behavior reported in the literature [16].

Regarding the total performance of the instrumented insole, it is in line with what would be expected in relation to the activation order of each sensor-cell: heel, followed by the metatarsal zones and finally the hallux [14], which also shows the good isolation between points of analysis.

V. OVERALL DEVICE ARCHITECTURE

The overall optically instrumented insole system comprises three components: the sensing element (insole), the interrogator system, and the mobile app on a smartphone (Fig. 13). The first component, the instrumented insole with optical fiber sensors (FBGs), has been substantially explained throughout the paper.

The second component is the interrogator system, required to acquire the signal modulated in the sensor-cells of the insole. The acquisition signal, in Bragg wavelength shift, can be translated into plantar and shear forces, using the proposed equations' system (3).

The third component is the mobile app designed for smartphones and/or tablets. This multiple functionality app is used as a data processing tool to analyze the values acquired from our system. It also displays the real-time results and statistics from the measured data over a period of time, when required by the patient (or doctor/caregiver). It may also be configured

FIGURE 13. The overall optically instrumented insole system for gait plantar and shear force monitoring.

to provide alerts of critical force levels to the user, allowing to instantaneously correct the gait and body positioning. Finally, this app can also use the smartphone connectivity as a gateway for transmitting the results to a cloud. Thus, the medical team has continuous access to these data and may perform a more elaborate analysis of the patients' condition, allowing for better medical care.
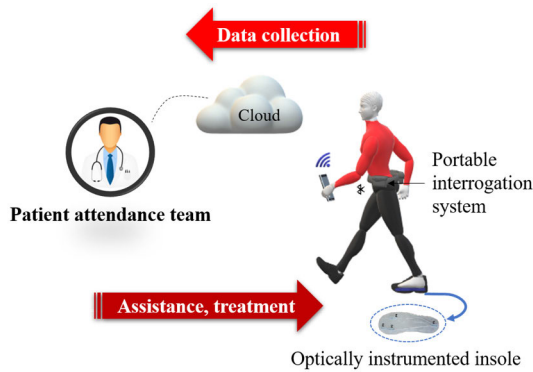
The implementation of such architecture, which can be adapted to the sensors here presented, has been reported and detailed in [36].

VI. CONCLUSION

In this work, a reliable optical fiber based solution for real-time monitoring of the plantar and shear forces in different zones of an insole was proposed. The developed system consists of a mesh of sensor-cells positioned in four key-points to measure plantar and shear forces. Each sensor-cell is composed by two in-line FBGs, that can be multiplexed in a single optical fiber cable. For ease of assembly, in the case of the insole here reported, we used two optical fibers.

This work stands out from the previous ones for its ability to measure two forces applied simultaneously in different directions with the same sensor, with a high level of detail.

The presented architecture, based on the optical fiber technology, is a small, compact and reliable solution, with low complexity. Because conventional electronic sensors have some problems when used in this application field, which include their inoperability to be used in damp/humid environments and sensitivity to electromagnetic interferences, an alternative detection system is proposed.

An overall device architecture was also presented aiming to the development of a portable system with a mobile software application which offers the user the real-time visualization of the forces that are being applied at each of the key-points in the insole and to alert him if the values exceed the recommended ones. Therefore, the application of this optical sensing device, as an e-Health tool, can be advantageous for users who are likely to have problems with pressure ulcers, or other problems related to the foot and/or the spine.

REFERENCES

[1] V. Kontis, J. E. Bennett, C. D. Mathers, G. Li, K. Foreman, and M. Ezzati, "Future life expectancy in 35 industrialised countries: Projections with a Bayesian model ensemble," *Lancet*, vol. 389, no. 10076, pp. 1323–1335, Apr. 2017.

[2] M. Domingues, C. Tavares, C. Leitão, A. Neto, N. Alberto, C. Marques, P. Antunes, and P. André, "Insole optical fibre Bragg grating sensors network for dynamic vertical force monitoring," *J. Biomed. Opt.*, vol. 22, no. 9, pp. 91507–91515, 2017, doi: 10.1117/1.JBO.22.9.091507.

[3] C. Tavares, M. F. Domingues, T. Paixão, N. Alberto, H. Silva, and P. Antunes, "Wheelchair pressure ulcer prevention using FBG based sensing devices," *Sensors*, vol. 20, no. 1, p. 212, Dec. 2019, doi: 10.3390/s20010212.

[4] M. F. Domingues, C. Tavares, V. Rosa, L. Pereira, N. Alberto, P. Andre, P. Antunes, and A. Radwan, "Wearable eHealth system for physical rehabilitation: Ankle plantar-dorsi-flexion monitoring," in *Proc. IEEE Global Commun. Conf. (GLOBECOM)*, Waikoloa, HI, USA, Dec. 2019, pp. 9–13, doi: 10.1109/GLOBECOM38437.2019.9014293.

[5] M. F. Domingues, N. Alberto, C. S. J. Leitao, C. Tavares, E. R. de Lima, A. Radwan, V. Sucasas, J. Rodriguez, P. S. B. Andre, and P. F. C. Antunes, "Insole optical fiber sensor architecture for remote gait analysis—An e-health solution," *IEEE Internet Things J.*, vol. 6, no. 1, pp. 207–214, Feb. 2019, doi: 10.1109/JIOT.2017.2723263.

[6] M. Verbunt and C. Bartneck, "Sensing senses: Tactile feedback for the prevention of decubitus ulcers," *Appl. Psychophysiol. Biofeedback*, vol. 35, no. 3, pp. 243–250, Sep. 2010, doi: 10.1007/s10484-009-9124-z.

[7] H. Brem, J. Maggi, D. Nierman, L. Rolnitzky, D. Bell, R. Rennert, M. Golinko, A. Yan, C. Lyder, and B. Vladeck, "High cost of stage IV pressure ulcers," *Amer. J. Surg.*, vol. 200, no. 4, pp. 473–477, Oct. 2010, doi: 10.1016/j.amjsurg.2009.12.021.

[8] L. Wang, D. Jones, G. Chapman, H. Siddle, D. Russell, A. Alazmani, and P. Culmer, "A review of wearable sensor systems to monitor plantar loading," *IEEE. Trans. Biomed. Eng.*, vol. 67, no. 7, pp. 1989–2004, Dec. 2020, doi: 10.1109/TBME.2019.2953630.

[9] S. Rajala and J. Lekkala, "Plantar shear stress measurements—A review," *Clin. Biomech.*, vol. 29, no. 5, pp. 475–483, 2014, doi: 10.1016/j.clinbiomech.2014.04.009.

[10] C. Bayón, S. Lerma, O. Ramírez, J. I. Serrano, M. D. Del Castillo, R. Raya, J. M. Belda-Lois, I. Martínez, and E. Rocon, "Locomotor training through a novel robotic platform for gait rehabilitation in pediatric population: Short report," *J. Neuroeng. Rehabil.*, vol. 13, no. 1, pp. 98–104, Dec. 2016, doi: 10.1186/s12984-016-0206-x.

[11] D. Zou, M. J. Mueller, and D. J. Lott, "Effect of peak pressure and pressure gradient on subsurface shear stresses in the neuropathic foot," *J. Biomech.*, vol. 40, no. 4, pp. 883–890, Jan. 2007, doi: 10.1016/j.jbiomech.2006.03.005.

[12] T. W. Kernozek, E. E. LaMott, and M. J. Dancisak, "Reliability of an in-shoe pressure measurement system during treadmill walking," *Foot Ankle Int.*, vol. 17, no. 4, pp. 204–209, Apr. 1996, doi: 10.1177/107110079601700404.

[13] M. N. Orlin and T. G. McPoil, "Plantar pressure assessment," *Phys. Therapy*, vol. 80, no. 4, pp. 399–409, Apr. 2000, doi: 10.1093/ptj/80.4.399.

[14] A. Completo and F. Fonseca, *Fundamentos de Biomecânica Músculo-esquelÉtica e Ortopédica*. Porto, Portugal: Publindustria, 2011.

[15] A. Muro-de-la-Herran, B. Garcia-Zapirain, and Mendez-Zorrilla, "Gait analysis methods: An overview of wearable and non-wearable systems," *Sensors*, vol. 14, no. 2, pp. 3362–3394, 2014, doi: 10.3390/s140203362.

[16] A. H. A. Razak, A. Zayegh, R. K. Begg, and Y. Wahab, "Foot plantar pressure measurement system: A review," *Sensors*, vol. 12, no. 7, pp. 9884–9912, 2012, doi: 10.3390/s120709884.

[17] R. Correia, S. James, S.-W. Lee, S. P. Morgan, and S. Korposh, "Biomedical application of optical fibre sensors," *J. Opt.*, vol. 20, no. 7, Jul. 2018, Art. no. 073003, doi: 10.1088/2040-8986/aac68d.

[18] D. Tosi, E. Macchi, and A. Cigada, "Fiber-optic temperature and pressure sensors applied to radiofrequency thermal ablation in liver phantom: Methodology and experimental measurements," *J. Sensors*, vol. 2015, Jan. 205, Art. no. 909012, doi: 10.1155/2015/909012.

[19] A. Lekholm and L. Lindström, "Optoelectronic transducer for intravascular measurements of pressure variations," *Med. Biol. Eng.*, vol. 7, no. 3, pp. 333–335, May 1969, doi: 10.1007/BF02474776.

[20] B. He, M. Li, J. Chen, W. Guo, G. Xu, and J. Xie, "An intensity-modulated fiber optic pressure sensor for hand-exoskeleton interactive force detection," in *Proc. 16th Int. Conf. Ubiquitous Robots (UR)*, Jeju, South Korea, Jun. 2019, pp. 750–754, doi: 10.1109/URAI.2019.8768686.

[21] D. Jia, J. Chao, S. Li, H. Zhang, Y. Yan, T. Liu, and Y. Sun, "A fiber Bragg grating sensor for radial artery pulse waveform measurement," *IEEE Trans. Biomed. Eng.*, vol. 65, no. 4, pp. 839–846, Apr. 2018, doi: 10.1109/TBME.2017.2722008.

[22] T. Allsop, K. Carroll, G. Lloyd, D. J. Webb, M. Miller, and I. Bennion, "Application of long-period-grating sensors to respiratory plethysmography," *J. Biomed. Opt.*, vol. 12, no. 6, 2007, Art. no. 064003, doi: 10.1117/1.2821198.

[23] A. V. Koulaxouzidis, M. J. Holmes, C. V. Roberts, and V. A. Handerek, "A shear and vertical stress sensor for physiological measurements using fibre Bragg gratings," in *Proc. 22nd Annu. Int. Conf. IEEE Eng. Med. Biol. Soc.*, Jul. 2000, pp. 23–28, doi: 10.1109/IEMBS.2000.900666.

[24] Z. F. Zhang, X. M. Tao, H. P. Zhang, and B. Zhu, "Soft fiber optic sensors for precision measurement of shear stress and pressure," *IEEE Sensors J.*, vol. 13, no. 5, pp. 1478–1482, May 2013, doi: 10.1109/JSEN.2012.2237393.

[25] K. Chethana, A. Prasad, S. Omkar, and S. Asokan, "Design and development of optical sensor based ground reaction force measurement platform for gait and geriatric studies," *Int. J. Mech. Mechatron. Eng.*, vol. 10, no. 1, pp. 60–64, 2016, doi: 10.5281/zenodo.1338606.

[26] M. Domingues, C. Tavares, C. Leitão, A. Neto, N. Alberto, C. Marques, A. Radwan, J. Rodriguez, O. Postolache, E. Rocon, P. André, and P. Antunes, "Insole optical fiber Bragg grating sensors network for dynamic vertical force monitoring," *J. Biomed. Opt.*, vol. 22, no. 9, p. 91507, 2018, doi: 10.1117/1.JBO.22.9.091507.

[27] D. Vilarinho, A. Theodosiou, C. Leitão, A. Leal-Junior, M. Domingues, K. Kalli, P. André, P. Antunes, and C. Marques, "POFBG-embedded cork insole for plantar pressure monitoring," *Sensors*, vol. 17, no. 12, p. 2924, 2017, doi: 10.3390/s17122924.

[28] C. Tavares, M. Domingues, A. Frizera-Neto, C. Leitão, N. Alberto, C. Marques, A. Radwan, E. Rocon, P. André, and P. Antunes, "Biaxial optical fiber sensor based in two multiplexed Bragg gratings for simultaneous shear stress and vertical pressure monitoring," *Proc. SPIE*, vol. 10680, May 2018, Art. no. 106802R, doi: 10.1117/12.2306889.

[29] C. Tavares, M. Domingues, A. Frizera-Neto, T. Leite, C. Leitão, N. Alberto, C. Marques, A. Radwan, E. Rocon, P. André, and P. Antunes, "Gait shear and plantar pressure monitoring: A non-invasive OFS based solution for e-health architectures," *Sensors*, vol. 18, no. 5, p. 1334, 2018, doi: 10.3390/s18051334.

[30] C. Tavares, M. Domingues, N. Alberto, A. Ramos, E. Rocon, P. André, H. Silva, and P. Antunes, "Bioinspired optical fiber sensor for simultaneous shear and vertical forces monitoring," *Proc. SPIE*, vol. 11028, Apr. 2019, Art. no. 110282M, doi: 10.1117/12.2522330.

[31] O. Al-Mai, J. Albert, and M. Ahmadi, "Development and characterization of compliant FBG-based, shear and normal force sensing elements for biomechanical applications," *IEEE Sensors J.*, vol. 20, no. 10, pp. 5176–5186, May 2020, doi: 10.1109/JSEN.2020.2969866.

[32] E. A. Al-Fakih, N. B. Arifin, G. Pirouzi, F. R. M. Adikan, H. N. Shasmin, and N. A. A. Osman, "Optical fiber Bragg grating-instrumented silicone liner for interface pressure measurement within prosthetic sockets of lower-limb amputees," *J. Biomed. Opt.*, vol. 22, no. 8, Aug. 2017, Art. no. 087001, doi: 10.1117/1.JBO.22.8.087001.

[33] J. R. Galvão, C. R. Zamarreño, C. Martelli, J. C. D. Silva, F. J. Arregui, and I. R. Matías, "Smart carbon fiber transtibial prosthesis based on embedded fiber Bragg gratings," *IEEE Sensors J.*, vol. 18, no. 4, pp. 1520–1527, Feb. 2018, doi: 10.1109/JSEN.2017.2786661.

[34] L. Armitage, G. Rajan, L. Kark, A. Simmons, and B. G. Prusty, "Simultaneous measurement of normal and shear stress using fiber Bragg grating sensors in prosthetic applications," *IEEE Sensors J.*, vol. 19, no. 17, pp. 7383–7390, Sep. 2019, doi: 10.1109/JSEN.2019.2914702.

[35] T. Leite, "Optical fiber solutions to physical rehabilitation systems and e-health applications," Univ. Aveiro, Aveiro, Portugal, Tech. Rep., 2018, pp. 616–718, vol. 535.

[36] J. Monge, O. Postolache, R. Alexandre, M. F. Domingues, and P. V. A. Viegas, "Fiber Bragg gratings solution for gait assessment," in *Proc. IEEE Int. Instrum. Meas. Technol. Conf. (IMTC)*, Dubrovnik, Croatia, May 2020, pp. 1–6.

CÁTIA TAVARES was born in Aveiro, Portugal, in July 1992. She received the master's degree in physics engineering from the University of Aveiro, Portugal, in 2016. She currently holds a DAEPHYS Ph.D. scholarship at Physics Department, Institute of Nanostructures, Nanomodelling and Nanofabrication, University of Aveiro. Her current research interest includes the development of optical fiber sensors for e-Health solutions.

FLÁVIA LEITE is currently pursuing the integrated master's degree in biomedical engineering with the University of Aveiro. Her research interests include projects in biomedical engineering area, namely in optical biosensors and medical imaging.

MARIA DE FÁTIMA DOMINGUES (Member, IEEE) received the M.Sc. degree in applied physics and the Ph.D. degree in physics engineering from the University of Aveiro, Portugal, in 2008 and 2014, respectively. In 2015, she held a research fellow position with the Instituto de Telecomunicações–Aveiro and the Consejo Superior de Investigaciones Científicas (CSIC), Madrid, Spain. She is currently a Researcher with the Instituto de Telecomunicações–Aveiro. She has authored or coauthored more than 80 journals and conference papers, several book chapters, and two books. Her current research interests include solutions of optical fiber-based sensors and its application in robotic exoskeletons and e-Health scenarios, with a focus in physical rehabilitation architectures.

TIAGO PAIXÃO received the B.S., M.S., and Ph.D. degrees in physics engineering from the University of Aveiro, Portugal, in 2014, 2016, and 2021, respectively. From 2016 to 2017, he was a Research Fellow with the Institute for Nanostructures, Nanomodelling and Nanofabrication (I3N) and the Telecommunications Institute (IT), Aveiro, Portugal. He is currently a Researcher with I3N and the University of Aveiro. His research interests include the development, optimization, and application of new optical fiber sensing architectures, based on fiber gratings and interferometers produced by nano and femtosecond lasers, to monitor physical and chemical parameters.

NÉLIA ALBERTO received the Ph.D. degree in physics from the University of Aveiro, Portugal, in 2011.

From 2012 to 2017, she worked under an FCT Postdoctoral Research Fellowship. In 2018, she was hired as a Researcher by the Instituto de Telecomunicações, Aveiro, Portugal. She has acquired expertise in the design and development of optical fiber sensors, fiber coatings, and application in different contexts, with special focus for medical environments. She is the author or coauthor of six book chapters, 44 articles in international peer-reviewed journals, and more than 60 papers in conference proceedings.
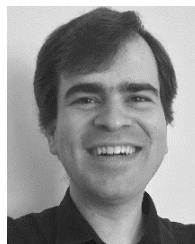
HUGO SILVA (Senior Member, IEEE) received the Ph.D. degree in electrical and computer engineering from the Instituto Superior Técnico (IST), University of Lisboa (UL). He has been a Researcher with the Instituto de Telecomunicações, since 2004. He has been a Co-Founder of multiple technology-based healthcare companies, since 2007. He is currently a Professor with the Instituto Superior Técnico, Universidade de Lisboa (IST-UL). His current research interests include biosignal research, systems engineering, signal processing, and pattern recognition. His work has been internationally distinguished with several academic and technical awards.

PAULO FERNANDO DA COSTA ANTUNES received the B.Sc. degree in physics engineering, the M.Sc. degree in applied physics, and the Ph.D. degree in physics engineering from University of Aveiro, Aveiro, Portugal, in 2005, 2007, and 2011, respectively. From 2017 to 2019, he was an Assistant Researcher with the Physics Department, Institute of Nanostructures, Nanomodelling and Nanofabrication (I3N), University of Aveiro. He is currently an Assistant Professor with the Department of Physics, University of Aveiro, and a Researcher with I3N and the Telecommunications Institute (IT). His research interests include the study and simulation of optical fiber sensors based on silica and polymeric fibers, for static and dynamic measurements, data acquisition, optical transmission systems, and sensor networks for several applications, such as temperature and strain measurements in extreme environments, structural monitoring, physical rehabilitation, and among others.

ANTÓNIO RAMOS received the Ph.D. degree in mechanical engineering from the University of Aveiro, Portugal, in 2005. From 2007 to 2019, he worked as a Researcher with TEMA–Aveiro, Portugal. His research interests include the study of medical devices, including long-term behavior focused in bone implant interaction, using experimental and computational model to predict the behavior and other field is product development in medical devices and clean energy.

. . .

MANUSCRIPT 5

sensors

Article

Wheelchair Pressure Ulcer Prevention Using FBG Based Sensing Devices

Cátia Tavares [1,2,*], M. Fátima Domingues [2,*], Tiago Paixão [1], Nélia Alberto [2], Hugo Silva [2,3,4] and Paulo Antunes [1,2]

[1] Department of Physics & I3N, University of Aveiro, Campus Universitário de Santiago, 3810-193 Aveiro, Portugal; tiagopaixao@ua.pt (T.P.); pantunes@ua.pt (P.A.)
[2] Instituto de Telecomunicações, Campus Universitário de Santiago, 3810-193 Aveiro, Portugal; nelia@ua.pt (N.A.); hsilva@lx.it.pt (H.S.)
[3] Department of Bioengineering, Instituto Superior Técnico, University of Lisbon, 1049-001 Lisboa, Portugal
[4] PLUX—Wireless Biosignals, S.A, Avenida 5 de Outubro n. 70, 1050-059 Lisboa, Portugal
[*] Correspondence: catia.tavares@ua.pt (C.T.); fatima.domingues@ua.pt (M.F.D.)

check for updates

13

Wheelchair Pressure Ulcer Prevention Using FBG Based Sensing Devices

Cátia Tavares [1,2,*] (ID)**, M. Fátima Domingues** [2,*] (ID)**, Tiago Paixão** [1] (ID)**, Nélia Alberto** [2] (ID)**,
Hugo Silva** [2,3,4] **and Paulo Antunes** [1,2] (ID)

[1] Department of Physics & I3N, University of Aveiro, Campus Universitário de Santiago, 3810-193 Aveiro,
   Portugal; tiagopaixao@ua.pt (T.P.); pantunes@ua.pt (P.A.)
[2] Instituto de Telecomunicações, Campus Universitário de Santiago, 3810-193 Aveiro, Portugal;
   nelia@ua.pt (N.A.); hsilva@lx.it.pt (H.S.)
[3] Department of Bioengineering, Instituto Superior Técnico, University of Lisbon, 1049-001 Lisboa, Portugal
[4] PLUX—Wireless Biosignals, S.A, Avenida 5 de Outubro n. 70, 1050-059 Lisboa, Portugal
* Correspondence: catia.tavares@ua.pt (C.T.); fatima.domingues@ua.pt (M.F.D.)

Abstract: In this work, a fiber Bragg grating (FBG) based sensing system for wheelchair pressure ulcer prevention was developed. Six FBGs were strategically positioned in a wheelchair to monitor the more prominent bone areas, namely scapulas (right (SR) and left (SL)), ischiatic zone (right (IR) and left (IL)), and heels (right (HR) and left (HL)). The sensing architecture was tested by a female user during pressure relief exercises, to verify its effectiveness on pressure monitoring. The proposed system proves to be a compact and reliable solution for wheelchair pressure ulcer prevention, making it a suitable alternative to existing conventional electronic sensors, with the advantage of being immune to electromagnetic interferences and usable in humid environments. In addition to the pressure, the breathing rate was also monitored. By combining the proposed sensing architecture with a wheelchair user detection software, it is possible to create alerts for the user to know when a new position should be adopted, in order to relieve the pressure in a specific area, thus avoiding one of the biggest problems for such patients, pressure ulcers.

Keywords: fiber Bragg grating; pressure ulcers; wheelchair; pressure sensors; breathing rate

1. Introduction

Pressure ulcers are localized lesions of the skin or underlying tissues that occur due to the decrease of the blood circulation inflicted by the increased pressure in specific zones of the body [1]. These injuries are directly related to life quality loss, higher risk of death, and higher healthcare costs due to all the treatment needed. In 2004, a scientific study revealed that in the USA, the cost of each pressure ulcer treatment could be up to $70.000/year, and the estimated total cost per year was around $1.6 billion [2]. There are more recent financial studies, but their focus is mainly on the specific causes of ulceration [3,4].

All patients who are permanently or even temporarily immobilized, for example in post-surgery situations, present high risk of developing pressure ulcers [5]. Wheelchair users, who are permanently immobilized, sitting in the wheelchair for more than eight hours a day, are one of the most at risk groups [5].

For a wheelchair user, the prominent areas of the body where the user is seated (scapulas, ischiatic zones, and heels) are the most prone zones to develop this pathology, see Figure 1 [1].
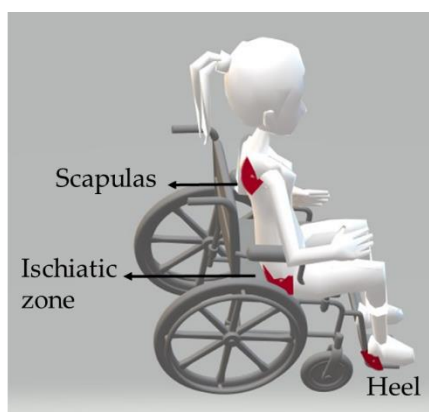
Figure 1. Representation of the most prominent bone zones for a wheelchair user.

Previous studies indicated that prevention is the key to reduce the health costs related to this pathology and improve the life quality of immobilized patients [2]. Thus, the scientific community has been investigating the influence of different parameters towards the reduction of the occurrence of this pathology, namely through the use of different support surfaces [6], types of diet [7,8], and patient repositioning [9,10]. At the same time, other scientific works have been published reporting the use of electronic sensors for wheelchair monitoring. These include devices for posture control and detection of the areas of higher pressure [1,5,10–14], sensors to identify fall risk postures [15], and a solution with an air cushion and pressure sensors that control the quantity of air in the cushion, according to the exerted pressure [16].

In this work, we present an alternative solution based on optical fiber Bragg grating (FBG) for the monitoring of pressure relief exercises for wheelchair users, targeting the prevention of ulcerations. Although the experimental setup used involves the use of an off-the-shelf interrogator, which may have some associated financial costs, this system can be replaced by other cost-effective interrogation techniques, like the ones based in edge filtering [17], which can considerably reduce both the size and the price of the overall sensing system.

Compared to their electronic counterparts, the advantages of the FBG technology include the ability to multiplex several sensors in one optical fiber, immunity to electromagnetic interferences, the possibility to be used in wet/humid areas without any encapsulation, and reduced weight and size [18–21]. Additionally, since no electrical current is needed at the measuring point, this sensing technique is intrinsically safer, allowing the design and implementation of a versatile and non-invasive sensing system, which can be used without affecting or compromising the user's comfort. Note that this system will be in contact with the subject's body, and the use of electronic sensors is not the most advisable, as they may suffer malfunctions due to the sweat of the body (humidity), or even be harmful to the patient/wheelchair user, due to the need to use electrical signals at the measuring point.

The proposed sensing system consists of a network with six FBGs sensors distributed over strategic zones of the wheelchair (chair back, chair seat, and footrest). The information retrieved with the proposed system will allow the monitoring of pressure relief exercises and further to evaluate if the users are performing them properly, and, consequently, to correctly instruct them. The potential connection of this sensing solution to an eHealth architecture [22] will also provide the medical staff with a continuous monitoring of the wheelchair user, offering a constant evaluation of the pressure exerted at the ulceration points. From the pressure results, the breathing rate can also be estimated. Based on the monitoring of such a vital sign, it is possible to detect critical situations as, for instance, the unconsciousness of the subject, or to collect relevant information for the early detection of diseases. This will contribute to increasing the quality and the efficiency of health treatment.

The paper is organized as follows. After this initial introduction (Section 1), Section 2 describes the produced FBG sensing element principle of operation. Section 3 focuses on the sensors development

and their calibration results. The implemented experimental protocols, the results, and discussion are addressed in Section 4, and the conclusion is presented in Section 5.

2. Fiber Bragg Grating Sensing Principle

The pressure in different wheelchair zones was monitored using FBGs. These sensors are characterized by presenting a perturbation in the refractive index along the fiber core. When an optical fiber containing an FBG is illuminated by a broadband light source, only a set of wavelengths that meet the Bragg condition are reflected, all the others are transmitted. The Bragg condition is given by the following equation:

$$\lambda_B = 2n_{eff}\Lambda \tag{1}$$

where λ_B is the reflected Bragg wavelength, n_{eff} is the effective refractive index of the optical fiber core, and Λ is the grating period.

The λ_B can be affected by changes in strain (Δl) and/or temperature (ΔT). Consequently, the reflected Bragg wavelength varies ($\Delta\lambda_B$), according to the following equation:

$$\Delta\lambda_B = \Delta\lambda_{B,l} + \Delta\lambda_{B,T} = 2\Big(\Lambda\frac{\partial n_{eff}}{\partial l} + n_{eff}\frac{\partial\Lambda}{\partial l}\Big)\Delta l + 2\Big(\Lambda\frac{\partial n_{eff}}{\partial T} + n_{eff}\frac{\partial\Lambda}{\partial T}\Big)\Delta T$$
$$= S_l\Delta l + S_T\Delta T \tag{2}$$

where the first term is related to the strain induced wavelength shift, and the last to the thermal effect on the same parameter. S_l and S_T represent the strain and temperature sensitivity coefficients of the FBG.

Aiming to improve the implementation procedures and protect the physical integrity of the sensing elements when subjected to pressure variations, the FBGs for the pressure monitoring were embedded into a thermosetting epoxy resin (LiquidLens) cylinder (Figure 2). Thus, when a pressure is applied to the upper face of the resin cylinder, it will distend, causing a strain also in the optical fiber, and consequently modulating the reflected Bragg wavelength (Figure 2).
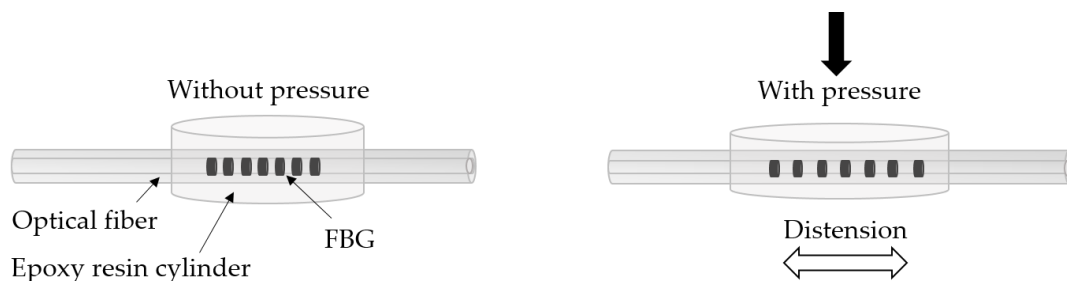
Figure 2. Sensor design and effect of pressure on the sensor.

3. Sensing System Preparation and Calibration

In this work, eight FBGs were inscribed into photosensitive optical fiber (GF1 Thorlabs), using a pulsed Q-switched Nd: YAG laser system (LOTIS TII LS-2137U Laser), lasing at the fourth harmonic (266 nm). The FBGs were recorded through the phase mask technique, employing a laser pump energy of 25 J, a repetition rate of 10 Hz, and an exposure time of 1 min, approximately.

Six Bragg gratings were recorded and multiplexed in the same optical fiber cable, spaced so that it is possible to monitor the pressure at the interest points on the wheelchair, namely both scapulas (right (SR) and left (SL)), both ischiatic zones (right (IR) and left (IL)), and both heels (right (HR) and left (HL)). The other two FBGs were inscribed in separated optical fiber cables for the temperature monitoring.

Each of the six FBGs multiplexed in the same fiber cable were subsequently embedded in an epoxy resin cylinder of 2 cm diameter, with the sensors positioned in the middle point of the cylinder (called cell).

After the FBG embedding process, the cells were characterized to pressure variations, ranging from 0 to 319 kPa, using a Shimadzu® AGS-5kND mechanical testing machine. Due to limitations in the

equipment, a non-constant pressure step was used, however the range was always the same (from from 0 to 319 kPa). The tests were repeated three times for each cell, and additionally the hysteresis phenomenon was also evaluated by decreasing the pressure applied on the sensing cells after increasing. The response of the optical sensors was monitored using an interrogation system with an acquisition rate of 960 Hz (I-Mon USB 512, Ibsen).

The results of the calibration test for the SL cell, for the three tests, are shown in Figure 3a. In Figure 3b the experimental data obtained from the hysteresis test for the same cell is depicted.
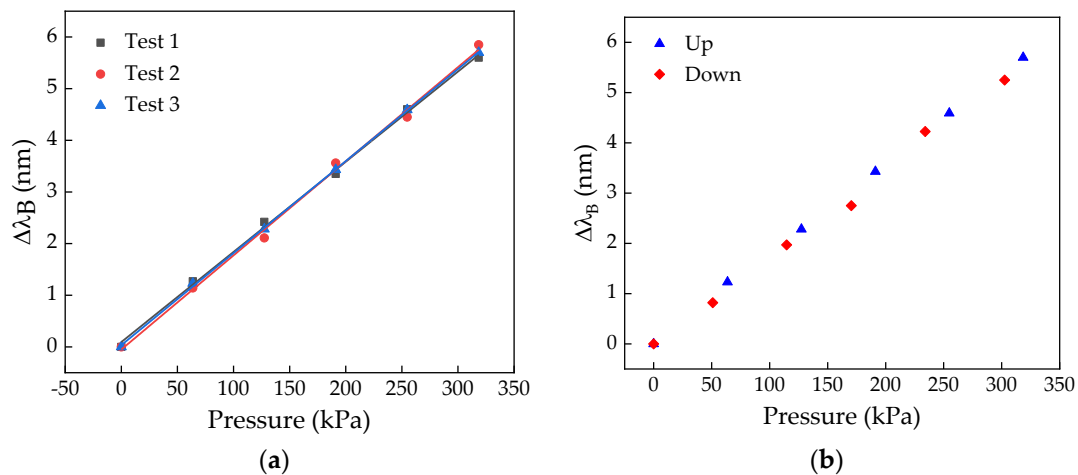
Figure 3. Results of the calibration (**a**) and hysteresis (**b**) tests for the left scapula (SL) cell.

For all the tests, a linear dependence of the Bragg wavelength shift with the applied pressure was verified, being the sensitivity coefficient given by the mean value of the slopes of the linear fits to the experimental data, in this particular case 17.8 ± 0.3 pm/kPa. As can be observed from the data in Figure 3b, the hysteresis effect is very low, and thus can be neglected.

Table 1 shows the sensitivity coefficient of each cell to the pressure variations. The values are not the same for all the cells, since it is difficult to precisely reproduce the sensing cells. However, this behavior has no influence on the final results, given that it is necessary to calibrate all cells individually, prior to their application.

Table 1. Sensitivity coefficient of each cell to the applied pressure.

Cell	Sensitivity Coefficient (pm/kPa)
Right heel (HR)	9.6 ± 0.1
Left heel (HL)	10.2 ± 0.2
Right scapula (SR)	18.2 ± 0.2
Left scapula (SL)	17.8 ± 0.3
Right ischiatic (IR)	17.9 ± 0.3
Left ischiatic (IL)	18.5 ± 0.2

Since the Bragg wavelength varies with pressure (induced strain) and temperature changes (Equation (2)), after the pressure calibration, and before the wheelchair pressure monitoring, the thermal sensitivity of the sensing cells was determined. The temperature was increased from 10.0 to 45.0 °C, with a step increment of 5.0 °C, using a climatic chamber (CH340, Angelantoni Industrie). For each temperature level, and after a stabilization period of 20 min, the reflected Bragg wavelength was registered. As for the pressure tests, different thermal sensitivity coefficients were obtained, ranging from 17.8 pm/°C to 19.1 pm/°C, for the SR and SL cells, respectively. These values are almost double with regard to the thermal sensitivity of 10 pm/°C obtained for a standard FBG. This difference is attributed to the thermal expansion coefficient of the epoxy resin where the FBGs were embedded [23].

4. Wheelchair Pressure Monitoring

4.1. Protocol and Implementation

After the calibration process, the six cells were strategically placed in high pressure zones for wheelchair users, namely SL, SR, IL, IR, HL, and HR, as shown in Figure 4a. In the case of the scapulas and ischiatic zones, the cells were glued with a strong double-sided duct tape to the wheelchair, where it contacted with the bony prominence regions of the user. The sensors for heel pressure monitoring were implemented into cork insoles [22] of appropriate size, which were adapted to the user's shoes. In Figure 4b we present a schematic representation of the overall experimental setup, which comprises the multiplexed FBG sensor network attached to the wheelchair and insoles, the optical interrogator, and the computer for data acquisition. The tests were realized in indoor conditions with the temperature almost constant during the entire experiment (21 °C).

(a)   (b)
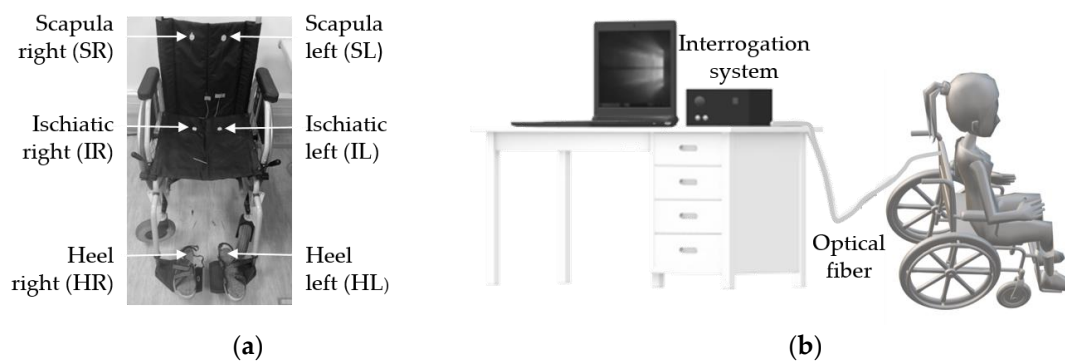
Figure 4. (**a**) Wheelchair with the six sensing cells; (**b**) Schematic representation of the experimental setup.

With the cells placed in the target zones, a volunteer was asked to sit in the wheelchair and the FBG modulated signal was continuously monitored while the subject executed different pressure relief exercises. As the name suggest, the performed exercises were intended to relieve the pressure in areas most prone to pressure sores in wheelchair users, i.e., in scapulas, ischiatic, and heel zones [14].

Figure 5 shows the user positions during the exercises implemented for pressure relief, corresponding to the normal position (NP) and the different pressure relief situations: small frontward lean (A), intermediate frontward lean (B), full frontward lean (C), without feet support (D), intermediate sideward lean (Left—E; Right—G), and full sideward lean (Left—F; Right—H). To standardize the movements, the subject always put his hands, arms, and feet as represented in Figure 5. In the intermediate sideward lean position, only one scapula is in contact with the wheelchair, while in the full sideward lean position there is no contact with the wheelchair. In these positions (E, G and F, H), the arm is supported on a table, 10 and 20 cm apart from the wheelchair, respectively.
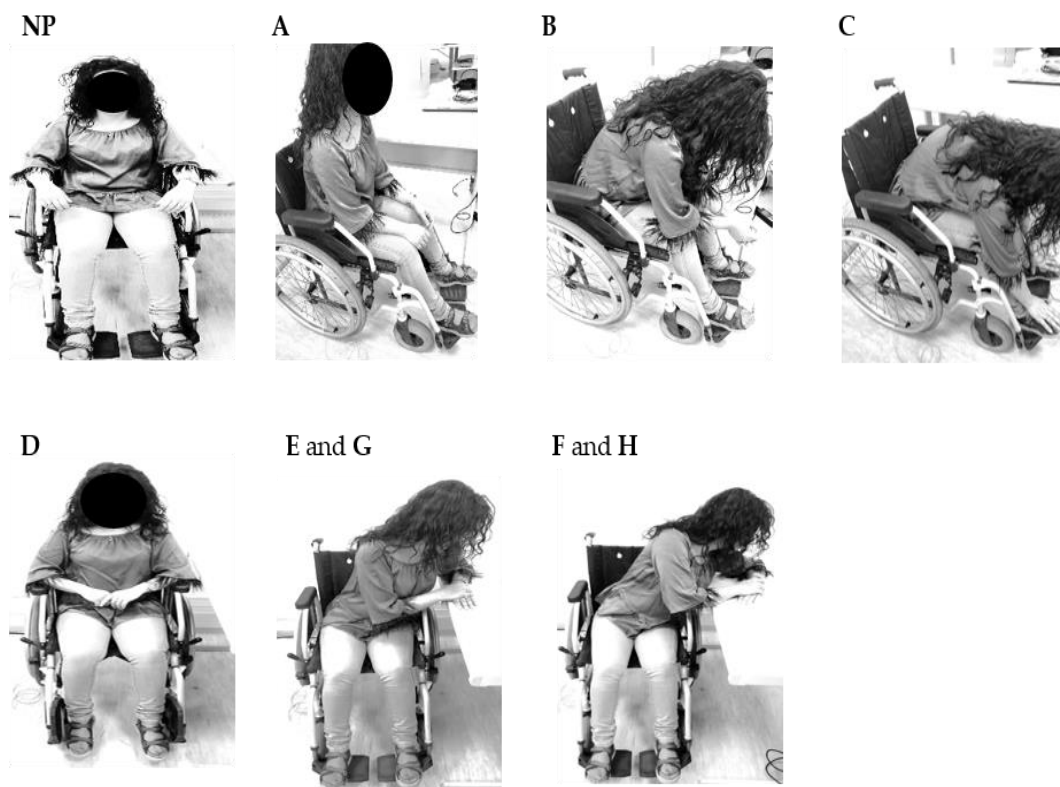
Figure 5. Representation of the nine positions adopted during the pressure relief tests.

The tests were performed on a female person (37 years), without mobility pathologies, with the aim to assess the capability of this system to detect pressure variations during different pressure relief positions.

According to the work reported in [14], before performing any pressure relief position, the subject should be in the NP for at least 2 min, to stabilize blood flow, and therefore the pressure on the skin surface. Nevertheless, since the Bragg wavelength varies simultaneously with the pressure (strain) and the temperature (Equation (2)), a waiting period of 14 min (12 min plus the 2 min recommended on [14]) was used in the NP position, before the volunteer moved to the first pressure relief position (A). After this temperature stabilization period, a significant temperature variation was not expected to be registered during the tests. As suggested in the previous study [14], the volunteer was also asked to remain in the NP position for 2 min before moving to the other pressure relief positions. The relief positions were maintained for 1 min.

To investigate the thermal influence on the pressure values, two temperature sensors, consisting of FBGs inside a double needle [24] for strain isolation, were put on the wheelchair. One was positioned close to the right scapula, and the other close to the right ischiatic, since these were the areas in which a higher temperature variation was expected during the pressure relief exercises. The heels were not included in this study, since, except for the D position, the location of the feet remains unchanged. In the case of the D position, the feet are removed from the wheelchair supports, and although there is a pressure relief, it is not expected that there is a significant temperature change, since the feet remain in contact with the cells/cork insoles. This is corroborated by results of previous studies, regarding the use of FBG sensors in the production of an insole for gait analysis, which showed that the temperature variation for this type of application can be neglected [25].

The sequence of the pressure relief exercises carried out in this temperature test was the same as that described for the pressure test. Briefly, prior to any exercise, there was a stabilization period of 14 min (12 min + 2 min corresponding to the NP position), followed by several pressure relief positions during 1 min, intercalated by 2 min in the NP position. Note that in this work there is no temperature

compensation on the pressure results, and the main aim of this test was to assess the error induced on the pressure results when the thermal effect is not compensated.

4.2. Results and Discussion

Figure 6 shows the response of the sensing cells for the several pressure relief positions. These values were obtained from the Bragg wavelength shift collected during the experimental tests and considering the sensitivity coefficient for each cell (Table 1). The negative pressure values are due to pressure relief in those areas. Upon data analysis, the initial Bragg wavelength was considered at the beginning of the tests, with the subject already seated in the chair, and therefore, with an initial pressure already applied on the sensors. In that way, when the pressure is relieved in a given sensor, there is a decrease in the grating modulation period, and consequently a negative wavelength shift compared with the reference initial Bragg wavelength. For simplicity of nomenclature, each graph is called by the name of the relief position that was tested (A, B, C, D, F, G, and H). However, all the tests started in the NP position, which was maintained during 2 min, followed by the position to be monitored. To simplify the results interpretation, only the signals related to the sensors where significant pressure changes were obtained are represented. Therefore, the response of the cells positioned in the heel is only represented in the graph corresponding to the pressure relief in the feet (D).

In general, all sensors responded to the wheelchair user position changes by sudden variations in the detected signal amplitudes. Also, it should be noted that, the oscillations for the SR, SL, IR, IL signals can be attributed to the subject's breathing, allowing the estimation of the breathing rate, which is also evaluated in this discussion. In the following, a detailed analysis of the results obtained by the optical sensors (Figure 6) during the various pressure relief positions (Figure 5) is presented.

In test A, the user places herself in a position where the posture angle is approximately 90° and her back is only slightly in contact with the wheelchair. This position change is reflected in the signal detected by the sensors, which in the case of SR there is a reduction of 6.5 kPa, and an increase of 22.1 kPa in the case of IR.

In test B, the user leans forward and places her arms over the legs. As expected, there is a decrease of the pressure registered in the cells positioned in the scapulas, and an increase in the case of the ischiatics, slightly less than in test A, because the upper body is positioned more over the ischiatic sensors in position A than in position B. The higher pressure relief detected in the left scapula intensities (13.7 kPa difference from the right scapula) is an indication that the user was slightly tilted to the left in the NP position, applying a stronger pressure in that sensor, which leads to a higher wavelength shift variation upon the position change (pressure relief).

In test C, the user bends totally forward putting her hands in contact with her feet. In this test, as in the previous ones, the pressure decreases in the scapulas and increases in the ischiatic regions. Again, a greater pressure relief is felt on the left side than on the right side with about 7.2 kPa difference.

In test D, the user is normally seated in the wheelchair but without the footrest, so as expected, a lower pressure is felt in the HL and HR. As the feet are raised, higher pressure is transferred to the ischiatic area, as also detected by the sensors located in that zone. Since this exercise only involves removing of the feet from the wheelchair supports, the pressure exerted by the feet on the insoles, and consequently on the sensing cells is much lower than that exerted on the scapulas and ischiatic regions. Thus, the amplitude of the pressure is different for the pressure values registered for the others pressure relief positions. Further, in previous work [22], a similar cork insole was used for the gait analysis, and higher pressures than those reported in this work were measured, which indicates that there is no limitation on the sensitivity.
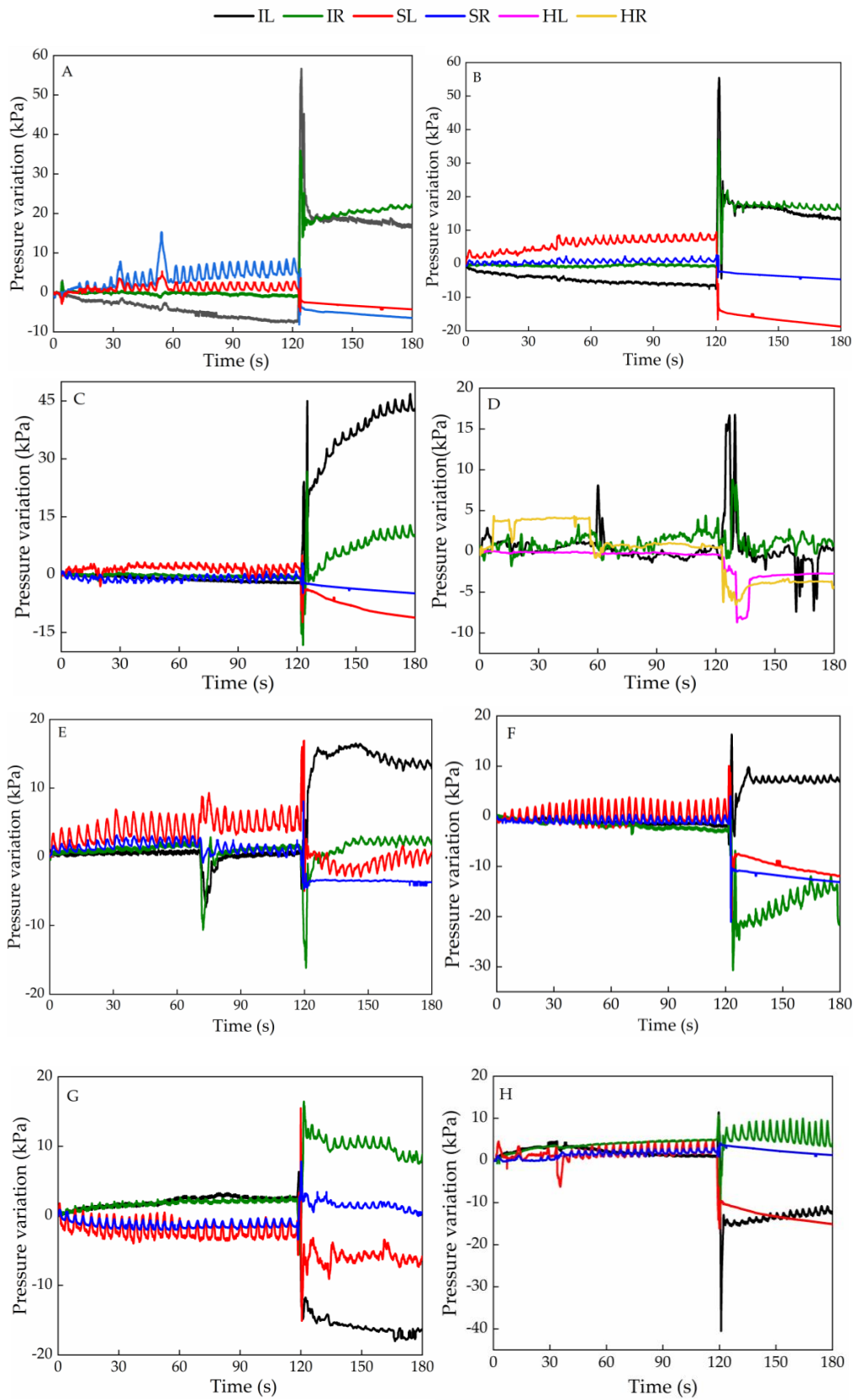
Figure 6. Pressure variation registered in different cells during the pressure relief exercises (**A–H**).

In test E, the user places the left arm on a side table 10 cm from the wheelchair so that the right scapula is not in total contact with the wheelchair. In this test a decrease on the signal amplitude of SR

and the IR is expected. In this case, a decrease of 3.6 kPa and an increase of 2.2 kPa were obtained, respectively. Contrarily, there is an increase for the case of the sensors at the SL zone (slight initial increase) and IL (increasing 15.0 kPa). As test G corresponds to the same pressure relief exercise, but to the right side, an opposite behavior should be expected. According to the results obtained, there should be greater contact (increasing of the pressure) between the right shoulder blade and the chair, as well as an increase in the pressure felt at the IR. This was detected by the sensors placed at those locations (1.7 and 9.8 kPa for the SR and IR, respectively). As for the IL and the SL, a pressure relief was also detected by the sensors placed in those specific locations with a decrease in the pressure values, 16.4 and 6.5 kPa, respectively.

In test F, the user places her left arm on the side table 20 cm away. In this position both scapulas are no longer in contact with the wheelchair. As expected, a decrease in the pressure on the SL and SR sensors was obtained, 11.7 and 13.1 kPa, respectively. A relief on the IR (14.1 kPa) and an increase in the IL (7.3 kPa) was registered as the user shifts her weight to the left side. In test H, the user repeats the pressure relief position, but this time to the right side, and also in this test the sensors respond as expected: decrease in the pressure felt at the IL (11.9 kPa) and at the SL (15.1 kPa) and slight increase of pressure felt at the IR (6.4 kPa) and SR (1.3 kPa).

Considering the pressure range used in the sensor characterization tests and the pressure amplitude in the graphs of Figure 6, we predict that the proposed architecture could be used by heavier subjects without breaking risk. The pressure values are dependent on the subject´s weight. Regarding the time of contact for the ulcer occurrence, in the literature, there is no agreement about that value, nevertheless, it is known that it varies according to the person's physiology and skin condition, and the authors from [14] advise the execution of pressure relief exercises during 30 s every 30 min.

Figure 7 shows the temperature variation obtained during the pressure relief tests, for the sensors positioned on the right scapula and right ischiatic, identified as SR_T and IR_T, respectively. Note that this experiment was carried out after the wheelchair test. An accentuated increase in the temperature, mainly in the first 10 min (about 7 °C) was observed. Hence, initially, a stabilization period of 14 min was considered, during which the temperature changes as the result of the temperature difference between the environment and the wheelchair user's body. After the first 14 min of the experiment, and as expected, a small temperature variation (about 0.6 °C) was registered by the sensor positioned in the IR, since the sensor is in contact with the wheelchair user during the whole experimental test (different pressure relief positions). In the case of the sensor positioned in the SR, a notable decrease of the temperature was obtained during the pressure relief exercises involving the loss of contact between the wheelchair user and the sensors. Examples of this situation are the positions B, C, and F. The maximum temperature difference obtained for these cases was about 2 °C. Considering the thermal sensitivity difference between the temperature sensors and the cells (as result of the resin where the FBG was embedded), the 2 °C may lead to an error of around 2 kPa in the pressure determination. However, we point out that this will be the maximum error, and for most of the pressure relief positions it will be lower. In future work, a rigorous temperature control will be carried out, with the inclusion of temperature sensors in the experimental setup. Moreover, each sensing cell could have embedded two FBGs with distinct sensitivities (separation of effects by the matrix method), or, for instance, to be composed of two FBGs, with one of them encapsulated, eliminating the sensitivity to strain/pressure variations.

Parallel to the pressure detected according to the user's position, a smaller oscillation in the signal is also detected in the first 2 min in the NP, related to the subject's breathing rate, Due to the sensing cell positions, this phenomenon is not as clear in the IR and IL zones as it is in the case of the SR and SL, so the breathing rate is estimated from the data obtained for the sensors located at the scapula, Figure 8a.
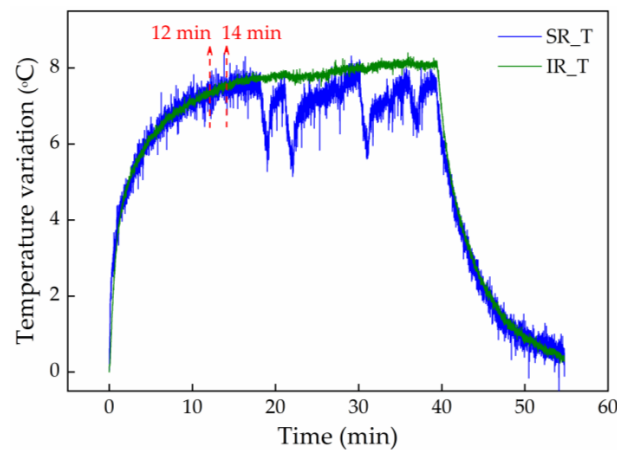
Figure 7. Thermal variation obtained during pressure relief exercises for the sensors positioned in the right scapula and ischiatic.

(**a**)　　　　　　　　　　　　　　　　　　　　　　　　　(**b**)
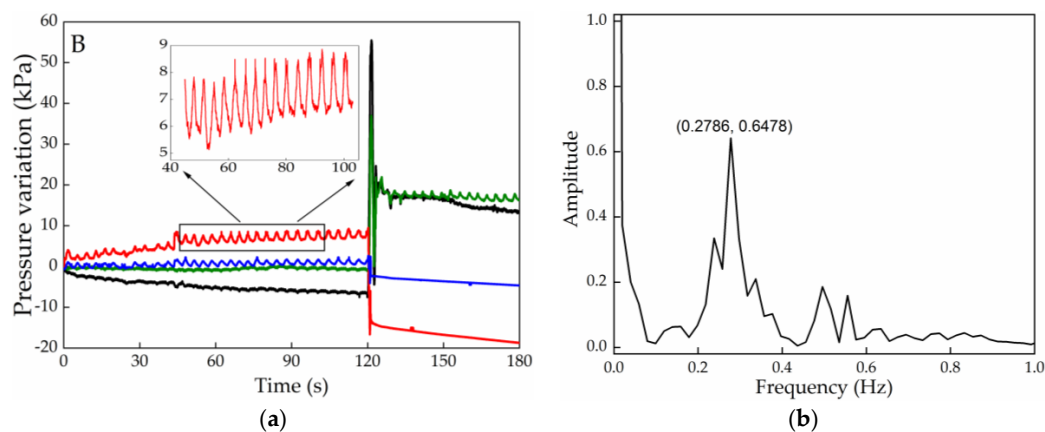
Figure 8. (**a**) Pressure variation registered in different cells, highlighting the SL cell results, during the pressure relief exercise B; (**b**) Fourier transform applied to the optical signal detected by the SL and highlighted in Figure 8a, for wheelchair user breathing rate determination.

Figure 8b depicts data of the Fourier transform applied to the initial values registered by the SL cell during the initial part of test B. The highest intensity peak corresponds to a frequency of 0.28 Hz, which is within the frequency range expected for a resting adult (up to 20 breaths/min, which equals a frequency of 0.33 Hz [26]). For the IR position a similar value was also obtained (0.29 Hz). Such results give also a new prospective on the application of this sensing architecture for detecting breathing related pathologies, such as asthma episodes and the moment when they are triggered, or even some psychological related disorders such as anxiety conditions.

5. Conclusions

In this work, a reliable solution for monitoring, in real time, the pressure in different zones of a wheelchair was proposed. The system consists of a mesh of six FBGs positioned in prominent bone areas, namely scapulas (R and L), ischiatic zone (R and L), and heels (R and L). The results showed that the use of this system based on optical fiber sensors offers a solution that is reliable, fast, small, and compact, making it an alternative solution to conventional electronic sensors.

The application of this system as an e-Health tool can offer advantages to patients prone to develop neuropathic ulcers in risk zones, where a continuous evaluation of the pressure points can be accessed, and the data retrieved can be continuously transferred to care centers or to associated medical staff. On envisaging a full stand-alone application associated with such architecture, alerts for pressure relief

exercises can be given to the user and emergency warnings can be sent to hospitals in critical situations. Additionally, with the proposed system it is possible to retrieve information regarding the breathing rate of the user, important information when considering the pathologies that can be inferred from it, particularly for elderly or debilitated users.

On contemplating the application of this sensing architecture in real context, and considering scenarios of the movement of patients with reduced mobility, special attention should be given to the robustness of the whole sensing system. This includes the improvement of the junction between the epoxy resin cylinder and the outgoing fiber (specially designed protection sleeves can be considered). The protection of the optical fiber connecting the multiplexed sensors should also be optimized.

In the future, it is also planned to compensate the temperature effect during pressure monitoring, and to provide the system with a mobile application that alerts the user to change his/her position to avoid ulcers. Also, the interrogation system will be replaced by including edge filtering techniques for the sensors analysis, which will be a financially affordable solution for the broader use of the proposed technology.

Author Contributions: C.T. and M.F.D. designed and implemented the experiments, and wrote the manuscript. N.A. realized the thermal characterization and contributed to the manuscript writing. T.P. inscribed the fiber Bragg gratings and revised the manuscript. H.S. and P.A. contributed to the results discussion and the manuscript revision. All authors have read and agreed to the published version of the manuscript.

Conflicts of Interest: The authors declare no conflict of interest. The founding sponsors had no role in the design of the study; in the collection, analyses, or interpretation of data; in the writing of the manuscript, and in the decision to publish the results.

References

1. Verbunt, M.; Bartneck, C. Sensing senses: Tactile feedback for the prevention of decubitus ulcers. *Appl. Psychophysiol. Biofeedback* **2010**, *35*, 243–250. [CrossRef] [PubMed]
2. Gordon, M.; Gottschlich, M.; Helvig, E.; Marvin, J.; Richard, R. Review of evidenced-based practice for the prevention of pressure sores in burn patients. *J. Burn Care Res.* **2004**, *25*, 388–410. [CrossRef] [PubMed]
3. Banks, M.; Graves, N.; Bauer, J.; Ash, S. The costs arising from pressure ulcers attributable to malnutrition. *Clin. Nutr.* **2010**, *29*, 180–186. [CrossRef] [PubMed]
4. Brem, H.; Maggi, J.; Nierman, D.; Rolnitzky, L.; Bell, D.; Rennert, R.; Michael, M.; Alan, M.; Courtney, N.; Bruce, V. High cost of stage IV pressure ulcers. *Am. J. Surg.* **2010**, *200*, 473–477. [CrossRef] [PubMed]
5. Dai, R.; Sonenblum, S.; Sprigle, S. A robust wheelchair pressure relief monitoring system. In Proceedings of the 2012 Annual International Conference of the IEEE Engineering in Medicine and Biology Society, San Diego, CA, USA, 28 August–1 September 2012.
6. Brienza, D.; Kelsey, S.; Karg, P.; Allegretti, A.; Olson, M.; Schmeler, M.; Zanca, J.; Geyer, M.; Kusturiss, M.; Holm, M. A randomized clinical trial on preventing pressure ulcers with wheelchair seat cushions. *J. Am. Geriatr. Soc.* **2010**, *58*, 2308–2314. [CrossRef] [PubMed]
7. Houwing, R.; Rozendaal, M.; Wouters-Wesseling, W.; Beulens, J.; Buskens, E.; Haalboom, J. A randomised, double-blind assessment of the effect of nutritional supplementation on the prevention of pressure ulcers in hip-fracture patients. *Clin. Nutr.* **2003**, *22*, 401–405. [CrossRef]
8. Bourdel-Marchasson, I.; Barateau, M.; Rondeau, V.; Dequae-Merchadou, L.; Salles-Montaudon, N.; Emeriau, J.; Manciet, G.; Dartigues, J. A multi-center trial of the effects of oral nutritional supplementation in critically ill older inpatients. *Nutrition* **2000**, *16*, 1–5. [CrossRef]
9. Defloor, T.; Bacquer, D.; Grypdonck, M. The effect of various combinations of turning and pressure reducing devices on the incidence of pressure ulcers. *Int. J. Nurs. Stud.* **2005**, *42*, 37–46. [CrossRef]

10. Young, T. The 30 degree tilt position vs the 90 degree lateral and supine positions in reducing the incidence of non-blanching erythema in a hospital inpatient population: A randomised controlled trial. *J. Tissue Viability* **2004**, *14*, 88–96. [CrossRef]

11. Shirreffs, B.; Ferguson-Pell, M. Remote monitoring of sitting behavior of people with spinal cord injury. *J. Rehabil. Res. Dev.* **2002**, *39*, 513–520.

12. Chenu, O.; Vuillerme, N.; Bucki, M.; Diot, B.; Cannard, Y. TexiCare: An innovative embedded device for pressure ulcer prevention. Preliminary results with a paraplegic volunteer. *J. Tissue Viability* **2013**, *22*, 83–90. [CrossRef] [PubMed]

13. Sonenblum, S.; Stephen, H.; James, S. Everyday sitting behavior of full-time wheelchair users. *J. Rehabil. Res. Dev.* **2016**, *53*, 585–598. [CrossRef] [PubMed]

14. Sonenblum, S.; Vonk, T.; Janssen, T.; Sprigle, S. Effects of wheelchair cushions and pressure relief maneuvers on ischial interface pressure and blood flow in people with spinal cord injury. *Arch. Phys. Med. Rehabil.* **2014**, *95*, 1350–1357. [CrossRef] [PubMed]

15. Ma, C.; Li, W.; Gravina, R.; Fortino, G. Activity recognition and monitoring for smart wheelchair users. In Proceedings of the 2016 IEEE 20th International Conference on Computer Supported Cooperative Work in Design (CSCWD), Nanchang, China, 4–6 May 2016.

16. Arias, S.; Cardiel, E.; Garay, L.; Tovar, B.; Pla, M.; Rogeli, P. A pressure distribution measurement system for supporting areas of wheelchair users. In Proceedings of the 35th Annual International Conference of the IEEE Engineering in Medicine and Biology Society (EMBC), Osaka, Japan, 3–7 July 2013.

17. Domingues, M.; Tavares, C.; Alberto, N.; Radwan, A.; André, P.; Antunes, P. High rate dynamic monitoring with Fabry–Perot interferometric sensors: An alternative interrogation technique targeting biomedical applications. *Sensors* **2019**, *19*, 4744. [CrossRef]

18. Antunes, P.; Leitão, C.; Rodrigues, H.; Travanca, R.; Lemos-Pinto, J.; Costa, A.; Varum, H.; André, P. Optical fiber Bragg grating based accelerometers and applications. In *Accelerometers: Principles, Structure and Applications*; Nova Publishers: New York, NY, USA, 2013.

19. Tavares, C.; Domingues, M.F.; Frizera-Neto, A.; Leite, T.; Leitão, C.; Alberto, N.; Marques, C.; Radwan, A.; Rocon, E.; André, P.; et al. Gait shear and plantar pressure monitoring: A non-invasive OFS based solution for e-Health architectures. *Sensors* **2018**, *18*, 1334. [CrossRef]

20. Carvalho, L.; Alberto, N.; Gomes, P.; Nogueira, R.; Lemos-Pinto, J.; Fernandes, M. In the trail of a new bio-sensor for measuring strain in bone: Osteoblastic biocompatibility. *Biosens. Bioelectron.* **2011**, *26*, 4046–4052. [CrossRef]

21. Antunes, P.; Varum, H.; André, P. Optical FBG sensors for static structural health monitoring. *Procedia Eng.* **2011**, *14*, 1564–1571. [CrossRef]

22. Domingues, M.; Alberto, N.; Leitão, C.; Tavares, C.; Lima, E.; Radwan, A.; Sucasas, V.; Rodriguez, J.; André, P.; Antunes, P. Insole optical fiber sensor architecture for remote gait analysis-an eHealth Solution. *IEEE Internet Things J.* **2019**, *6*, 207–214. [CrossRef]

23. Ferreira, L.; Antunes, P.; Domingues, F.; Silva, P.; André, P. Monitoring of sea bed level changes in nearshore regions using fiber optic sensors. *Measurement* **2012**, *45*, 1527–1533. [CrossRef]

24. Alberto, N.; Bilro, L.; Antunes, P.; Leitão, C.; Lima, H.; André, P.; Nogueira, R.; Pinto, J. Optical fiber technology for eHealthcare. In *Handbook of Research on ICTs and Management Systems for Improving Efficiency in Healthcare and Social Care*; Cruz-Cunha, M., Miranda, I., Gonçalves, P., Eds.; Medical Information Science Reference; IGI global: Hershey, PA, USA, 2013; pp. 180–200.

25. Domingues, M.; Tavares, C.; Leitão, C.; Neto, A.; Alberto, N.; Marques, C.; Radwan, A.; Rodriguez, J.; Postolache, O.; Rocon, E.; et al. Insole optical fiber Bragg grating sensors network for dynamic vertical force monitoring. *J. Biomed. Opt.* **2017**, *22*, 091507. [CrossRef]

26. Cretikos, M.; Bellomo, R.; Hillman, K.; Chen, J.; Finfer, S.; Flabouris, A. Respiratory rate: The neglected vital sign. *Med. J. Aust.* **2008**, *188*, 657–659. [CrossRef] [PubMed]

MANUSCRIPT 6

Article

Sensor Cell Network for Pressure, Temperature and Position Detection on Wheelchair Users

Cátia Tavares [1,2,*], Daniela Real [1], Maria de Fátima Domingues [2,*], Nélia Alberto [2], Hugo Silva [3,4] and Paulo Antunes [1,2]

[1] Department of Physics & I3N, University of Aveiro, Campus Universitário de Santiago, 3810-193 Aveiro, Portugal; danielafreal@ua.pt (D.R.); pantunes@ua.pt (P.A.)

[2] Instituto de Telecomunicações and University of Aveiro, Campus Universitário de Santiago, 3810-193 Aveiro, Portugal; nelia@ua.pt

[3] Instituto de Telecomunicações, Instituto Superior Técnico, University of Lisbon, 1049-001 Lisbon, Portugal; hsilva@lx.it.pt

[4] PLUX—Wireless Biosignals, S.A, 1050-059 Lisboa, Portugal

* Correspondence: catia.tavares@ua.pt (C.T.); fatima.domingues@ua.pt (M.d.F.D.)

Article

Sensor Cell Network for Pressure, Temperature and Position Detection on Wheelchair Users

Cátia Tavares [1,2,*], Daniela Real [1], Maria de Fátima Domingues [2,*], Nélia Alberto [2], Hugo Silva [3,4] and Paulo Antunes [1,2]

1 Department of Physics & I3N, University of Aveiro, Campus Universitário de Santiago, 3810-193 Aveiro, Portugal; danielafreal@ua.pt (D.R.); pantunes@ua.pt (P.A.)
2 Instituto de Telecomunicações and University of Aveiro, Campus Universitário de Santiago, 3810-193 Aveiro, Portugal; nelia@ua.pt
3 Instituto de Telecomunicações, Instituto Superior Técnico, University of Lisbon, 1049-001 Lisbon, Portugal; hsilva@lx.it.pt
4 PLUX—Wireless Biosignals, S.A, 1050-059 Lisboa, Portugal
* Correspondence: catia.tavares@ua.pt (C.T.); fatima.domingues@ua.pt (M.d.F.D.)

Abstract: This work proposes an optical sensing network to monitor pressure and temperature in specific areas of a wheelchair to prevent pressure ulcers and to monitor the position of the wheelchair user by analyzing its pressure distribution. The sensing network is composed of six optical fiber Bragg grating (FBG)-based sensor cells. Each sensor cell is built from a polylactic acid (PLA) base and has two FBGs, one embedded in epoxy resin to monitor pressure variations (FBG_P) and another without resin to monitor temperature (FBG_T). Once produced, all sensor cells were experimentally characterized for pressure and temperature variations, resulting in an average pressure sensitivity of 81 ± 5 pm/kPa (FBG_P) and -5.0 ± 0.4 pm/kPa (FBG_T), and an average temperature sensitivity of 25 ± 1 pm/°C (FBG_P) and 47.7 ± 0.7 pm/°C (FBG_T). The sensor cells were then placed in six specific areas of a wheelchair (four in the seat area and two in the shoulder blade area) to carry out experimental tests, wherein the response of the sensors to a specific sequence of relief positions was tested. During the execution of the test, the optical signal of all sensors was monitored, in real time, with the pressure and temperature values detected in each zone of the wheelchair. In addition, random position changes were performed in order to evaluate the precision of the proposed sensing network in the identification of such positions.

Keywords: wheelchair user; fiber Bragg grating; pressure and temperature sensors; pressure ulcers; position detection

Publisher's Note: MDPI stays neutral with regard to jurisdictional claims in published maps and institutional affiliations.

1. Introduction

The advances in knowledge associated with the development of science and technology, as well as the increase in the average life expectancy of people, has led to a constant search for solutions in the field of health to improve the quality of life of the population. Often, these solutions do not lead to the cure of a pathology, but instead focus on its treatment and/or prevention. In this work, we propose a solution to improve the life quality of people who, for various reasons, have limited mobility and are bound to the daily use of a wheelchair. Due to the prolonged use of such mobility aid, wheelchair users may suffer from different pathologies, with pressure ulcers being one of the most recurrent, which in more severe cases may precede a generalized infection and lead to the death of the patient [1]. A pressure ulcer is a lesion on the skin and/or underlying tissue, resulting from prolonged exposure of a given anatomical region to pressure or pressure combined with torsional forces [2,3]. Additional pressure applied to a specific area of the skin impairs blood flow, resulting in a decrease in oxygen and nutrients to that area (ischemia) when sustained for a long period of time [4]. If this pressure is not relieved, an ulcer will begin

to form. Therefore, in wheelchair users, this additional pressure combined with limited mobility, low sensitivity, poor nutrition, ageing of the skin, and increase in temperature and humidity can eventually lead to the development of ulcers [5,6]. The most common areas for the development of this pathology are ischium and sacrum; scapulae; and, in some cases, trochanters and posterior region of the knee, depending on the chair and the position most frequently assumed by the user [7,8] (Figure 1). It is estimated that 95% of wheelchair users develop pressure ulcers during their lifetime [7], which is why it is considered one of the most critical secondary complications for patients with bone marrow damage [9]. Additionally, several studies show that the treatment of pressure ulcers causes high costs for both patients and health services. An article published in 2010 mentions that the treatment of a stage 4 pressure ulcer can cost as much as USD 129,248 per patient [10].
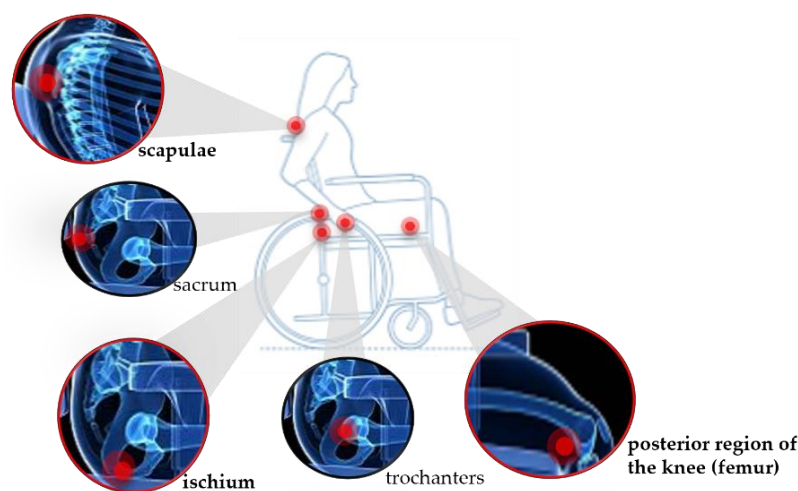
Figure 1. Schematic representation of the most common areas for the development of pressure ulcers, highlighting the areas studied in this work.

The most common methods to prevent this pathology are movements that relieve pressure and cushions in wheelchairs. Among these, the most cost-effective is the regular repositioning; frequent changes in posture, even sitting, can change the pressure at the skin surface and restore blood flow, improving the tissue health [9]; therefore, individuals with risk of developing pressure ulcers are recommended to change their positions regularly [3,6,9,11]. These repositioning movements include vertical push-ups and side and forward tilts in order to reduce the duration and amount of pressure [6]. Nevertheless, there is no scientific consensus on the frequency with which this type of exercise should be performed nor on the duration of the exercises. To date, the maximum pressures above which their application to specific parts of the body can be considered harmful have not yet been identified [4]. The tolerance of tissues to pressure varies according to the patient, depends on the nature of the tissue and its location, age, hydration, and metabolism.

There are already some published works with devices designed to monitor pressure in wheelchairs. In 2008, Gassara et al. designed a smart wheelchair with multiple electronic sensors (FlexiForce A201 sensor, optical pulse sensor and SCA11H sensor) for force, temperature, and heart rate monitoring [3]. Later, in 2009, a system was reported for problematic posture detection and notification of the user [8]. In 2012, an article was published on monitoring pressure relief using electronic sensors [4], and in the following year, Chenu's team published a paper on textile sensors to measure pressure at the interface between the mattress and the ischial area [12]. In 2014 and 2016, other teams reported the pressure monitoring by using electronic sensors to evaluate pressure relief movements [7,13]. More recently, Yang et al. included electronic sensors on wheelchair cushions for temperature and humidity monitoring in ischial tuberosities and thighs, with the aim of preventing pressure ulcers [14]. There is only one paper published in 2019 that reports the use of fiber Bragg grating (FBG)-based sensor network to monitor pressure in different areas

of a wheelchair, namely, scapulars, ischiatic, and heels, but this work does not provide temperature compensation at each point of analysis [15].

With this work, we intend to develop a non-electronic system for simultaneous real-time pressure and temperature detection in different areas of wheelchairs in order to help the wheelchair user and their caregivers/medical staff to prevent and control pressure ulcers. This system consists of a network of six sensor-cells, capable of measuring pressure and temperature at each point. This network of sensor-cells has two optical fibers as the main sensing component, each with six FBGs (one fiber for pressure measurement, and the other one for temperature monitoring). This is a system that can be easily adapted to different wheelchairs.

The manuscript is structured as follows: after the introduction provided in Section 1, Section 2 focuses on the sensor-cells sensing principle and design; Section 3 deals with the characterization and calibration of the sensor cells; Section 4 describes the implementation of the sensor cells in the wheelchair and the tests results; Section 5 presents the discussion; and, finally, Section 6 focuses on conclusion and future work perspectives.

2. Sensor Cells Sensing Principle and Design

The sensing network, proposed here to monitor pressure and temperature on the wheelchair, is composed by 12 multiplexed FBGs, divided into two optical fibers with six FBGs each.

The Bragg gratings are characterized by a periodic disturbance of the refractive index of the fiber core, normally produced with a UV laser. When an optical fiber with an FBG is illuminated by a broadband light source, only a set of wavelengths that meet the Bragg condition are reflected, with the others being transmitted. The Bragg condition is given by:

$$\lambda_B = 2n_{eff}\Lambda \tag{1}$$

where λ_B is the reflected Bragg wavelength, n_{eff} is the effective refractive index of the optical fiber core, and Λ is the grating period [15].

As mentioned previously, the λ_B can be affected by changes in strain (Δl) and/or temperature (ΔT). Consequently, the reflected Bragg wavelength varies ($\Delta\lambda_B$) according to the following equation:

$$\Delta\lambda_B = \Delta\lambda_{B,l} + \Delta\lambda_{B,T} = 2\left(\Lambda\frac{\partial n_{eff}}{\partial l} + n_{eff}\frac{\partial \Lambda}{\partial l}\right)\Delta l + 2\left(\Lambda\frac{\partial n_{eff}}{\partial T} + n_{eff}\frac{\partial \Lambda}{\partial T}\right)\Delta T = S_l\Delta l + S_T\Delta T \tag{2}$$

where the first term is the strain-induced wavelength shift, and the last is the thermal effect on the same parameter, with S_l and S_T representing the strain and temperature sensitivity coefficients of the FBG.

The goal of this work was to build a sensing system with six optical sensor cells that monitor the temperature and pressure in specific areas of the seat and backrest of the wheelchair and allow conclusions to be drawn about the position of the user. The six sensor cells have the same design and components, as shown in Figure 2. The base, shown in blue in Figure 2a,b, was printed in polylactic acid (PLA) using a 3D printer (Ultimaker 3D Extended). Each sensor cell contains two FBGs that were inscribed into photosensitive optical fibers (GF1 Thorlabs) using a pulsed Q-switched Nd:YAG laser system operating at the fourth harmonic at 266 nm. The FBGs were recorded using the phase mask technique, employing a laser pump energy of 25 J with a repetition rate of 10 Hz and an exposure time of approximately 1 min. One FBG is responsible for the temperature monitoring (FBG$_T$), being protected by a small cover to avoid pressure interferences. In this case the Bragg wavelength change is mostly due to temperature variations. The FBG$_P$ is embedded into a block of thermosetting epoxy resin (LiquidLens), with a Young modulus around 6.5 MPa that is in contact with the surface. When pressure is applied to the top of the resin block, it expands, causing strain in the optical fiber that modulates the Bragg wavelength. At the same time, the epoxy resin is also sensitive to temperature variations, changing its shape

with temperature fluctuations, and therefore it is expected that there will be variations in the wavelength of the FBG_P due to temperature.
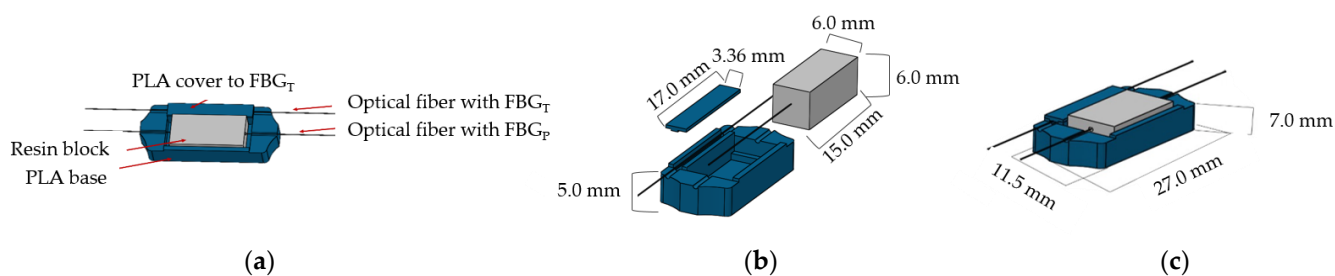

Figure 2. 3D design of sensor cell with: (**a**) all components; (**b**) components dimensions; and (**c**) final assembled sensor cell with its dimensions.

The sensor cell design was created with higher PLA walls on the sides of the resin (0.5 mm) and lower walls on the transverse tops so that the resin moves longitudinally and promotes elongation of the optical fiber when it is under pressure. Each sensor cell resin block, shown in shades of gray in Figure 2a,b, is 15 mm long, 6 mm wide, and 6 mm high. Figure 2c depicts the final assembled sensor cell.

Following this design, we produced six sensor cells for pressure and temperature detection on the scapulas (S), ischium (I), and femur (F). Both sides (left and right) were considered, and thus the sensor cells were identified as SL, SR, IL, IR, FL, and FR. As an example, the IR corresponds to the sensor cell positioned on the ischium (I) of the right side (R).

3. Sensor Cell Characterization and Calibration

3.1. Response Time of the Sensor Cell to Pressure and Temperature Variations

The response time of the projected sensor cells to pressure variations was determined by placing and quickly removing a mass of approximately 4 kg on the six sensor cells. The data were collected using an I-Mon USB512 interrogator (Ibsen Photonics) due to its high acquisition frequency ($\approx$1 kHz), with a resolution of 5 pm and wavelength range of 70 nm. According to the results shown in Figure 3a, for the IR sensor cell, as expected, no Bragg wavelength shift was obtained in the case of the FBG_T sensor. The determination of the response times of FBG_P for the rise and fall of all cycles only considered the analysis of the elapsed time between 10 and 90%, as shown in Figure 3b. An average rise time of 0.30 s and a fall time of 0.38 s were obtained. The difference between the values may have been due to the fact that the resin itself took time during the descent to return to its original position. In any case, both values were quite low for the type of movement to be detected in this work, and therefore the sensor design here proposed was proven to be suitable for the intended application. Since the response time is about 0.5 s, the sm125–500 interrogator (Micron Optics), another interrogation system available in our laboratory, which registers two points per second with a resolution of 1 pm and a wavelength range of 80 nm, is suitable for the sensor calibration, and therefore it was the interrogator used during all tests.

To obtain the response time of the sensors with respect to temperature variations, we placed one of the six sensor cells, in this case the SL, in a climate test chamber (CH340, Angelantoni Industries). The results are presented in Figure 4.

Int. J. Environ. Res. Public Health **2022**, *19*, 2195

5 of 14
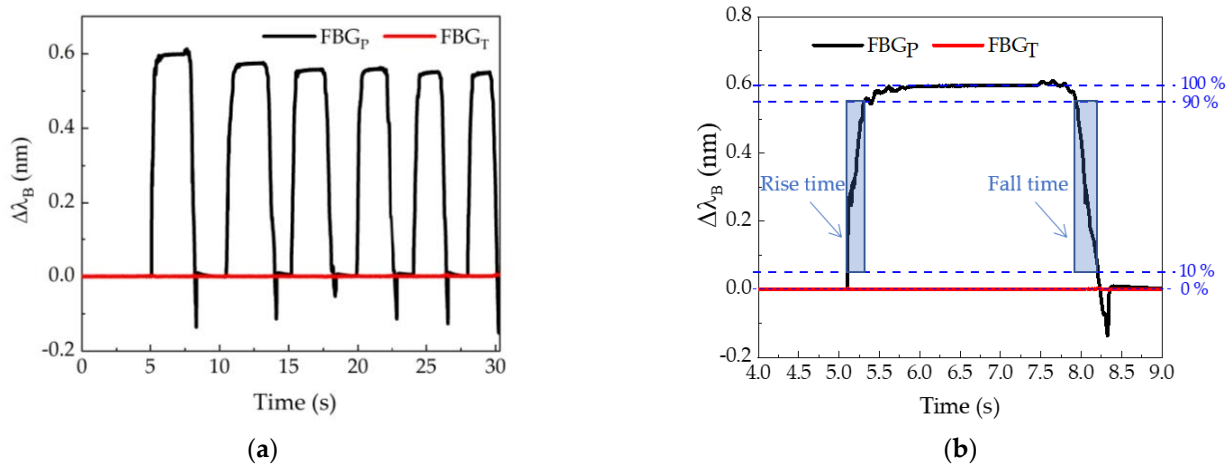
Figure 3. Determination of the response time of the IR sensor cell to pressure variations: (**a**) entire test; (**b**) zoom of first peak to show the methodology used to find the rise and fall times.
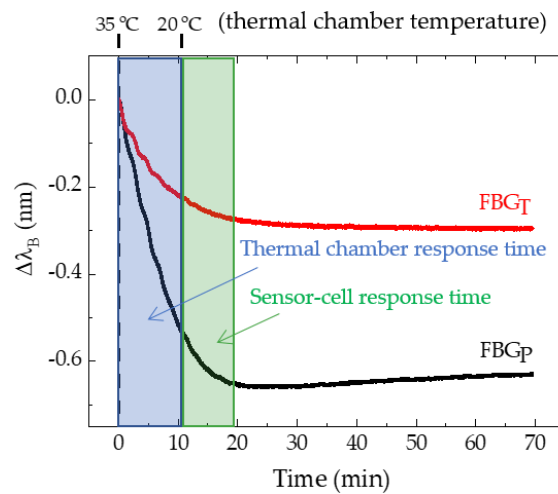
Figure 4. Determination of the response time of the SL sensor cell to 15 °C of temperature variation.

The Micron Optics sm125–500 interrogator was used to record the Bragg wavelength for FBG_P and FBG_T. At the beginning of the test, at minute 0.0, the thermal chamber displayed 35.0 °C, having been programmed to 20.0 °C at that time. The desired temperature was reached 10.6 min after the start of the test. As shown in Figure 4, 20.0 min after the thermal chamber was turned on, the temperature of the FBGP and FBGT was considered stabilized.

3.2. Calibration to Pressure and Temperature

The pressure calibration test was performed for all sensor cells, ranging from 0 to 15 kPa (using several loads), at a controlled temperature. Results of the calibration test for the FR sensor cell are shown in Figure 5. Since the sensor cell response was also tested for the decrease of the pressure load, the hysteresis of the sensors was evaluated as well.

Int. J. Environ. Res. Public Health **2022**, *19*, 2195

6 of 14
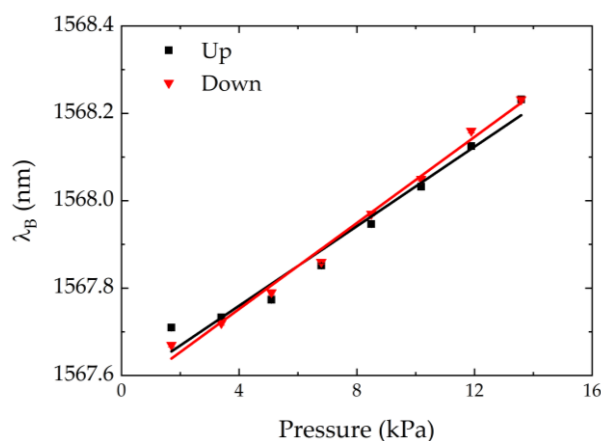
Figure 5. FR sensor cell calibration test to pressure variations. The symbols correspond to experimental data, and the lines to the linear fits.

For all sensor cells, these tests resulted in a linear dependence of the Bragg wavelength change with the applied pressure. The sensitivity coefficient of each sensor cell was given by the average of the slopes of the linear fits for the up and down pressure. The results are presented in Table 1. From Figure 5, it can be deduced that the hysteresis effect was very low and can therefore be neglected. The same occurred with the other sensor cells.

Table 1. Pressure (S_P) and temperature (S_T) sensitivity coefficients for the FBGs of all sensor cells.

Sensitivity Coefficient	SR Scapula Right	SL Scapula Left	IR Ischium Right	IL Ischium Left	FR Femur Right	FL Femur Left
$S_{P,FBGP}$ (pm/kPa)	87.0 ± 8.0	46.0 ± 3.0	83.7 ± 0.7	16.0 ± 1.0	89.0 ± 6.0	163.0 ± 11.0
$S_{P,FBGT}$ (pm/kPa)	-4.5 ± 0.4	-2.7 ± 0.3	-1.5 ± 0.3	-10.0 ± 1.0	-11.4 ± 0.4	-0.2 ± 0.1
$S_{T,FBGP}$ (pm/°C)	22.0 ± 0.2	54.0 ± 5.0	21.5 ± 0.2	15.0 ± 0.3	18.2 ± 0.1	21.6 ± 0.2
$S_{T,FBGT}$ (pm/°C)	89.0 ± 1.0	19.6 ± 0.1	27.1 ± 0.7	25.3 ± 0.4	116.0 ± 2.0	9.3 ± 0.1

For temperature calibration, all the sensor cells placed in the thermal chamber were subjected to temperature variations ranging from 15 to 40 °C with a 5 °C step, and without any external applied pressure. Although it was verified that the stabilization time of the temperature sensor was around 10 min after the thermal chamber reached the desired value (Figure 4), the response of the FBG$_P$ and FBG$_T$ was registered 15 min after the temperature stabilization in the climate test chamber in order to ensure more accuracy of the results. The test was carried out for the increase and decrease of the temperature. During this test, the relative humidity of the thermal chamber was stabilized at 70%.

Figure 6 shows the results obtained only for the FBG$_T$ of the sensor cell IL, both for the temperature increase and decrease. The values were very close, and this trend was verified for all FBG$_T$, indicating that the developed sensor cells do not have hysteresis to temperature variations. In terms of sensitivity coefficient of each sensor cell, we considered the mean value of the sensitivity coefficient obtained for the increase and decrease of the temperature (values shown in Table 1).

Figure 6. Temperature IL sensor cell calibration test.

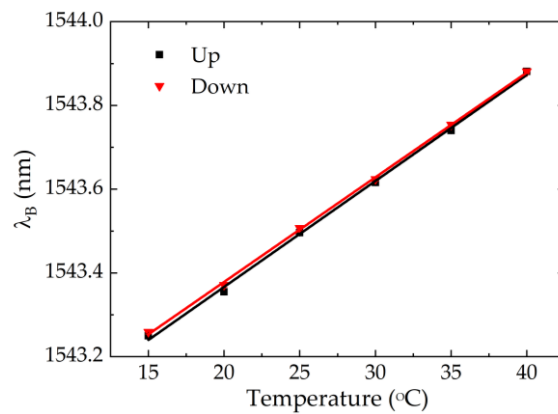With the obtained data and respective adjustments and averages, we summarize the main findings in Table 1, wherein the pressure and temperature sensitivity coefficients of FBG$_P$ and FBG$_T$ are listed for all the sensor cells. The differences of sensitivity coefficients between sensors may have been due to different factors. Although we tried to reproduce the sensor cells in the same way, there were small geometrical discrepancies between sensor cells. Additionally, there were still some steps manually controlled in the process, e.g., placing the resin and gluing and tensioning of the optical fiber. Moreover, the resin can produce small air bubbles that are difficult to control and that can easily change its elasticity and thermal properties, which justifies the differences in the sensitivities observed in Table 1. Concerning the negative values obtained for the FBG$_T$ pressure sensitivity coefficient—$S_{P,FBGT}$, this may have been due to a bending of the optical fiber caused by the deformation of the PLA under the applied pressure. Since this bending resulted in a longitudinal compression of the fiber, it will be reflected in a negative wavelength variation. However, the discrepancy in the sensitivity coefficients and the negative wavelength variations achieved in the thermal characterization had no influence on the final results, as the calculations took into account the values present in this table.

3.3. Compensation for the Temperature Effect

The pressure and temperature characterization tests were performed, assuming that only one of these parameters varied while the other remained constant. Nonetheless, during the application of the proposed sensing system in the wheelchair, both parameters can vary at the same time. As the FBGs were simultaneously sensitive to temperature and strain under the pressure applied to the sensor cells, it is relevant to compensate the temperature effect on the FBG$_P$ response in order to obtain the precise pressure that is applied at each analysis point. For this, a matrix represented by Equation (3) can be considered:

$$
\begin{bmatrix} \Delta\lambda_{\mathrm{FBG}_T} \\ \Delta\lambda_{\mathrm{FBG}_P} \end{bmatrix} = \begin{bmatrix} S_{P,\mathrm{FBG}_T} & S_{T,\mathrm{FBG}_T} \\ S_{P,\mathrm{FBG}_P} & S_{T,\mathrm{FBG}_P} \end{bmatrix} \begin{bmatrix} \Delta P \\ \Delta T \end{bmatrix}, \tag{3}
$$

where $\Delta\lambda_{\mathrm{FBG}_T}$ and $\Delta\lambda_{\mathrm{FBG}_P}$ correspond to the Bragg wavelength shift measured in FBG$_T$ and FBG$_P$, respectively; S_{P,FBG_T} and S_{P,FBG_P} are the pressure sensitivities of FBG$_T$ and FBG$_P$, respectively; S_{T,FBG_T} and S_{T,FBG_P} are the temperature sensitivities of FBG$_T$ and FBG$_P$, respectively; and ΔP and ΔT are pressure and temperature variations, respectively. Solving Equation (3) to ΔP and ΔT, we obtain Equation (4):

$$
\begin{bmatrix} \Delta P \\ \Delta T \end{bmatrix} = \frac{1}{\det(A)} \begin{bmatrix} S_{T,\mathrm{FBG}_P} & -S_{T,\mathrm{FBG}_T} \\ -S_{P,\mathrm{FBG}_P} & S_{P,\mathrm{FBG}_T} \end{bmatrix} \begin{bmatrix} \Delta\lambda_{\mathrm{FBG}_T} \\ \Delta\lambda_{\mathrm{FBG}_p} \end{bmatrix}, \tag{4}
$$

$$
\text{with } A = \begin{bmatrix} S_{P,\mathrm{FBG}_T} & S_{T,\mathrm{FBG}_T} \\ S_{P,\mathrm{FBG}_P} & S_{T,\mathrm{FBG}_P} \end{bmatrix} \tag{5}
$$

4. Implementation of Sensor Cells in the Wheelchair

The sensor cells were attached to the specific areas of interest of a wheelchair, as depicted in Figure 7. Special care was also taken with the optical fiber in order to minimize the curvature, not only to reduce the possibility of breakage, but also to avoid reducing the optical power intensity of the Bragg wavelength peak (due to the optical attenuation caused by the fiber curvature). Although this is not relevant for the measurement itself, as the parameter of interest is encoded in the spectral shift of the Bragg wavelength, this may cause fails on the peak detection by the interrogation system. After the sensor cell network was implemented, foam pads were placed on the back and seat of the chair to protect the sensors and provide more comfort for the user.
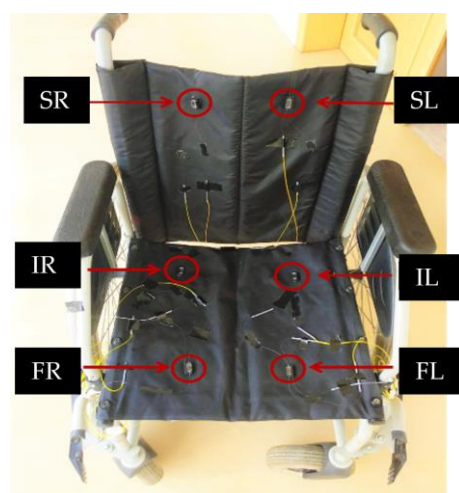
Figure 7. Photography of the wheelchair with the identification of six FBG-based sensor cells for pressure and temperature monitoring.

All the tests were performed by the same person, who weighed 58 kg, had no identified pathologies, and was able to move and perform the different positions without external assistance. In accordance with the areas most prone to the development of pressure ulcers, we carried out the protocol demonstrated in Figure 8, consisting of a set of pressure relief positions, as recommended in the literature [7,15]. The tests were realized in a closed indoor environment at a constant temperature.
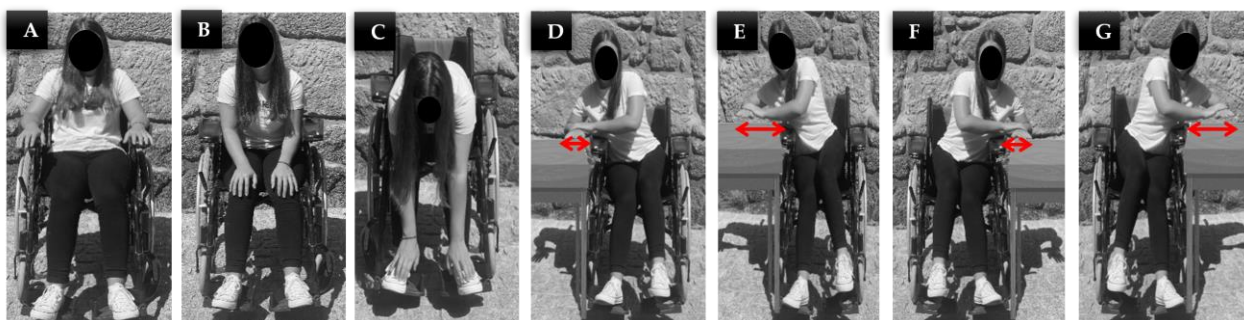
Figure 8. Positions performed during the test: (**A**) reference position, person sitting normally; (**B**) leaning slightly forward with hands on knees; (**C**) leaning strongly forward with hands on feet; (**D**) slight tilt to the right; (**E**) too tilted to the right; (**F**) slight tilt to the left; (**G**) too tilted to the left.

4.1. First Test: Sequence of Pressure Relief Positions

The first test with the instrumented wheelchair aimed at verifying the reliability of the optical sensor network to monitor, in real time, the pressure and temperature in specific

Int. J. Environ. Res. Public Health **2022**, 19, 2195

9 of 14

areas of the wheelchair during different positions. The test began with the user sitting in position A, during 15 min for temperature and pressure stabilization. The other positions, presented in Figure 8, were performed for 1 min, always interrupted by 2 min in the initial position A for blood flow stabilization. Figure 9 describes the sequence of relief positions during the first test.

Figure 9. Scheme showing the sequence of pressure relief positions and their time at the first test.

Since it is known that the Bragg wavelength increases with pressure, it is possible to predict the FBG$_P$ sensor cells response during this test, as described in Table 2.

Table 2. Expected variations to be observed for each FBG$_P$ of the sensor cells throughout the test.

Sensor Cells	Expected Results
SR and **SL**	After the initial position A, in general, there should be a negative variation of the Bragg wavelength in the periods corresponding to positions B, C, D, E, F, and G, since the body is no longer in contact with the sensors when these relief positions are exercised.
IR and **FR**	Increased Bragg wavelength shift in the period corresponding to positions B, C, D, and E. Decrease in the periods corresponding to positions F and G, with the latter being more accentuated. In position C, a greater variation on the FR sensor cell than the IR sensor cell is expected.
IL and **FL**	Increased Bragg wavelength shift in the periods corresponding to positions B, C, F, and G. Decrease in the positions D and E (more accentuated in this case). In position C, a greater variation on the FL sensor cell than on the IL sensor cell is expected.

Figure 10 shows the Bragg wavelength shift registered for the FBG$_P$ (a) and FBG$_T$ (b) of the SR sensor cell during the sequence of relief positions identified in Figures 8 and 9.
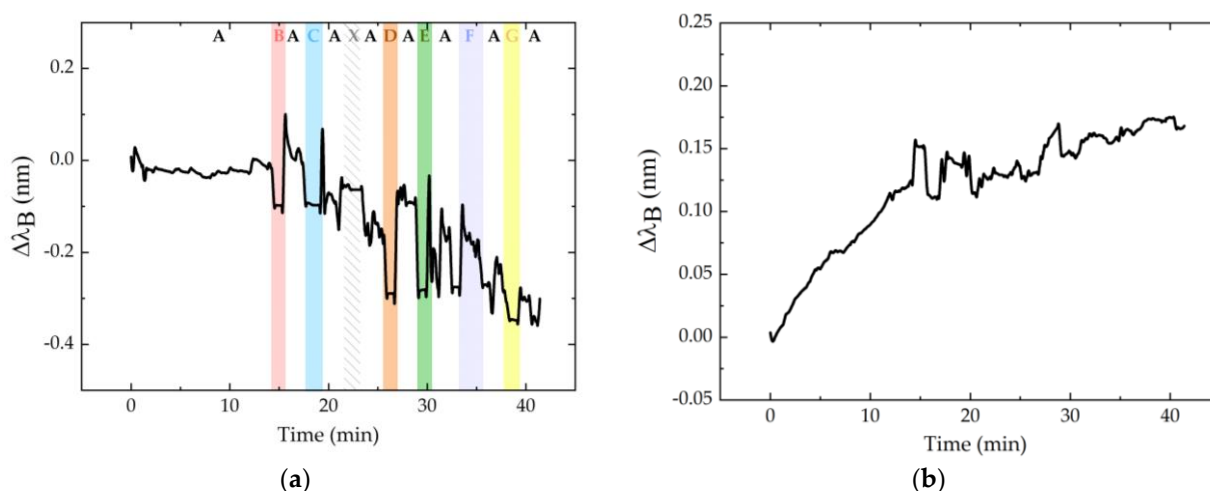
Figure 10. Bragg wavelength shift for the FBG$_P$ (**a**) and FBG$_T$ (**b**) of the SR sensor cell. In the first graph (**a**), each color refers to the position that was exercised at that moment: position A in white; B in red; C in blue; D in orange; E in green; F in dark blue; and G in yellow. The white area with pattern corresponds to a random movement of the volunteer (identified as X).

Using Equation (4) and the sensitivities presented in Table 1, we were able to convert these data to pressure and temperature, represented in Figure 11a,b, respectively. Com-

Int. J. Environ. Res. Public Health **2022**, *19*, 2195

10 of 14

paring the Figures 10a and 11a, we found that the difference between the shape of system response before and after temperature compensation, respectively.

(**a**)   (**b**)
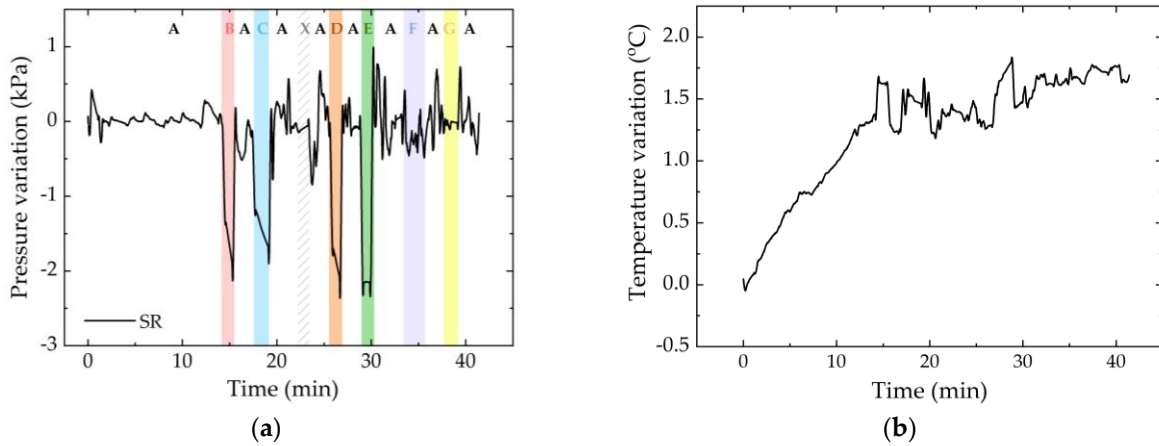
Figure 11. Pressure with temperature compensation (**a**) and temperature (**b**) of the SR sensor cell during the test. In the first graph, each color refers to the position that was exercised at that moment: position A in white; B in red; C in blue; D in orange; E in green; F in dark blue; and G in yellow. The white area with pattern corresponds to a random movement of the volunteer (identified as X).

For comparison purposes, Figure 12 shows the pressure variation registered for all the sensor cells.

Figure 12. *Cont.*

Int. J. Environ. Res. Public Health **2022**, *19*, 2195

11 of 14
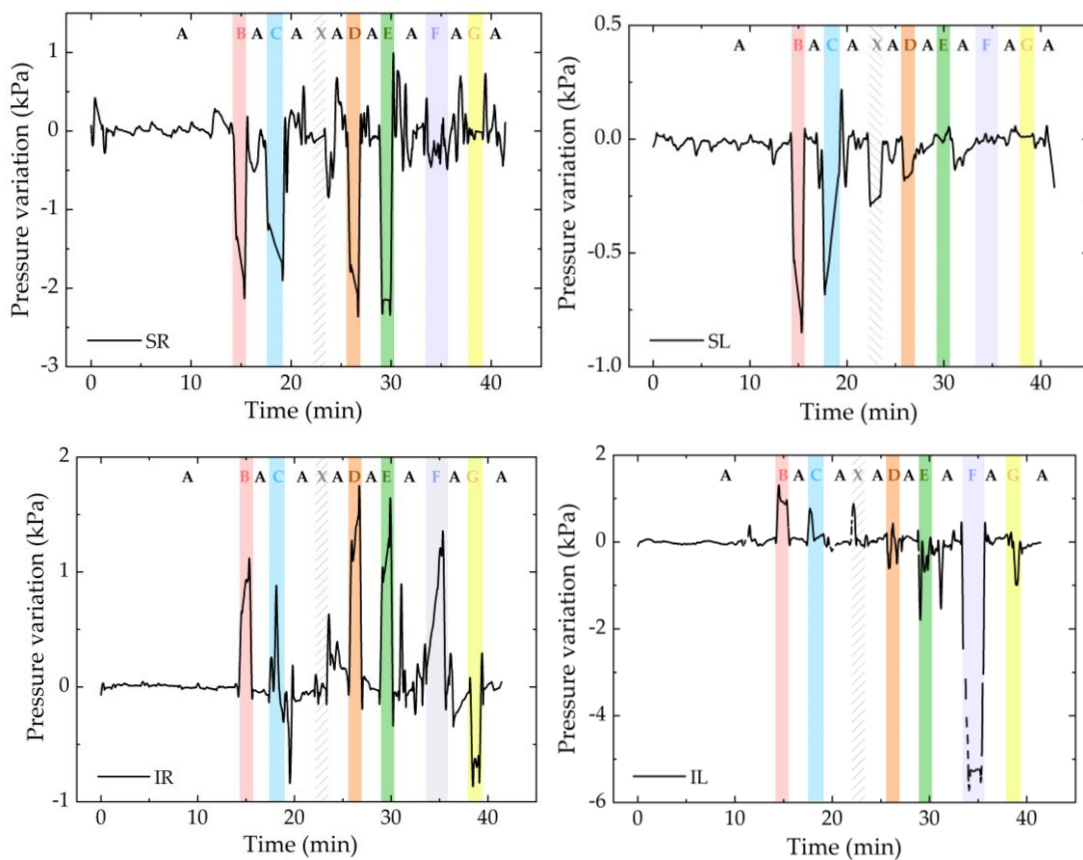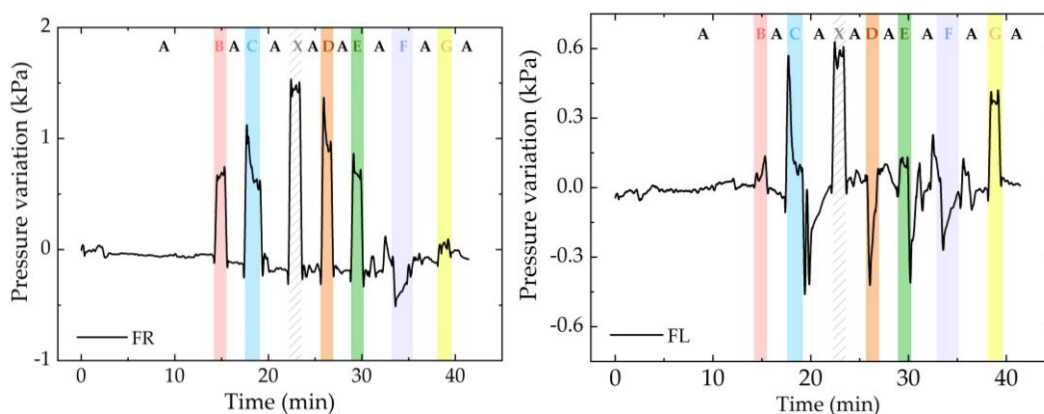
Figure 12. Pressure variation for all sensor cells during the test. In the graphs, each color refers to the position that was exercised at that moment: position A in white; B in red; C in blue; D in orange; E in green; F in dark blue; and G in yellow. The white area with pattern corresponds to a movement of the volunteer (identified as X).

In general, the response of the sensor cells is similar to the one already predicted (Table 2), although in some cases there were some pressure peaks that affected the values detected immediately afterwards, mainly in position 7. The discrepancy could have been caused by sudden movements that exerted pressure on the FBG_T and led to errors in the temperature compensation or even torsion and strain of the optical fibers. However, with time and normalization of the position, these errors can certainly be eliminated.

During the test, the greatest pressure variation, with about 6 kPa, was found in the ischial region (IL), and the greatest thermal variation was also found in the same region (IR), with an increase of 5 °C. This is consistent with the state of the art [7,8], which identifies the ischial tuberosity area as one of the most likely areas for the development of pressure ulcers in wheelchair users.

4.2. Second Test: Random of Pressure Relief Positions

This test aimed to verify the reliability of the proposed optical sensor network for real-time detection of the wheelchair user's position. For this, the volunteer sat in the wheelchair and randomly adopted the positions described in Figure 8. Since this test was performed immediately after the one described previously in Section 4.1, the initial 15 min required for the temperature stabilization was not considered (this condition was already guaranteed). To identify the seven positions of the wheelchair user, we only needed to analyze the response of three sensors as long as they met two criteria: use of sensors from opposite sides of the seat and use of sensors from all areas of analysis (scapulae, ischium, and femur). Thus, to simplify the analysis, we show in Figure 13 the pressure variation plots only for three sensors, namely, FR, IL, and SR sensor cells.

By observing the data from each of these sensor cells, we were able to deduce the position in which the wheelchair user was in. Table 3 describes the sensor cell behavior and the predicted position, as well as the real position adopted by the volunteer.
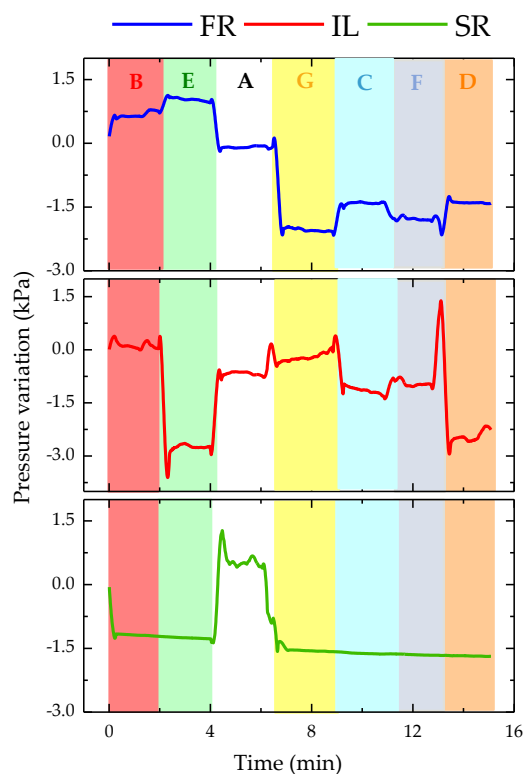
Figure 13. Pressure variation for SR, IL, and FR sensor cells during the random test of relief positions: position A in white; B in red; C in blue; D in orange; E in green; F in dark blue; and G in yellow. The white area with pattern corresponds to a movement of the volunteer (identified as X).

Table 3. Sensor cells behavior and correspondent position.

Sensor Cell Behavior and Predicted Position	Real Position
In the first 2 min, there was a positive pressure variation in FR and IL, and a decrease in SR, that is, the user did not have the shoulder blades supported on the wheelchair structure and there was pressure in both the femoral and ischial areas (left and right), corresponding only to position B.	B
The pressure in SR was maintained, increased even more in relation to the previous position in FR, and decreased abruptly in IL. This was only verified when the wheelchair user was too inclined to the right, corresponding to position E.	E
There was a positive variation in SR corresponding to the position in which the wheelchair user supported the shoulder blades in the area where the sensor cell was located. This variation occurred exclusively for position A, and was confirmed by the variations observed in the remaining sensor cells.	A
There was a null variation in SR for the rest of the test, that is, position A was not checked again. As there was an abrupt negative variation in FR and a positive variation in IL, it was concluded that the wheelchair user was excessively tilted to the left, being in the G position.	G
The pressure increased in FR and decreased in IL, that is, the wheelchair user was not only exercising pressure on the sensor cells positioned on the left side. As the pressure was higher in the femur area, the user should have been in position C.	C
There was again a pressure decrease in the FR sensor cell and an increase in IL; however, this was not so pronounced, corresponding to position F.	F
There was an increase in the pressure felt by the FR and a decrease in IL; however, both were slight variations, corresponding to position D.	D

Int. J. Environ. Res. Public Health **2022**, *19*, 2195

13 of 14

Knowing the positions assumed by the wheelchair user, we were able to compare those with the conclusions drawn from the observation of the data presented in Figure 13. In fact, it was possible to deduce the position that the wheelchair user was assuming at that moment from the pressure analysis. However, it should be noted that it was not possible to draw conclusions from the response of only one sensor cell. For unambiguous identification, one must have the response of at least three sensor cells, preferably one from the shoulder blade area and two from the seat area.

5. Discussion

Compared with the system proposed by Tavares et al. [15], this work had an improved sensor cell arrangement that allows for the detection of several positions of wheelchair users and a new sensor cell design enabling them to simultaneously monitor temperature and pressure at each point. It was found that the temperature is an important parameter to be monitored, not only because it increases with friction and therefore it is indirectly related to the occurrence of pressure ulcers [14], but also because the FBGs are simultaneously sensitive to both pressure and temperature variations. Therefore, the design of the sensor cell proposed in this work allows for a compensation of the temperature effects on the sensors dedicated to pressure measurements, enabling a precise value of both the temperature and pressure exerted at each point to be obtained.

To validate the performance of the sensor network, we implemented two tests: one consisted of the execution of a well-defined sequence of pressure relief movements (as de-scribed in the literature [7,15]) for real-time monitoring of temperature and pressure; the other test consisted of a random sequence of movements in order to check if it is possible to identify the different positions with the proposed optical sensing network. The pressure variations obtained were within the expected order of magnitude [16]. The sensor network was proven to be reliable, not only for real-time pressure and temperature monitoring, but also for the detection of the wheelchair user position.

On the basis of the proposed sensing system, we were able to perceive the position in which the wheelchair user was in, in order to warn when they are exceeding the recommended pressure values and advise a relief position. However, it is important to note that these values are dependent on factors that are currently not measured, such as the skin's condition.

6. Conclusions

In this work, a sensing network with six FBG-based sensor cells was developed for simultaneous and real-time pressure and temperature monitoring in a wheelchair. The motivation for monitoring these physical parameters in specific positions of a wheelchair is based on the need for solutions that help in the prevention of pressure ulcer development.

Six specific areas of the wheelchair (four in the seat area and two in the shoulder blade area) were instrumented with the sensor cells. This enabled us to carry out experimental tests in which the response of the sensors to a specific sequence and a random sequence of pressure relief positions was tested. On the basis of the proposed sensing system, we were able to differentiate the response of sensors to pressure and temperature variations, as well as to perceive the position in which the wheelchair user was in, in order to warn when they were exceeding the recommended pressure values and advise a relief position.

In the future, the development of a low-cost, stand-alone interrogation system installed on the wheelchair can be considered, capable of being powered by a battery. Moreover, regarding the sensor cells production, different casing materials and filling resins could be tested to improve the cell reproducibility and/or performance. Additionally, for the optimization of the sensor cells, it will be important to carry out applicability and usability studies in which a large number of users with and without ulcers can test the system for several hours.

References

1. Han, D.K.; Kim, J.M.; Cha, E.J.; Lee, T.S. Wheelchair type biomedical system with event-recorder function. In Proceedings of the Annual International Conference of the IEEE Engineering in Medicine and Biology Society, Vancouver, CB, Canada, 21–24 August 2008.
2. Kim, J.M.; Hong, J.H.; Cho, M.C.; Cha, E.J.; Lee, T.S. Wireless biomedical signal monitoring device on wheelchair using noncontact electro-mechanical film sensor. In Proceedings of the 29th Annual International Conference of the IEEE Engineering in Medicine and Biology Society, Lyon, France, 22–26 August 2007.
3. Gassara, H.E.; Almuhamed, S.; Moukadem, A.; Schacher, L.; Dieterlen, A.; Adolphe, D. Smart wheelchair: Integration of multiple sensors. In Proceedings of the IOP Conference Series: Materials Science and Engineering, Putrajaya, Malaysia, 20–22 October 2017.
4. Dai, R.; Sonenblum, S.E.; Sprigle, S. A robust wheelchair pressure relief monitoring system. In Proceedings of the 2012 Annual International Conference of the IEEE Engineering in Medicine and Biology Society, San Diego, CA, USA, 28 August–1 September 2012.
5. Brem, H.; Maggi, J.; Nierman, D.; Rolnitzky, L.; Bell, D.; Rennert, R.; Golinko, M.; Yan, A.; Lyder, C.; Vladeck, B. High cost of stage IV pressure ulcers. *Am. J. Surg.* **2010**, *200*, 473–477. [CrossRef] [PubMed]
6. Presti, D.L.; Massaroni, C.; Leitão, C.; Domingues, M.F.; Sypabekova, M.; Barrera, D.; Floris, I.; Massari, L.; Oddo, C.; Sales, S.; et al. Fiber Bragg gratings for medical applications and future challenges: A review. *IEEE Access* **2020**, *8*, 156863–156888. [CrossRef]
7. Sonenblum, S.E.; Vonk, T.E.; Janssen, T.W.; Sprigle, S.H. Effects of wheelchair cushions and pressure relief maneuvers on ischial interface pressure and blood flow in people with spinal cord injury. *Arch. Phys. Med. Rehabil.* **2014**, *95*, 1350–1357. [CrossRef] [PubMed]
8. Verbunt, M.; Bartneck, C. Sensing senses: Tactile feedback for the prevention of Decubitus ulcers. *Appl. Psychophysiol. Biofeedback* **2010**, *35*, 243–250. [CrossRef] [PubMed]
9. Gadd, M.M. Preventing hospital-acquired pressure ulcers: Improving quality of outcomes by placing emphasis on the braden subscale scores. *J. Wound Ostomy Cont. Nurs.* **2012**, *39*, 292–294. [CrossRef] [PubMed]
10. Demarré, L.; Van Lancker, A.; Van Hecke, A.; Verhaeghe, S.; Grypdonck, M.; Lemey, J.; Annemans, L.; Beeckman, D. The cost of prevention and treatment of pressure ulcers: A systematic review. *Int. J. Nurs. Stud.* **2015**, *52*, 1754–1774. [CrossRef] [PubMed]
11. Sprigle, S.; Sonenblum, S. Assessing evidence supporting redistribution of pressure for pressure ulcer prevention: A review. *J. Rehabil. Res. Dev.* **2011**, *48*, 203–213. [CrossRef] [PubMed]
12. Chenu, O.; Vuillerme, N.; Bucki, M.; Diot, B.; Cannard, F.; Payan, Y. TexiCare: An innovative embedded device for pressure ulcer prevention. Preliminary results with a paraplegic volunteer. *J. Tissue Viability* **2013**, *22*, 83–90. [CrossRef] [PubMed]
13. Sonenblum, S.E.; Sprigle, S.H.; Martin, J.S. Everyday sitting behavior of full-time wheelchair users. *J. Rehabil. Res. Dev.* **2016**, *53*, 585–598. [CrossRef]
14. Yang, Y.S.; Pan, C.T.; Ho, W.H. Sensor-based remote temperature and humidity monitoring device embedded in wheelchair cushion. *Sens. Mater.* **2018**, *30*, 1807–1814. [CrossRef]
15. Tavares, C.; Domingues, M.F.; Paixão, T.; Alberto, N.; Silva, H.; Antunes, P. Wheelchair pressure ulcer prevention using FBG based sensing devices. *Sensors* **2020**, *20*, 212. [CrossRef]
16. Agrawal, K.; Chauhan, N. Pressure ulcers: Back to the basics. *Indian J. Plast. Surg.* **2012**, *45*, 244–254. [CrossRef] [PubMed]

Instrumented Office Chair With Low-Cost Plastic Optical Fiber Sensors for Posture Control and Work Conditions Optimization

CÁTIA TAVARES[1,2], **JOÃO OLIVEIRA E. SILVA**[3], **ANDRÉ MENDES**[3], **LEONOR REBOLO**[1], **MARIA DE FÁTIMA DOMINGUES**[2], (Member, IEEE), **NÉLIA ALBERTO**[2], **MÁRIO LIMA**[2,3], **HUGO PLÁCIDO SILVA**[5,6], (Senior Member, IEEE), **AND PAULO FERNANDO DA COSTA ANTUNES**[1,2]

[1]Department of Physics & I3N, University of Aveiro, Campus Universitário de Santiago, 3810-193 Aveiro, Portugal
[2]Instituto de Telecomunicações and University of Aveiro, Campus Universitário de Santiago, 3810-193 Aveiro, Portugal
[3]Department of Electronics, Telecommunications and Informatics, Campus Universitário de Santiago, 3810-193 Aveiro, Portugal
[4]Department of Physics, University of Aveiro, Campus Universitário de Santiago, 3810-193 Aveiro, Portugal
[5]Instituto de Telecomunicações, Instituto Superior Técnico, Universidade de Lisboa, 1049-001 Lisboa, Portugal
[6]PLUX–Wireless Biosignals, S.A, 1050-059 Lisboa, Portugal

Instrumented Office Chair With Low-Cost Plastic Optical Fiber Sensors for Posture Control and Work Conditions Optimization

CÁTIA TAVARES [1,2], **JOÃO OLIVEIRA E. SILVA**[3], **ANDRÉ MENDES**[3], **LEONOR REBOLO**[1],
MARIA DE FÁTIMA DOMINGUES[2], **(Member, IEEE), NÉLIA ALBERTO**[2], **MÁRIO LIMA**[2,3],
HUGO PLÁCIDO SILVA[5,6], **(Senior Member, IEEE),**
AND PAULO FERNANDO DA COSTA ANTUNES[1,2]

[1]Department of Physics & I3N, University of Aveiro, Campus Universitário de Santiago, 3810-193 Aveiro, Portugal
[2]Instituto de Telecomunicações and University of Aveiro, Campus Universitário de Santiago, 3810-193 Aveiro, Portugal
[3]Department of Electronics, Telecommunications and Informatics, Campus Universitário de Santiago, 3810-193 Aveiro, Portugal
[4]Department of Physics, University of Aveiro, Campus Universitário de Santiago, 3810-193 Aveiro, Portugal
[5]Instituto de Telecomunicações, Instituto Superior Técnico, Universidade de Lisboa, 1049-001 Lisboa, Portugal
[6]PLUX–Wireless Biosignals, S.A, 1050-059 Lisboa, Portugal

Corresponding authors: Cátia Tavares (catia.tavares@ua.pt) and Nélia Alberto (nelia@ua.pt)

ABSTRACT People spend more and more time sitting and this habit has been shown to cause spine pathologies. Thus, the scientific community and the industry have become interested in instrumented chairs development to detect incorrect user postures. In this work we present the development and implementation of invisibles and non-intrusive plastic optical fiber sensor cells to monitor the posture and evaluate the ergonomic behavior of a seated person. The low-cost plastic optical fiber (POF) based sensing devices developed in this work, were implemented in an office chair, to evaluate the workers posture throughout their work day. In addition to the sensors, Android and PC software applications were developed, to provide real time feedback and alerts to the user whenever an inadequate posture is detected, or the seating position is the same for a long time. The proposed approach was evaluated in a study involving six users, and results show that it can detect the user's position with 96.6% accuracy.

INDEX TERMS Pressure sensors, plastic optical fiber, work conditions, ergonomic posture.

I. INTRODUCTION

Nowadays, there is an increasingly higher number jobs in which the worker is seated [1]. At the same time, there are also a range of leisure activities carried out in the same way (e.g. eSports) [1]. This increase in sedentary lifestyle is associated with the development of different health pathologies among which postural problems, especially related to the

The associate editor coordinating the review of this manuscript and approving it for publication was Gyorgy Eigner.

spine, are in a growing number. Studies indicate that spinal disorders are the second leading cause of requests for medical leave from work and are also a reason for early retirement [2]. In recent years, research in intelligent office chairs with sensors has started to grow in interest, aiming to advise the user to correct their posture or take short breaks for relaxation or muscle repositioning. Furthermore, despite not reaching a consensus on the correct sitting position, the medical community defends that there are several recommended positions and that, even if the user is in an adequate position, he/she

should only remain in the same position for a maximum of 4 hours [1]–[4]. However, the ideal is to take short and regular breaks to get up and allow muscular relaxation [1].

Most of the available technologies to monitor posture are based on pressure maps obtained by the incorporation of electronic sensors at different points of the chair [5]–[10]. Nevertheless, electronic sensors exhibit limitations, one of the biggest being the use of electrical signals at the point of measurement, which makes them susceptible to catastrophic failure if in contact with liquids (in case of an accident or even cleaning), increases the risk of short circuit and/or electric fire, and even user safety. That is one of the reasons driving the community to study other types of sensors, namely optical fiber sensors. These have been increasingly researched in recent years, especially for the measurement of physical and physiological parameters [11]–[13]. They offer several advantages comparatively to conventional electronic sensors, such as: no need for electricity at the measurement point; immunity to electromagnetic interference; robustness, flexibility, and smaller size and weight [11], [14]–[16].

Plastic optical fiber (POF) sensors are particularly advantageous over other optical fiber sensors due to the low cost and robustness, although few works are reported in the literature so far, they already have been used for pressure or vital signals detection in beds or seats (e.g.). In [17] a system based on POF pressure sensors was developed for detecting a passenger in a car seat, consisting of an optical fiber embedded in a fabric and attached to the side. When the optical fiber is subjected to pressure, it stretches and consequently changes the transmitted optical power. This system was shown to perform well in a pressure range between 0.18 and 0.21 N/cm^2. Lee *et al.* [18] also used POF sensors embedded in a fabric, but with stable perpendicular cylindrical structures placed under the fiber. The working principle was the same as the one reported in [17], i.e. the optical power varies as a function of the pressure applied on the optical fiber. Sartiano *et al.* proposed a pressure sensor with POF sensors incorporated in a mattress for vital signs monitoring [19]. The system consisted of a matrix of POFs that changed their optical performance under pressure. To increase the sensitivity of the sensor, the POFs were cut at the points where they intersect. The results obtained showed that the sensor could detect movement and respiratory rate. Recently, a system similar to that of [19], i.e. POF matrix with cuts embedded in a mattress, was used for sleep monitoring [20]. The system has been shown to be able to distinguish four sleep-related behavioral states, as well as to obtain breathing and heart rate data in different sleep positions and postures.

Nonetheless, to our best knowledge this work is the first to explore the use of non-wearable POF based sensors for posture detection. In this paper, we propose a novel design and implementation of POF sensors to infer the posture of a person sitting in an office chair, considering five different positions. In addition to the sensors' production, end-user software applications were also designed and developed, both for Windows PC and Android. The data acquisition system

and software were integrated with a cloud service (Google Firebase). The developed tools are responsible for the data collection, its processing, and storage in a cloud. They also allow real-time interaction with the user, providing the alerts and prompting for posture adjustments when/if needed.

The paper is organized as follows. Section 1 provides the motivation and introduction to the work. Section 2 describes the proposed sensing architecture. Section 3 focuses on sensors design and calibration. The implemented protocols and results are discussed in Section 4 and, lastly, the conclusions and future work are presented in Section 5.

II. ARCHITECTURE DESIGN AND OPERATION PRINCIPLE
A. FIBER OPTIC SENSORS DESIGN
The optical sensors developed in this work detect variations in light intensity, comprising three main elements: a LED - light emitting diode (IF-E93 LED, 520 nm, Industrial Fiber Optics, Tempe, USA); a POF (polymethyl-methacrylate optical fiber model SH-4001, Mitsubishi Chemical Corporation, Wiesbaden, Germany) inserted in a cell developed for pressure detection; and a photodetector (IF D92, Industrial Fiber Optics, Tempe, USA). The type of optical fiber used (POF), is a standard 1 mm core fiber, available on the market and chosen not only due to its robustness, but also because it is a low-cost solution, allowing the use of lower cost photodetectors and LEDs. That way it's possible to implement a low-cost optical interrogation system, unlike the ones used for instance with fiber Bragg gratings (FBGs). The interrogation system for FBGs is substantially more expensive than the photodetectors used in this work. This system was designed so that pressure applied to the cell containing the POF (sensor cell) causes a controlled bending of the optical fiber, which in turn increases the optical attenuation and decreases the optical power detected at the end of the fiber by the photodetector. Consequently, as the pressure on the sensor increases, the optical power detected by the photodetector decreases. By performing a controlled calibration of each POF sensor cell, it is possible to determine the magnitude of the pressure applied on it.

A transimpedance amplifier circuit was designed to convert the current generated by the photodiode, which is inversely proportional to the pressure change applied to the sensor, into a voltage variation. For the transimpedance circuit, we chose the AD8615 operational amplifier (AnalogDevices, Wilmington, USA), and a 1 MΩ potentiometer was used as feedback resistor, thus enabling more precise calibration adjustments/tuning. To better match the output voltage of the sensors to the dynamic range of the analog-to-digital converter (ADC), and to allow an individual calibration of each sensor, one potentiometer per sensor cell was used.

The sensor cell is composed of a 3D printed (Ultimaker 3D Extended, Ultimaker, Utrecht, Netherlands) housing that accommodates the POF (Figure 1). Our cell was designed in such way that when the optical fiber is subjected to pressure, an attenuation on the optical power is obtained, returning
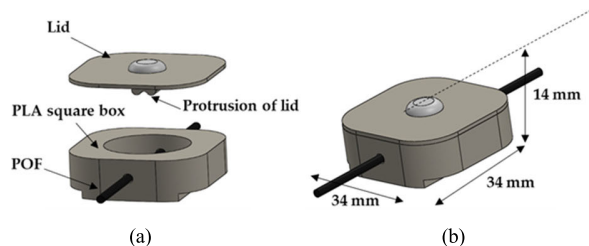
FIGURE 1. Sensor cell design: (a) identification of all components and (b) dimensions.

FIGURE 2. Schematic representation of: (a) three types of lids and (b) three resin heights.

to its original shape when no pressure is applied. This cell was produced in polylactic acid (PLA, Ultimaker, Utrecht, Netherlands) using standard 3D printing processes, consisting of a square box with a large cavity at the top and two holes on the sides through which the fiber is passed, and a lid with a protrusion that is inserted into the hole and can move up and down depending to the existence or not of pressure. PLA was the material chosen for the sensor body composition because it is the most used polymer for 3D printing, widely available, low-cost and capable of giving the needed sensor robustness. Figure 1a shows the 3D drawing of the box with the optical fiber and the lid design chosen for testing, depicting how the components are assembled to form the sensor cell; Fig. 1b presents the sensor cell dimensions.

The cell was then filled with epoxy resin, with the aim of helping the optical fiber to restore its position after the pressure is applied. In order to achieve the best sensitivity for the system, with the lowest hysteresis, three lid configurations and three resin heights were tested (Table 1).

TABLE 1. Summary of all tested optical sensor cell configurations.

Sensor identification	Lid configurations	Epoxy resin configurations
A	L1	Without resin
B	L2	Without resin
C	L3	Without resin
D	L1	With resin - H1
E	L2	With resin - H1
F	L3	With resin - H1
G	L1	With resin - H2
H	L2	With resin - H2
I	L3	With resin - H2
K	L1	With resin - H3
J	L2	With resin - H3
L	L3	With resin - H3

The difference between the three lids was only in its surface: lid 1 (L1) had a circular shape with a diameter smaller than the diameter of the box cavity, allowing it to move vertically; lid 2 (L2) also had a circular shape and the diameter was larger than the box cavity, allowing only the center of the lid to move vertically; lid 3 (L3) had a square shape with the same dimensions as the top of the box (see schematic 3D in Fig. 2a). The three configurations of resin height are depicted in Fig. 2b and consist of: resin until touching the optical
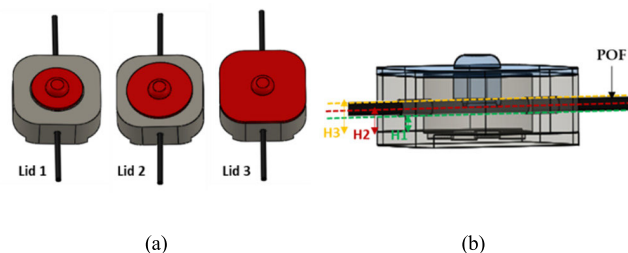
fiber (H1); resin to half the height of the optical fiber (H2); and resin to cover the optical fiber (H3).

A total of twelve configurations were tested in two pressure tests, to assess the best relationship between the sensor cell ability to return to zero when pressure is released and its sensitivity to mass variations. In the first test, a mass of 5 kg was applied and removed after 1 minute, while in the second, a mass of 20 kg was used. All cells without resin in the cavity had difficulty returning to their initial values after being subjected to the second mass, which implied to configurations A, B and C being excluded. In the configurations where the resin height tested was H1 (sensors D, F and F) the same was verified, although the recovery to the initial values ended up happening, it took many minutes, which was not plausible for the developed system. In the sensor cells in which the resin height was H3, the opposite was verified, the cell was not sensitive to the pressure exerted, especially for the first mass (5 kg), for the second mass (20 kg) only the K sensor showed to have some sensitivity. Finally, analyzing the cells with H2 resin height, all were sensitive to both tested masses. However, after exerting the weight, only the configuration with Lid 3 (sensor I) showed a return to the initial position within a few seconds, so it was the configuration chosen for our work.

B. IMPLEMENTATION OF THE SENSORS IN AN OFFICE CHAIR

The seat of an office chair was instrumented with several sensor cells (in the configuration identified as I on Table 1) aiming to monitor the pressure and consequently the position of the user. The sensor cells were placed in four distinct areas: right (IR) and left ischial (IL) tuberosities, and right (TR) and left thigh (TL) (Fig. 3a top). The sensor cells were installed in a wooden board like what already existed in the original chair seat, inside cavities drilled in the wood with the outer dimensions of the cells. Subsequently, two aluminum sheets (3 mm thick) were fixed: one above the sensors to provide a larger contact area (Fig. 3a bottom), and the other to the base of the wood to increase its resistance. The only part of the cell above the level of the wooden top is a drop-like structure 3D printed on the lid, which will serve as a pressure transfer point from the top aluminum sheet plate to the cell. To complete the assembly process of the office chair, the optical fibers of

FIGURE 3. Office chair seat instrumentation process: (a) sensor cells installed on the wooden seat plate (top); aluminum plate fixed on the seat over the sensor cells (bottom); (b) finalized instrumented chair; and (c) schematic representation of sensor cell connection.
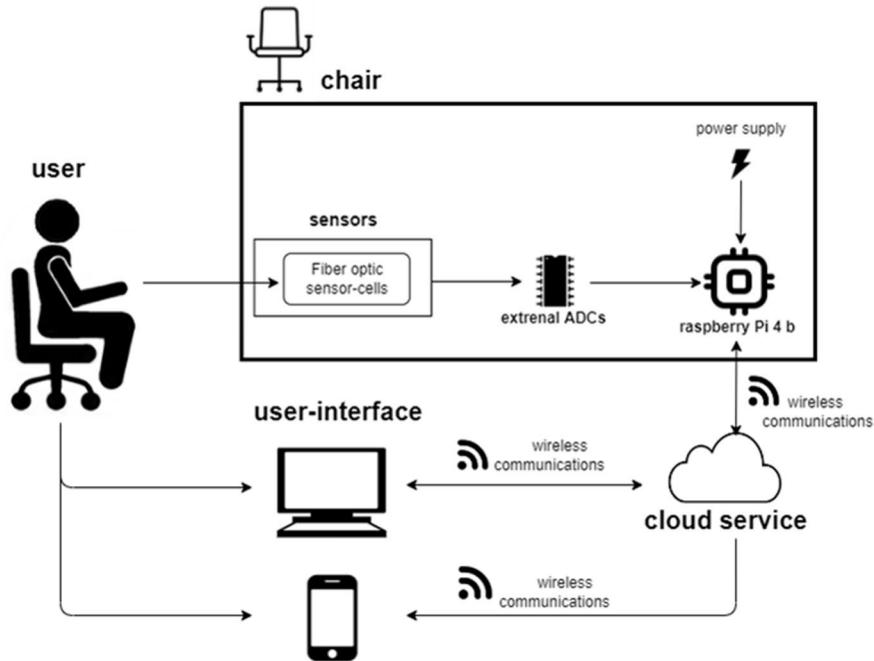
FIGURE 4. Overall architecture of the implemented system.

the four sensor cells are connected to the LEDs and correspondent photodetectors, placed in the box under the chair, along with the hardware for the data acquisition, processing, and transmission system (according to the schematic shown in Fig. 3c). Following the chair instrumentation, the original chair sponge is placed over the seat's aluminum plate. Finally, the chair fabric is added (Fig. 3b).

C. DATA ACQUISITION SYSTEM AND SOFTWARE
In the developed system, the data are collected, processed, and sent to a database by a microcomputer, a Raspberry Pi (RPi) 4 B 2G (OKdo, London, England), which requires the use of external MCP3008 ADCs (Microchip, Arizona, USA). The whole system is powered by an external power supply connected to the mains and using a 230 V AC to 9 V DC transformer. The collected data is stored in a Realtime Database (RD) hosted in Google's Firebase cloud service [21]. The software developed for data acquisition can be divided into three sections: the RPi firmware; the computer application (Windows); and the smartphone application (Android). Fig. 4 shows the overall system architecture supporting our proposed implementation of the office chair.

1) RASPBERRY PI 4 B

The data from the four sensor cells are collected and processed by the RPi using Python, which also handles the streaming to the RD. To make the system user friendly, the data is processed in such a way that the information reaching the user is simply the position he/she is adopting at that moment. However, to reach this conclusion, it is necessary to go through three data processing steps: first, the data read by each sensor cell are converted into kgV using its sensitivity coefficients; then an analysis is performed by group percentage, that is, the sum of the values measured by each sensor at each moment corresponds to 100%; and finally, the values of each sensor cell (already in percentage) will relate to the user's posture through the conditions that will be described later in Section 4. The RPi sends the detected position to the RD only if it detects the same position twice in a row.

2) COMPUTER AND MOBILE APPLICATIONS

Computer (Windows) and mobile (Android) applications were developed to visualize the user's position in real-time, which also shows whether the chair is empty or not. For the Window application, the interface was created using the Tkinter library, which is the default toolkit in Python for the standard GUI (Graphic User Interface) applications. The interface consists of a schematic image related to the position adopted (or the empty chair) and informs if the position being adopted is correct or not (Fig. 5). In the case of the Android application, the interface is created using Android Studio with Kotlin language, which is the standard for Android applications. The GUI is very similar in comparison to the Window application, in which the information displayed is the same.

(a)   (b)   (c)
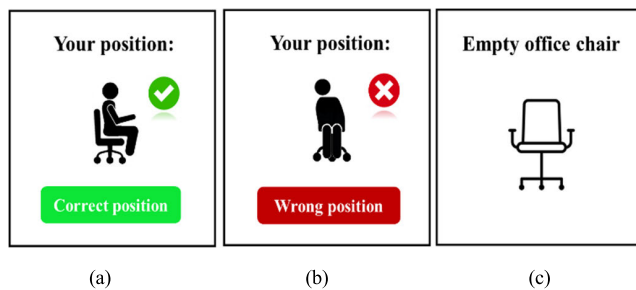
FIGURE 5. Examples of the displayed information about the user's position for both the mobile phone and computer applications: (a) when he/she is in the correct position; (b) when he/she in an incorrect position; and (c) when the chair is empty.

To warn the user that he/she has been sitting for more than 30 minutes in the same position or if he/she is incorrectly sitting, a pop-up window opens in the lower right corner of the computer, as represented in Fig. 6a and 6b, respectively. The 30 minutes is the time defined by default by the software based on some publications [4], [22], however the user can change it according to their needs.

(a)   (b)
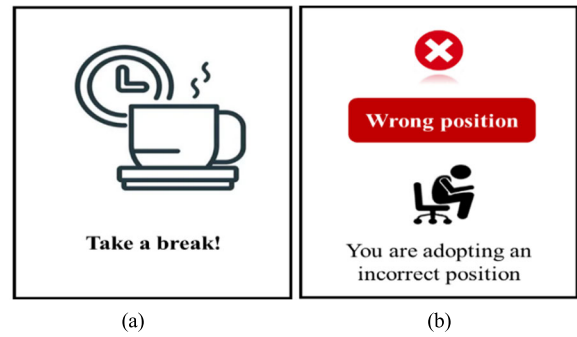
FIGURE 6. Examples of pop-ups that will appear on the user's computer or mobile phone.

III. SENSING SYSTEM CALIBRATION

The four sensor cells were calibrated for mass increase and decrease, in a range of 0-25 kg, using several loads over the seat zone of each sensor. The range tested allows to know the sensors' response for an exerted mass of up to 100 kg by a user. Fig. 7 illustrates the response of the TR sensor cell obtained during this calibration process.
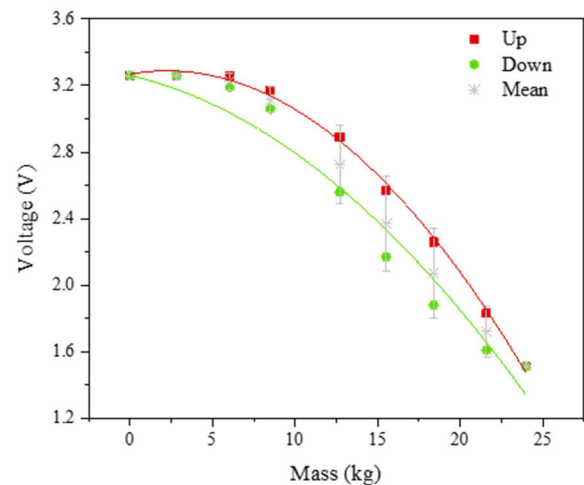
FIGURE 7. Calibration test to mass variations for the TR sensor cell. The lines correspond to the polynomial fits.

Polynomial approximations were made to all results and their coefficients are summarized in Table 2. The differences of sensitivity coefficients between sensors may be due to different factors. Although we have tried to reproduce the sensor cells in the same way, there are small geometrical discrepancies between sensor cells. In addition, there are still some manually controlled steps in the process, such as: placing the resin, gluing and tensioning of the optical fiber. The resin itself can still produce small air bubbles that are difficult to control and that can easily change its elasticity, which explains the differences in the sensitivities observed in Table 2. As it is the largest factor, we only consider the linear factor (b) as the sensitivity value to pressure. Therefore, from

TABLE 2. Sensitivity coefficients to the polynomial fits.

Optical sensor cell	Sensitivity coefficient (V/kg)
TR	$a=1.32\text{x}10^{-4}$; $b=-7.37\text{x}10^{-2}$
TL	$a=-3.02\text{ x}10^{-4}$; $b=-1.75\text{x}10^{-4}$
IR	$a=5.72\text{ x}10^{-4}$; $b=-1.46\text{x}10^{-1}$
IL	$a=-1.60\text{ x}10^{-3}$; $b=-3.10\text{x}10^{-2}$

TABLE 3. Descriptive characteristics of the participants enrolled in our study.

User	Gender	Height (cm)	Mass (kg)
#1	male	172	77
#2	male	178	74
#3	female	167	59
#4	male	173	70
#5	female	165	54
#6	male	180	100

FIGURE 9. Representation of the five adopted positions throughout the protocol.
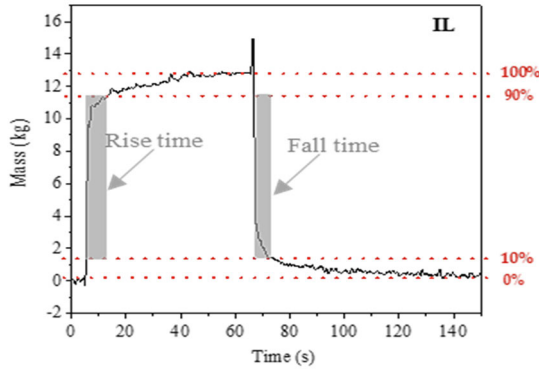
FIGURE 8. Characterization of the response time of the sensor cell IL.

FIGURE 10. The logic used in the software to identify the user's positions.

the same table we can conclude that the sensor cells have an average sensitivity of 62.7 mV/kg. From the response of each cell to the rise and fall of weights, it is still possible to assess its hysteresis. For this sensor cell, the average hysteresis obtained was 22.7%. This value is considerably high, and it may be due to the structure and operating principle of the sensor cells, as it is made of viscoelastic materials that tend to have higher hysteresis. As the final results showed, for this particular application it was still possible to correctly detect the user position, because the final outcome is an average value dependent on the simultaneous measurement of the 4 sensors simultaneously. Nevertheless, hysteresis effect re-duction is important, and the team is working on it.

The POF sensors cell response times were also tested. To do so, a person sat down in the chair and stood up again after around one minute, while the values obtained by the sensor cells were recorded. Fig. 8 illustrates the response of the IL sensor cell during this test. To determine the response time, analysis of the time elapsed between 10 and 90% of the sensor cell response to the impulse was considered. Average response times of 7.33 s (with standard deviation of 1.55 s) and 3.42 s (with standard deviation of 0.17 s) were obtained for the ascend and decrease of the mass, respectively. As the purpose of the sensors is to monitor the pressure over several hours and determine the user's position over time, response times of a few seconds do not affect the performance of all system.

As the thermal variations to which the sensor cells are subject are expected to be low and equal in all sensor cells and as the end result of the user's position is relative to percentage ratios of all sensor cells, this temperature influence ends up

be removed. Therefore, the thermal characterization has been neglected.

IV. EXPERIMENTAL EVALUATION
A. PROTOCOL AND IMPLEMENTATION
Posture recognition tests on the office chair with the sensor cells were performed by six adults (2 females and 4 males) without known pathologies and able to move without external assistance. Table 3 presents the users' physical characteristics. The tests were performed in a closed indoor environment, at a constant room temperature,

TABLE 4. Relative load distribution (in %) obtained for each user in the five positions tested and confirmation of the logic of the software to validate the positions.

Positions	1	2	3	4	5
Logical condition	Reference	$TR_2+TL_2>TR_1+TL_1$	$TR_3+TL_3>60\%$	$TR_4+IR_4>50\%$	$TL_5+IL_5>50\%$
User 1	-	✓	✓	✓	✓
User 2	-	✓	✓	✓	✓
User 3	-	✗	✓	✓	✓
User 4	-	✓	✓	✓	✓
User 5	-	✓	✓	✓	✓
User 6	-	✓	✓	✓	✓

in which the voluntaries performed the postures presented in Fig. 9 respectively:

- Position 1: correctly seated;
- Position 2: leaning forward;
- Position 3: leaning forward with the hips wrongly positioned;
- Position 4: leaning on the right side;
- Position 5: leaning to the left side.

In the first time that the user sits in the chair, he/she must be positioned correctly according to Position 1 (Fig. 9), and he/she must tare the chair. Afterwards, according to the data of Position 1, and through the logic present in the flowchart (Fig. 10), the software will detect the user's position. It is important to highlight that, after the first stage, the values are converted into percentages (as explained in section 3.2.1) to make its analysis easier.

B. RESULTS AND DISCUSSION

The percentages obtained for all users during the test positions, the logic of the software and the result achieved by the sensor cells are presented in Table 4.

Six users with different masses (from 54 to 100 kg) were tested, and from the results presented in Table 4, we can conclude that the office chair instrumented with the POF sensor cells was able to predict with 96.6% accuracy four of the five tested posture (Positions 1, 3, 4 and 5). Although in all other users, the Position 2 was correctly detected, in user 3 this was not the case. In fact, Position 2 becomes the most difficult posture to detect since it is an intermediate between Positions 1 and 3, i.e. the user is far from the back of the chair but may not be leaning forward enough to validate the Position 2 condition. The analysis of this position would be easier if the information taken from the sensor cells of the seat was complemented with the response of sensor cell positioned on the back of the chair, in order to indicate to the

software if there would be contact in this area of the chair. However, despite allowing us to detect Position 2 with greater certainty and possibly also allowing the detection of other incorrect positions, an instrumented chair also with sensors on the back would make the whole system more complex and expensive.

V. CONCLUSION

In this work, an office chair seat was instrumented with four optical fiber-based sensor cells to monitor the user's posture. Each sensor cell has a box configuration, 3D printed in PLA, with epoxy resin stabilizing a POF that crosses the 3D printed box. Different lids and resin heights were tested. The sensitivity and response time of these cells was evaluated, from which it was found that the best performance (sensitivity and response time) was the one obtained from the sensor cell with configuration I. Based on this primary study, four sensor cells, similar to the configuration I were produced and incorporated into the seat of a chair, presenting an average sensitivity of 62.7 mV/kg.

Real world tests were performed with six users, considering 5 pre-defined postures. The data was acquired in a quite random scenario: we considered the most common positions adopted by users (correct and wrong ones), have done so for different subjects, both in height and in weight, which grants the system, a wide sample characterization both according to the position/posture adopted and with the characteristics of the user. The results showed that the proposed system is a promising solution, allowing to estimate four positions with 96.6% of confidence. Position 2 was not correctly detected in only one user; this posture is the most difficult one to detect because it is an intermediate position between Position 1 and 3, and the user may not be leaning forward enough to validate the Position 2 condition.

Due to the results presented, considering the inherent advantages of using optical fibers over electronic sensors and the simplicity and low-cost, the proposed solution is a promising method to replace the existing electronic technology to detect user postures in office chairs, and advise on the posture improvements. The lower complexity, yet high efficiency of the used algorithms, requires lower computational capacities and times, which is and added advantage of the solution here proposed. The developed software already allows the user to receive notifications to take a break if he/she is sitting in the same position for more than 30 minutes (default time), but this time can be adjusted by the user. This work was developed for an office chair, but it can be used in other types of seats with structures capable of embedding the produced sensor cells (so that they do not interfere with the user's well-being), such as in sofas or beds.
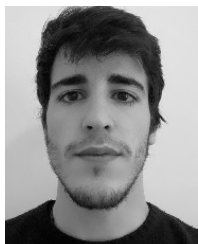
In the future, it would be of added value improve these sensor cells (testing new materials/designs) in order to have a solution with less hysteresis, test a solution with sensors built into the back of the chair to allow the detection of more positions, and to incorporate other optical sensors to monitor the user's physiological parameters and parameters related of the environment. Regarding the developed software, as the data is sent to an online database, it is only necessary to authorize access to the database to the person or systems of interest (for example, hospitals) that can handle them in the most appropriate way for the intended purpose. Therefore, in the future it can be adapted to other e-Health systems. For example, for medical teams to study the posture of a team of workers during a certain period and relate it to their spinal injuries, or for people with special needs the sending urgent and emergency information in case of detection of long periods of inactivity that suggests a risk situation (it can even send alerts not only to the user's cell phone but also to the caregiver's cell phone or to medical assistance).

REFERENCES

[1] Y. Ding, Y. Cao, V. G. Duffy, and X. Zhang, "It is time to have rest: How do break types affect muscular activity and perceived discomfort during prolonged sitting work," *Saf. Health Work*, vol. 11, no. 2, pp. 207–214, Jun. 2020.

[2] N. Marques, C. Z. Hallal, and M. Gonçalves, "Biomechanic, ergonomic, and clinical features of the sitting posture: A review," *Fisioter. Pesqui.*, vol. 17, no. 3, pp. 270–276, 2010.

[3] A. P. Claus, J. A. Hides, G. L. Moseley, and P. W. Hodges, "Is 'ideal' sitting posture real?: Measurement of spinal curves in four sitting postures," *Manual Therapy*, vol. 14, no. 4, pp. 404–408, Aug. 2009.

[4] V. Korakakis, K. O'Sullivan, P. B. O'Sullivan, V. Evagelinou, Y. Sotiralis, A. Sideris, K. Sakellariou, S. Karanasios, and G. Giakas, "Physiotherapist perceptions of optimal sitting and standing posture," *Musculoskeletal Sci. Pract.*, vol. 39, pp. 24–31, Feb. 2019.

[5] M. Huang, I. Gibson, and R. Yang, "Smart chair for monitoring of sitting behavior," in *Proc. DesTech Int. Conf. Design Technol., Knowl. E*, Jan. 2017, pp. 274–280.

[6] L. Russell, R. Goubran, and F. Kwamena, "Posture detection using sounds and temperature: LMS-based approach to enable sensory substitution," *IEEE Trans. Instrum. Meas.*, vol. 67, no. 7, pp. 1543–1554, Jul. 2018.

[7] B. Prueksanusak, P. Rujivipatand, and K. Wongpatikaseree, "An ergonomic chair with Internet of Thing technology using SVM," in *Proc. 4th Technol. Innov. Manage. Eng. Sci. Int. Conf. (TIMES-iCON)*, Dec. 2019, pp. 1–5.

[8] D. Bibbo, M. Carli, S. Conforto, and F. Battisti, "A sitting posture monitoring instrument to assess different levels of cognitive engagement," *Sensors*, vol. 19, no. 3, p. 455, Jan. 2019.

[9] A. A. Ishaku, A. Tranganidas, S. Matuska, R. Hudec, G. McCutcheon, L. Stankovic, and H. Gleskova, "Flexible force sensors embedded in office chair for monitoring of sitting postures," in *Proc. IEEE Int. Conf. Flexible Printable Sensors Syst. (FLEPS)*, Jul. 2019, pp. 1–3.

[10] W. Kim, B. Jin, S. Choo, C. S. Nam, and M. H. Yun, "Designing of smart chair for monitoring of sitting posture using convolutional neural networks," *Data Technol. Appl.*, vol. 53, no. 2, pp. 142–155, Jun. 2019.

[11] L. Dziuda, "Fiber-optic sensors for monitoring patient physiological parameters: A review of applicable technologies and relevance to use during magnetic resonance imaging procedures," *J. Biomed. Opt.*, vol. 20, no. 1, 2015, Art. no. 10901.

[12] D. L. Presti, C. Massaroni, C. Leitão, M. F. Domingues, M. Sypabekova, D. Barrera, I. Floris, L. Massari, C. Oddo, D. Tosi, and E. Schena, "Fiber Bragg gratings for medical applications and future challenges: a review," *IEEE Access*, vol. 8, pp. 156863–156888, 2020.

[13] C. P. Mayoral, J. G. Gutiérrez, J. L. C. Pérez, M. V. Treviño, I. B. G. Velasco, P. A. H. Cruz, R. T. Rosas, L. T. Carrillo, J. A. Ríos, E. L. Apreza, and R. R. Laguna, "Fiber optic sensors for vital signs Monitoring. A review of its practicality in the health field," *Biosensors*, vol. 11, no. 2, p. 58, Feb. 2021.

[14] M. F. Domingues, N. Alberto, C. Leitão, C. Tavares, E. de Lima, A. Radwan, V. Sucasas, J. Rodriguez, P. André, and P. Antunes, "In-sole optical fiber sensor architecture for remote gait analysis—An eHealth solution," *IEEE Internet Things J.*, vol. 6, no. 1, pp. 207–214, Feb. 2017.

[15] C. Leitão, P. Antunes, J. L. Pinto, J. M. Bastos, and P. André, "Carotid distension waves acquired with a fiber sensor as an alternative to tonometry for central arterial systolic pressure assessment in young subjects," *Measurement*, vol. 95, pp. 45–49, Jan. 2017.

[16] D. Lo Presti, C. Monssaroni, J. D'Abbraccio, L. Massari, M. Caponero, U. G. Longo, D. Formica, C. M. Oddo, and E. Schena, "Wearable system based on flexible FBG for respiratory and cardiac monitoring," *IEEE Sensors J.*, vol. 19, no. 17, pp. 7391–7398, Sep. 2019.

[17] D. Haroglu, N. Powell, and A.-F.-M. Seyam, "A textile-based optical fiber sensor design for automotive seat occupancy sensing," *J. Textile Inst.*, vol. 108, no. 1, pp. 49–57, Jan. 2017.

[18] T. H. Lee, E. S. Kim, T. H. Kim, and M. Y. Jeong, "Simple pressure sensor for a vehicle seat using a woven polymer optical-fiber sheet," *J. Korean Phys. Soc.*, vol. 67, no. 11, pp. 1947–1951, Dec. 2015.

[19] D. Sartiano and S. Sales, "Low cost plastic optical fiber pressure sensor embedded in mattress for vital signal monitoring," *Sensors*, vol. 17, no. 12, p. 2900, Dec. 2017.

[20] P. Han, L. Li, H. Zhang, L. Guan, C. Marques, S. Savovic, B. Ortega, R. Min, and X. Li, "Low-cost plastic optical fibre sensor embedded in mattress for sleep performance monitoring," *Opt. Fiber Technol.*, vol. 64, pp. 102–541, Jul. 2021.

[21] Google. *Firebase Realtime Database*. Accessed: Oct. 2021. [Online]. Available: https://firebase.google.com

[22] Environment, Health and Safety UNC EHS. *Office Ergonomics*. Accessed: Dec. 2021. [Online]. Available: https://ehs.unc.edu/workplace-safety/ergonomics/office/

CÁTIA TAVARES was born in Aveiro, Portugal, in July 1992. She received the master's degree in engineering physics from the University of Aveiro, in 2016. Currently, she is a DAEPHYS Ph.D. Scholarships at the Physics Department, Aveiro University, and the Institute of Nanostructures, Nanomodelling and Nanofabrication. Her current research interest includes the development of optical fibre sensors for e-Health solutions.

JOÃO OLIVEIRA E. SILVA was born in Aveiro, Portugal, in March 1997. He received the master's degree in electronics and telecommunications engineering from the University of Aveiro, Aveiro, in 2021. He also received the defending his master's thesis. His thesis was titled ''Implementation of a data acquisition and transmission system for an e-Health platform'' and the work described in it was used within the scope of this project. His research interests include work related to embedded devices, sensorization, machine learning, signal processing, and noise recognition.

ANDRÉ MENDES was born in Porto, Portugal, in August 1997. He received the master's degree in electronics and telecommunications engineering from the University of Aveiro, Portugal, in 2021. His thesis was titled ''Conception of a data processing system for an e-Health platform'' and the work described in it was used as a complement for the writing of this project. His research interests include 5G network data analysis and optimization and server maintenance.

LEONOR REBOLO was born in Funchal, Portugal, in 1999. She is currently pursuing the integrated master's degree in biomedical engineering with the University of Aveiro. In 2020, her third year's final project was on ''Smart office chair for working conditions optimization.'' Currently, she is working on her master's thesis, on medical imaging devices optimization for cancer therapies.

MARIA DE FÁTIMA DOMINGUES (Member, IEEE) received the M.Sc. degree in applied physics and the Ph.D. degree in physics engineering from the University of Aveiro, Portugal, in 2008 and 2014, respectively. In 2015, she started a research fellow position at the Instituto de Telecomunicações—Aveiro and the Consejo Superior de Investigaciones Científicas (CSIC)—Madrid, Spain. She is currently a Researcher with the Instituto de Telecomunicações. She has authored or coauthored more than 100 journals and conference papers, several book chapters and five books. Her current research interests include new solutions of photonic-based sensors and its application in e-Health scenarios, with a focus in physical rehabilitation architectures.

NÉLIA ALBERTO received the Ph.D. degree in physics from the University of Aveiro, Portugal, in 2011.

From 2012 to 2017, she worked under a FCT Postdoctoral Research Fellowship, and in 2018, she was hired as a Researcher by the Instituto de Telecomunicações—Aveiro, Portugal. She has acquired expertise in the design and development of optical fiber sensors, fiber coatings and application in different contexts, and with special focus for medical environments. She is the author/coauthor of one book, six book chapters, 52 papers in international peer-reviewed journals, and more than 70 papers in conference proceedings.

MÁRIO LIMA received the bachelor's degree in electronics engineering and telecommunications, the M.Sc. degree in telecommunications systems, and the Ph.D. degree in electrical engineering from the University of Aveiro, Portugal, in July 1994, June 1998, and July 2003, respectively. He is currently an Assistant Professor with the Department of Electronics, Telecommunications, and Informatics, University of Aveiro, and a Researcher at the Optical Communications Group, Institute of Telecommunications—Aveiro. He has participated in several national (FCT and QREN support) and international projects included in the European Union (EU) Telecommunications Research and Development Programs, such as ACTS and IST. He has/is supervised seven Ph.D. students and 65 M.Sc. students. He has contributed to one book, three books chapters, one patent, published 56 papers in journals, and more than 120 resumes in conferences proceedings.

HUGO PLÁCIDO SILVA (Senior Member, IEEE) was born in Vila Franca de Xira, Portugal, in August 1979. He received the Ph.D. degree in electrical and computers engineering from the University of Lisbon, Lisbon, Portugal, in 2015. Since 2004, he has been a Researcher in IT with the Instituto de Telecomunicações. He has been a Professor with the Instituto Superior Técnico, since 2019, and the Co-Founder and the Chief Innovation Officer at PLUX—Wireless Biosignals, S.A., since 2007. His research interests include biosignal research, system engineering, signal processing, and machine learning. His work has been distinguished with numerous academic and technical awards.

PAULO FERNANDO DA COSTA ANTUNES received the degree in engineering physics, the M.Sc. degree in applied physics, and the Ph.D. degree in physics engineering from Aveiro University, Portugal, in 2005, 2007, and 2011, respectively. From 2017 to 2019, he was an Assistant Researcher with the Physics Department, Aveiro University, and the I3N (Institute of Nanostructures, Nanomodelling and Nanofabrication), Aveiro, Portugal. Currently, he is an Assistant professor with the Physics Department, Aveiro University, and a Researcher at the I3N and IT institutes. His research interests include the study and simulation of optical fiber sensors based on silica and polymeric fibers, for static and dynamic measurements, data acquisition, optical transmission systems, and sensor networks for several applications, such as temperature and strain measurements in extreme environments, structural monitoring, and physical rehabilitation.

● ● ●

MANUSCRIPT 8

Respiratory and heart rate monitoring using an FBG 3D-printed wearable system

CÁTIA TAVARES,[1,2,*] CÁTIA LEITÃO,[1,2] DANIELA LO PRESTI,[3] M. F. DOMINGUES,[2] NÉLIA ALBERTO,[2] HUGO SILVA,[4,5] AND PAULO ANTUNES[1,2]

[1]*Department of Physics & I3N, University of Aveiro, Campus Universitário de Santiago, 3810-193 Aveiro, Portugal*
[2]*Instituto de Telecomunicações and University of Aveiro, Campus Universitário de Santiago, 3810-193 Aveiro, Portugal*
[3]*Unit of Measurements and Biomedical Instrumentation, Departmental Faculty of Engineering, Università Campus Bio-Medico di Roma, 00128 Rome, Italy*
[4]*Instituto de Telecomunicações, Instituto Superior Técnico, University of Lisbon, 1049-001 Lisbon, Portugal*
[5]*PLUX - Wireless Biosignals, S.A, Lisboa, Portugal*
*catia.tavares@ua.pt

Respiratory and heart rate monitoring using an FBG 3D-printed wearable system

CÁTIA TAVARES,[1,2,*] **CÁTIA LEITÃO,**[1,2] **DANIELA LO PRESTI,**[3] **M. F. DOMINGUES,**[2] **NÉLIA ALBERTO,**[2] **HUGO SILVA,**[4,5] **AND PAULO ANTUNES**[1,2] (iD)

[1]*Department of Physics & I3N, University of Aveiro, Campus Universitário de Santiago, 3810-193 Aveiro, Portugal*

[2]*Instituto de Telecomunicações and University of Aveiro, Campus Universitário de Santiago, 3810-193 Aveiro, Portugal*

[3]*Unit of Measurements and Biomedical Instrumentation, Departmental Faculty of Engineering, Università Campus Bio-Medico di Roma, 00128 Rome, Italy*

[4]*Instituto de Telecomunicações, Instituto Superior Técnico, University of Lisbon, 1049-001 Lisbon, Portugal*

[5]*PLUX - Wireless Biosignals, S.A, Lisboa, Portugal*

*catia.tavares@ua.pt

Abstract: This work proposes a 3D-printed sensor based on fiber Bragg grating (FBG) technology for respiratory rate (RR) and heart rate (HR) monitoring. Each sensor is composed of a single FBG fully encapsulated into a 3D-printable *Flexible*, during the printing process. Sensors with different material thicknesses and infill densities were tested. The sensor with the best metrological properties was selected and preliminary assessed in terms of capability of monitoring RR and HR on three users. Preliminary results proved that the developed sensor can be a valuable easy-to-fabricate solution, with high reproducibility and high strain sensitivity to chest wall deformations due to breathing and heart beating.

1. Introduction

Fiber Bragg grating (FBG) is an optical technology widely used to produce sensors for medical applications [1]. FBG sensors have many advantages, such as high sensitivity, multiplexing capability, small size and weight, and electromagnetic interference immunity. Moreover, FBG sensors are highly safe, including in humid environments since there is no electrical current at the sensing point [1,2]. In the last decades, the use of FBG sensors for medical applications has experienced a rapid evolution: from surgical tools instrumentation [3–6] to wearable garments [7–10] and biosensors [11,12] development.

In biomedical scenarios, the FBG aforementioned advantages make them very appealing for wearables designed to monitor physiological parameters, without interfering with the user's daily life. Bearing this in mind, the main focus of this work is the development of wearable sensors based on a single FBG for monitoring two vital signs: the respiratory rate (RR) and heart rate (HR). Commonly, when integrated into wearables, FBGs work as strain sensors and must meet the requirements of reduced size and weight, comfort, and flexibility [13,14]. Once placed in contact with the body, the sensors must be able to suffer deformations according to the mechanical movements caused by the user chest wall and reflect them in its output signal [13,14].

Previous work has proposed FBGs to monitor vital signs, items and smart garments in the form of wearables [15,16]. In 2011, Silva et al. designed and fabricated a wearable system based on a single FBG sensor to monitor RR and HR [7]. The main innovation of this system was the structure in which the FBG sensor was embedded: a foil made of polyvinyl chloride (PVC). A year later, a paper was published proposing a sensor consisting of a FBG embedded in

a pneumatic cushion placed between the backrest of a seat and the back of the monitored person [17]. Laboratory studies have shown that the sensor was able to monitor dynamic strains (μ) in the range of 50-124 μμ, caused by the respiration, and about 8.3 μμ due to the heartbeat.

Years later, in 2017, Lo Presti et al. proposed a smart textile based on an array of 12 FBGs, evaluating its feasibility of monitoring RR and HR in healthy subjects in two body positions (standing and supine) [18]. In the same year, Nedoma et al. published a paper focused on a novel FBG-based system suitable for the simultaneous monitoring of RR and HR during magnetic resonance imaging (MRI) examinations [19]. The developed sensor was encapsulated in a polydimethylsiloxane polymer (PDMS). Still in 2017, a novel non-invasive optical ballistocardiography technique that allowed simultaneous measurement of cardiac and respiratory activities was reported. The unique design of this device provided additional capabilities, such as monitoring nascent morphology of cardiac and respiratory activity, HR and HR variability (HRV) [20].

There are several techniques and materials exploited to encapsulate FBGs to measure vital signs, like embedding FBGs in resin or plastic composites (for example in PDMS [20,21], Dragon skin [13,22], Ecoflex [17] or PVC [7]). These materials are very flexible and confer to the FBGs good robustness, high adaptability to the skin, and good compliance with the chest movements. However, some uncontrolled factors which may occur during the manufacturing process, such as a non-uniform bonding strength at the fiber-polymer interface and the presence of some bubbles of air in the cured polymer matrixes, may affect the performance of the final system.

To overcome these issues, recently, fused deposition modeling (FDM) has been proposed as a promising method for fabricating various components, including sensors [23]. The FDM technique allows to develop a sensing element very quickly and with high printing precision [23,24]. It is establishing therefore a good alternative to the most common polymer encapsulation methods. The FDM technique has been mainly used in the fabrication of sensors for civil engineering [25–27]. Few papers proposed this technique in the fabrication of sensors for medical applications [28,29], but none of them for monitoring respiration and cardiac activity.

The paper aims at evaluating if the FDM method can be an innovative technique to build a FBG-based wearable system able to monitor the users' vital signs in real time, namely RR and HR. This sensing element is composed of an optical fiber with a single FBG sensor into 3D-printed material (i.e., the *Flexible)*. The optical fiber with FBG was fully embedded in the material during the printing process. To optimize the strain sensitivity of the wearable system, the influence of three infills percentages and two different thicknesses on the sensor response was investigated. Then, the most sensitive sensor was worn and tested on three different users during normal breathing and apnea.

This paper is organized as follows: the first section presents the introduction to the work, the second section explains the working principle, followed by the development of the sensor (section 3), section 4 presents the tests performed on users, and finally the discussion and conclusion follows (section 5).

2. Working principle

A FBG is a periodic perturbation of the refractive index along the fiber core. The modulation of the refractive index generates a grating, which reflects a narrowband of wavelengths centered at the Bragg wavelength (λ_B), when the Bragg condition is met:

$$\lambda_B = 2n_{eff}\Lambda \tag{1}$$

where λ_B is the reflected Bragg wavelength, n_{eff} is the effective refractive index of the optical fiber core and Λ is the grating period, which corresponds to the periodic modulation of the refractive index.

The FBGs can be affected by changes in strain (Δl) and/or temperature (ΔT). Consequently, λ_B varies ($\Delta\lambda_B$), according to the following equation:

$$\Delta\lambda_B = \Delta\lambda_{B,\iota} + \Delta\lambda_{B,T} = 2\left(\Lambda\frac{\partial n_{eff}}{\partial l} + n_{eff}\frac{\partial \Lambda}{\partial l}\right)\Delta l + 2\left(\Lambda\frac{\partial n_{eff}}{\partial T} + n_{eff}\frac{\partial \Lambda}{\partial T}\right)\Delta T = S_l\Delta l + S_T\Delta T \quad (2)$$

The first term is related to the strain induced wavelength shift, and the second one to the thermal effect on the same parameter. S_l and S_T represent the FBG sensitivity coefficients to strain and temperature, respectively.

When the FBG is embedded into a 3D printed polymer matrix, S_l and S_T are largely influenced by the elastic and thermal properties of the material, much thicker than the silica fiber [27]. The elastic properties will influence the response to strain, however the T contribution may be ignored, because the parameters to be measured have considerably higher dynamic behavior than temperature variations, which are time dependent.

The developed sensor is intended to be worn on the chest to measure RR and HR. Therefore, it should be able to measure the displacement occurring on the chest during respiration (from 4 to 12 mm) and heart beating (from 0.2 to 0.5 mm) [13]. These chest deformations stretch the surface of the 3D-printed polymer, being transferred up to the sensor, and leading to a change in the FBG output ($\Delta\lambda_B$) as depicted in Fig. 1.
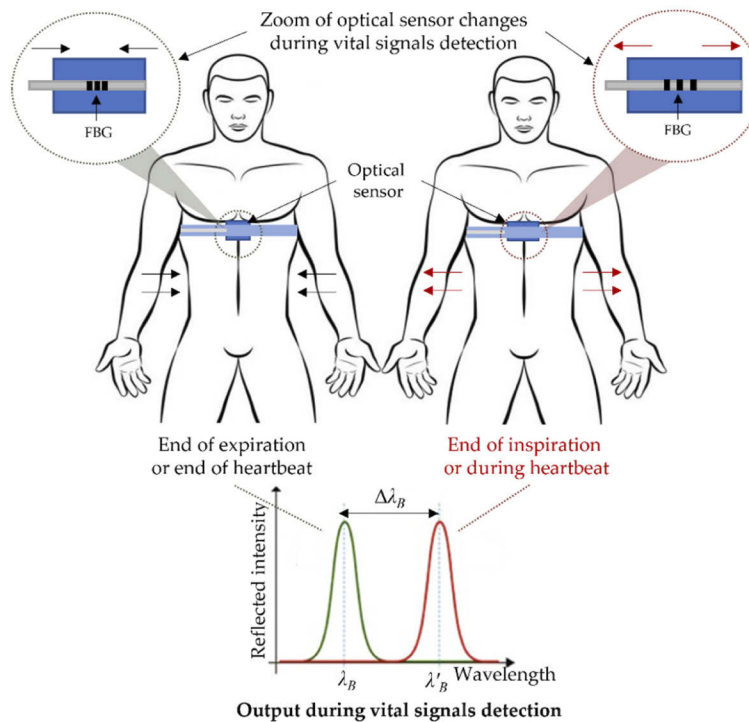
Fig. 1. Schematic representation of the optical sensor response during vital sign measurements.

3. 3D-printed sensor development: design, fabrication, and metrological characterization

3.1. Design and production

The sensor developed for measuring RR and HR values consists of an elastic material (*Flexible*, Fish box mini model, Avistron, Bergheim, Germany) printed by a 3D printer (Ultimaker 3D Extended, Ultimaker, Utrecht, Netherlands) and a single optical fiber with a single FBG (Fig. 2). The FBGs were inscribed into photosensitive optical fiber (GF1, Thorlabs, New Jersey, United States of America) for a length around 5 mm, using a pulsed Q-switched Nd: YAG laser system (LS-2137U, LOTIS TII, Minsk, Belarus), emitting at the fourth harmonic (266 nm). The FBGs were recorded through the phase mask technique, employing a laser pump energy of 25 J, a repetition rate of 10 Hz, and an exposure time of 1 min, approximately.
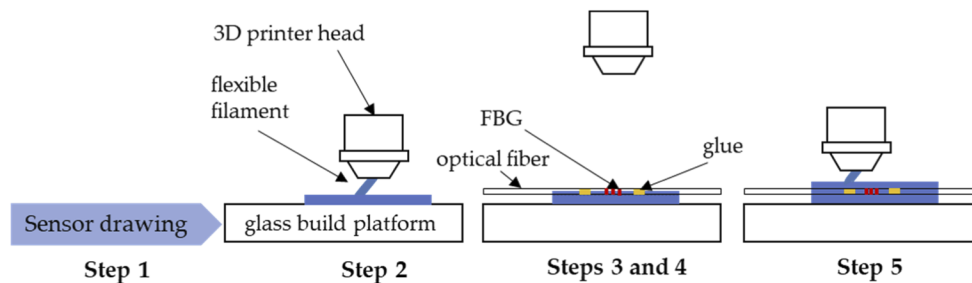
Fig. 2. Schematic diagram of fabrication process of the optical sensor using an 3D printer.

As the aim of the present study was to develop a FBG-based fully printed 3D sensor with high robustness and able to detect chest wall deformations due to respiration and the heart beating pumping, an elastic material was chosen, due to its stretchability without tearing.

The fabrication process consists of the following steps (Fig. 2):

1. 3D drawing of the sensor (Step 1);

2. Sensor printing on a 3D printer with the *Flexible* filament (Step 2);

3. When the 3D-printed part is halfway through its printing, the process is paused, and the optical fiber containing the FBG is placed into the corresponding groove (Step 3);

4. The optical fiber is tensioned and fixed with cyanoacrylate glue on each side of the FBG, after which, it was given a resting time of 10 s, for the glue to cure (Step 4);

5. Printing is resumed (Step 5).

The 3D drawing of the piece was designed with several grooves, so that the optical fiber and glue have space to be placed, without interrupting the printing of the posterior layers (Fig. 3). After defining all the details of the design, in order to successfully place the FBG, two more factors responsible for improving the performance of the sensor were investigated: the thickness of the 3D-printed sensor and the infilling density of the print [30]. In details, two thicknesses (2 and 3 mm), and three infills (20, 60 and 100%) were tested (Fig. 3 b). Therefore, six different sensors were produced (Table 1).

3.2. Metrological characterization

The experimental setup to analyze the sensors response to strain was composed by a waveform generator (33220A, Agilent Technologies, Santa Clara, California) to produce sinusoidal waves
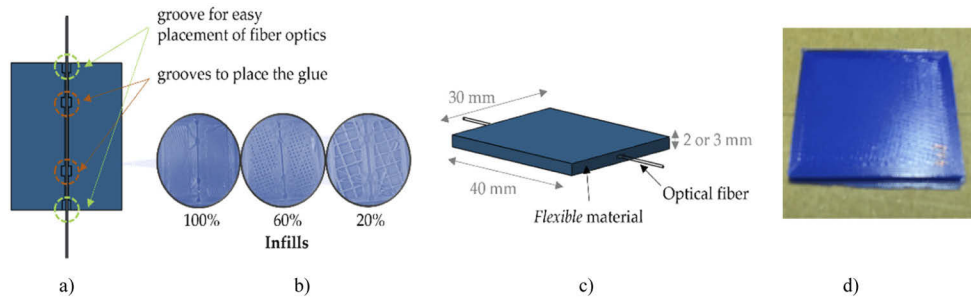
Fig. 3. Schematics of the sensor: (a) cut in the middle of the 3D drawing to show the grooves inside the sensor; (b) infills photographs; (c) representation of all sensor components and dimensions; and (d) sensor photography.

Table 1. Characteristics of the six sensors produced

Name of sensor	Thickness (mm)	Infill (%)
A	3	100
B	3	60
C	3	20
D	2	100
E	2	60
F	2	20

that fed a Z/Tilt Piezoelectric Flexure Stage (P287.70, Physik Instrumente, Karlsruhe, Germany), via a high-voltage piezoelectric amplifier (E-508.00, Physik Instrumente, Karlsruhe, Germany). This specific actuator was chosen due to its movement range being close to the chest movements during breathing and heart beats, presenting a maximum displacement of 700 μm. The sensors' responses were characterized by pressing the sensor with the actuator, causing 150 μm (displacement amplitude) sinusoidal movements in the cardiac frequency range (from 0.5 to 10.0 Hz), and of 450 μm, in the respiratory frequency range (from 0.1 to 0.3 Hz). The study of the higher frequencies (and small amplitude motion, 150 μm) was done sequentially for the frequencies of 0.5, 1, 2, 4, 6, 8, and 10 Hz. For lower frequencies (and greater range of motion, 450 μm), the frequencies studied were 0.1, 0.15, 0.2, and 0.3 Hz. The signal frequency sweeps were made in loop, firstly by increasing the frequency and then decreasing it, until the value of the first frequency applied.

After testing, the 3 mm thick sensors did not show the necessary sensitivity to amplitudes related with cardiac activity. Therefore, no graph of sensors A, B and C will be presented. The same did not happen for the sensors with 2 mm, so the Fig. 4 a) and b) show the Bragg wavelength shift signals obtained from each sensor (D, E and F) for 150 and 450 μm displacement amplitudes, respectively.

For the 150 μm signal, which is representative of cardiac activity, sensor F with ≈ 0.024 nm of Bragg wavelength shift was the one that achieved a signal with greater amplitude, i.e., greater sensitivity. To the 450 μm signal, representative of respiration, sensors D and F showed a similar Bragg wavelength shift amplitude (≈ 0.090 nm). Considering the data from sensor F acquired at the lower frequency (0.1 Hz) for the greater amplitude movements (450 μm), a sensitivity of 0.190 ± 0.001 pm/μm was reached. On the other hand, as expected, for the higher frequency (10 Hz), acquired at lower amplitude movements (150 μm), a slightly lower sensitivity was attained (0.120 ± 0.004 pm/μm). These results supported that the sensor with the best sensitivity to both parameters was sensor F and therefore it was chosen to be used in the tests with users.
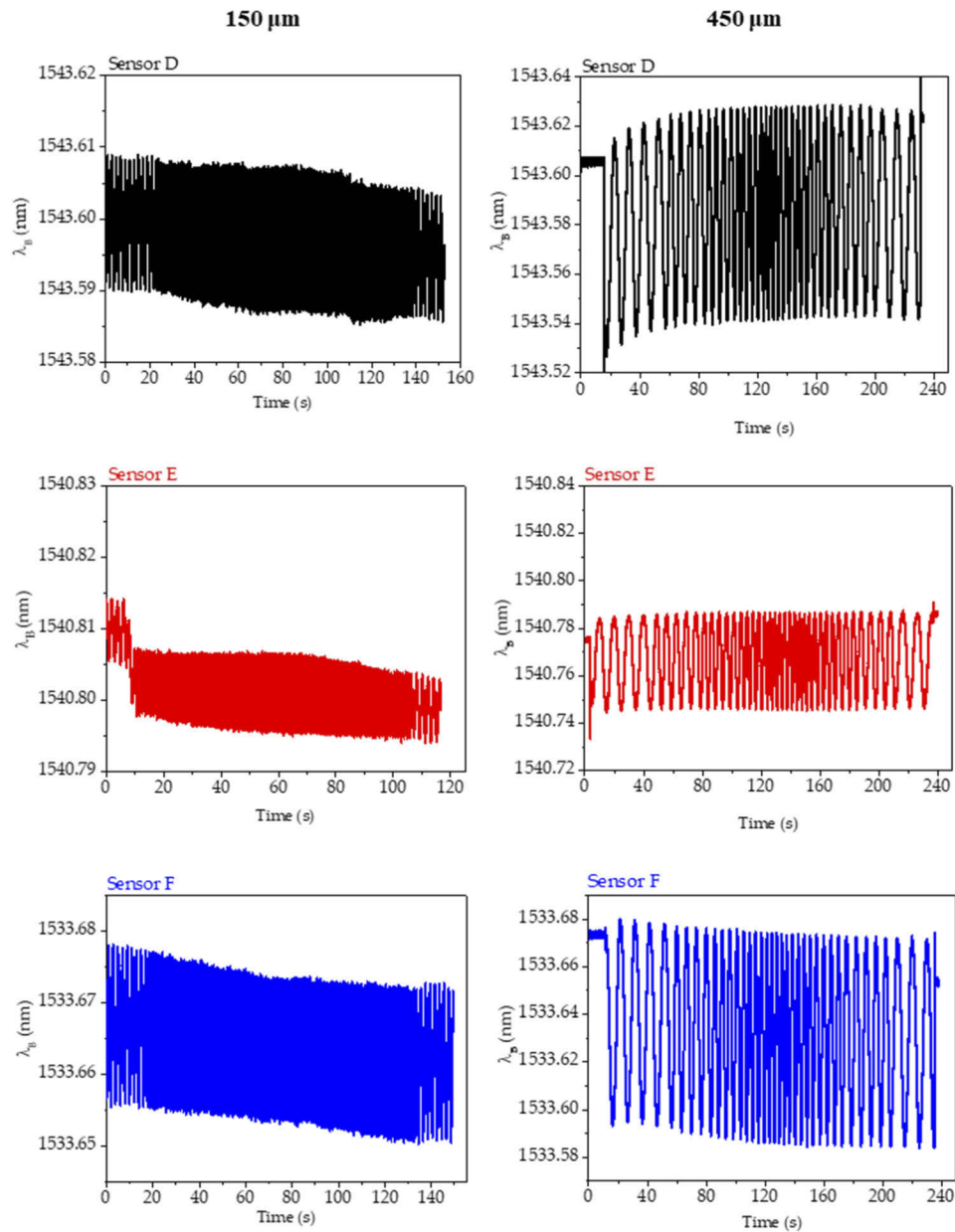
Fig. 4. Sensors D, E and F sensitivity test results to: (a) 150 μm; and (b) 450 μm amplitude movements.

Since the measurements performed using this sensor are expected to be very dynamic compared to the variation in body temperature, this variation can be removed from the signal by digital filtering. Therefore, the thermal characterization has been neglected.

4. Tests on users

The preliminary assessment of the optical sensor (OS) feasibility to monitor RR and HR was evaluated on three users with the respective anthropometric characteristics presented in Table 2.

Table 2. Anthropometric characteristics of the users

User	Gender	Age	"Height (m)	Weight (kg)
1	Female	34	1.65	71
2	Female	33	1.59	57
3	Male	30	1.80	83

The BioHarness (BH) device (ZEPHYR performance systems, Medtronic, Colorado, United States of America) was used as a reference for both the RR and HR. It records the respiration waveform at 25 samples/s and the ECG at 250 samples/s. As shown in Fig. 5, each user was asked to place the two systems – the BH elastic band around the chest and the 3D-printed sensor under the BH on the left side of the chest. The output of the developed sensor was collected by an optical interrogation system composed by a spectrometer (I MON 512E, Ibsen photonics, Farum, Denmark), a circulator (6015-3, Thorlabs, New Jersey, United States of America) and an optical source (AS4500, BA Technology, Shanghai, China) with an acquisition rate of 1000 Hz. Each user was invited to lie down on a physiotherapy bed to perform three tests of two types of breathing: 30 s of apnea (Ap) followed by 90 s of normal breathing (NB). The data gathered by the optical sensor during the test of each user are shown in Fig. 6.
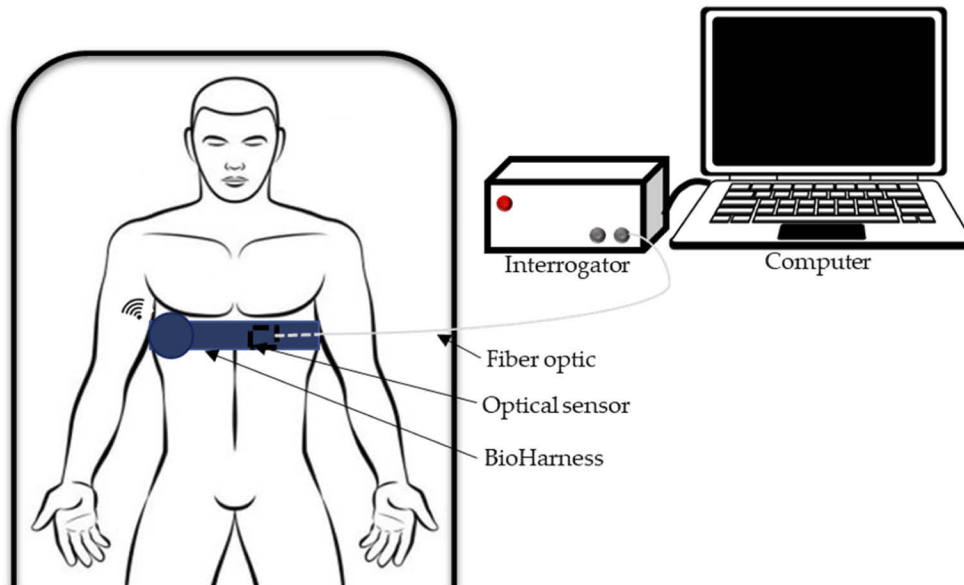
Fig. 5. Schematic diagram of the experimental arrangement for the vital signals acquisition during the tests on users.

In order to obtain the RR and HR from the recorded signals, different signal processing steps were applied to evidence each signal component aimed to be detected (respiratory and heart beat signals). For RR estimation, due to be a high amplitude movement of the chest and therefore presenting a high signal-to-noise ratio, only a smooth filter was applied. For the HR monitoring, since the vibrations of the heart have a higher frequency and much lower amplitude than the respiratory movements, knowing that the normal HR is between 50 to 120 bpm, a bandpass
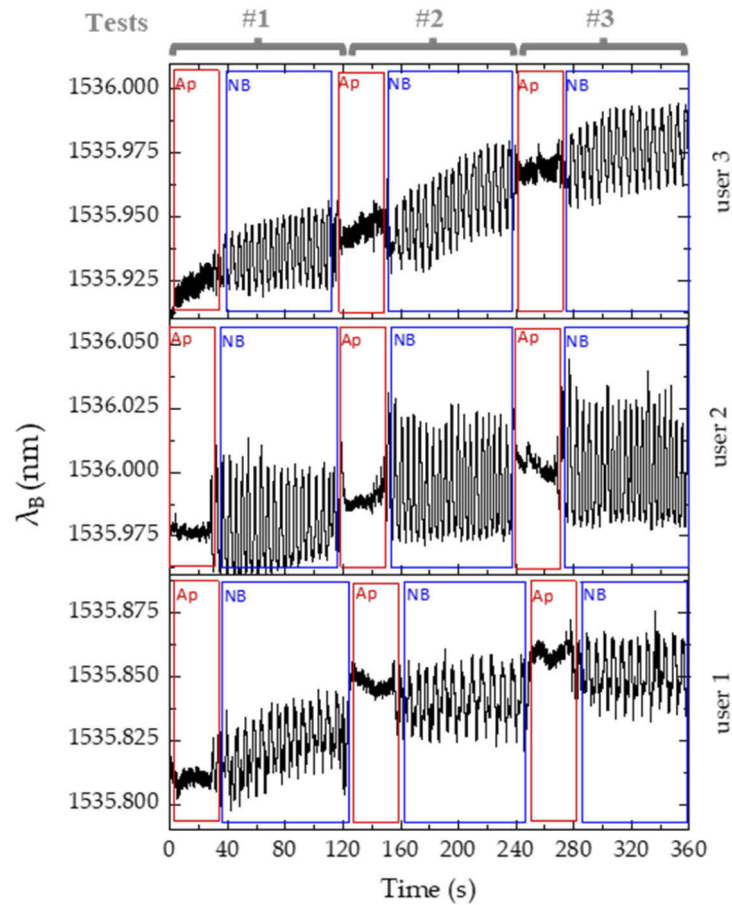
Fig. 6. Bragg wavelength shift results of the optical sensor during tests realized on three users.

frequency (0.8 Hz - 2.0 Hz) was applied [13] to reveal the heart beat signal. Both RR and HR were calculated as the number of maximum peaks over time windows of 30 s. Afterward, these values were converted into rpm and bpm, respectively by multiplying the number of maximum peaks per 2.

For cardiac and respiratory activities, a maximum will correspond to one heartbeat and one breath, respectively. Figure 7 shows the comparison between the signals of the two sensors during the tests to detect the vital signs (respiratory and heart signals) of the three users.

The RR and HR results comparison, obtained using both sensors, is shown in Fig. 8 and Fig. 9, respectively.
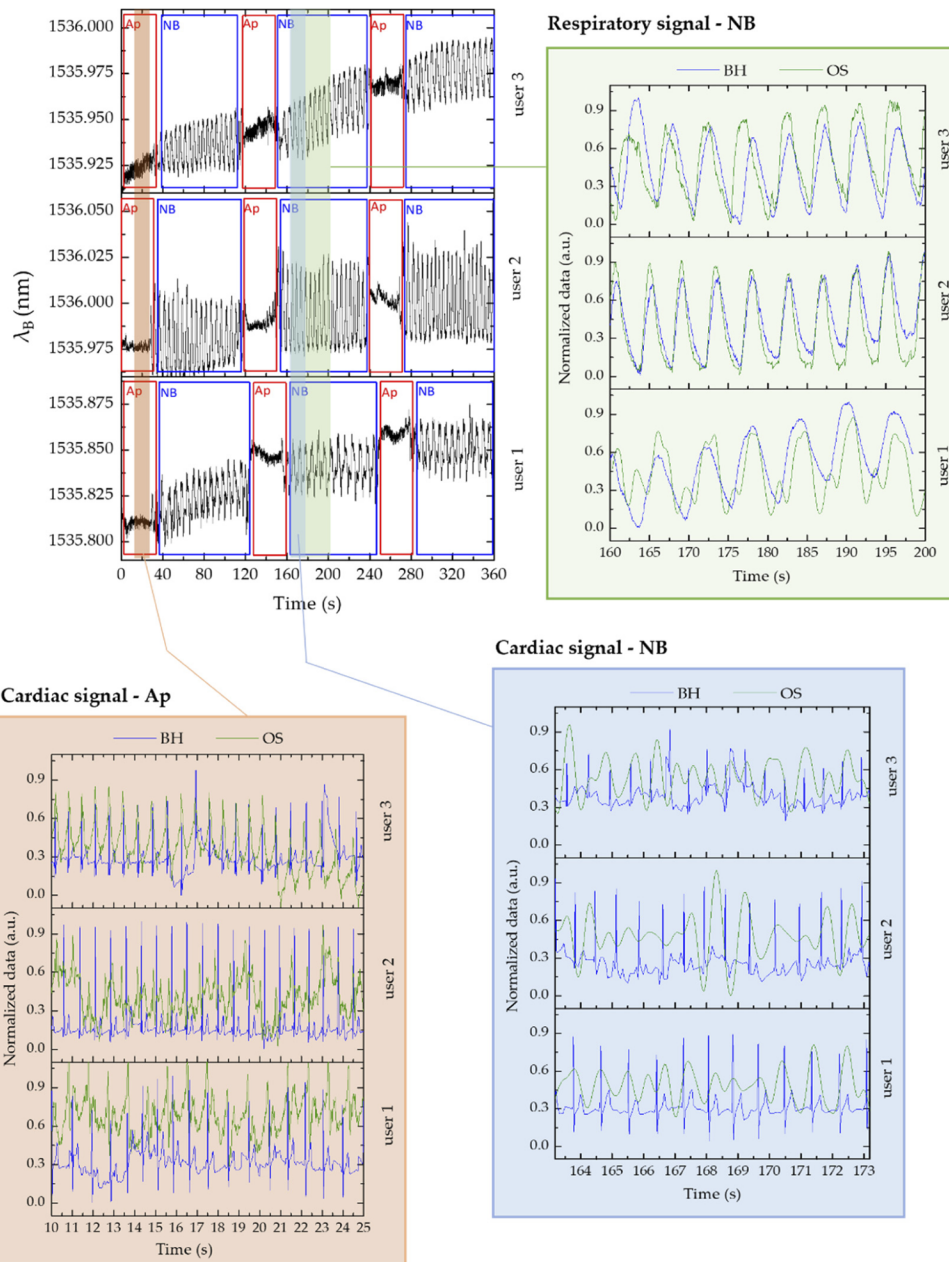
Fig. 7. Comparison between the signals from the two sensors during the tests performed by each user.

Figure 8 shows the RR in time slots of 30 seconds, for normal breathing. The average RR of users 1-3 was 10, 14, and 13 rpm, respectively (values obtained by the two sensors). It can be seen that the signals from the two sensors completely match for all the tests of the three users.

Figure 9 shows heart rate throughout the test, with users 1-3 having mean HRs of 67, 85, and 91 bpm, respectively (values obtained by the reference sensor). It can be verified that the HR registered by the two devices is very similar. Also, the maximum difference between rates of two
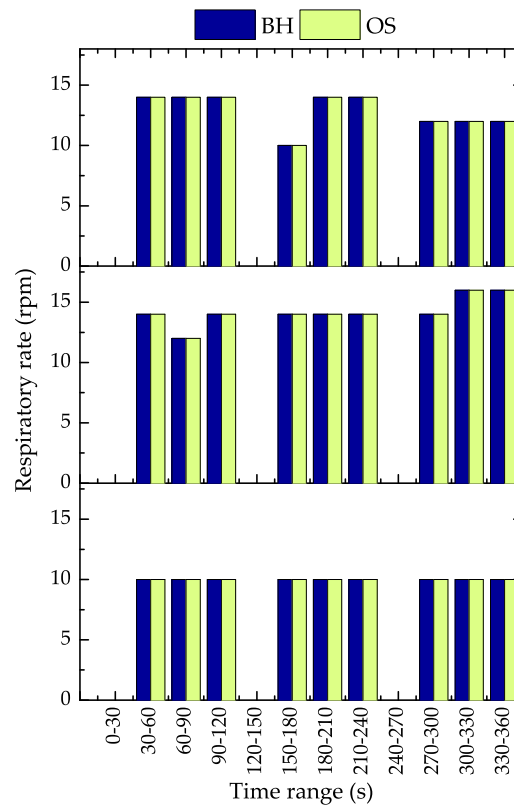
Fig. 8. Comparison between the RR obtained from the two sensors during the tests performed by each user.

sensors occurred mainly in the range time corresponding to the first change from Ap to NB (see Fig. 9, range time 30-60 s for users 1 and 2).

The developed sensor results were compared with the reference (BH using paired difference, paired absolute difference and percent difference). Using the BH as the standard, the paired difference was assessed by calculating the difference between both techniques in each time range, being calculated as (HR_{BH}-HR_{OS}). Absolute values were also considered, in order to better assess the magnitude of difference without considering direction. Percent differences were calculated as [($HR_{BH} - HR_{OS}$)/HR_{BH}]×100. Results are presented and compared with two commercial HR monitors in Table 3.

Table 3. Heart rate (bpm and %) differences between BH and OS and comparison of the results with commercial HR monitors that also used ECG as reference.

Device	HR differenced from ECG (mean ± Standard deviation)			References
	Paired differences	Absolute paired differences	Percent difference	
FBG	0.8 ± 5.9 bpm	3.8 ± 4.6 bpm	0.6 ± 7.6%	This work
Polar Chest Strap	0.2 ± 1.4 bpm	0.7 ± 1.2 bpm	0.9 ± 1.6%	[31]
Apple Watch	-1.7 ± 10 bpm	5.0 ± 9.0 bpm	5.5 ± 9.4%	[31]
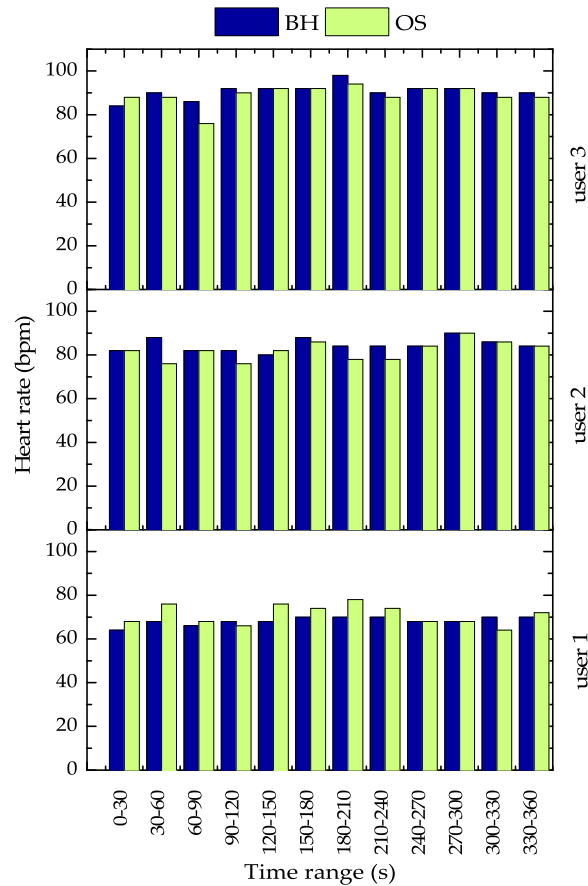
Fig. 9. Comparison between the cardiac signals from the two sensors during the tests performed by each user.

5.   Discussion and conclusions

In this work, a 3D printed sensor produced with *Flexible*, with an embedded FBG was developed to monitor two vital signs, namely HR and RR. Six different configurations were tested for this sensor, varying two thicknesses and three infill percentages. To define the best sensor for the target application, all sensors were tested for frequencies between 0.1 and 10.0 Hz, and two different movement amplitudes, 150 and 450 μm. The sensor that showed higher sensitivity for both types of signals was the device with the least thickness and less filling, which was referred to as the sensor F throughout the paper.

Since this is a sensor for monitoring very dynamic parameters, the optical fiber sensors calibration is normally performed for very low frequency parameters, such as, temperature, pressure and relative humidity, was neglected [13].

Applicability tests were performed with three users, to preliminarily evaluate the system's ability to detect chest wall excursions related to respiratory and cardiac activities. An electronic commercial sensor was used as a reference to compare the obtained signals. The results showed that the proposed system is a wearable solution, and it is able to estimate the users' RR and HR during normal breathing and apnea. Although the displacements caused by the heartbeat are smaller than those induced by the respiration, the values obtained for the HR only differ 0.8 ± 5.9 bpm, which is in line with other commercial wearable devices.

Due to the reliability of the results presented, the inherent advantages of using optical fibers over electronic sensors, and the simple, inexpensive and high reproducibility of the sensor, the proposed solution constitutes a promising method to replace existing electronic technology for detecting heart and respiration rates.

In the future, it would be of added value to develop a portable and low-cost, stand-alone interrogation system to install on elastic band, capable of being powered by a battery.

Disclosures. The authors declare no conflict of interest.

Data availability. Data underlying the results presented in this paper are not publicly available at this time but may be obtained from the authors upon reasonable request.

References

1. D. Lo Presti, C. Massaroni, C. Leitão, M. F. Domingues, M. Sypabekova, D. Barrera, I. Floris, L. Massari, C. Oddo, S. Sales, I. Iordachita, D. Tosi, and E. Schena, "Fiber Bragg gratings for medical applications and future challenges: a review,," IEEE Access **8**, 156863–156888 (2020).
2. D. Tosi, S. Poeggel, I. Iordachita, and E. Schen, "Fiber optic sensors for biomedical applications," in *Opto-Mechanical Fiber Optic Sensors* (Heinemann, 2018), 301–333.
3. X. He, J. Handa, P. Gehlbach, R. Taylor, and I. Iordachita, "A submillimetric 3-DOF force sensing instrument with integrated fiber Bragg grating for retinal microsurgery," IEEE Trans. Biomed. Eng. **61**(2), 522–534 (2014).
4. C. Kim and C. Lee, "Development of a 6-DoF FBG force-moment sensor for a haptic interface with minimally invasive robotic surgery," J. Mech. Sci. Technol. **30**(8), 3705–3712 (2016).
5. C. Lv, S. Wang, and C. Shi, "A high-precision and miniature fiber Bragg grating-based force sensor for tissue palpation during minimally invasive surgery," Ann. Biomed. Eng. **48**(2), 669–681 (2020).
6. R. Xue, B. Ren, J. Huang, Z. Yan, and Z. Du, "Design and evaluation of FBG-based tension sensor in laparoscope surgical robots," Sensors **18**(7), 2067 (2018).
7. A. F. Silva, A. F. Gonçalves, P. Mendes, and J. Correia, "FBG sensing glove for monitoring hand posture," IEEE Sensors J. **11**(10), 2442–2448 (2011).
8. S. Ambastha, S. Umesh, S. Dabir, and S. Asokan, "Comparison of force required for lumbar puncture with different gauges of spinal needle using fiber Bragg grating force device," IEEE Sensors J. **18**(19), 8028–8033 (2018).
9. C. Tavares, M. F. Domingues, A. Frizera-Neto, T. Leite, C. Leitão, N. Alberto, C. Marques, A. Radwan, E. Rocon, and P. André, "Gait shear and plantar pressure monitoring: A non-invasive OFS based solution for e-Health architectures," Sensors **18**(5), 1334 (2018).
10. M. F. Domingues, C. Tavares, A. Nepomuceno, N. Alberto, P. André, H. R. Chi, and A. Radwan, "Non-invasive wearable optical sensors for full gait analysis in e-Health architectures," IEEE Wirel. Commun. **28**(3), 28–35 (2021).
11. M. Loy, E. Hassan, M. Lobry, F. Liu, C. Caucheteur, R. Wattiez, M. DeRosa, W. Willmore, and J. Albert, "Rapid detection of circulating breast cancer cells using a multiresonant optical fiber aptasensor with plasmonic amplification," ACS Sens. **5**(2), 454–463 (2020).
12. C. Leitão, S. O. Pereira, N. Alberto, M. Lobry, M. Loyez, F. M. Costa, J. L. Pinto, C. Caucheteur, and C. Marques, "Cortisol in-fiber ultrasensitive plasmonic immunosensing," IEEE Sens. J. **21**(3), 3028 (2020)..
13. D. Lo Presti, C. Massaroni, J. D'Abbraccio, L. Massari, M. Caponero, U. Longo, D. Formica, C. Oddo, and E. Schena, "Wearable system based on flexible FBG for respiratory and cardiac monitoring," IEEE Sens. J. **19**(17), 7391–7398 (2019).
14. I. Aizhan, A. Beisenova, D. Tosi, and C. Molardi, "Fiber-optic based smart textiles for real-time monitoring of breathing rate," Sensors **20**(12), 3408 (2020).
15. C. Mayoral, J. Gutiérrez, J. Pérez, M. Treviño, I. Velasco, P. Cruz, R. Rosas, L. Carrillo, J. Ríos, E. Apreza, and R. Laguna, "Fiber optic sensors for vital signs monitoring. A Review of its practicality in the health field," Biosensors **11**(2), 58 (2021).

16. C. Massaroni, M. Zaltieri, D. Lo Presti, A. Nicolò, D. Tosi, and E. Schena, "Fiber Bragg grating sensors for cardiorespiratory monitoring: A review," IEEE Sens. J. **21**(13), 14069–14080 (2021).
17. L. Dziuda, F. W. Skibniewski, M. Krej, and J. Lewandowski, "Monitoring respiration and cardiac activity using fiber Bragg grating-based sensor," IEEE Trans. Biomed. Eng. **59**(7), 1934–1942 (2012).
18. D. Lo Presti, C. Massaroni, D. Formica, P. Saccomandi, F. Giurazza, M. A. Caponero, and E. Schena, "Smart textile based on 12 fiber Bragg gratings array for vital signs monitoring," IEEE Sensors J. **17**(18), 6037–6043 (2017).
19. J. Nedoma, M. Fajkus, R. Martinek, and V. Vasinek, "Non-invasive fiber-optic biomedical sensor for basic vital sign monitoring," Adv. Electr. Electron. Eng. **15**, 336–342 (2017)..
20. K. Chethana, A. S. Prasad, A. S. Omkar, and S. Asokan, "Fiber Bragg grating sensor based device for simultaneous measurement of respiratory and cardiac activities," J. Biophotonics. **10**(2), 278–285 (2017).
21. M. Fajkus, J. Nedoma, R. Martinek, V. Vasinek, and H. Nazeran, "A non-invasive multichannel hybrid fiber-optic sensor system for vital sign monitoring," Sensors **17**(12), 111 (2017).
22. D. Lo Presti, F. Santucci, C. Massaroni, D. Formica, R. Setola, and E. Schena, "A multi-point heart rate monitoring using a soft wearable system based on fiber optic technology," Sci. Rep. **11**(1), 21162 (2021).
23. S. B. Kesner and R. D. Howe, "Design principles for rapid prototyping forces sensors using 3-D printing," IEEE/ASME Trans. Mechatronics **16**(5), 866–870 (2011).
24. T. M. Llewellyn-Jones, B. W. Drinkwater, and S. R. Trask, "3D printed components with ultrasonically arranged microscale structure," Smart Mater. Struct. **25**(2), 02LT01 (2016).
25. C. Hong, Y. Zhang, Z. Lu, and Z. Yin, "A FBG tilt sensor fabricated using 3D printing technique for monitoring ground movement," IEEE Sens. J. **19**(15), 6392–6399 (2019).
26. C. Hong, Y. Zhang, D. Su, and Z. Yin, "Development of a FBG based hoop-strain sensor using 3D printing method," IEEE Access **7**, 107154–107160 (2019).
27. G. Teng, T. Zhang, Y. Li, and X. Qiao, "Highly sensitive FBG seismometer with a 3D-printed hexagonal configuration," J. Lightwave. Technol. **38**(16), 4588–4595 (2020).
28. A. Leal-Junior, C. Marques, M. Ribeiro, M. Pontes, and A. Frizera, "FBG-embedded 3-D printed ABS sensing pads: the impact of infill density on sensitivity and dynamic range in force sensors," IEEE Sens. J. **18**(20), 8381–8388 (2018).
29. Z. Hao, K. Cook, J. Canning, H. Chen, and C. Martelli, "3D printed smart orthotic insoles: monitoring a person's gait step by step," IEEE Sens. Lett. **4**(1), 1–4 (2020).
30. C. Lubombo and M. A. Huneault, "Effect of infill patterns on the mechanical performance of lightweight 3D-printed cellular PLA parts," Mater. Today Commun. **17**, 214–228 (2018).
31. M. Etiwy, Z. Akhrass, L. Gillinov, A. Alashi, R. Wang, G. Blackburn, S. M. Gillinov, D. Phelan, A. M. Gillinov, P. L. Houghtaling, H. Javadikasgari, and M. Y. Desai, "Accuracy of wearable heart rate monitors in cardiac rehabilitation," Cardiovasc. Diagn. Ther. **9**(3), 262–271 (2019).

Cátia Vanessa Rodrigues Tavares

Sensores de fibra ótica para arquiteturas *e-Health*

Fiber optic sensors for e-Health architectures

Relatório Complementar

Relatório escrito elaborado nos termos dos artigos 63.º e 64.º-A do Regulamento de Estudos da Universidade de Aveiro

Supplementary Report

Written report prepared under the terms of articles 63 and 64-A of the University of Aveiro Studies Regulation

Cátia Tavares

Symbols and constants

Λ_{Bragg}	Bragg Grating period
$\Delta\Lambda_{\text{Bragg}}$	Bragg Grating period variation
λ_{Bragg}	Bragg's wavelength
$\Delta\lambda_{Bragg}$	Bragg's wavelength variation
$(\theta m/2)$	Diffraction angle of the maximized order
m	Diffracted order
d	Distance between planes
n_{eff}	Effective refractive index
FBG_P	FBG to monitor pressure
FBG_T	FBG to monitor temperature
Λ	Grating period
θ/θ_i	Incident angle
n	Integer
λ_{laser}	Laser wavelength
Λ_{pm}	Phase mask period
f_R	Respiratory frequency
S_ε	Sensitivity coefficients to ε
S_T	Sensitivity coefficients to T
$\Delta\varepsilon$	Strain variation
e	Strain
T	Temperature
ΔT	Temperature variation
λ	wavelength

Acronyms

ASE	Amplified Spontaneous Emission
BCG	Ballistocardiogram
BCM	Body Center Of Mass
BH	BioHarness
bpm	Breaths per minute
BPM	Beats Per Minute
BT	Body Temperature
ECG	Electrocardiogram
FBG	Fiber Bragg Gratings
FDM	Fused Deposition Modelling
HR	Heart Rate
IC	Intrinsic Capacities
IFOS	Intensity Fiber Optic Sensor
IoT	Internet of Things
MRI	Magnetic Resonance Imaging
NA	Numerical Aperture
OFS	Optical Fiber Sensor
PD	Photodetector
PDMS	Polydimethylsiloxane Polymer
PF	Plantar Force
PLA	Polylactic Acid
PMMA	Polymethyl Methacrylate
PND	Peripheral Diabetes Neuropathy
POF	Plastic Optical Fiber
PZT	Piezoelectric Sensors
rh	Relative Humidity
RR	Respiratory Rate
R&D	Research and Development
SCG	Seismocardiogram

SF	Shear Force
SOF	Silica Optical Fiber
TPU	Thermoplastic Polyurethanes
UV	Ultraviolet
VGRF	Vertical Ground Reaction Force
WHO	World Health Organization

Figures Index

Tables Index

Cátia Tavares

Index

Cátia Tavares

CHAPTER 1

INTRODUCTION AND MOTIVATION

Cátia Tavares

1.1 MOTIVATION AND OBJETIVES

Advances in medicine and health care have resulted in an increase in the population's lifespan. These advances are changing the way and time in which diseases are diagnosed and how the patient is followed. Therefore, many scientists defend that we are facing a technological revolution in healthcare, which many call Healthcare 4.0 [1-3].

Fiber optic sensor technology has been extensively studied for medical applications, showing several advantages when compared to conventional electronic sensors. Such sensors are light, small, chemically inert, immune to electromagnetic interference, capable of operating in hostile and humid environments, flexible, don't need any electric signal at the measuring point and are non-toxic [4-7]. Although these sensors have many advantages, there are still challenges within the scientific community that studies this topic, especially in the development of sensors suitable for their application in clinical practices [8-10].

The present work has the general objectives of development and characterization of fiber optic sensors for several medical applications. Due to the differentiating characteristics of optical fiber, it offers the possibility of developing sensors with applicability in various areas of medicine through different sensing techniques. As the research progressed and different challenges emerged, there was an increase in the motivation to develop new sensors with optical fibers and provide new medical solutions both to aid in diagnosis and to monitor patients with the most varied pathologies.

That said, the objectives of this doctoral program were the:

- Implementation of a network of FBG sensors in insole for pressure monitoring and later for pressure and shear monitoring.
- Implementation of a network of FBG sensors to monitor pressure at several points of a wheelchair, and later to monitor pressure and temperature and detect the posture of the wheelchair user.
- Implementation of lower cost plastic optical fiber (POF) sensors on the seat of an office chair for pressure monitoring and detection of the user's posture. In parallel with the implementation of several electronic sensors to monitor physical and physiological parameters of the user and parameters of the surrounding environment.
- Development and testing of a fully encapsulated FBG sensor during the 3D printing process on an elastic material to monitor respiratory and heart rates.

Cátia Tavares

1.2   OPTICAL FIBER SENSOR – A BRIEF OVERVIEW

Optical Fiber Sensors (OFS) have been generating great interest in recent decades, not only by the scientific community but also by the industry. This interest is mainly due to their advantages when compared to conventional sensors; in addition to the advantages highlighted in Section 1.1, OFS tend to have a rapid response, good linearity, and high sensitivity to external perturbations [11]. Due to its properties, OFS are used to monitor the most diverse parameters: temperature, deformation and torsion, magnetic fields, refraction index, pressure, etc. Therefore, many works with OFS have been published in several engineering areas such as aerospace [12], civil [13], environmental [14], and biomedical [15].

There are several types of OFS, which differ not only in the material composing the optical fiber (the most common being: silica optical fiber (SOF) and polymer optical fiber (POF)), but also in the properties of the propagated optical signal (intensity, phase, frequency, or spectral content). The silica fibers have their core and cladding of silica, whereas POFs are typically fabricated of poly (methyl 2-methylpropenoate), usually known as polymethyl methacrylate - PMMA, or other polymers such as amorphous fluorinated polymer, polystyrene and polycarbonate [16]. The fibers used in this work were: the photosensitive optical fiber GF1 (Thorlabs) for FBG engraving and the POF model SH-4001 (Mitsubishi Chemical Corporation) for the intensity-based sensor. The main features of the referred optical fibers are presented on Table 1. Depending on the application, the two types of optical fiber can be chosen, conventional POFs are more robust and require simpler and cheaper interrogation systems, whereas SOFs are lighter and smaller, allowing not only sensing over longer distances, but more importantly the multiplexing capabilities using FBGs [16, 17].

Table 1. Main features of the SOF and POF used during my PhD.

Features	GF1	SH-4001
Total diameter (µm)	250	2200
Core diameter (µm)	9	980
Core material	silica	PMMA
Operation wavelength (nm)	1500-1600	530-650
Numerical aperture	0.13	0.5

Optical fiber sensing systems are generally composed by four components: a light source, the optical fibers, the sensing element, and a photodetector or spectrometer. The light source emits light to the optical fiber, that is transmitted through the optical fiber. The sensing element can be on the fiber itself or it can be external to the fiber, and it act as a transducer that change the properties of light with the measurand. In the end, the light is received in the photodetector/spectrometer. Given the variety of optical technologies available, only those used in this PhD work are discussed in this section.

Cátia Tavares

1.2.1 Fiber Bragg grating sensors

In 1978 Hill et al. from the Canadian Communication Research Center reported the formation of the first FBG, inscribed in a germanosilic fiber [18]. An FBG consists of a periodic modulation of the refractive index along an optical fiber core. When a wideband light spectrum is injected into the optical fiber with an FBG, this optical signal will interact with the FBG, where a sharp peak centred on the Bragg wavelength is reflected, and all other wavelengths are transmitted [18-21]. As can be seen from the schematic in Figure 1.

After several years of inscribing methods optimization in different optical fibers and different applications, it now very well established that FBGs are particularly suitable for sensing purposes, becoming the most promising and reliable optical fiber sensing technology in the world, mainly due to the relatively simple fabrication methods, and their inherent unique advantages. Besides sensing, FBGs are used as passive optical filters in optical communications.
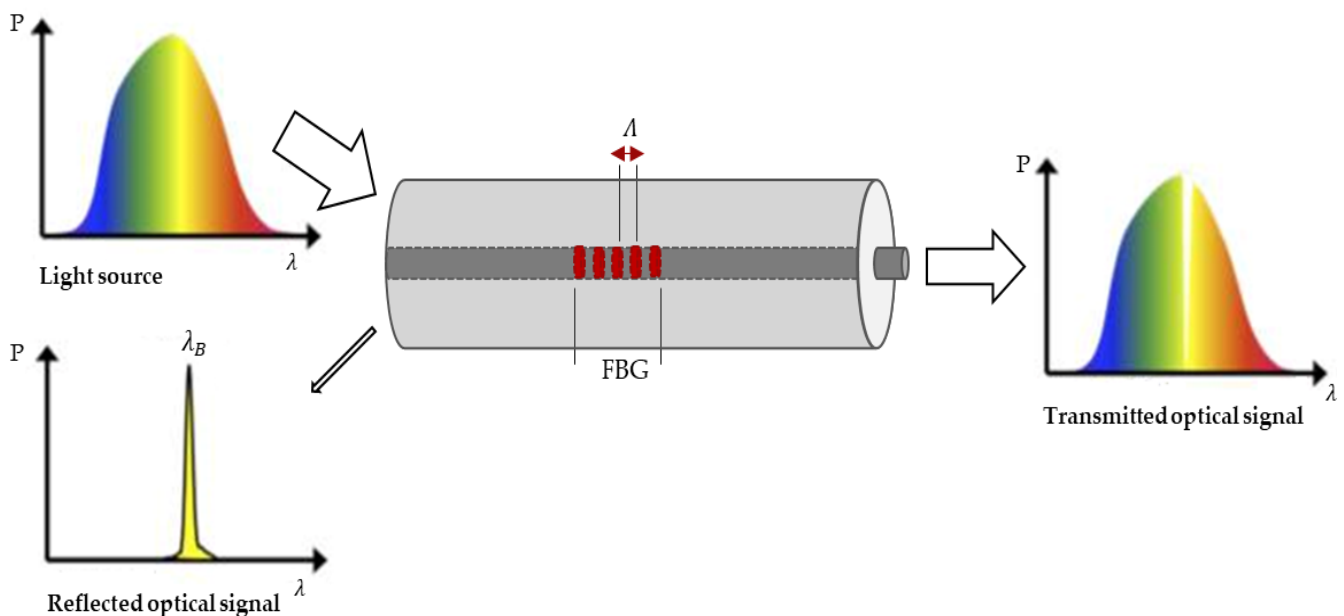
Figure 1. FBG working scheme.

The term fiber Bragg grating was borrowed from the Bragg law, and it was applied to the periodical structures inscribed inside the core of conventional optical fibers [18-21]. So, before entering the theory of fiber Bragg grating itself, it is important to go back in 1912, the year the British physicist and X-ray crystallographer Sir William Lawrence Bragg, discoverered the Bragg law of X-ray diffraction [22-26]. This principle is used until today for the study and determination of crystal structure. For a crystalline solid with lattice planes separated by a distance d the waves are scattered and interfere constructively if the path difference of length of the waves is equal to an integer multiple

of the wavelength (Figure 2) [25, 26]. The Bragg's law describes the condition for this constructive interference:

$$2\,d\,sin(\theta) = n\,\lambda \tag{1}$$

where ϑ is the incident angle, n is an integer and λ is the wavelength.
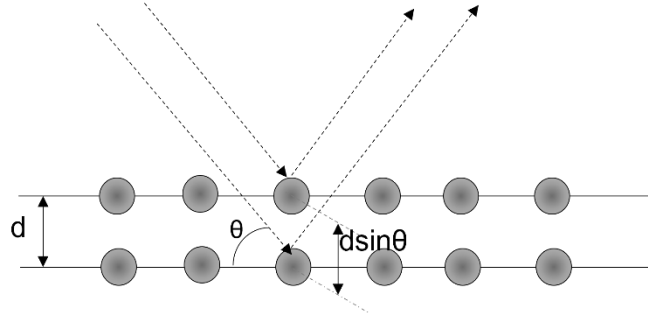
Figure 2. Schematic representation of the constructive interaction between incident radiation and the lattice structure of a crystalline material.

The bridge between this fundamental law and its application in fiber Bragg gratings was established by Hill et al. [18], as previously mentioned. To get the well-known Bragg's wavelength (λ_{Bragg}) equation, we must assume that $\theta = 90\,°$ and d as the distance between consecutive planes of the refractive index modulation imposed in the fiber core, and adapt Equation (1) to include the refractive index of the propagating mode, the following equation is deduced:

$$\lambda_{Bragg} = \frac{2\,n_{eff}\,\Lambda}{m} \tag{2}$$

Where n_{eff} is the effective refractive index of the propagating medium, m is the diffraction order (equivalent of n in Equation 1)) and Λ the grating period (equivalent of d in the same equation).

From Equation 2 we can see that the Bragg wavelength only depends on the distance between the grating modulation planes (Λ) and the effective index of refraction (n_{eff}). So, any external agent that is capable of changing Λ (for example a longitudinal deformation, due to an external force) may change both Λ and n_{eff}, and consequently will shift the reflected spectrum centred at Bragg wavelength [19-21]. Equally, a variation in temperature can also change both parameters, via thermal expansion and thermo-optic effect respectively. Therefore, FBGs are essentially a strain and temperature sensors.

The FBGs can be affected by changes in strain ($\Delta\varepsilon$) and/or temperature (ΔT). Consequently, λ_B varies ($\Delta\lambda_B$), according to the Equation 3 [19-21]:

$$\Delta\lambda_B = \Delta\lambda_{B,\iota} + \Delta\lambda_{B,T} = 2\left(\Lambda\frac{\partial n_{eff}}{\partial l} + n_{eff}\frac{\partial \Lambda}{\partial l}\right)\Delta\varepsilon + 2\left(\Lambda\frac{\partial n_{eff}}{\partial T} + n_{eff}\frac{\partial \Lambda}{\partial T}\right)\Delta T = S_\varepsilon\,\Delta\varepsilon + S_T\,\Delta T \tag{3}$$

Cátia Tavares

The first term is related to the strain induced wavelength shift, and the second one to the thermal effect on the same parameter. $S\varepsilon$ and S_T represent the FBG sensitivity coefficients to ε and T, respectively.

Different techniques can be used for the inscription of a FBG in the fiber core, these can be divided into two main groups: interferometric and non-interferometric techniques. In the interferometric technique, two coherent laser beams are used, which are later recombined, originating an interference pattern in order to determine the induced modulation profile, which allows the inscribing of Bragg gratings in a photosensitive fiber. The characteristics of the FBG inscribed with this technique are closely related to the characteristics of the light source. However, this method has some limitations regarding the light sources used, which need temporal and spatial coherence, the low repeatability of the process and the strong influence of small external vibrations in the process [27, 28].

As for the non-interferometric techniques, there are three distinct inscriptions: point-by-point exposure, amplitude mask and phase mask. The first process consists of modifying the refractive index of the core of a photosensitive fiber through the individual recording of each plane that makes up the grating by exposure to pulses from a laser [29, 30]. After recording a plane, the fiber or laser beam is moved longitudinally to the core at a distance corresponding to the period of the grating, and the process is then repeated. The technique using the amplitude mask consists of projecting an ultraviolet beam through an amplitude mask in order to guarantee the modification of the refractive index of the core of an optical fiber, it is used specially to produce long-period gratings, with modulation periods greater than 1μm [31-34]. The most common, simple, and effective method to fabricate FBGs in photosensitive fibers is through the use of a phase mask, which was the method used during this thesis. The main advantage of this technique is the low coherence required by the laser source (which significantly reduces the final cost of the process) and the ease of reproducing this process to obtain specific Bragg wavelengths. In general, the setup required for this technique comprises a laser source, a mirror system to guide the light beam (optional), a cylindrical convex lens to focus the beam and a phase mask (responsible for setting the inscription pattern) [35-37] (Figure 3).

Cátia Tavares
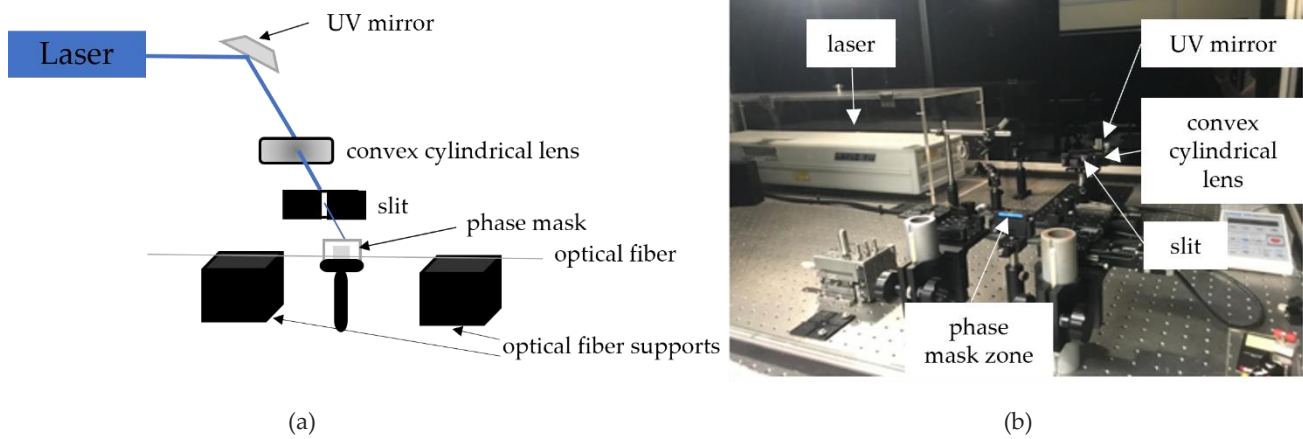
Figure 3. Setup to inscribe FBGs in optical fibers in our laboratory: a) scheme and b) photography.

Regarding their functioning, these masks act as diffraction gratings, dividing the transmitted beam into several diffraction orders. The recombination of diffraction orders (typically +1/0 and +1/-1) over the fiber core creates an interference pattern that leads to the formation of Bragg gratings. Phase masks are often designed to minimize the 0-diffraction order and maximize the -1 and +1 orders. The interference pattern created depends only on the phase mask period; to produce a FBG with different wavelength it is necessary to use a distinct phase mask [27, 28]. To determine the Λ_{PM} of a phase mask, the Equation 4 should be used [28]:

$$\Lambda_{PM} = \frac{m\,\lambda_{laser}}{sin\left(\frac{\theta m}{2}\right) - sin(\theta)} \tag{4}$$

where m is the diffracted order, λ_{laser} the laser wavelength, $(\theta m/2)$ is the diffraction angle of the maximized order and θ is the incident angle of the laser beam. When considering a normal incidence of the laser beam, the orders +1/-1 will be maximized so $\theta = 0$, giving rise to a grating period on the fiber core (Λ) specified by the Equation 5 [28]:

$$\Lambda = \frac{\Lambda_{PM}}{2} \tag{5}$$

Using Equations 2 and 5, is possible to define the Λ_{PM} value of phase mask able to inscribe a desired Bragg wavelength through Equation 6 [28].

$$\Lambda_{PM} = \frac{m\,\lambda_{Bragg}}{n_{eff}} \tag{6}$$

The sensing of a parameter thought an optical fiber with an FBG requires a physical connection to an optical interrogator, through a standard optical connector. Normally, the optical interrogator consists of a scanning tuneable laser coupled through an optical circulator to the FBG and the reflected optical signal deviated throughout the same circulator to a photodetector (PD) followed by a transimpedance amplifier; or a broadband light source like a superluminescent LED or an Amplified

Cátia Tavares

Spontaneous Emission (ASE) source instead of the tuneable laser, but in that case, instead of the photodetector, a spectrometer must be used [27, 28]. These systems allow the detection of the whole reflection spectrum, and using a peak tracking method, it is normally possible to estimate the λ_B with an accuracy ≤ 1 pm and follow its shift over time.

Due to its advantages, enumerated above, and as it is possible to inscribe several FBGs in a single fiber, multiplexing several sensors into the same fiber cable (allowing to measure different parameters with a single fiber and acquisition system simultaneously), with the evolution of this technology, optical sensing with FBGs has become one of the most used techniques for the development of OFS.

1.2.2 Intensity sensors

The working principle of Intensity Fiber Optic Sensors (IFOSs) is directly related to the variation of light intensity according to the variation of measurand.

IFOSs can be used in intrinsic or extrinsic configurations. The intrinsic intensity sensors have several configurations, but in general are characterized by side disorders of fiber caused by measurand, which induce micro or macro blending in fiber optic and change the intensity of the output optical signal [38-42]. Examples of this configuration's schemes can be seen in Figure 4. The intensity sensors in extrinsic configurations, on the other hand, can be subdivided into two configurations: reflection and transmission configuration (Figure 5). In the first configuration, the applied optical signal leaves the fiber, contact with the measurand, is reflected, and enters in the same optical fiber again. In the second, the optical signal leaves the fiber, contact with the measurand, and enters in a different optical fiber (Figure 5).
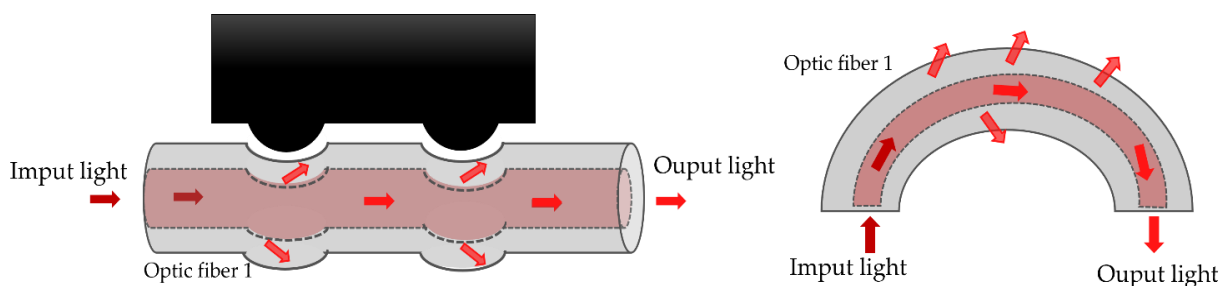
Figure 4. Schematic examples of intrinsic IFOSs configurations.

Cátia Tavares
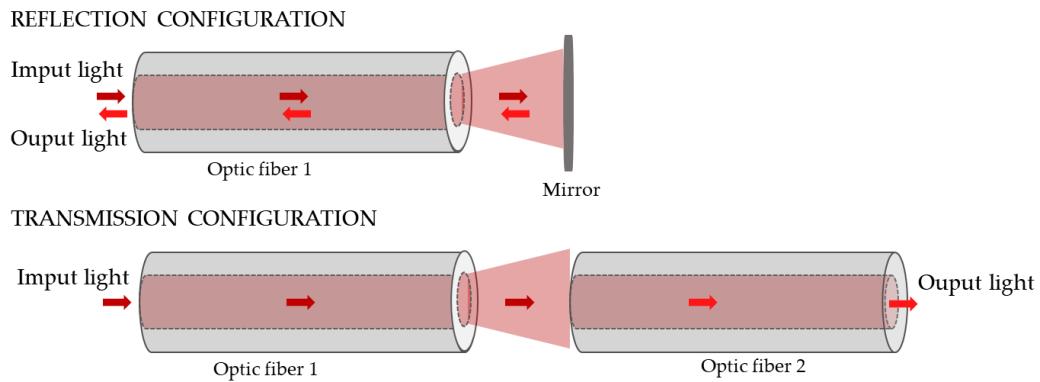
Figure 5. Schematic examples of extrinsic IFOSs configurations.

In IFOSs, it is fundamental to potentiate the light intensity transmitted through the fiber, and an easy and lower cost way to achieve this is to use multimode fibers, due to their larger cores and Numerical Aperture (NA), which is a measure for its acceptance of incoming light, than for single mode fibers. The greatest advantage of this technique is to obtain robust and low-cost sensors since they feature a simple interrogation system: based on LEDs as power sources and photodetectors (PDs) to detect the intensity variations.

During this work only one IFOS configuration was used: the intrinsic IFOS. In brief, a box was designed where the plastic optical fiber was subject to bending when this box was under pressure. This bending caused changes in the output signal of the optical fiber and with this it was possible to measure the force applied to the sensor. This work will be explained later in the section dedicated to the instrumentation work of an office chair.

1.3 OPTICAL FIBER SENSOR FOR BIOMEDICAL APPLICATIONS – A BRIEF OVERVIEW AND STATE OF THE ART

Recent advances in Internet of Things, wearable, or invisible devices (or "off-the-person" sensing) approaches in which the sensors are integrated in everyday use objects [43, 44]), added to the miniaturization of sensors and electronic components, have significantly increased the capabilities of the biomedical sensing devices by expanding the range of applications. These solutions can perform both real time and long-term telemonitoring of individuals with limited access to health services, enabling early diagnosis and intervention on diseases, allowing to reduce the frequency of visits or long-term stays at medical facilities, without compromising the treatment [45]. Throughout this topic, the most relevant works with optical sensors related to applications in biomechanics and applications in physiological monitoring will be covered, as these are the areas of medical application of the developed sensors during the PhD work.

1.3.1 Applications in biomechanics

The classic definition says that biomechanics is mechanics applied to the study of living bodies with special emphasis on the human body [46, 47]. In this section, an overview of wearable or invisibles (not wearable) systems based on optical sensors is described, with the aim to monitor the interaction between the human body and other objects such as insoles, wheelchairs, and office chairs to evaluate important parameters for the individual's health status (Figure 6).
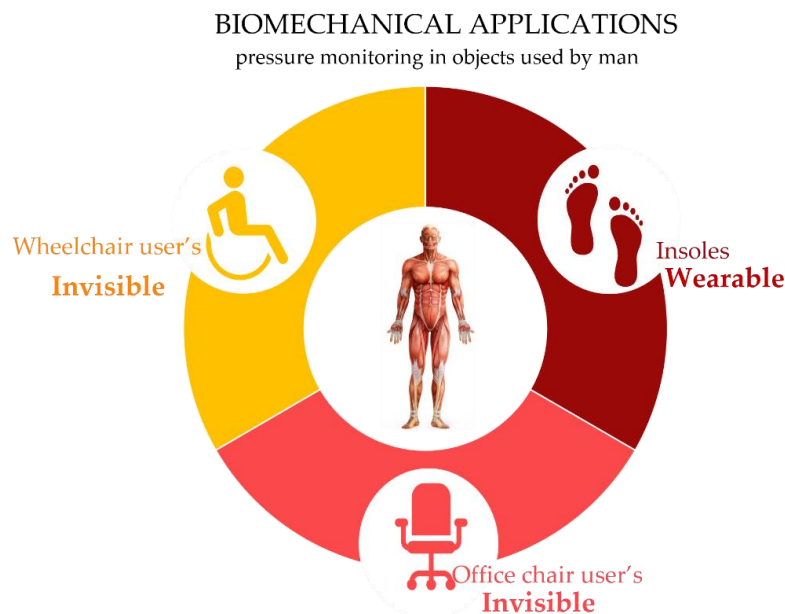
Figure 6. Schematic representation of objects where sensors were applied for biomechanical applications during this PhD.

Insoles

A foot health monitoring system based on instrumented insoles is a solution that can allow an individual's general health status to be monitored in a cost-effective and simple way during day-to-day life [47-52]. The foot is used in locomotion activities, it supports the weight and provides balance to the individual, which requires the proper functioning of the neuromuscular system. A healthy and normal gait also presupposes an adequate functioning of the cardiovascular, respiratory, nervous, and musculoskeletal systems [50]. For all these reasons, it is recognizable that the health of gait and feet is indirectly related to the health condition of an individual [51]. For example, patients with Parkinson's, even at an early stage, are easily identified by gait anomalies such as smaller, shuffled steps [53, 54] or have periodic difficulties in turning, stopping, starting, or lifting their feet while walking. On the other hand, diabetic patients with peripheral diabetes neuropathy (PND) tend to have areas of greater plantar pressure on the foot, resulting in a greater propensity for pressure ulcers to occur [51, 55, 56]. In parallel with plantar pressure, abnormally high shear values on the sole of the foot were also indicated as causes of this pathology [56-58].

Thus, devices to monitor and assess gait, plantar pressure or shear can be of immense use for early diagnose of the previously mentioned pathologies or, if the pathologies have already been diagnosed, to carry out a regular follow-up of the patient.

The scientific community has been working and publishing some results with the application of fiber optic sensors in insoles for gait analysis [59-63], plantar pressure mapping [59, 63-65] and pressure and shear mapping [66-68].

At the beginning of this doctoral program, few works had been published in which silica fiber optic sensors with FBG were used as plantar pressure sensors in equipment for in-shoe use, similar to insoles. The first work was published in 2003 and consisted of an insole made up of ten layers of carboepoxy between which an optical fiber of silica with five FBGs was placed. FBGs were strategically placed to measure plantar pressure at the points that the authors considered most relevant to the study of plantar pressure and were able to obtain sensitivities of 5.44 pm / N [59]. Ten years later, Suresh et al. published an article comparing the use of plantar pressure sensors with FBG and piezoelectric sensors (PZT) during gait at low and high speeds [60]. To produce the optical devices, the FBGs were embedded between layers of carbon composite material in the shape of an arch, and for clinical tests were glued to the sole of a shoe available on the market. The study concluded that FBG sensors revealed to have a better sensitivity at static moments and at lower speeds, while piezoelectric sensors had greater sensitivity at higher speeds. The following year, another work was published on an insole instrumented with six FBGs embedded in a silicone rubber, capable of detecting 4 different types of

feet in 11 users [64]. The first works of our team appeared in 2017 with wearable solutions in silica optic fiber with FBGs [61, 65]. One of them consisted in the design and implementation of a non-invasive platform and an insole both using a network of fiber Bragg grating sensors to monitor the vertical ground reaction forces (VGRF) distribution (induced in the foot plant surface during gait) and the displacement of the body´s center of mass (BCM) [65]. Another work focused on a non-invasive architecture adaptable to a shoe sole to plant pressure remote monitoring, which is suitable to be integrated in an IoT e-Health solution to monitor the wellbeing of individuals [61]. Later, in 2019 [63] a work was published with a fully 3D printed intelligent insole with the FBGs encapsulated during the printing process and with results for both the standing position and the walking cycles. Solutions using FBGs on silica optical fibers capable of monitoring two types of forces on the sole of the foot have also been published: pressure and shear forces [66, 68].

Very few works with insoles instrumented with POF were published and all of them to only monitor pressure. Vilarinho et al. proposed a cork insole embedded with one POFs with five FBGs [62]. The proposed POF sensor system showed a pressure sensitivity of 8.14 pm/kPa with the possibility of measuring a larger range of users due to POFs higher strain limits. Later, an instrumented insole fabricated by 3D printing was proposed with fifteen sensing points using POF intensity variation-based sensors [67], with only two photodetectors to monitor the whole system. The developed device was used to assess the plantar pressure distribution during the gait of 20 volunteers, where the sensor system was able to detect the plantar pressure at each sensing point and was also able to identify the gait phases. Table 4 presents the main characteristics of the different insoles instrumented with optical fiber sensors reported in the literature.

Table 2. Summary of published works with FBGs optical fiber sensors in insoles.

Device	Parameters to monitor	Type of fiber	Sensor technology	No. of sensors	Sensibility	Type of tests performed	Ref.
Insoles	pressure	SOF	FBG	5	5.44 pm/N	Normal standing gait and abnormal standing gait	[59]
	pressure	SOF	FBG	2	1.3 pm/kPa	Low and high-speed walking	[60]
	pressure	SOF	FBG	6	-	Detect different feet types	[64]
	pressure	SOF	FBG	6	8.3 pm/kPa	Gait motion	[61] [2]
	pressure	POF	FBG	5	8.14 pm/kPa	Gait motion	[62]
	pressure and shear	SOF	FBG	5	1.4 pm/N (pr.); 2.6 pm/N (sh.)	Gait motion	[66] [2]
	pressure	POF	intensity variation	15	-	Standing position, BCM displacement and gait motion	[67]

Cátia Tavares

	pressure	SOF	FBG	4	-	Standing position and gait motion	[63]
	pressure and shear	SOF	FBG	4	-	Gait motion	[68] [2]
Insoles and platform	VGRF and pressure	SOF	FBG	5/6	max 11.06 pm/kPa	Gait motion and BCM displacement	[65] [2]

Wheelchair

In wheelchair users the additional pressure combined with limited mobility, low sensitivity, poor nutrition, ageing of the skin and increase in temperature and humidity can lead to the development of pressure ulcers [69]. It is estimated that 95% of wheelchair users develop pressure ulcers during their lifetime [70]. The most common areas for the development of this pathology are ischium and sacrum, scapulae and, in some cases, trochanters and coccyx, depending on the chair and the positions of wheelchair users [70, 71].

For this reason, it is important to change their body position regularly and monitor the pressure forces at the bony prominences to ensure that the recommended limits for each patient are not exceeded [72-74]. Ideally, this monitoring should be done daily and in real time, to alert the user when they need to perform pressure relief exercises. There are already some published works with electronic devices designed to monitor pressure in wheelchairs [75-79], however, we were the first team to publish works with OFS for this application. In 2019 we published our first work in this area, with a network of six fiber optic sensors for monitoring pressure in scapula's, ischiatic zones and heels [80]. A second work was later published in which six sensor cells (four in the seat area and two in the shoulder blade area) composed by twelve FBGs, not only monitoring the pressure but also the temperature at each point [81]. In addition, the developed system was also able to detect the user's position. Then, in Table 4, the characteristics of the published works related to this application are summarized.

---

[2] Our works

Table 3. Summary of published works with FBGs optical fiber sensors in wheelchair.

Device	Parameters to monitor	Type of fiber	Sensor technology	No. of sensors	Sensibility	Type of tests performed	Ref.
Wheelchair	pressure and RR	SOF	FBG	6	17.8 pm/kPa	7 positions	[80][3]
	pressure and temperature	SOF	FBG	6	81 pm/kPa and 47 pm/°C	7 positions	[81][3]

Office chairs

There is an increasingly higher number jobs in which the worker is seated. At the same time, there are also a range of leisure activities carried out in the same way [82]. This sedentary lifestyle is associated with the development of different health pathologies among which postural problems, especially related with the spine. There are even studies that indicate that spinal disorders are the second leading cause of requests for medical leave from work and are also a reason for early retirement [83]. In recent years, research in intelligent office chairs with sensors has started to grow in interest, aiming to advise the user to correct their posture or take short breaks for relaxation or muscle repositioning.

Some researchers have published works in which they apply electronic sensors to office chairs to analyse user's posture: with pressure maps [84-86], with load cells [87, 88], with accelerometers [89], digital photogrammetry [90], and temperature sensors [91].

However, there are few studies that use SFOs in seats and most are not intended to detect pressure, but other physiological parameters such as breathing [92, 93]. Two papers were published in 2015 and 2016, respectively, that used the variation of optical power in the POF to monitor pressure in seated people [94, 95]. Both works use POF embedded in a fabric, the first uses stable cylindrical structures perpendicularly under the fiber [94], and the second was for detecting a passenger presence in a car seat [95]. This system showed good performance in a pressure range between 0.18 and 0.21 N/cm^2. Nonetheless, no work has been published on the use of non-wearable optical sensors for posture detection in chairs. Our work, published in 2022, reports the application of four sensor cells with POF based on the variation of optical power, in the seat of an office chair [96]. These sensors, allow the detection of five user postures (four of them incorrect postures), through a software developed for this purpose. The software was developed so that through the information given by the POF sensors, the system detects the user's position and, if necessary, warn him to reposition himself in the chair or to

---

[3] Our works

take short breaks. Table 4 summarizes the main characteristics of optical devices produced to monitor office chairs.

Table 4. Summary of published works with FBGs optical fiber sensors in office chairs.

Device	Parameters to monitor	Type of fiber	Sensor technology	No. of sensors	Sensibility	Type of tests performed	Ref.
Office chair	RR and HR	SOF	FBG	2	-	-	[93]
	RR	SOF	FBG	4	38.13 pm/N	-	[94]
	pressure	POF	intensity variation	4	62.7 mV/kg	5 positions	[96] [4]

1.3.2 Applications in physiological monitoring

In the scope of this work, vital signs monitoring refers to a series of physiological parameters that can be acquired non-invasively through invisibles and that are fundamental in medicine, in particular: heart rate (HR), respiratory rate (RR), blood pressure, temperature, volume and oxygenation of the blood.

Cardiovascular diseases are the leading cause of death in the world [97], and periodic monitoring of vital signs in ambulatory is prone to promote timely detection of abnormalities that may be important in the diagnosis and treatment of these diseases. Hence the importance of monitoring these parameters and the great interest shown by the scientific community on this topic. As previously mentioned, fiber optic sensors have several advantages over conventional sensors when it comes to biomedical applications. The combination of these two factors is the main reason why monitoring of vital signs is the area of application of optical sensors with the largest number of published works [98-101].

Due to the large number of publications in this area, this section describes an overview of non-invasive systems based only on optical sensors with silica optical fibers with FBGs, to be used in several parts of the body for monitoring the two types of vital signs addressed throughout my PhD work: HR and RR (Figure 7).

---

[4] Our work

Cátia Tavares
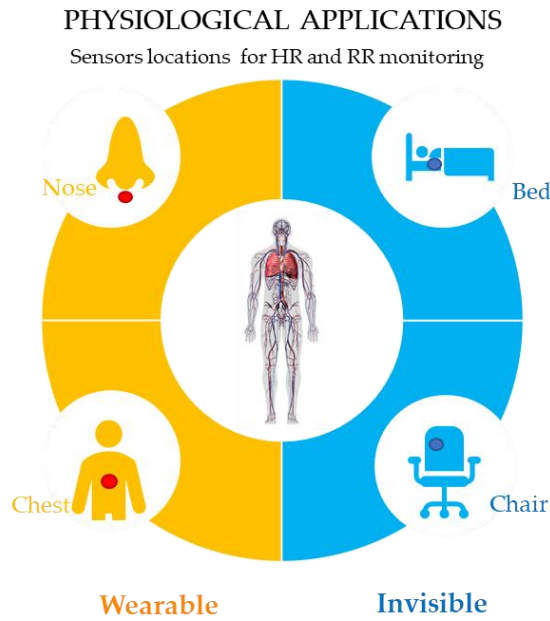
Figure 7. Schematic representation of typical sensor locations for HR and RR monitoring.

FBG technology has been widely used in optical sensors for the reasons listed in Section 1.2.1. In breathing and heart rate monitoring, the FBG operating principle is mostly related to the monitoring of periodic displacements of the body caused by movements of lungs and heart, which in turn, lengthen the FBGs and cause changes in its Bragg wavelength, as explained in Figure 8.

In the literature it is possible to find both fiber optic sensors that monitor only one type of vital sign, as well as sensors that monitor more than one vital sign simultaneously. To close this section, Table 5 summarizes the main characteristics of the works published about this topic.
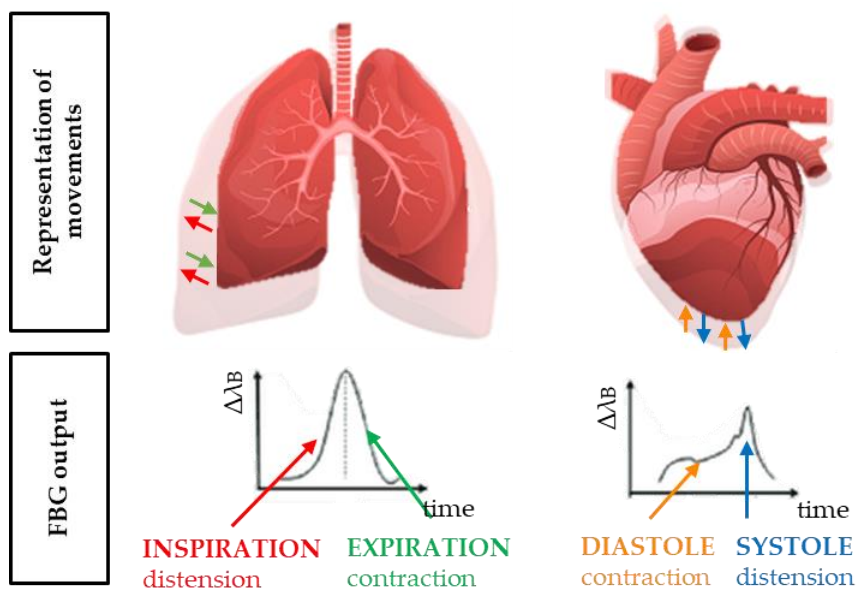
Figure 8. FBG output variations due breathing and heart beating (adapted from [102]).

Cátia Tavares

Respiratory rate (RR) monitoring

A healthy resting adult human has a respiratory rate of 12 to 18 breaths per minute (bpm) [100], however premature infants have the highest respiratory rates 40-60 bpm. This section describes of the most popular and recent FBGs-based solutions for monitoring respiratory parameters. An overview of the anatomical locations used for respiratory monitoring is shown in Figure 7. The published solutions can be divided in two groups related with the measured parameters used to infer about the breath: solutions based on the monitoring of the body movements caused by the respiratory activity (specially of the chest wall); and solutions based on the respiratory airflow, relative humidity (rh) or temperature between inspiratory and expiratory air.

<u>Solutions based on the body movements:</u>

During normal breathing, the rib cage normally suffers displacements of 3-5 mm in the ventral part and 1-2 mm in the side parts [103]. By being able to monitor the body displacement resulting from respiration it is possible to deduce the respiratory rate. FBGs are highly suitable for this purpose and have been widely used in recent years since their sensitivity to tension allows a direct relationship between the displacement of the Bragg wavelength and the displacement of the thorax induced by breathing. In this sense, measuring thorax displacement with FBGs works as follows: when the sensor undergoes a deformation, the tension is transmitted to the optical fiber with the FBG that experiences longitudinal deformation, inducing a $\Delta\lambda_B$; the maximum and minimum deformation of the sensors corresponds to the end of the inspiratory and expiratory phases, respectively (Figure 8); by calculating the time elapsed between two consecutive maximums or minimums, it is possible to estimate the respiratory period and subsequently the respiratory frequency (f_R).

FBGs can be naked or embedded in elastic materials. The most varied works have been published, wearable and non-wearable, for applications in hospital environments, in sports environments or even for continuous monitoring in everyday life [98-101]. The first published work on RR monitoring by an FBG was in 2001, consisting of a fiber embedded in an elastic band over the thorax [104]. After that, many works were published on wearable solutions based on movements of body due breath, the most common being elastic bands placed on the chest (with FBGs encapsulated or not in other materials and glued to the band [104-106] or sewn to the band [107, 108], but there were also instrumented shirts for monitoring this parameter [109-111]. There is also non-wearable but invisible solutions, which consist of incorporating FBGs into objects that are in contact with the body, such as: pillows [112], beds [113-115], wheelchairs [80], or seats [93, 94].

Cátia Tavares

<u>Solutions based on the respiratory airflow, relative humidity, or temperature:</u>

Spirometry measures air volume as a function of time during inhaling and exhaling and is the most used technique to assess respiratory health. There are several conventional (electronic) flow meters on the market and in recent years some works with FBGs have also been published to measure the air flow during breathing with optical sensors. Several works were published in which FBGs were introduced in spirometers to measure respiration through elongation, temperature, or relative humidity (rh) differences [116-118]. At the same time, studies were also published in which FBGs were applied to wearable solutions to detect airflow by elongation [119] and by variations in relative humidity [120]. There is yet another kind of solution, based on a hot wire anemometer using one or two FBGs [121, 122]. The work principle of this type of sensor is about the phenomenon of heat transfer, in which the sensing part (FBG) is heated by an external energy source (laser source) and when the airflow hits the FBG there is heat exchange. The equilibrium temperature or the energy used to maintain the FBG at a constant temperature can be used as an indirect measure of the airflow velocity. After that, the flowrate can be estimated by the velocity. Table 5 lists published works with FBGs as sensors to monitor RR.

Heart rate (HR) monitoring

Cardiovascular dynamics has been used in clinical practice for many years on the basis of heart sounds alone, often using a stethoscope. Today, this analysis is extended to other types of signal sources, such as force, frequency, or pressure sensors. Optical sensors are increasingly used as an alternative approach to conventional sensors, especially sensors with FBGs. The HR has been monitored simultaneously to RR mostly through FBG-based solutions that measure chest displacements [105, 106, 110]. Once, the cardiac activity causes vibrations of lower amplitude and higher frequency than respiratory activity, through complex filtering systems it is possible to differentiate the two signals. The representation of the vibrations of thorax induced by the heartbeat is called seismocardiogram (SCG), and the representation of the ballistic forces generated by the heart measured in the center of mass of the body is called a ballistocardiogram (BCG).

There are some reference values that must be known when analysing the HR of an adult at rest: the normal pulse or HR is between 60 and 100 beats per minute (BPM), that is between 1 and 1.7 Hz, in people over 10 years old. HR greater than 100 BPM is called tachycardia and less than 60 BPM is called bradycardia. In children and infants, the pulse is naturally faster [124]. The displacements induced by cardiac activities typically range from 0.2 to 0.5 mm [125]. Several factors can affect the HR, such as fever, heart problems, infections, hypovolemia, anxiety, physical condition, and medications, hence the

importance of monitoring this vital sign on a regular basis, especially in people with morbidities. In this sense, in the last decades the interest in discrete methods based on one or more FBGs to record these signals has grown more and more. Wearable and invisible solutions have been investigated to monitor this parameter.

To the best of our knowledge, the first published work with FBGs to monitor HR was in 2011 [126], Chen et al. published a paper were an elastic Plexiglas board with a bonded FBG element is placed on the magnetic resonance imaging (MRI) couch behind the back of the patient and close to the heart. The proposed method allowed to analyse the signals in semi-real-time with an accuracy of +/- 2 beats. The method was tested in a group of seven subjects and the root-mean-square error obtained did not exceed 6.0 BPM. After this, many other works followed, some based on wearable solutions [102, 106, 110, 127, 128] others on non-wearable solutions [93, 112, 129]. The works based on wearable solutions mostly monitored the HR by attaching the sensors to the users' chest, both through elastic bands and through t-shirts [98]. The works based on invisible solutions to measure HR are applied to objects in contact with the body, such as beds [112] and pillows [93]. Regarding the configuration of the sensors, as with the RR sensors mentioned above, the sensors for monitoring HR can also be composed of only naked FBGs as well as FBGs encapsulated in elastic materials such as: epoxy [93], Polimetilmetacrilato (PMMA) [130], polydimethylsiloxane polymer (PDMS) [105, 106, 112] or dragon skin [102, 131]. These materials are flexible and confer to the FBGs good robustness, high adaptability to the skin or to the fabrics, and good compliance with the body movements. However, some uncontrolled factors which may occur during the manufacturing process, such as a non-uniform bonding strength at the fiber-polymer interface and the presence of some bubbles of air in the cured polymer matrixes, may affect the performance of the final system, especially the sensitivity, range of measurement and reproducibility. To overcome these issues, recently, fused deposition modelling (FDM) by 3D printing has been proposed as a promising method for fabricating various components, including optical fiber sensors [132-134]. Few papers proposed this technique in the fabrication of OFS for medical applications [135, 136], and the first work using this technique for monitoring vital signs was published in 2022 by our research group [128]. In this work, a 3D printed sensor produced with a material named "Flexible" (Fish box mini model, Avistron), with an embedded FBG during the printing process, was developed to monitor two vital signs: HR and RR. Applicability tests were performed with three users, to preliminarily evaluate the system's ability to detect chest wall excursions related to respiratory and cardiac activities during normal breathing and apnoea. An electronic commercial sensor was used as a reference to compare the obtained signals. The results showed that the proposed system can be integrated in a wearable solution and is able to accurately estimate the users' RR and HR during two types of breathing.

Cátia Tavares

Table 5 lists published works with FBGs as sensors to monitor RR and HR, identifying important characteristics such as: the type of fiber used, the configuration of the sensor, the position of the sensor and the variation errors.

Table 5. Published works with FBGs silica optical fiber sensors to monitor RR and HR.

To monitor	Type of sensor	Nº of sensors	Embedded	Sensor test position	Error variation	Ref.
RR	wearable	1 FBG	no	attached to an elastic band on the chest	-	[104]
RR	invisible	12 FBGs	in reinforced carbon fiber (CFRP)	attached to a bed	max ± 1 breaths	[114]
RR	wearable	2 FBGs	no	glued to a t-shirt on the chest	max 9.5 %	[109]
RR	wearable	1 FBG	in PDMS	attached to an elastic band on the chest	-	[137]
RR	invisible	1 FBG	no	glued to a cantilever inside of spirometer	max 24 %	[117]
RR	wearable	2 FBGs	no	glued to a cantilever over the nose	-	[119]
RR	wearable	1 FBG	in hygroscopic material (agar)	object placed at the entrance to the nose	max 2.29 %	[120]
RR	invisible	4 FBGs	no	glued to a pillow to put on back of office chair	max 2.95 bpm	[94]
RR	invisible	2 FBGs	in polyurethane diaphragm	glued to a sponge to put on back of office chair	max 1.91 bpm	[94]
RR, T, rh	invisible	1 FBG	in agar	glued inside of spirometer	max 2 %	[118]
RR, HR	wearable	1 FBG	in polymeric foil	glued to a t-shirt on chest	-	[138]
RR, HR	invisible	2 FBGs	in epoxy	glued to a pillow in contact with the chest	max 12 %	[93]
RR, HR, T	wearable	2 FBGs	in PDMS	attached to an elastic band on the chest	95.01% within the ±1.96 SD RR; 95.34% HR; max 0.55% BT	[105]
RR, HR, T	wearable	2 FBGs	in PDMS	attached to an elastic band on the chest	3.9% RR; 96.54% HR within the ±1.96 SD; 0.36% TB	[106]

Cátia Tavares

RR, HR	wearable	12 FBGs	in adhesive silicon rubber	glued to a t-shirt on chest and back	max 0.38% RR; ± 1.13 bpm HR	[110]
RR, HR	invisible	1 FBG	in cyanoacrylate adhesive	glued across the diaphragm, placed on a Velcro strap placed on the chest	-	[129]
RR, HR	invisible	1 FBG	in PDMS	attached to a bed	96.10% within the ±1.96 SD RR; 95.49% HR	[112]
RR, HR	invisible	1 FBG	in fiberglass	attached to an elastic band on the chest	95.36% within the ±1.96 SD RR; 95.13% HR	[127]
RR, HR	wearable	1 FBG	in dragon skin	attached to an elastic band on the chest	-	[131]
RR, HR	wearable	2 FBGs	in dragon skin	attached to two elastic bands on the chest	max. 1.97% RR; 5.74% HR	[102]
RR, HR	wearable	1 FBG	in 3D printed material (flexible)	attached to an elastic band on the chest	0.6% HR	[128][5]
HR	invisible	2 FBGs	in PMMA	in standing position, under the feet	± 2.68 bpm	[130]
HR	invisible	1 FBG	in Plexiglas	in the sitting position between the back and the chair	± 2.57 bpm	[130]

---

[5] Our work

1.4 SUPPLEMENTARY REPORT ORGANIZATION

This Supplementary Report is divided in three chapters, organized as follows.

In Chapter 1, the motivation for the work developed during of this thesis is presented, together with the theoretical foundation needed to understand the different types of OFS. Then, a brief overview and state of the art on OFS for biomedical applications is presented, followed by a presentation of the document's structure. This chapter ends with the list of the main outputs and contributions attained during the PhD.

Chapter 2 comprises the detailed description of each article that makes up this doctoral thesis, as well as my contribution to its publication and the relevance of the work presented.

Finally, in Chapter 3, the general conclusions of the work developed during the PhD are summarized, as well as some future perspectives.

1.5 MAIN CONTRIBUTIONS AND PUBLICATIONS

The work presented in this thesis allowed the publication of several documents, namely 2 book chapters, 13 papers in Scimago Journal Ranking indexed journals (6 as first author), 13 scientific communications in international conferences (5 as first author), and 8 prototypes of the devices with embedded fiber optic sensors. In addition, it also allowed participation in 2 R&D scientific projects and participation in various scientific dissemination events. During this work I was also part of the scientific orientation team of several University of Aveiro students. The complete documents' list and the students' list are presented below.

1.5.1 List of published documents

Book chapters

[1]   M. F. Domingues, C. Tavares, T. Silva, C. Leitão, N. Alberto, C. Marques, A. Radwan, P. André, P. Antunes "Fiber Bragg Gratings as e-Health enablers: an overview for gait analysis applications", in Applications of Optical Fibers for Sensing, IntechOpen, London, 2019.

[2]   A. Leal-Junior, M. F. Domingues, R. Min, D. Vilarinho, A. Theodosiou, C. Tavares, N. Alberto, C. Leitão, K. Kally, A. Frizera-neto; P. André, P.Antunes, C. Marques, "Fiber Bragg Based Sensors for

Foot Plantar Pressure Analysis. in International Joint Conference on Biomedical Engineering Systems and Technologies (pp. 3-25). Springer, Cham, 2018.

Published papers on international peer-reviewed journals

[1] C. Tavares, J. Silva, A. Mendes, L. Rebolo, M.F. Domingues, N. Alberto, M. Lima, H. Silva, P. Antunes, "Instrumented office chair with low-cost plastic optical fiber sensors for posture control and work conditions optimization" Accepted in *IEEE Access*, 2022.

[2] M. Rocha, C. Tavares, A. Nepomuceno, P. Antunes, M. F. Domingues, N. Alberto, "FBGs based system for muscle effort monitoring in wheelchair users" *IEEE Sensors Journal*, 2022.

[3] C. Tavares, C. Leitão, D. Lo Presti, M. F. Domingues, N. Alberto, H. Silva, P. Antunes, "Respiratory and heart rate monitoring using an FBG 3D-printed wearable system" *Biomedical Optics Express*, 2022, vol. *13*, pp. 2299-2311.

[4] C. Tavares, D. Real, M. F. Domingues, N. Alberto, H. Silva, P. Antunes, "Sensor Cell Network for Pressure, Temperature and Position Detection on Wheelchair Users" *International Journal of Environmental Research and Public Health*, 2022, vol. 1*9*, pp. 2195.

[5] C. Tavares, F. Leite, M. F. Domingues, T. Paixão, N. Alberto, A. Ramos, H. Silva, P. Antunes, "Optically Instrumented Insole for Gait Plantar and Shear Force Monitoring" *IEEE Access*, 2021, vol. *9*, pp. 132480-132490.

[6] M. F. Domingues, C. Tavares, A. C. Nepomuceno, N. Alberto, P. André, P. Antunes, H. R. Chi, A. Radwan. "Non-Invasive Wearable Optical Sensors for Full Gait Analysis in E-Health Architecture" *IEEE Wireless Communications*, 2021, vol. 28, no. 3, pp. 28-35.

[7] M. F. Domingues, V. Rosa, A. Nepomuceno, C. Tavares, N. Alberto, P.S André, A. Radwan, P. Antunes, "Wearable devices for remote physical rehabilitation using a Fabry-Perot optical fiber sensor: ankle joint kinematic" *IEEE Access*, vol. 8, pp. 109866 - 109875, June, 2020.

[8] C. Tavares, M. F. Domingues, T. Paixão, N. Alberto, H. Silva, P. Antunes, "Wheelchair Pressure Ulcer Prevention Using FBG Based Sensing Devices" *Sensors*, 2020, vol. 20, pp. 212-225.

[9] M. F. Domingues, C. Tavares, N. Alberto, A. Radwan, P. André, P. Antunes, "High Rate Dynamic Monitoring with Fabry–Perot Interferometric Sensors: An Alternative Interrogation Technique Targeting Biomedical Applications" *Sensors*, 2019, vol. 19, pp. 4744-4744.

[10] <u>C. Tavares</u>, M. F. Domingues, A. Frizera-Neto, T. Leite, C. Leitão, N. Alberto, C. Marques, A. Radwan, E. Rocon, P. André, P. Antunes, "Gait Shear and Plantar Pressure Monitoring: A Non-Invasive OFS Based Solution for e-Health Architectures" *Sensors*, 2018, vol. 18, pp. 1334.

[11] M. F. Domingues, C. Rodriguez, J. Martins, <u>C. Tavares</u>, C. Marques, N. Alberto, P. André, P. Antunes, "Cost-effective optical fiber pressure sensor based on intrinsic Fabry-Perot interferometric micro-cavities" *Optical Fiber Technology*, 2018, vol. 42, pp. 56-62.

[12] M. F. Domingues, N. Alberto, C. Leitão, <u>C. Tavares</u>, E. de Lima, A. Radwan, V. Sucasas, J. Rodriguez, P. André, P. Antunes, "Insole optical fiber sensor architecture for remote gait analysis-an eHealth solution" *IEEE Internet of Things Journal*, 2017.

[13] M. F. Domingues, <u>C. Tavares</u>, C. Leitão, A. Frizera-Neto, N. Alberto, C. Marques, P. André, P. Antunes, "Insole optical fiber Bragg grating sensors network for dynamic vertical force monitoring" *Journal of Biomedical Optics*, vol. 22, no. 9, pp. 091507-1 – 091507-8, 2017.

Submitted papers on international peer-reviewed journals

[14] <u>C. Tavares</u>, J. Silva, A. Mendes, L. Rebolo, M.F. Domingues, N. Alberto, M. Lima, A. Radwan, H. Silva, P. Antunes, "Smart office chair for working conditions optimization" Submitted in *IEEE Internet of Things Journal*, 2022.

Papers in international conferences

[1]   A. Ferreira, <u>C. Tavares</u>, C. Leitão, D. Lo Presti, M. F. Domingues, N. Alberto, H. P. da Silva, P. Antunes "3D printed FBG based sensor for vital signal monitoring – Influence of the infill printing parameters" accepted in *European Optical Society Annual Meeting - EOSAM*, Porto, Portugal, September 2022.

[2]   <u>C. Tavares</u>, C. Leitão, D. Lo Presti, E. Schena, M. F. Domingues, N. Alberto, H. P. da Silva, P. Antunes "3D Printed Wearable FBG based Devices: A Proof of Concept for Heart Rate Monitoring" *IEEE International workshop on Metrology for Industry 4.0 and IoT*, Trento, Italy, June 2022.

[3]   M. Rocha, <u>C. Tavares</u>, A.C. Nepomuceno, P. Antunes, M.F. Domingues, N. Alberto "Monitoring of the muscle effort in wheelchair users using FBG-based sensors" *Optical Sensing and Detection VII*, Strasbourg, France, May 2022.

[4] M. F. Domingues, <u>C. Tavares</u>, V. Rosa, L. Pereira, N. Alberto, P. André, P. Antunes, A. Radwan " Wearable eHealth System for Physical Rehabilitation: Ankle Plantar-Dorsi-Flexion Monitoring" *GLOBECOM-IEEE Global Communications Conference*, Waikoloa, USA, December 2019.

[5] <u>C. Tavares</u>, A. Nepumocemo, V. Rosa, F. Leite, L. Pereira, T. Paixão, N. Alberto, P. André, P. Antunes, M. F. Domingues "Towards a Complete Gait Analysis using Optical Fiber Bragg Gratings" *International Microwave and Optoelectronics Conf. – IMOC*, Aveiro, Portugal, November 2019.

[6] <u>C. Tavares</u>, M. F. Domingues, L. Pereira, N. Alberto, A. Ramos, E. Rocon, P. André, H. Silva, P. Antunes, "Fiber optic sensor for monitoring tangential and vertical forces for wheelchair application" *International Conference on Applications in Optics and Photonics (AOP)*, Lisbon, Portugal, June 2019.

[7] <u>C. Tavares</u>, M. F. Domingues, N. Alberto, A. Ramos, E. Rocon, P. André, H. Silva, P. Antunes, "Bio-inspired optical fiber sensor for simultaneous shear stress and vertical pressure monitoring" *SPIE Optics+ Optoelectronics*, Prague, Czech Republic, April 2019.

[8] M. F. Domingues, A. Nepumocemo, <u>C. Tavares</u>, N. Alberto, A. Radwan, P. André, P. Antunes, " Low-cost intrinsic optical fibre FPI sensor for knee kinematic gait analysis and e-Health architecture" *SPIE Optics+ Optoelectronics*, Prague, Czech Republic, April 2019.

[9] M. F. Domingues, A. Nepomuceno, <u>C. Tavares</u>, A. Radwan, N. Alberto, C. Marques, J. Rodriguez, P. André, P. Antunes, "Energy-aware wearable e-Health architecture using optical FBG sensors for knee kinematic monitoring" *IEEE Global Communications Conference (GLOBECOM)*, Abu Dhabi, United Arab Emirates, December 2018.

[10] <u>C. Tavares</u>, M. F. Domingues, A. Frizera-Neto, C. Leitão, N. Alberto, C. Marques, A. Radwan, E. Rocon, P. André, P. Antunes, "Biaxial optical fiber sensor based in two multiplexed Bragg gratings for simultaneous shear stress and vertical pressure monitoring" *Photonics Europe 2018*, Strasburg, France, April 2018.

[11] C. Leitão, M. F. Domingues, <u>C. Tavares</u>, J. Pinto, P. André, C. Marques, P. Antunes, "Arterial pulses assessed with FBG based films - a smart skin approach" *Photonics Europe 2018*, Strasburg, France, April 2018.

[12] M. F. Domingues, J. Martins, C. Rodriguez, <u>C. Tavares</u>, N. Alberto, P.S André, P. Antunes, "Low cost intrinsic Fabry-Perot interferometric optical fiber strain and pressure sensor" *III International Conference on Applications in Optics and Photonics (AOP 2017)*, Faro, Portugal, May 2017.

[13] M. F. Domingues, <u>C. Tavares</u>, N. Alberto, C. Leitão, P. Antunes, P. André, E. de Lima, V. Sucasas, A. Radwan, J. Rodriguez, "Non-invasive insole optical fiber sensor architecture for monitoring foot anomalies" *IEEE GLOBECOM 2017*, Singapure, December 2017.

1.5.2 Supervising activities:

Co-orientation (4)

1. 2021/2022 | Biomedical Engineering |3rd year Project | **Alexandra Ferreira** |
   Impressão 3D de sensores em fibra ótica para monitorização de sinais vitais.
2. 2020/2021 | Biomedical Engineering | 3rd year Project | **Daniela Real** |
   Rede de sensores de fibra ótica para monitorização de pressão e temperatura em cadeiras de rodas.
3. 2019/2020 | Biomedical Engineering | 3rd year Project | **Francisco Soares** |
   Sensores óticos para prevenção de úlceras de pressão em cadeirantes.
4. 2018/2019 | Electronic Eng. and Telecommunications | Industrial Project | **Álvaro Vaz, Daniel Fernandes, Joaquim Melim |** *Integração de sensores de fibra ótica na Plataforma Bitalino.*

Orientation support (4)

1. 2020/2021|Electronic Eng. and Telecommunications | Master's dissertation | **André Mendes |**
   Conceção de um sistema de processamento de dados para uma Plataforma e-Health.
2. 2020/2021| Electronic Eng. and Telecommunications | Master's dissertation | **João Silva |**
   Implementação de um sistema de aquisição e transmissão de dados para plataforma e-Health.
3. 2018/2019 | Biomedical Engineering | 3rd year Project | **Flávia Leite |**
   Sensores óticos para monitorização de forças verticais e cisalhamento em aplicações biomédicas.
4. 2017/2018 | Physical Engineering | Master's dissertation | **Tiago Leite |**
   Soluções em fibra ótica para sistemas de reabilitação física e aplicações e-Health.

1.5.3 Participation in scientific projects/events

Scientific projects

1. 01-04-2020 to 31-03-2021 | E-Health4workplace Plataforma e-Health para otimização de condições no local de trabalho | Funded by AlticeLabs@UA.

2. 01/11/2016 to 31/10/2018|WeHope – Wearable e-health optical fiber monitoring system | Funded by Instituto de Telecomunicações/ Projet UID/EEA/50008/2013.

Cátia Tavares

Scientific dissemination events

1. Research Summit
2. Xperimenta
3. Academia de Verão

Cátia Tavares

CHAPTER 2

RELEVANCE AND ORIGINAL CONTRIBUTIONS

Cátia Tavares

2.1 Insole Sensors

2.1.1 Introduction

With the progressive increase in life expectancy the medical and scientific community has been concerned with creating programs that promote healthy aging [139, 140]. In 2015 the World Health Organization (WHO) published a report called "World Report on Ageing and Health", which defines the concept of healthy aging as a process of developing and maintaining the functional ability that enables wellbeing in older age and sets the goal of reducing dependent elderly people by 15 million by 2025 [139, 140]. For this, the WHO considered essential to promote the integrated care to maintain people's Intrinsic Capacities (IC). It was also described IC as the combination of the individual's physical and mental capacities, and functional dividing them into five distinct categories: locomotion, sensory, psychological, vitality and cognition. The advances in research areas like e-Health are driven by this purpose, as well as for the necessary help to medical staff in the early diagnosis of anomalies.

The work developed during this thesis was partially motivated to assist in the locomotion category, developing wearable systems with fiber optic sensors. Thus, the objective was the development of systems with the potential to detect anomalies in the gait cycle that may be related to serious pathologies in the spine, as well as the detection of warning signs related to the appearance of pressure ulcers on the feet (very common in people with diabetes).

2.1.2 Manuscript 1: Insole optical fiber sensor architecture for remote gait analysis - an eHealth Solution

Summary

The advances and fast spread of mobile devices and technologies witnessed today, have extended the advantages of medical and health practices supported by mobile devices, giving rise to the growing research of Internet of Things (IoT), especially the e-Health field. The features provided by mobile technologies revealed to be of major importance when considering the continuous aging of population and the consequent increase of its debilities. In addition to the increase of lifetime span of population, also the increase of health risks and their locomotive impairments increases, requiring a close monitoring and continuous evaluation. Such monitoring should be as non-invasive as possible, in order not to compromise the mobility and the day-to-day activities of citizens. Therefore, we present the development of a non-invasive optical fiber sensor architecture adaptable to a shoe sole for plantar pressure remote monitoring, which is suitable to be integrated in an IoT e-Health solution to monitor the wellbeing of individuals. The paper explores the production of the optical fiber sensor multiplexed network (using Fiber Bragg Gratings) to monitor the foot plantar pressure distribution during gait

Cátia Tavares

(walking movement). From the acquired gait data, it is possible to infer health conditions of the patient's foot and spine posture. To guarantee the patients mobility, the proposed system consists of an optical fiber sensor network integrated with a wireless transceiver to enable efficient ubiquitous monitoring of patients. The paper shows the calibration and measurement results, which reflect the accuracy of the proposed system, under normal walking in controlled area.

Figure 9. Graphical abstract of Manuscript 1.

Novelty

The dynamic and continuous monitor of gait parameters requires that the sensing mechanisms implemented are mobile, with limited or non-existent wiring, preferably adaptable to a shoe, low cost, and with low power consumption. Although a considerable number of solutions for plantar pressure have been already reported, they are mainly based on electronic or imaging devices, presenting some drawbacks such as fragility, instability, and inconsistent feedback. As an alternative to these electronic devices, optical fiber-based sensors offer some advantages. The optical fiber technology had already been used to monitor static VGRF and plantar pressure values. Nevertheless, to date of this publication, no reports on dynamic continuous measurements during gait had been presented. On that note, the achievement of our work regarding the dynamic and continuous optical data acquisition during gait was of great significance for the field.

My contributions

This work was carried out at a very early stage of my PhD, nevertheless, I participated in most stages of this work, namely in the pressure characterization of the six sensor elements of the instrumented insole. This calibration was performed by me on a mechanical test machine (Shimadzu® AGS-5kND), where the applied force ranged from 10 to 200 N. The load sets were applied independently in each sensing point (from FBG 1 to FBG 6). I also participated in the processing of data collected during calibration, which resulted in the pressure sensitivities of each sensing points. After calibration, the insole was tested to monitor plantar pressure during gait, and I participated in these experimental trials along with other co-authors. The treatment of the data collected during these experimental trials was performed by me and by two other co-authors of this manuscript. In the end, I also participated in the writing of the manuscript.

2.1.3 Manuscript 2: Insole optical fiber Bragg grating sensors network for dynamic vertical force monitoring

Summary

In an era of unprecedented progress in technology and increase in population age, continuous and close monitoring of elder citizens and patients is becoming more of a necessity than a luxury. Contributing toward this field and enhancing the life quality of elder citizens and patients with disabilities, this work presents the design and implementation of a non-invasive platform and insole fiber Bragg grating sensors network to monitor the vertical ground reaction forces distribution induced in the foot plantar surface during gait and body center of mass displacements. The acquired measurements are a reliable indication of the accuracy and consistency of the proposed solution in monitoring and mapping the vertical forces active on the foot plantar sole, with a sensitivity up to 11.06 pm/N. The acquired measurements can be used to infer the foot structure and health condition, in addition to anomalies related to spine function and other pathologies (e.g., related to diabetes); also, its application in rehabilitation robotics field can dramatically reduce the computational burden of exoskeletons' control strategy. The proposed technology has the advantages of optical fiber sensing (robustness, non-invasiveness, accuracy, and electromagnetic insensitivity) to surpass all drawbacks verified in traditionally used sensing systems (fragility, instability, and inconsistent feedback).

Cátia Tavares
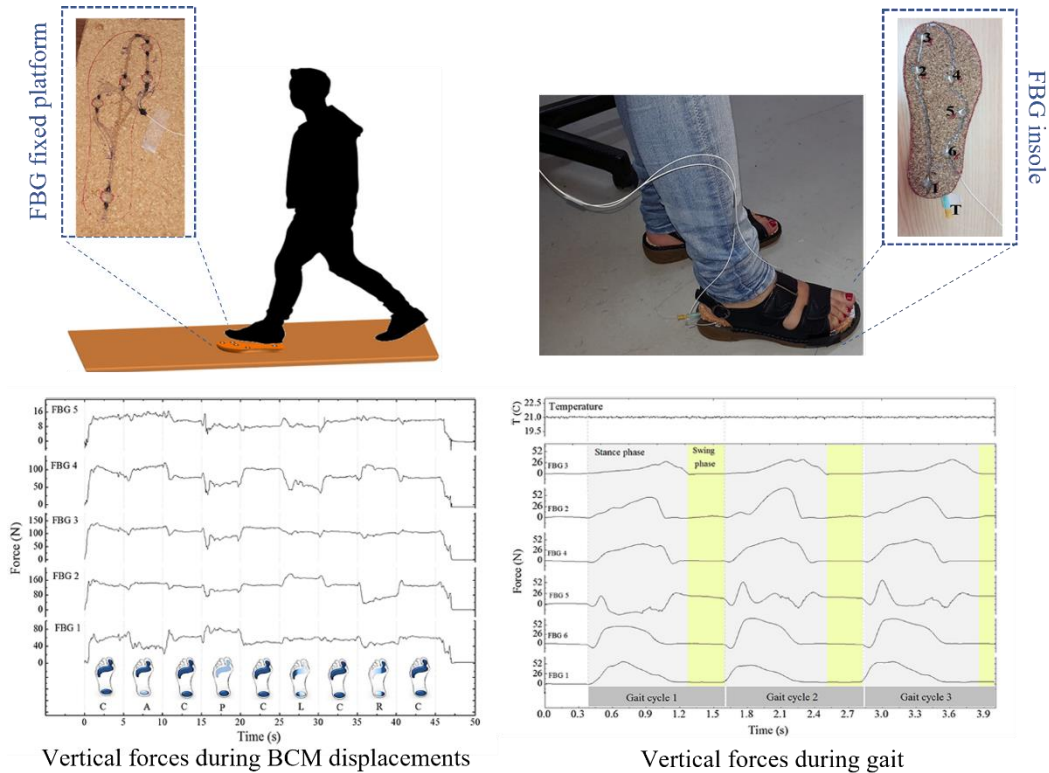
Figure 10. Graphical abstract of Manuscript 2.

Novelty

Compared with the previous manuscript, this work presents two solutions: one to monitor vertical ground reaction forces (VGRF) induced in the foot plantar surface during gait, and another to monitor body center of mass (BCM) displacements. A platform-shaped solution (static solution) and another as insole (mobile solution). As the two manuscripts (1 and 2) were published at about the same time, the novelty of this work is also related to the analysis of the VGRF and BCM during dynamic tests.

My contributions

Like in the previous manuscript, this manuscript was written at an early stage of my PhD. Despite not following all the stages of the work, hence not being the main author, I participated in most of the stages, from the design of the platform to measure plantar pressure to the writing of the manuscript. Briefly, my contribution to this work began by helping to implement the optical sensor network on the cork platform, then I performed the calibration of all the sensing points on both the platform and the insole, in the mechanical testing machine. With other co-authors, I processed the data resulting from the pressure characterisation, which resulted in the sensitivities of each of the detection points. After that, I also participated in the experimental testing of the two devices during the different protocols.

After the experimental tests, together with two other co-authors, I performed the data processing. At the end, I also participated in the writing of the article.

2.1.4 Manuscript 3: Gait shear and plantar pressure monitoring: a non-invasive OFS based solution for e-Health architectures

Summary

In an era of unprecedented progress in sensing technology and communication, health services are now able to closely monitor patients and elderly citizens without jeopardizing their daily routines through health applications on their mobile devices in what is known as e-Health. Within this field, we propose an optical fiber sensor (OFS) based system for the simultaneous monitoring of shear and plantar pressure during gait movement. These parameters are two key factors in gait analysis that can help in the early diagnosis of multiple anomalies, such as diabetic foot ulcerations or in physical rehabilitation scenarios. The proposed solution is a biaxial OFS based on two in-line fiber Bragg gratings (FBGs), which were inscribed in the same optical fiber and placed individually in two adjacent cavities, forming a small sensing cell. Such design presents a more compact and resilient solution with higher accuracy when compared to the existing electronic systems. The implementation of the proposed elements into an insole is also described, showcasing the compactness of the sensing cells, which can easily be integrated into a non-invasive mobile e-Health solution for continuous remote gait monitoring of patients and elder citizens. The reported results show that the proposed system outperforms existing solutions, in the sense that it can dynamically discriminate shear and plantar pressure during gait.
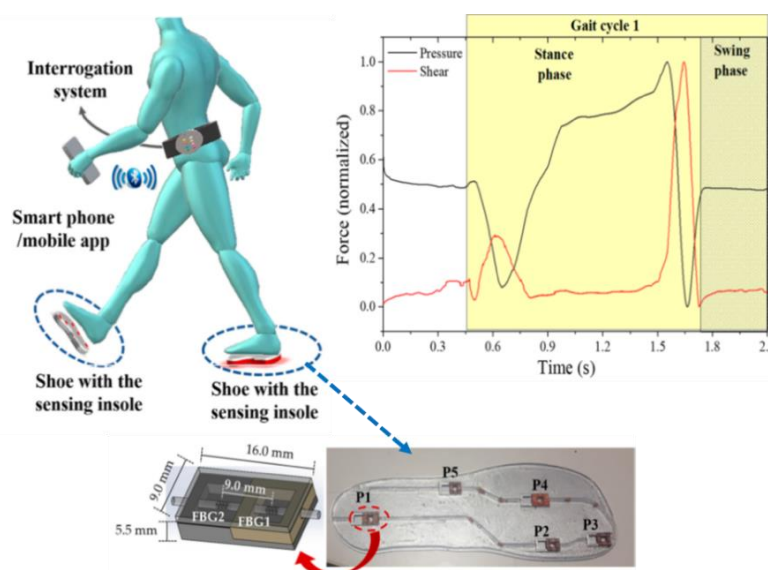
Figure 11. Graphical abstract of Manuscript 3.

Cátia Tavares

Novelty

During the last decades some methods have been proposed for the measurement of plantar shear stress, however, there was a lack of systems capable of simultaneously and at the same point monitoring both shear and pressure during gait. This is because abnormal forces of this type on the sole of the foot are the main cause of plantar pressure ulcers in people with diabetes. This innovative work aimed to bridge this gap by providing an ambulatory solution based on state-of-the-art OFS technology capable of being integrated as an enabler in e-Health architectures.

My contributions

In general, I led the development throughout all the steps of this work: from researching the importance of monitoring shear in the sole of the foot, planning the design of the sensor cell, then also designing, implementing, and testing the sensor cell already in the insole, and finally in data processing. The only process that was not performed by me was the recording of the Bragg gratings.

Being totally innovative, this work started with extensive research on the importance of monitoring other parameters in the sole of the foot during walking, concluding that the monitoring of shear was essential to prevent numerous pathologies related to the health of diabetic patients and/or patients with prolonged age.

This was followed by the study of the design of a sensor cell capable of being placed in an insole without causing discomfort and capable of simultaneously monitoring pressure and shear at the same point. These were the most time-consuming stages of this work. After finding the ideal design, the sensor cells were inserted into the insole, this whole process was mostly done by me but accompanied by other co-authors. After being placed in the insole, each cell was individually characterized to shear and pressure, and an electronic triaxial force sensor was used as reference sensor. This process was performed by me with the help of a master's student that I helped to supervise in his master's dissertation. Subsequently, the instrumented insole was tested during walking. The whole data processing, both characterization and experimental tests, was mainly done by me. Finally, the writing of the article was done by me with the collaboration of the other co-authors.

2.1.5 Manuscript 4: Optically instrumented insole for gait plantar and shear force monitoring

Summary

In this work, a Fiber Bragg Gratings (FBGs) based sensing insole, capable of simultaneously measure plantar force (PF) and shear force (SF) is proposed. The insole has four measuring points,

strategically located for a full gait analysis. Each sensing point contains a sensor-cell which consists of a polylactic acid (PLA) structure, covered by an epoxy resin layer, and crossed by one optical fiber with two FBGs, FBG1 and FBG2, respectively. Due to the specific design of the system, the FBG1 is sensitive to both forces (with higher sensitivity to the PF), while the FBG2 is designed to detect only the SF. The instrumented insole was tested during static and gait exercises, and the results, obtained for the PF and SF monitoring, were according to those theoretically expected.

Figure 12. Graphical abstract of Manuscript 4.

Novelty

With this paper, was proposed a new instrumented insole capable of simultaneously measuring plantar and shear forces at the same point of analysis. There was until that moment only one published work that fulfilled the same purpose (my manuscript 3), however it was presented some complexity of production due to the manual cutting of all the pieces involved in the sensor-cell production (pieces of only a few millimetres in dimension). So, in this work was presenting a new sensor-cell design that reduced the production complexity, since only two materials were used and fewer manual production steps was involved, due to the use of 3D printing to produce the body of the sensor-cell and the base of the insole.

My contributions

Once again in this work I led the development throughout in almost every step, except for recording the Bragg gratings. However, most of my time was dedicated to the sensor design to achieve a less complex production solution: thinking about the cell design, choice of materials and dimensions. After trying out various configurations, a sensor was chosen, which was tested and implemented in the

insole. All these processes were carried out by me and other team members (co-authors of the article), and the calibration processes were very similar to those of manuscript 3. Afterwards, experimental tests were carried out with the insole and the data acquired during them were later treated by me. Finally, I wrote the article presented here with all the detailed information of this work. The remaining authors of the article helped in the review of the paper. Parallel to this work, I also helped a student in her 3rd year Project, this student also participated in several stages of this work and, therefore, she is also one of the co-authors of the presented article.

2.1.6 Main Conclusions

When I started my PhD, very few works had been published using optical fibers as sensors implemented in insoles, so our group contributed significantly to this area state of the art. The first works started only with pressure monitoring (and VGRF and BCM displacement), but we quickly realized that in addition to pressure monitoring being useful, shear monitoring was also worthwhile, as it is one of the biggest indicators of the propensity to develop pressure ulcers (a pathology that can be fatal and affects many people with diabetes). So, the last two works published by me were pioneering contributions in the monitoring of shear and pressure at the same point of the foot. Therefore, in general, this type of sensors has high potential in different contexts/scenarios, including the prevention and study of pressure ulcers or in monitoring the performance of athletes during training; in electronic skin (e-skin) technologies; intelligent and rehabilitation robotic exoskeletons; human-machine interaction devices or even biomimetic prosthesis.

2.2 WHEELCHAIRS SENSORS

2.2.1 Introduction

According to the WHO, about 1% of world population need a wheelchair [141], which is an expressively high number of people, justifying the need for investment in development of devices that contribute to improve their quality of life. Following this purpose, during this thesis work, two papers were published with fiber optic sensor solutions that may contribute to that.

These people, that for various reasons, have limited mobility are obliged to an extensive, daily, and prolonged use of a wheelchair. The consequences are that wheelchair users are more prone to suffer from several pathologies, with pressure ulcers being one of the most recurrent, which in more severe cases can precede a generalized infection and lead to the patient's death. The most common methods to prevent this pathology are related with relieve pressure movements and the use of special cushions

in wheelchairs. Among these, the most cost-effective is the regular repositioning; frequent changes in posture, even sitting, can change the pressure at the skin surface and restore blood flow, improving the tissue health. Therefore, individuals with risk of developing pressure ulcers are recommended to change their positions regularly. To the date of our paper's publication, there were already some published works with electrical devices designed to monitor pressure in wheelchairs, but none with optical sensors. Because, for this particular application, we believe that optical sensors have several advantages over conventional sensors, we decided to start implementing optical sensors in wheelchairs: the first work consisted of a fiber optic sensor network with FBGs capable of monitoring the pressure in six areas of the wheelchair (both scapulas (right and left), both ischiatic zones, and both heels), in addition, it was also possible to measure the patient's heart rate; the second work consisted on a network of six fiber optic sensors with FBGs that is a little more complex, because in addition to monitoring the pressure at different positions (right and left scapulas, both ischiatic zones and both femur zones), it also allowed to detect the user's posture and temperature.

2.2.2 Manuscript 5: Wheelchair pressure ulcer prevention using FBG based sensing devices

Summary

In this work, a fiber Bragg grating (FBG) based sensing system for wheelchair pressure ulcer prevention was developed. Six FBGs were strategically positioned in a wheelchair to monitor the more prominent bone areas, namely scapulas (right (SR) and left (SL)), ischiatic zone (right (IR) and left (IL)), and heels (right (HR) and left (HL)). The sensing architecture was tested by a female user during pressure relief exercises, to verify its effectiveness on pressure monitoring. The proposed system proves to be a compact and reliable solution for wheelchair pressure ulcer prevention, making it a suitable alternative to existing conventional electronic sensors, with the advantage of being immune to electromagnetic interferences and usable in humid environments. In addition to the pressure, the breathing rate was also monitored. By combining the proposed sensing architecture with a wheelchair user detection software, it is possible to create alerts for the user to know when a new position should be adopted, to relieve the pressure in a specific area, thus avoiding one of the biggest problems for such patients, pressure ulcers.

Cátia Tavares
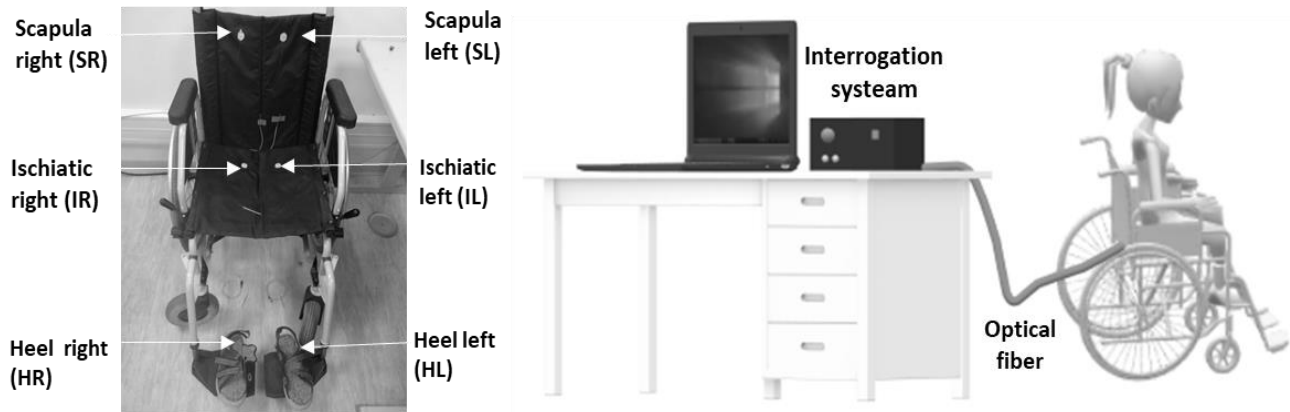
Figure 13. Graphic abstract of Manuscript 5.

Novelty

As previously mentioned, there were no published works with optical sensors in wheelchairs to monitor pressure and posture before this one. That is why all the work developed in this paper is a novelty in itself.

My contributions

It was on my initiative that this work was started and developed, after realizing that there were no published articles with optical sensors applied to wheelchairs, and the huge number of wheelchair users in the world. We believe this is an important topic, deserving attention and research investment, contributing to the wellbeing of many people. Consequently, I did intensive research on this topic, focusing on the needs and problems of wheelchair users. After doing all the research, I was responsible for designing the sensors and defining the wheelchair locations to be instrumented. In this work I recorded the FBGs, implemented the sensor network and performed the tests (both for the calibration of each sensor cell and for the experimental tests). Regarding the acquired data processing and article writing, these tasks were also carried out in collaboration with the other co-authors of the document.

2.2.3 Manuscript 6: Sensor-cell network for pressure, temperature and position detection on wheelchair users

Summary

This work proposes an optical sensing network to monitor pressure and temperature in specific areas of a wheelchair to prevent pressure ulcers and to monitor the position of the wheelchair user by analysing its pressure distribution. The sensing network is composed of six optical fiber Bragg gratings (FBGs) based sensor-cells. Each sensor-cell is built from a polylactic acid (PLA) base and has two FBGs, one embedded in epoxy resin, to monitor pressure variations (FBG$_P$) and another without resin to

Cátia Tavares

monitor temperature (FBG$_T$). Once produced, all sensor-cells were experimentally characterized for pressure and temperature variations, resulting in an average pressure sensitivity of 81 ± 5 pm/kPa (FBG$_P$) and -5.0 ± 0.4 pm/kPa (FBG$_T$), and an average temperature sensitivity of 25 ± 1 pm/^{o}C (FBG$_P$) and 47.7 ± 0.7 pm/^{o}C (FBG$_T$). The sensor-cells were then placed in six specific areas of a wheelchair (four in the seat area and two in the shoulder blade area) to carry out experimental tests, where the response of the sensors to a specific sequence of relief positions was tested. During the execution of the test, the optical signal of all sensors was monitored, in real time, with the pressure and temperature values detected in each zone of the wheelchair. In addition, random position changes were performed, to evaluate the precision of the proposed sensing network in the identification of such positions.

Zones prone to pressure ulcers in wheelchair users

Instrumented wheelchair with six FBGs based sensor-cells for pressure and temperature monitoring

Motivation

Work done

Figure 14. Graphical abstract of Manuscript 6.

Novelty

At the time of publication of this work, there was only other one (our manuscript 4) published using optical sensors to monitor pressure in wheelchairs, therefore, we can consider this work as an optimization of the previous system. In this new work, the wheelchair is also monitored with six sensors, but besides the pressure, the temperature is also monitored, which made it possible to perform a point-to-point temperature compensation in the pressure measurement and to indirectly conclude about the friction in each of the points under analysis. Despite the number of sensors being the same, the location of two of them was changed, moving from the heels in manuscript 5 to the femur area in this new work. This allowed the sensors, besides monitoring pressure and temperature, to be able to assess the posture adopted by the user, so this new system is capable of detecting 7 different positions.

Cátia Tavares

My contributions

In this work I was responsible, along with three other co-authors, for the design of a new sensor cell capable of measuring pressure and temperature at the same point. Everything was thought and produced by us. The recording of twelve FBGs, the production of the six cells, their characterization at pressure and temperature and their subsequent implementation in the wheelchair was coordinated by me and was carried out with the help of other co-authors, namely a student of the third-year project of which I was co-supervisor. In the exploratory tests, the user who tested the wheelchair was my student, while I followed the whole process, ensuring that the protocols were followed, and that the data were acquired correctly and safely. The processing stage of all the acquired data was carried out by me and my student. Finally, the article was written by me and reviewed by the other co-authors.

2.2.4 Main Conclusions

Prior to our team, work with OFS for instrumenting wheelchairs to monitor pressure, posture and temperature had never been published. Fiber optic sensors have several advantages when compared to conventional electronic sensors, so we hope to have opened a door for this type of sensors to continue to be implemented in wheelchairs to improve the quality of life for wheelchair users. As we are at a very preliminary stage of the applicability of this technology to wheelchairs, there is still a lot of work to be done, mainly related to the acquisition system that needs to be cheaper and smaller, nevertheless seminal, and pioneering contributions have been made to this topic. Work is also needed to deliver a mobile application that alerts the user to change his/her position regularly to avoid ulcers.

2.3 OFFICE CHAIR SENSORS

2.3.1 Introduction

Nowadays, there is an increasingly higher number of jobs in which the worker is seated. At the same time, there are also a range of leisure activities carried out in the same way. This increase in sedentary lifestyle is associated with the development of different health pathologies among which postural problems, especially related to the spine, are in a growing number. In recent years, research in intelligent office chairs with sensors has started to grow in interest, aiming to advise the user to correct their posture or take short breaks for relaxation or muscle repositioning. There are several systems that have been developed allowing the user's sitting posture to be monitored using non-wearable sensors, suitable for use in the work environment. In most of these projects, electronic pressure sensors are used to study posture through the pressure applied at different points of the chair. Although back pain is

the main cause of discomfort for office workers, there are other factors related to the indoor environment that can also affect their performance at work, such as: excessive noise, annoying temperatures, and insufficient light. In this sense, it is important to constantly monitor these parameters to provide a healthy and comfortable work environment, to maximize the productivity of its workers. During my PhD, two works were published with instrumented office chairs. The first one only uses electronic sensors and therefore not considered in the scope of this thesis, in which the chair is instrumented with many sensors that allowed to monitor not only the user posture but also environmental parameters. The second work consists in the instrumentation of an office chair with optical intensity low-cost sensors, only to detect posture, being able to detect five different postures. These systems are intended to optimize working conditions, providing the worker, employers, and health institutions a tool to alert seated workers to correct posture, need to rest/get up times, added to the possibility of automaticity adjust environmental parameters, such as lightning. Comfort and safety parameters, such as humidity and CO_2 concentration are also monitored. This work followed an R&D project funded by AlticeLabs@UA.

2.3.2 Manuscript 7: Instrumented office chair with low-cost plastic optical fiber sensors for posture control and work conditions optimization

Summary

People spend more and more time sitting and this habit has been shown to cause spine pathologies. Thus, the scientific community and the industry have become interested in instrumented chairs development to detect incorrect user postures. In this work we present the development and implementation of invisibles and non-intrusive plastic optical fiber sensor cells to monitor the posture and evaluate the ergonomic behaviour of a seated person. The low-cost Plastic Optical Fiber (POF) based sensing devices developed in this work, were implemented in an office chair, to evaluate the workers posture throughout their workday. In addition to the sensors, Android and PC software applications were developed, to provide real time feedback and alerts to the user whenever an inadequate posture is detected, or the seating position is the same for a long time. The proposed approach was evaluated in a study involving six users, and results show that it is able to detect the user's position with 96.6% accuracy.

Cátia Tavares
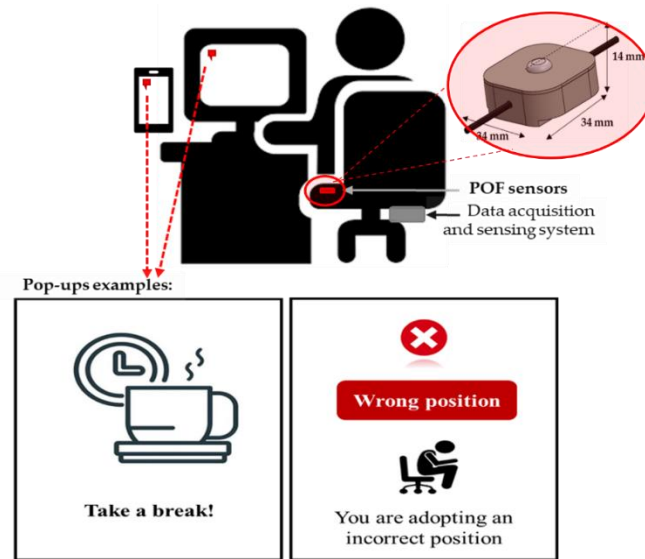
Figure 15. Graphical abstract of Manuscript 7.

Novelty

To our best knowledge this work is the first to explore the use of non-wearable POF based sensors for posture detection. This paper, propose a novel design and implementation of POF sensors to infer the posture of a person sitting in an office chair, considering five different positions. In addition to the sensor's development, end-user software applications were also designed and developed, both for Windows PC and Android. The data acquisition system and software were integrated with a cloud service (Google Firebase). The developed tools are responsible for the data collection, its processing, and storage in a cloud. They also allow real-time interaction with the user, providing the alerts and prompting for posture adjustments when/if needed.

My contributions

This work arose with the implementation of an AlticeLabs financed R&D Project called " E-Health4workplace Plataforma e-Health para otimização de condições no local de trabalho". In which the general objective would be to equip an office chair with sensors to monitor the posture and basic health conditions of the user and monitor the workspace in order to make work more productive. This project was divided in two stages: the first would be to instrument an office chair only with electronic sensors and the second would replace the posture sensors by optical sensors. Although my doctoral work was with optical sensors, I followed this work from the beginning participating in the researcher's team. We started the work by researching what had already been published on the subject: existing devices (electronic and optical), what was considered a good posture for the office chair user, and what were the most frequent incorrect postures. After this initial research phase, we started thinking about

the number of sensors needed to be able to distinguish different postures. I helped my fellow co-authors with the instrumentation of electronic sensors, but I was not the lead researcher in this first stage process nor in the development of all the software for data processing, storage and mobile applications. I participated the most on the second stage, on the production and testing of several optical posture sensor cells. All the design, production and testing of the sensor cells configurations were guided by me, with the help of several co-authors. Subsequently, the implementation of optical sensors and experimental tests (both pressure calibration and applicability tests with different users) were also performed by me. The data processing and writing of this article and the article with electronic sensors only was also done by me and reviewed by the other co-authors. The work with only electronic sensors is currently under analysis for publication, but as it is not part of the theme of my PhD we decided not to include it in the document.

2.3.3 Main Conclusions

The results presented in this work and considering the inherent advantages of using optical fibers over electronic sensors and the simplicity and low cost, showed that the proposed optical sensors solution is a promising method to replace the existing electronic technology. Thus, in the future, it would be of added value to incorporate other optical sensors to help monitor: posture, physiological parameters and the environment in which the chair is located.

2.4 VITAL SIGNS SENSORS

2.4.1 Introduction

The FDM technology by 3D printing for the construction of optical sensors with embedded FBGs has been used in recent years mainly due to the speed, high accuracy, low complexity, and reproducibility in the production of these sensors. Its application has been vast, however in the field of medical applications very few works have been published. In this sense, at a later stage of my PhD I started to explore the application of FBGs during the 3D printing process in parts built with various types of filaments (PLA - polylactic acid, TPU - Thermoplastic Polyurethanes, Flexible) to produce pressure sensors. The sensor produced with Flexible proved to be very sensitive and was therefore tested as a sensor for vital signs monitoring.

The importance of vital signs monitoring is more than known, standing out as the application area of optical sensors with the largest number of published works. Its periodic monitoring can even

detect abnormalities related to several pathologies, mainly those related to cardiovascular diseases, which, as already mentioned, are the main cause of death in the world [97].

There are many teams that over the years have published works with new optical devices to monitor vital signs, but as far as we know, none has produced its sensor using only the FDM technique.

2.4.2 Manuscript 8: Respiratory and heart rates monitoring using a FBG 3D-printed wearable system

Summary

This work proposes a 3D-printed sensor based on fiber Bragg grating (FBG) technology for respiratory rate (RR) and heart rate (HR) monitoring. Each sensor is composed of a single FBG fully encapsulated into a 3D-printable Flexible, during the printing process. Sensors with different material thicknesses and infill densities were tested. The sensor with the best metrological properties was selected and preliminary assessed in terms of capability of monitoring RR and HR on three users. Preliminary results proved that the developed sensor can be a valuable easy-to-fabricate solution, with high reproducibility and high strain sensitivity to chest wall deformations due to breathing and heart beating.

Figure 16. Graphical abstract of Manuscript 8.

Cátia Tavares

Novelty

As already discussed in section 1.3.2, there are several techniques and materials already exploited to encapsulate FBGs to measure vital signs, such as resin or plastic composites, which are very flexible and confer to the FBGs good robustness, high adaptability to the skin, and good compliance with the chest movements. However, some uncontrolled factors which may occur during the manufacturing process, such as a non-uniform bonding strength at the fiber-polymer interface and the presence of some bubbles of air in the cured polymer matrixes, that may affect the performance of the final system and decrease its reproducibility. Recently, fused deposition modelling (FDM) has been proposed as a promising method for sensors fabricating, allowing to develop a sensing element very quickly and with high printing precision. Few papers proposed this technique in the fabrication of sensors for medical applications, but none of them for monitoring respiration and cardiac activity. This paper aims at evaluating if the FDM method can be an innovative technique to build an FBG-based wearable system able to monitor the users' vital signs in real time, namely RR and HR.

My contributions

This work started with my curiosity to incorporate fibre optic sensors into a part printed on a 3D printer during printing. I tested several designs for the parts and several materials, starting with the most common (PLA), but quickly moving on to other materials less used, but with higher elasticity and therefore more practical as wearable solutions (TPU and *Flexible*). *Flexible* was the material chosen for this work, because we get very good results already from the first experiments, having produced very sensitive sensors to pressure/vibration. As the developed sensor exhibited high sensitivity to pressure, it was tested as HR and RR sensor, offering excellent results. Besides testing several materials and several designs, I also tested several fillers to further optimize the produced sensor. This article reflects that path of trying to optimize a sensor for this specific application, where the sensor configuration that results in higher sensitivity is tested: two sensor thicknesses (2 or 3 mm) and three infills (20, 60 or 100 %) are compared. I was responsible for this whole process of sensor optimization, from the design to the 3D printing and even the recording of the Bragg gratings. After all this, the individual characterization of each sensor cell was performed at different deformation amplitudes and at different frequencies. This characterization was performed by me, and another co-author of the article and we used as reference sensor the BioHarness (BH) device (ZEPHYR performance systems, Medtronic). The

exploratory tests on the three users were also all monitored by me, as well as the management of all data. Finally, the paper was written by me and reviewed by the other authors. The continuation of this work also gave rise to two more papers accepted at international conferences and a work of the third-year project of the Biomedical Engineering graduation degree of a student that I co-supervised during the final part of my PhD.

2.4.3 Main Conclusions

In this work, a 3D printed sensor produced with Flexible, with an embedded FBG was developed to monitor two vital signs, namely HR and RR. Six different configurations were tested for this sensor, varying two thicknesses and three infill printing percentages. The sensor that showed higher sensitivity for both types of signals was the device with the least thickness and less filling. Applicability tests were performed with three users, to preliminarily evaluate the system's ability to detect chest wall excursions related to respiratory and cardiac activities. The results showed that the proposed system, a wearable solution, can be used to measure the users' RR and HR during normal breathing and apnoea. Although the displacements caused by the heartbeat are smaller than those induced by the respiration, the values obtained for the HR only differ 0.8 ± 5.9 bpm, which is in line with other commercial wearable devices. Due to the reliability of the results presented, the inherent advantages of using optical fibers over electronic sensors, and the simple, inexpensive, and high reproducibility of the sensor manufacturing process, the proposed solution constitutes a promising method to replace existing electronic technology for detecting heart and respiration rates.

CHAPTER 3

GENERAL CONCLUSIONS AND FUTURE
PRESPECTIVES

Cátia Tavares

3.1 GENERAL CONCLUSIONS

This Thesis was structured according to Art. 63.º and 64.º-A of Study Regulations of the University of Aveiro and consists of the presentation of the most relevant published papers during the course of the Doctoral Programme, followed by a Complementary Report. This report aims to provide an overview of all the work done and to clarify my contribution to the publication of each article. The Complementary Report, structured in 3 chapters, starts by reviewing the importance of constant health monitoring nowadays and the parallel emergence of fiber optic sensor technology in this research topic. This has happened mainly due to the advantages of these sensors when compared to conventional sensors. In the area of biomedical applications these sensors stand out for their stability, immunity to electromagnetic interference, high sensitivity, and safety. A brief overview about optical fibers, OFS and the application of these sensors in biomedical applications was also done.

During the present work, OFS were developed for different biomedical applications: beginning with the development of insoles instrumented with silica optical fiber sensors with several FBGs to monitor initially pressure and later pressure and shear; then by the development of a sensor network of the same type but for application in wheelchairs for monitoring the posture of the wheelchair user; later plastic optical fiber sensors were developed to monitor the posture of an office chair user; and finally, a sensor completely embedded in a 3D printed part capable of monitoring HR and RR was developed. This last sensor uses silica fiber sensor with only one FBG.

Before the presentation of the developed work, Section 1.3 was dedicated to the literature review, where greater focus was given to the published works in which fiber optic sensors were used in the applications described above, i.e., insoles, wheelchairs, office chairs and vital signs monitoring (RR and HR).

The first two articles (Sections 2.1.2 and 2.1.3) are focused on the development of an insole instrumented with OFS to monitor plantar pressure. The next two articles (Sections 2.1.4 and 2.1.5) are about instrumented insoles for monitoring plantar pressure and shear. In Table 6, the main features such as the number of FBGs and materials used for their production are compared, and the all works are classified quantitatively on a scale from I to V (where I means minimum and V maximum) according to the ease of production and their robustness. In addition to the articles published in SJR indexed journals, three first author works were also presented in scientific communications in international conferences during the years 2018 and 2019 related to this topic: in 2018 SPIE Photonics Europe (Strasbourg, France); in 2019 IMOC (Aveiro, Portugal); and SPIE Optics+ Optoelectronics (Prague, Czech Republic).

Table 6. Main differences between published manuscripts related to insoles instrumentation.

	Manuscript 1 (pressure)	Manuscript 2 (pressure)	Manuscript 3 (pressure and shear)	Manuscript 4 (pressure and shear)
Sensitivity	8.30 pm/kPa	11.06 pm/kPa	0.014 nm/N (pr.) 0.024 nm/N (sh.)	0.186 nm/N (pr.) 0.127 nm/N (sh.)
Robustness*	III	III	II	III
Production facility*	IV	IV	I	III
No. of FBGs	6	5	10	8
Material	Cork and epoxy resin	Cork and epoxy resin	Cork, PLA and epoxy resin	PLA and epoxy resin

* Quantitative variable: minimum (I), maximum (V).

The first (Section 2.1.2) and the second (Section 2.1.3) manuscripts were devoted to the initial development of tools to analyse different parameters related to the gait, being the first one only for pressure monitoring and the second one for monitoring not only pressure but also body centre of mass displacements.

The third and fourth studies (Sections 2.1.3 and 2.1.4) are related with the previous works optimization and allowed the development a tool to simultaneously monitor not only plantar pressure but also shear during the gait. Shear forces were identified by several authors as one of the main reasons for the appearance of pressure ulcers in the feet [58]. The third paper presented in this thesis (manuscript 3) was the first published work using OFS to simultaneously monitor these two forces in an insole, reaching an equipment with appropriated sensitivities. The following work (manuscript 4) main motivation was to improve and optimize the design and production process. The modifications in the design of the insole and in the sensor cells, allowed to obtain a device capable of monitoring the same two forces, through a completely different production process, 3D printing was used to produce most of the details of the insole, with the remaining elements of the insole filled with epoxy resin. This optimization of the manufacturing process made it possible to reduce the manufacturing time, and to automate the process, reducing errors that arose due to the large part of the old process being manual. Besides the ease of the production method, this solution was more robust and composed of only two materials.

Section 2.2 is dedicated to wheelchairs instrumentation (manuscripts 5 and 6). In addition to these manuscripts, a communication was also presented at the IV International Conference on Applications of Optics and Photonics in Lisbon 2019, with the application of two sensor cells reported in Manuscript 4

on a pillow installed on a seat of a wheelchair to monitoring pressure and shear in two different locations. The manuscript 5 (Section 2.2.2) was the first paper published with OFS application for posture monitoring in wheelchair users. This monitoring is an important tool to aid preventing the appearance of postural and tissue lesions due to excessive hours in the same position. The instrumentation of wheelchairs with pressure sensors is the first step towards the development of a system that can alert the user to change position regularly, and it may greatly improve the life of a wheelchair user. OFS instrumentation, in this application, present specific advantages when compared with conventional electronic sensors, such as no electric signals at the measuring point, which is often humid due to transpiration (or regular cleaning), flexibility but robustness, light and small size, among others. In this work, it was possible to monitor the pressure in several areas of the wheelchair (scapulas, ischiatic zone and heels), and the respiratory rate. The temperature increase in certain areas of the wheelchair is usually related to areas of greater friction, which are areas where pressure ulcers are more likely to occur, one of the greatest scourges of wheelchair users. To make up for the lack of localized temperature detection in several areas of the wheelchairs, a second work arose. This last work (manuscript 6, Section 2.2.3) consisted in the production of a more complex sensor cell, capable of measuring pressure and temperature at the same point. The position of the sensors on the chair was different from the previous work (in this case, they were placed on the scapulas, ischiatic zone and femur), which allowed the detection of 7 different postures adopted by the user. Table 7 presents the main differences between the published works with FBGs in wheelchairs.

Table 7. Main differences between published manuscripts related to wheelchair instrumentation.

	Manuscript 4 (pressure, RR)	Manuscript 5 (pressure, temperature)
Sensitivity	17.8 pm/kPa	81.00 pm/kPa (pr.)
		5.00 pm/kPa (t.)
Robustness*	IV	III
Production facility*	IV	III
No. of FBGs	6	12
Material	epoxy resin	epoxy resin and PLA
No. of detected postures	6	7

*Quantitative variable: minimum (I), maximum (V).

After the development of sensor networks to monitor pressure and posture in wheelchair users, the work evolved to the office chairs thematic.

The following section (Section 2.3) is dedicated to the instrumentation of office chairs with optical and electronic sensors (manuscript 7). In addition to this publication, another manuscript was also submitted to the Internet of Things journal with instrumentation of an office chair with only electronic

Cátia Tavares

sensors. Manuscript 7 presented in this PhD thesis is about an office chair seat instrumented with four optical fiber-based sensor cells (with POF intensity sensors) to monitor the user's posture. The work describes the whole process from the choice of the sensor-cell design to the software developed for the user of the chair and finally shows the results obtained after exploratory tests with six users. The results showed a confidence of 96.6% for detection of four different postures. Considering the inherent advantages of the use of plastic optical fibres when compared to conventional electronic sensors, the simplicity, and the low cost, this is a promising solution to replace the electronic sensors. As far as we know there are no other works with the application of similar sensors in office chairs to monitor the user's posture. Despite the novelty, this is an important and increasingly fashionable topic due to the high number of hours we spend inactively seated (both at work and in various leisure activities), which often leads to postural injuries.

The work developed during this PhD program continued studying the embedding process of fiber optic sensors in 3D printed parts during their printing process. Initially it was tested in parts composed by PLA, for being the material most used in these printers, but due to its rigidity quickly the work progressed to more flexible materials and therefore more comfortable to be used as wearables equipment's. As a result of these experiments, a fast and very sensitive sensor was developed, fully embedded in a material called "Flexible", capable of monitoring both heart rate and respiration rate. Although OFSs for monitoring vital signs are a widely studied area, sensors with this type of encapsulation for this application had never been published before. The results obtained in this sensor are presented and compared with two commercial HR monitor in Table 8. The calculation of the difference in results presented by each device is according to the results obtained by ECG (electrocardiogram). In addition to giving rise to a paper published in the journal Biomedical Optics Express, the work with this device continued, and two works were also accepted for international conferences: the first employs the same sensor cell to the wrist to successfully detect HR and featured at MetroInd 4.0, Trento 2022; the second presents a study of the 3D printing filling percentage and the FBG positioning effects on the sensor sensitivity, allowing to optimize and adapt the sensor to different applications, this work was accepted and will be presented at European Optical Society Annual Meeting, Porto 2022.

Cátia Tavares

Table 8. Heart rate differences between BH and our published optical sensor and comparation of the results with commercial device, adapted by [128].

Device	HR differenced from ECG (mean ± standard deviation)		Ref.
	Paired differences	Percent difference	
Our device	0.8 ± 5.9 bpm	0.6 ± 7.6 %	[128]
Polar Chest Strap	0.2 ± 1.4 bpm	0.9 ± 1.6 %	[142]
Apple watch	-1.7 ± 10 bpm	5.5 ± 9.4 %	[142]

In summary, the main goals of the proposed workplan were attained and even exceeded, with the development of a total of eight devices with embedded fiber optic sensors: four to detect gait-related parameters, two to detect postures in wheelchairs, one to detect postures in office chairs and one to monitor vital signs.

3.2 FUTURE PRESPECTIVES

About pressure and shear sensors a lot of work was done and published by our group. The work has been evolving, not only by optimizing the devices created, but also because we were adding new parameters to be monitored. However, there is still work to be done, mainly in the acquisition systems that are expected to be simpler and cheaper, decreasing the sensors production time and increasing its reproducibility. Also, on the software development side, there is also work to be done, such as the development of user-friendly applications, as well as its connection to rehabilitation clinics and medical teams in real time for home remote rehabilitation programs.

Concerning the wheelchair sensors, two types of sensors were created to monitor the posture of the wheelchair user, however there are other types of sensors of equal importance that can be implemented in wheelchairs, and the future in this area can go down that path. Implementation of a network of sensors to monitor more parameters of the user (as for example vital signs, muscular effort, etc) and also of the surrounding environment, as in the work published in the manuscript 7 (ambient temperature, luminosity, etc). This type of tool can be extremely useful to improve the day by day of wheelchair users. As in the previous topic, here too the situation of decreasing the cost of acquisition systems is imperative and transversal to all fibre optic sensors with FBGs, where non-expensive acquisition systems are still needed.

Cátia Tavares

For the vital sign's sensors area, collaborations with other departments of the Aveiro University (Mechanics and Health School) and universities (University Campus Bio-Medico di Roma, Italia) are currently being contemplated for usability tests of the developed device to monitor vital signs.

In the future, work on optical fiber sensors in 3D printed parts are being thought for biomedical devices for areas of study other than vital signs monitoring, such as pressure measurement for posture control in chairs, couch's, cars, airplanes, etc. Also, the possibility of incorporating other types of optical sensors, such as FPI (Fabry Perrot Interferometers), or even light intensity variation sensors are being considered, especially to help lowering the cost related with the acquisition system.

In the instrumentation field, it would be of added value to develop a light, portable and low-cost, autonomous interrogation system for easy installation on clothing or wearable elements like belts, capable of being battery powered. That would be a big step to move from the use of these sensors only in laboratories to their effective use in the daily life of users.

REFERENCES

RFFERENCES

[1] Paul, S., Riffat, M., Yasir, A., Mahim, M.N., Sharnali, B.Y., Naheen, I.T., Rahman, A. and Kulkarni, A., 2021. Industry 4.0 applications for medical/healthcare services. *Journal of Sensor and Actuator Networks*, *10*(3), pp. 43.

[2] Wehde, M., 2019. Healthcare 4.0. *IEEE Engineering Management Review*, *47*(3), pp. 24-28.

[3] Tortorella, G.L., Fogliatto, F.S., Mac Cawley Vergara, A., Vassolo, R. and Sawhney, R., 2020. Healthcare 4.0: trends, challenges and research directions. *Production Planning & Control*, *31*(15), pp. 1245-1260.

[4] Dakin, J. and Culshaw, B., 1988. Optical fiber sensors: Principles and components. Volume 1. *Boston*.

[5] Gholamzadeh, B. and Nabovati, H., 2008. Fiber optic sensors. *World Academy of Science, Engineering and Technology*, *42*(3), pp. 335-340.

[6] Sabri, N., Aljunid, S.A., Salim, M.S., Ahmad, R.B. and Kamaruddin, R., 2013.Toward optical sensors: Review and applications. In *Journal of Physics: Conference Series*, 423(1), pp. 012064. IOP Publishing, April.

[7] Rajan, G., 2017. *Optical fiber sensors: advanced techniques and applications*. CRC press.

[8] Baldini, F., Giannetti, A., Mencaglia, A.A. and Trono, C., 2008. Fiber optic sensors for biomedical applications. *Current Analytical Chemistry*, *4*(4), pp. 378-390.

[9] Poeggel, S., Tosi, D., Duraibabu, D., Leen, G., McGrath, D. and Lewis, E., 2015. Optical fibre pressure sensors in medical applications. *Sensors*, *15*(7), pp. 17115-17148.

[10] Correia, R., James, S., Lee, S.W., Morgan, S.P. and Korposh, S., 2018. Biomedical application of optical fibre sensors. *Journal of Optics*, *20*(7), pp. 073003.

[11] Cuadrado-Laborde, C., 2019. *Applications of Optical Fibers for Sensing*. BoD–Books on Demand.

[12] García, I., Zubia, J., Durana, G., Aldabaldetreku, G., Illarramendi, M.A. and Villatoro, J., 2015. Optical fiber sensors for aircraft structural health monitoring. *Sensors*, *15*(7), pp. 15494-15519.

[13] Bado, M.F. and Casas, J.R., 2021. A review of recent distributed optical fiber sensors applications for civil engineering structural health monitoring. *Sensors*, *21*(5), pp. 1818.

[14] Joe, H.E., Yun, H., Jo, S.H., Jun, M.B. and Min, B.K., 2018. A review on optical fiber sensors for environmental monitoring. *International journal of precision engineering and manufacturing-green technology*, *5*(1), pp. 173-191.

[15] Kazanskiy, N.L., Khonina, S.N., Butt, M.A., Kaźmierczak, A. and Piramidowicz, R., 2021. State-of-the-art optical devices for biomedical sensing applications—A review. *Electronics*, *10*(8), p.973.

[16] Bartlett, R.J., Philip-Chandy, R., Eldridge, P., Merchant, D.F., Morgan, R. and Scully, P.J., 2000. Plastic optical fibre sensors and devices. *Transactions of the Institute of Measurement and Control*, *22*(5), pp. 431-457.

[17] Peters, K., 2010. Polymer optical fiber sensors—a review. *Smart materials and structures*, *20*(1), pp. 013002.

[18] Hill, K.O., Fujii, Y., Johnson, D.C. and Kawasaki, B.S., 1978. Photosensitivity in optical fiber waveguides: Application to reflection filter fabrication. *Applied physics letters*, *32*(10), pp. 647-649.

[19] Othonos, A., 1997. Fiber Bragg gratings. *Review of scientific instruments*, *68*(12), pp. 4309-4341.

[20] Hill, K.O. and Meltz, G., 1997. Fiber Bragg grating technology fundamentals and overview. *Journal of lightwave technology*, *15*(8), pp. 1263-1276.

[21] Kashyap, R., 2009. *Fiber Bragg gratings*. Academic press.

[22] Bragg, W.H., 1912. X-rays and Crystals, *Nature*, 90, pp. 219

[23] Bragg, W.L., 1912. The Specular Reflection of X-rays., *Nature*, 90, pp. 410.

[24] Bragg, W.H. and Bragg, W.L., 1913. The Structure of the Diamond, *Nature,* 91, pp. 557.

[25] Glazer, A.M., 2013. The first paper by W.L. Bragg – What and when?, *Crystallogr. Rev.* 19, pp. 117-124.

[26] Moscatelli, A., 2014. A new crystallography is born, *Nature*, 511, pp. 7.

[27] Araújo, F., 1999. Redes de Bragg em Fibra Ótica, Faculdade de Ciências da Universidade do Porto.

[28] Nogueira, R., 2005. Redes de Bragg em fibra óptica.

[29] Martinez, A., Dubov, M., Khrushchev, I. and Bennion, I., 2004. Direct writing of fibre Bragg gratings by femtosecond laser, *Electronics Letters*, 40, pp. 1170-1172.

[30] Slattery, S.A., Nikogosyan, D.N. and Brambilla, G., 2005. Fiber Bragg grating inscription by high intensity femtosecond UV laser light: comparison with other existing methods of fabrication, *Journal of the Optical Society of America*, 22, pp. 354.

[31] Patrick, H.J., Kersey, A.D. and Bucholtz F., 1998. Analysis of the response of long period fiber gratings to external index of refraction, *Journal of Lightwave Technology*, 16, pp. 1606-1612.

[32] Zhang, L. Liu, Y. Everall, L. Williams, J.A.R. and Bennion, I., 1999. Design and realization of long-period grating devices in conventional and high birefringence fibers and their novel applications as fiber-optic load sensors, *IEEE Journal of Selected Topics in Quantum Electronics*, 5 pp. 1373-1378.

[33] Bai-Ou Guan, A-Ping Zhang, Hwa-Yaw Tam, Chan, H.L.W., Chung-Loong Choy, Xiao-Ming Tao and Demokan, M.S., 2002. Step-changed long-period fiber gratings, *IEEE Photonics Technology Letters*, 14, pp. 657–659.

[34] Zhao, X.W. and Wang, Q., 2019. Mini review: Recent advances in long period fiber grating biological and chemical sensors. *Instrumentation Science & Technology*, *47*(2), pp. 140-169.

[35] Othonos, A and Kalli, K. 2001. Bragg gratings in optical fibers, *Handbook of Advanced Electronic and Photonic Materials and Devices*, 9, pp. 367-480.

[36] Singh, N., Jain, S.C., Aggarwal, A.K. and Bajpai, R.P., 2005. Fibre Bragg grating writing using phase mask technology.

[37] Markowski, K., Perka, A., Jędrzejewski, K. and Osuch, T., 2016. Custom FBGs inscription using modified phase mask method with precise micro-and nano-positioning. In *Photonics Applications in Astronomy, Communications, Industry, and High-Energy Physics Experiments 2016,* 10031, pp. 100311H. International Society for Optics and Photonics, September.

[38] Rothmaier, M., Luong, M.P. and Clemens, F., 2008. Textile pressure sensor made of flexible plastic optical fibers. *Sensors*, *8*(7), pp. 4318-4329.

[39] Silva, A.S., Catarino, A., Correia, M.V. and Frazão, O., 2013. Design and characterization of a wearable macrobending fiber optic sensor for human joint angle determination. *Optical Engineering*, *52*(12), pp.126106.

[40] Bilro, L., Alberto, N., Pinto, J. L. and Nogueira, R., 2012. Optical sensors based on plastic fibers. *Sensors*, 12(9), pp. 12184-12207.

[41] Jing, N., Zheng, J., Zhao, X. and Teng, C., 2014. Refractive index sensing based on a side-polished macrobending plastic optical fiber. *IEEE Sensors Journal*, *15*(5), pp. 2898-2901.

[42] Mesquita, E., Paixão, T., Antunes, P., Coelho, F., Ferreira, P., André, P. and Varum, H., 2016. Groundwater level monitoring using a plastic optical fiber. *Sensors and Actuators A: Physical*, *240*, pp. 138-144.

[43] Silva, H. P. Biomedical sensors as invisible doctors. *Regenerative Design in Digital Practice*, 324.

[44]   Silva, A. S., Correia, M. V., and Silva, H. P., 2021. Invisible ECG for High Throughput Screening in eSports. *Sensors*, *21*(22), pp. 7601.

[45]   Majumder, S., Mondal, T., Deen, M., 2017. Wearable Sensors for Remote Health Monitoring. *Sensors*, 17, pp. 130

[46]   Roriz, P., Ramos, A., Santos, J.L. and Simões, J.A., 2012. Fiber optic intensity-modulated sensors: A review in biomechanics. *Photonic Sensors*, *2*(4), pp. 315-330.

[47]   Roriz, P., and Ribeiro, A. B. L., 2018. Fiber Optical Sensors in Biomechanics. *Opto-Mechanical Fiber Optic Sensors*, pp. 263-300. Butterworth-Heinemann.

[48]   Subramaniam, S., Majumder, S., Faisal, A.I. and Deen, M.J., 2022. Insole-Based Systems for Health Monitoring: Current Solutions and Research Challenges. *Sensors*, *22*(2), pp. 438.

[49]   Chen, J. L., Dai, Y. N., Grimaldi, N. S., Lin, J. J., Hu, B. Y., Wu, Y. F., and Gao, S., 2022. Plantar Pressure-Based Insole Gait Monitoring Techniques for Diseases Monitoring and Analysis: A Review. *Advanced Materials Technologies*, *7*(1), pp. 2100566.

[50]   Ramirez-Bautista, J.A., Huerta-Ruelas, J.A., Chaparro-Cárdenas, S.L. and Hernández-Zavala, A., 2017. A review in detection and monitoring gait disorders using in-shoe plantar measurement systems. *IEEE Reviews in Biomedical Engineering*, *10*, pp. 299-309.

[51]   Fernando, M.E., Crowther, R.G., Lazzarini, P.A., Sangla, K.S., Wearing, S., Buttner, P. and Golledge, J., 2016. Plantar pressures are higher in cases with diabetic foot ulcers compared to controls despite a longer stance phase duration. *BMC endocrine disorders*, *16*(1), pp. 1-10.

[52]   Faisal, A.I., Majumder, S., Mondal, T., Cowan, D., Naseh, S. and Deen, M.J., 2019. Monitoring methods of human body joints: State-of-the-art and research challenges. *Sensors*, *19*(11), pp. 2629.

[53]   Majumder, S., Mondal, T. and Deen, M.J., 2018. A simple, low-cost and efficient gait analyzer for wearable healthcare applications. *IEEE Sensors Journal*, *19*(6), pp. 2320-2329.

[54]   Coutinho, E.S.F., Bloch, K.V. and Coeli, C.M., 2012. One-year mortality among elderly people after hospitalization due to fall-related fractures: comparison with a control group of matched elderly. *Cadernos de Saúde Pública*, *28*, pp. 801-805.

[55]   Stess, R.M., Jensen, S.R. and Mirmiran, R., 1997. The role of dynamic plantar pressures in diabetic foot ulcers. *Diabetes care*, *20*(5), pp. 855-858.

[56]   Wang, L., Jones, D., Chapman, G. J., Siddle, H. J., Russell, D. A., Alazmani, A., and Culmer, P., 2019. A review of wearable sensor systems to monitor plantar loading in the assessment of diabetic foot ulcers. *IEEE Transactions on Biomedical Engineering*, *67*(7), pp. 1989-2004.

[57]   Zou, D., Mueller, M.J. and Lott D. J, 2007. Effect of peak pressure and pressure gradient on subsurface shear stresses in the neuropathic foot. *Journal of Biomechanics*, 40(4), pp. 883-890.

[58]   Rajala S. and Lekkala, J., 2014. Plantar shear stress measurements: A review. *Clinical Biomechanics.*, 29(5), pp. 475-483.

[59]   Hao, J.Z., Tan, K.M., Tjin, S.C., Liaw, C.Y., Chaudhuri, P.R., Guo, X. and Lu, C., 2003. Design of a foot-pressure monitoring transducer for diabetic patients based on FBG sensors. In *Conference Proceedings-Lasers and Electro-Optics Society Annual Meeting-LEOS*, 1, pp. 23-24. IEEE, December.

[60]   Suresh, R., Bhalla, S., Hao, J. and Singh, C., 2015. Development of a high resolution plantar pressure monitoring pad based on fiber Bragg grating (FBG) sensors. *Technology and Health Care*, *23*(6), pp. 785-794.

[61]   Domingues, M.F., Alberto, N., Leitão, C.S.J., Tavares, C., de Lima, E.R., Radwan, A., Sucasas, V., Rodriguez, J., Andre, P.S. and Antunes, P.F., 2017. Insole optical fiber sensor architecture for remote gait analysis—An e-health solution. *IEEE Internet of Things Journal*, *6*(1), pp. 207-214.

[62] Vilarinho, D., Theodosiou, A., Leitão, C., Leal-Junior, A.G., Domingues, M.D.F., Kalli, K., André, P., Antunes, P. and Marques, C., 2017. POFBG-embedded cork insole for plantar pressure monitoring. *Sensors*, *17*(12), pp. 2924.

[63] Hao, Z., Cook, K., Canning, J., Chen, H.T. and Martelli, C., 2019. 3-D Printed Smart Orthotic Insoles: Monitoring a Person's Gait Step by Step. *IEEE Sensors Letters*, *4*(1), pp. 1-4.

[64] Liang, T.C., Lin, J.J. and Guo, L.Y., 2016. Plantar pressure detection with fiber Bragg gratings sensing system. *Sensors*, *16*(10), pp. 1766.

[65] Domingues, M.F., Tavares, C., Leitão, C., Neto, A., Alberto, N., Marques, C., Radwan, A., Rodriguez, J., Postolache, O., Rocon, E. and André, P., 2017. Insole optical fiber Bragg grating sensors network for dynamic vertical force monitoring. *Journal of Biomedical Optics*, *22*(9), pp. 091507.

[66] Tavares, C., Domingues, M.F., Alberto, N., Ramos, A., Rocon, E., André, P., Silva, H. and Antunes, P., 2019, Bioinspired optical fiber sensor for simultaneous shear and vertical forces monitoring. In *Optical Sensors 2019*, l(11028), pp. 110282M. International Society for Optics and Photonics, April.

[67] Leal-Junior, A.G., Diaz, C.R., Marques, C., Pontes, M.J. and Frizera, A., 2019. 3D-printed POF insole: Development and applications of a low-cost, highly customizable device for plantar pressure and ground reaction forces monitoring. *Optics and Laser Technology*, *116*, pp. 256-264.

[68] Tavares, C., Leite, F., Domingues, M.D.F., Paixão, T., Alberto, N., Ramos, A., Silva, H. and Antunes, P.F.D.C., 2021. Optically Instrumented Insole for Gait Plantar and Shear Force Monitoring. *IEEE Access*, *9*, pp.132480-132490.

[69] Brem, H., Maggi, J., Nierman, D., Rolnitzky, L., Bell, D., Rennert, R., Golinko, M., Yan, A., Lyder, C. and Vladeck, B., 2010. High cost of stage IV pressure ulcers. *The American Journal of Surgery*, *200*(4), pp. 473-477.

[70] Sonenblum, S.E., Vonk, T.E., Janssen, T.W. and Sprigle, S.H., 2014. Effects of wheelchair cushions and pressure relief maneuvers on ischial interface pressure and blood flow in people with spinal cord injury. *Archives of physical medicine and rehabilitation*, *95*(7), pp. 1350-1357.

[71] Verbunt, M. and Bartneck, C., 2010. Sensing senses: Tactile feedback for the prevention of decubitus ulcers. *Applied psychophysiology and biofeedback*, *35*(3), pp. 243-250.

[72] Sprigle, S. and Sonenblum, S., 2011. Assessing evidence supporting redistribution of pressure for pressure ulcer prevention: a review. *J Rehabil Res Dev*, *48*(3), pp. 203-13.

[73] Gadd, M.M., 2012. Preventing hospital-acquired pressure ulcers: improving quality of outcomes by placing emphasis on the Braden subscale scores. *Journal of Wound Ostomy and Continence Nursing*, *39*(3), pp. 292-294.

[74] Gassara, H.E., Almuhamed, S., Moukadem, A., Schacher, L., Dieterlen, A. and Adolphe, D., 2017. Smart wheelchair: Integration of multiple sensors. In *IOP Conference Series: Materials Science and Engineering,* 254(7), pp. 072008. IOP Publishing, October.

[75] Sonenblum, S.E., Vonk, T.E., Janssen, T.W. and Sprigle, S.H., 2014. Effects of wheelchair cushions and pressure relief maneuvers on ischial interface pressure and blood flow in people with spinal cord injury. *Archives of Physical Medicine and Rehabilitation*, *95*(7), pp. 1350-1357.

[76] Sonenblum, S.E., Sprigle, S.H. and Martin, J.S., 2016. Everyday sitting behaviour of full-time wheelchair users. *Journal of Rehabilitation Research and Development*, *53*(5).

[77] Yang, Y.S., Pan, C.T. and Ho, W.H., 2018. Sensor-based remote temperature and humidity monitoring device embedded in wheelchair cushion. *Sensors and Materials, 30*, pp. 1807-1814.

[78]   Takada, M., Wakimoto, S., Oshikawa, T., Ueda, T. and Kanda, T., 2020. Active Cloth Fabricated by a Flat String Machine and its Application to a Safe Wheelchair System. *Journal of Robotics and Mechatronics*, *32*(5), pp. 1010-1018.

[79]   Elevado, A.Z., Sagao, E., Sales, A.F., Ibarra, J.B. and Valiente, L., 2021. Discomfort Monitoring System using IoT applied to a Wheelchair. In *2021 IEEE International Conference on Automatic Control and Intelligent Systems (I2CACIS)*, pp. 120-125. IEEE, June.

[80]   Tavares, C., Domingues, M.F., Paixão, T., Alberto, N., Silva, H. and Antunes, P., 2019. Wheelchair pressure ulcer prevention using FBG based sensing devices. *Sensors*, *20*(1), pp. 212.

[81]   Tavares, C., Real, D., Domingues, M.D.F., Alberto, N., Silva, H. and Antunes, P., 2022. Sensor Cell Network for Pressure, Temperature and Position Detection on Wheelchair Users. *International Journal of Environmental Research and Public Health*, *19*(4), pp. 2195.

[82]   Silva A.S., Correia M.V. and Silva H.P., 2021. Invisible ECG for High Throughput Screening in eSports. *Sensors,* 21(22).

[83]   Salve, M. and Bankoff, A., 2003. Body posture - a problem that afflicts workers. *Brasileiro de Saúde Ocupacional*, 28, pp. 91-103.

[84]   Huang, M., Gibson I. and Yang R., 2017. Smart chair for monitoring of sitting behavior, *DesTech 2016: Proceedings of the International Conference on Design and Technology*, Knowledge E, pp. 274-280.

[85]   Prueksanusak, Rujivipatand P. and Wongpatikaseree, K., 2019. An Ergonomic Chair with Internet of Thing Technology using SVM, *2019 4th Technology Innovation Management and Engineering Science International Conference (TIMES-iCON)*, pp. 1-5.

[86]   Ishaku, A.A., Tranganidas, A., Matúška, S., Hudec, R., McCutcheon, G., Stankovic, L. and Gleskova, H., Flexible force sensors embedded in office chair for monitoring of sitting postures. *2019 IEEE International Conference on Flexible and Printable Sensors and Systems (FLEPS)*, pp. 1-3.

[87]   Cheng, J., Zhou, B., Sundholm, M. and Lukowicz, P., 2013. Smart chair: What can simple pressure sensors under the chairs legs tell us about user activity? *IARIA XPS Press.*

[88]   Roh, J., Park, H.J., Lee, K.J., Hyeong, J., Kim, S. and Lee, B., 2018. Sitting Posture Monitoring System Based on a Low-Cost Load Cell Using Machine Learning. *Sensors*.

[89]   Wong W.Y. and Wong M.S., 2008. Trunk posture monitoring with inertial sensors, *European Spine Journal.*

[90]   Annetts, S., Coales, P., Colville, R., Mistry, D., Moles, K., Thomas, B. and Van Deursen, R., 2012. A pilot investigation into the effects of different office chairs on spinal angles. *European Spine Journal*, 21(2), pp. 165-170.

[91]   Russell, L., Goubran R. and Kwamena, F., 2018. Posture Detection Using Sounds and Temperature: LMS-Based Approach to Enable Sensory Substitution. *IEEE Transactions on Instrumentation and Measurement*, 67(7), pp. 1543-1554.

[92]   Dziuda, L., Skibniewski, F. W., Krej, M. and Lewandowski, J., 2012. Monitoring respiration and cardiac activity using fiber Bragg grating-based sensor. *IEEE Transactions on Biomedical Engineering*, *59*(7), pp. 1934-1942.

[93]   Prata, D., Carvalho, A., Costa, F.M., Marques, C. and Leitão, C., 2021. Unobtrusive monitoring of the respiratory rate in an office desk chair with FBG sensors. In *2021 IEEE International Workshop on Metrology for Industry 4.0 & IoT (MetroInd4. 0&IoT)*, pp. 177-181. IEEE, June.

[94]   Lee, T.H., Kim E.S., Kim T.H. and Jeong, M. Y., 2015. Simple pressure sensor for a vehicle seat using a woven polymer optical-fibre sheet, *Journal of the Korean Physical Society*, 67(11), pp.1947–1951.

[95]   Haroglu, D., Powell, N. and Seyam, A.F.M., 2016. A textile-based optical fiber sensor design for automotive seat occupancy sensing. *The Journal of The Textile Institute,* 108(1), pp. 49-57.

[96]   Tavares, C., Silva, J., Mendes, A., Rebolo, L., Domingues, M.D.F., Alberto, N., Lima, M., Silva, H. and Antunes, P., 2022. Instrumented office chair with low-cost plastic optical fiber sensors for posture control and work conditions optimization. Accepted in IEEE Access.

[97]   Cardiovascular Diseases (CVDs). World Health Organization (WHO). Available online: https://www.who.int/health-topics/cardiovascular-diseases#tab=tab_1 (accessed in February 2022).

[98]   Massaroni, C., Zaltieri, M., Presti, D.L., Nicolò, A., Tosi, D. and Schena, E., 2020. Fiber Bragg grating sensors for cardiorespiratory monitoring: A review. *IEEE Sensors Journal*, *21*(13), pp. 14069-14080.

[99]   Presti, D.L., Massaroni, C., Leitão, C.S.J., Domingues, M.D.F., Sypabekova, M., Barrera, D. and Schena, E., 2020. Fiber bragg gratings for medical applications and future challenges: A review. *IEEE Access*, *8*, pp. 156863-156888.

[100]   Perezcampos Mayoral, C., Gutiérrez Gutiérrez, J., Cano Pérez, J.L., Vargas Treviño, M., Gallegos Velasco, I.B., Hernández Cruz, P.A., and Rojas Laguna, R., 2021. Fiber Optic Sensors for Vital Signs Monitoring. A Review of Its Practicality in the Health Field. *Biosensors*, *11*(2), pp. 58.

[101]   Lee, K.P., Yip, J., Yick, K.L., Lu, C. and Lo, C.K., 2021. Textile-based fiber optic sensors for health monitoring: A systematic and citation network analysis review. *Textile Research Journal*, pp. 00405175211036206.

[102]   Lo Presti D., Romano C., Massaroni C., D'Abbraccio J., Massari L., Caponero M.A., Oddo C.M., Formica D. and Schena E., 2019. Cardio-Respiratory Monitoring in Archery Using a Smart Textile Based on Flexible Fiber Bragg Grating Sensors. *Sensors,* 19(16), pp. 3581.

[103]   De Groote, A., Wantier, M., Cheron, G., Estenne, M. and Paiva, M., 1997. Chest wall motion during tidal breathing. *Journal of Applied Physiology*.

[104]   Wehrle, G., Nohama, P., Kalinowski, H.J., Torres, P.I. and Valente, L.C.G, 2001. A fibre optic Bragg grating strain sensor for monitoring ventilatory movements. *Measurement Science and Technology*, 12(7), pp. 805-809.

[105]   Nedoma, J., Fajkus, M., Martinek, R. and Vasinek, V., 2017. Non-Invasive Fiber-Optic Biomedical Sensor for Basic Vital Sign Monitoring. *Advances in Electrical and Electronic Engineering,* 15, pp. 336-342.

[106]   Fajkus, M., Nedoma, J., Martinek, R., Vasinek, V., Nazeran, H. and Siska, P., 2017. A Non-Invasive Multichannel Hybrid Fiber-Optic Sensor System for Vital Sign Monitoring. *Sensors,* 17, pp. 111.

[107]   Grillet, A., Kinet, D., Witt, J., Schukar, M., Krebber, K., Pirotte, F. and Depre, A., 2008. Optical fiber sensors embedded into medical textiles for healthcare monitoring, *IEEE Sensors Journal*, 8(7), pp. 1215-1222.

[108]   Witt, J., Narbonneau, F., Schukar, M., Krebber, K., De Jonckheere, J., Jeanne, M., Kinet, D., Paquet, B., Depre, A., D'Angelo, L.T., Thiel, T. and Logier, R., 2012. Medical textiles with embedded fiber optic sensors for monitoring of respiratory movement. *IEEE Sensors Journal,* 12(1), pp. 246-254.

[109]   Ciocchetti, M., Massaroni, C., Saccomandi, P., Caponero, M.A., Polimadei, A., Formica, D. and Schena, E., 2015. Smart Textile Based on Fiber Bragg Grating Sensors for Respiratory Monitoring: Design and Preliminary Trials. *Biosensors*, 5, pp. 602-615.

[110]   Presti, D.L., Massaroni, C., Formica, D., Saccomandi, P., Giurazza, F., Caponero, M.A. and Schena, E., 2017. Smart Textile Based on 12 Fiber Bragg Gratings Array for Vital Signs Monitoring. IEEE Sensors Journal, 17, pp. 6037-6043.

[111] Lo Presti, D., Massaroni, C., Saccomandi, P., Caponero, M.A., Formica, D. and Schena, E., 2017. A Wearable Textile for Respiratory Monitoring: Feasibility Assessment and Analysis of Sensors Position on System Response. *Annual International Conference of the IEEE*, pp. 4423-4426.

[112] Nedoma, J., Fajkus, M., Novak, M., Strbikova, N., Vasinek, V., Nazeran, H., Vanus, J., Perecar, F. and Martinek, R., 2017. Validation of a Novel Fiber-Optic Sensor System for Monitoring Cardiorespiratory Activities During MRI Examinations. *Advances in Electrical and Electronic Engineering*, 15, pp. 536-543.

[113] Fook, V.F.S., Leong, K.P., Zhong, E.H.J., Jayachandran, M., Wai, A.A.P., Biswas, J., Si, L.W. and Yap, P., 2008 Non-intrusive respiratory monitoring system using Fiber Bragg Grating sensor. In *HealthCom 2008-10th International Conference on e-health Networking, Applications and Services*, pp. 160-164. IEEE, July.

[114] Hao, J., Jayachandran, M., Kng, P.L., Foo, S.F., Aung Aung, P.W. and Cai, Z., 2010. FBG-based smart bed system for healthcare applications. *Frontiers of Optoelectronics in China*, 3(1), pp. 78-83.

[115] Zhu, Y., Maniyeri, J., Fook, V.F.S. and Zhang, H., 2015, Estimating respiratory rate from FBG optical sensors by using signal quality measurement. In *2015 37th annual international conference of the IEEE engineering in medicine and biology society (EMBC)*, pp. 853-856. IEEE, August.

[116] Iacoponi, S., Massaroni, C., Lo Presti, D., Saccomandi, P., Caponero, M.A., D'Amato, R. and Schena, E., 2018. Polymer-coated fiber optic probe for the monitoring of breathing pattern and respiratory rate. In *Annual International Conference of the IEEE Engineering in Medicine and Biology Society (EMBC)*, pp. 1616-1619. IEEE, July.

[117] Ambastha, S., Umesh, S., Maheshwari, U., and Asokan, S., 2016. Pulmonary function test using fiber Bragg grating spirometer. *Journal of Lightwave Technology*, 34(24), pp. 5682-5688.

[118] Massaroni, C., Presti, D.L., Saccomandi, P., Caponero, M.A., D'Amato, R. and Schena, E., 2018. Fiber Bragg Grating Probe for Relative Humidity and Respiratory Frequency Estimation: Assessment During Mechanical Ventilation. *IEEE Sensor Journal*, 18, pp. 2125-2130.

[119] Pant, S., Umesh, S. and Asokan, S., 2018. Fiber Bragg Grating Respiratory Measurement Device. *In Proceedings of the 2018 IEEE International Symposium on Medical Measurements and Applications (MeMeA)*, pp. 1-5. IEEE June.

[120] Lo Presti, D., Massaroni, C., Zaltieri, M, Sabbadini, R., Carnevale, A., Di Tocco, J., Longo, U.G., Caponero, M.A., D'Amato, R., Shena, E. and Formica D., 2020. A Magnetic Resonance-compatible wearable device based on functionalized fiber optic sensor for respiratory monitoring. *IEEE Sensor Journal*, pp. 1.

[121] Jewart, C., McMillen, B., Cho, S.K. and Chen, K.P., 2006. X-probe flow sensor using self-powered active fiber Bragg gratings. *Sensors and Actuators A: Physical*.

[122] Gao, S., Zhang, A.P., Tam, H.Y., Cho L.H. and Lu, C., 2011. All optical fiber anemometer based on laser heated fiber Bragg gratings. *Optics Express*, 19(11), pp. 10124.

[123] Gao, R. and Lu, D., 2019. Temperature compensated fiber optic anemometer based on graphene-coated elliptical core micro-fiber Bragg grating. *Optics Express*, 27(23), pp. 34011-34021.

[124] Seidel, H.M., Stewart, R.W., Ball, J.W., Dains, J.E., Flynn, J.A. and Solomon, B.S., 2010. Mosby's Guide to Physical Examination-E-Book. *Elsevier Health Sciences*.

[125] Shaq, G. and Veluvolu, K.C., 2014. Surface chest motion decomposition for cardiovascular monitoring. *Scientific Reports*, 4(1), pp. 19.

[126] Chen, Z., Teo, J.T., Ng, S.H. and Yim, H., 2011. Smart Pillow for Heart-Rate Monitoring Using a Fiber Optic Sensor. *In Proceedings of the Optical Fibers, Sensors, and Devices for Biomedical Diagnostics and Treatment XI*, 7894, pp. 789402. February.

[127] Nedoma, J., Fajkus, M., Martinek, R. and Nazeran, H., 2019. Vital sign monitoring and cardiac triggering at 1.5 tesla: a practical solution by an MR-ballistocardiography fiber-optic sensor. *Sensors*, *19*(3), pp. 470.

[128] Tavares, C., Leitão, C., Lo Presti, D., Domingues, M.F., Alberto, N., Silva, H. and Antunes, P., 2022. Respiratory and heart rate monitoring using an FBG 3D-printed wearable system. *Biomedical Optics Express*, *13*(4), pp. 2299-2311.

[129] Chethana, K., Prasad, A.S.G., Omkar, S.N. and Asokan, S., 2017. Fiber Bragg Grating Sensor Based Device for Simultaneous Measurement of Respiratory and Cardiac Activities. *Journal Biophotonics*, 10, pp. 278-285.

[130] Dziuda and Skibniewski, F.W., 2014. A new approach to ballistocardiographic measurements using fibre Bragg grating-based sensors. *Biocybernetics and Biomedical Engineering*, 34(2), pp. 101-116.

[131] Lo Presti, D., Massaroni, C., D'Abbraccio, J., Massari, L., Caponero, M., Longo, U.G., Formica, D., Oddo, C.M. and Schena E., 2019. Wearable system based on flexible FBG for respiratory and cardiac monitoring. *IEEE Sensors Journal*, 19(17), pp. 7391-7398.

[132] Kesner, S.B. and Howe, R.D., 2011. Design principles for rapid prototyping forces sensors using 3-D printing. *IEEE/ASME Transactions on Mechatronics*, 16(5), pp. 866-870.

[133] Khosravani, M.R. and Reinicke, T., 2020. 3D-printed sensors: Current progress and future challenges. *Sensors and Actuators A: Physical*, *305*, pp. 111916.

[134] Elst, L., Faccini de Lima, C., Gokce Kurtoglu, M., Koraganji, V.N., Zheng, M. and Gumennik, A., 2021. 3D printing in fiber-device technology. *Advanced Fiber Materials*, *3*(2), pp. 59-75.

[135] Leal-Junior, A., Marques, C., Ribeiro, M., Pontes, M. and Frizera, A., 2018. FBG-embedded 3-D printed ABS sensing pads: the impact of infill density on sensitivity and dynamic range in force sensors. *IEEE Sensor Journal*, 18(20), pp. 8381–8388.

[136] Hao, Z., Cook, K., Canning, J., Chen, H. and Martelli, C., 2020. 3D printed smart orthotic insoles: monitoring a person's gait step by step. *IEEE Sensor Letter*, 4(1), pp. 1–4.

[137] Fajkus, M., Nedoma, J., Siska, P. and Vasinek, V., 2016. FBG Sensor of Breathing Encapsulated into Polydimethylsiloxane. *In Proceedings of the Optical Materials and Biomaterials in Security and Defence Systems Technology XIII*, 9994, pp. 99940N. October.

[138] Silva, A.F., Carmo, J.P., Mendes, P.M. and Correia, J.H., 2011. Simultaneous cardiac and respiratory frequency measurement based on a single fiber Bragg grating sensor. *Measurement Science and Technology*, 22(7).

[139] WHO, 2015. Relatório Mundial de Envelhecimento e Saúde.

[140] Program on Maintaining intrinsic capacities with aging. World Health Organization (WHO). Available online: https://www.care-weekly.com/2551-w-h-o-world-health-organization-program-on-maintaining-intrinsic-capacities-with-aging.html#:~:text=W.H.O%20defines%20intrinsic%20capacity%20as,%2Dsensorial%3A%20Vision%2C%20Earing. (accessed in February 2022).

[141] WHO, 2008. Guidelines on the provision of manual wheelchairs in less resourced settings.